Gene expression and immune responses in tuberculosis: the effect of *Mycobacterium tuberculosis*-specific- and type I interferon stimulation

By

Florence Mutua

A Thesis Submitted to the Faculty of Graduate Studies of

The University of Manitoba

In partial fulfillment of the requirements of the degree of

DOCTOR OF PHILOSOPHY

Department of Medical Microbiology and Infectious Diseases

University of Manitoba

Winnipeg

Abstract

Type I interferon (IFN) signatures described in active TB (ATB) show potential as biomarkers for treatment monitoring and identification of individuals at risk of disease progression. The drivers or inducers of this profile have however not been identified

The research outlined in this thesis sought to examine potential drivers of the IFN signature and tested the hypothesis that IFN-α- and/or IFN-β-driven transcriptomic signatures and cytokine responses could distinguish clinical TB states. Peripheral blood mononuclear cells (PBMCs) from individuals with ATB, latent TB infection (LTBI as defined by the QuantiFERON test), tuberculin skin test-reactive (TST-positive, QuantiFERON-negative), and healthy controls (HC) were stimulated with IFN-α or IFN-β or *Mycobacterium tuberculosis* whole cell lysate (Mtb WCL). mRNA expression of 51 ISGs was assessed using RT-qPCR and cytokine production assessed from culture supernatants using Milliplex assays.

The results showed that LTBI could be distinguished from ATB by IFN-α-driven expression of FCGR1A gene; IFN-β-driven expression of *FCGR1A*, *FCGR1B*, and *SOCS3* genes; and Mtb WCL-driven expression of *IFI44*, *IFI44L*, *IFIT1*, and *IFITIM3* genes. Similarly, IFN-α- and IFN-β-driven IL-10 protein expression could distinguish LTBI from ATB. *FCGR1A*, *IFIT1* and *IL-10* genes drive disease progression, while SOCS3, *IFI44*, *IFI44L*, and *IFITM3* genes control infection. The data also showed that genes involved in macrophage polarization could distinguish ATB from either LTBI or HC. IFN-α induced expression of *MSR1* that drives a detrimental M2 phenotype, whereas IFN-β and Mtb WCL induced *SOCS3* and *STAT1* respectively, that drive a protective M1 phenotype. IFN-α/β and Mtb WCL stimulation induced divergent immune responses. IFN-α/β stimulation upregulated ISG expression but low cytokine induction whereas Mtb WCL stimulation induced low ISG expression but upregulated cytokines.

These results illustrate that ISG and cytokine responses show specificity to IFN-α, IFN-β or Mtb WCL and can distinguish LTBI from ATB. Differentially expressed genes and cytokines show protective or detrimental effects that can determine *M. tuberculosis* infection outcomes. This thesis research contributes to the knowledge of type I IFN responses in TB that could be used in identification of possible therapeutic targets, and of ISGs and cytokines that can be used in the diagnosis of active and latent TB.

Acknowledgements

I would like to thank the people who helped me through my graduate studies. First, I would like to thank Dr. Terry Blake Ball and Dr. Sandra Kiazyk for giving me the opportunity to study under their supervision and for their support, guidance, and encouragement during my studies. Thank you for supporting my research project and for the financial support.

Further, I would like to acknowledge the members of my PhD advisory committee, Dr.Ruey-Chyi Su, Dr. Stephanie Booth, and Dr. Neeloffer Mookherjee, for their constructive criticism, guidance, thought-provoking questions and encouragement over the years, and the motivation that kept my research work moving forward. Thanks also to the study participants from Winnipeg who provided the samples used for these experiments.

I wish to thank past and present members of the Ball lab for their contributions to this research. Thank you, Dr. Jennifer Juno, Dr. Jillian Waruk, and Christine Mesa for the discussions that kick-started this research. Thank you, Dr. Ruey-Chyi Su,for the many one-on-one discussions. Thank you to the Immunogenetics group for the helpful discussions and advice – Dr. Catherine Card, Dr. Sandra Gonzalez, Xuefen Yang, Bernard Abrenica, Hillary McCoubrey, Andrew Plesniarski, Abu Bakar Siddiq, and Zipporah Richard. Thanks to Dr. Tamsir Diallo, Linda Ares, Dana Cabiles, Tomasz Bielawny, Margot Plews, Max Abou, David Tang for the Quantstudio training, John Ho, and all other members of the JC Wilt lab.

I thank past and present staff of the Department of Medical Microbiology & Infectious Diseases. I specifically thank the Department Head Dr. Keith Fowke, Dr. Lyle McKinnon, Angela Nelson, Jude Zieske, Sharon Tardi, and Natasha Hollett. Thank you all MMID staff for an engaging and enjoyable learning experience. I also thank my fellow students in MMID for the many interactions in seminars, journal clubs and lively discussions that played a significant role in keeping our projects going. Thanks to Ruth Mwatelah, Kathleen Glover, Winnie Apidi, Kashem Mohammad, Dr. Robert Were Omange, Riley Tough, among others. Thank you to my fellow International Infectious Diseases and Global Health training program (IID and GHTP) trainees for a great, multidisciplinary experience, exciting discussions, and the discovery of many teaching techniques. I am grateful to the University of Nairobi (UoN) administration and the Department of Medical Microbiology & Immunology, UoN, for giving me time off work for my PhD studies.

And to all the friends who cheered me on through it all and kept the fire burning, I am truly grateful for your friendship. I am grateful to my family. My late dad, Peter Mutua Ngii, who always believed I could achieve whatever I set to do no matter the challenges, was a great inspiration and hoped to make it for my graduation (this one's for you, "Ndeti"); my Mum, Esther Ngii, who held me up in prayer everyday over the years – thank you both for the Saturday morning calls that I could always count on. My brothers and sisters – Mike, Joyce, Pamela, and Lennox. Thank you, Fred. And thank you Sally and Peter for keeping me going, especially during the challenging times.

I thank God Almighty for His grace and for His peace that passes all understanding. Thank You for walking with me every step of the way.

Dedication

I dedicate this thesis to my children, Sally and Peter, and to my late Dad, Peter Mutua Ngii, and to my Mum, Esther Ngii. Thank you for your love, support, encouragement, and prayers.

Table of Contents

List of Tables

List of Figures

Manuscripts arising from this thesis

Mutua F, Su R-C, Mwatelah R., Ball T.B., Kiazyk S. Type I interferon and *Mycobacterium tuberculosis* whole cell lysate induce different transcriptional responses in M. tuberculosis infection. *In preparation*

Mutua F, Su R-C, Ball T.B., Kiazyk S. Relationship between the transcriptional profile and cytokine/ chemokine responses induced by *Mycobacterium tuberculosis* antigen- and interferon-α/β in tuberculosis. *In preparation*

Mutua F, Su R-C, Ball T.B., Kiazyk S. The role of type I interferons in tuberculosis and in TB-risk associated comorbidities. *Review*. *In preparation*

CHAPTER ONE: GENERAL INTRODUCTION

1.1 Tuberculosis

1.1.1 Epidemiology of tuberculosis

Tuberculosis (TB) is a communicable disease of public health concern worldwide. Its causative agent, *Mycobacterium tuberculosis*, was first described in 1882 by Robert Koch and was previously known as the Koch bacillus.

More than 150 years later, this curable disease is among the top causes of death from a single infectious agent, with 1.3 million deaths in HIV-uninfected individuals and 214 000 in HIV-infected individuals from the 10 million cases reported in 2020 (1). In Canada, 1,796 cases of active TB (ATB) were reported in 2017 (2). Although the country has a low incidence rate of TB, 4.9 per 100 000 population, the distribution of cases is disproportionate and varies by province/ territory, ranging from 0.0 per 100 000 population in Prince Edward Island to 265.8 per 100 000 population in Nunavut. The proportions also vary by origin, with foreign-born persons being the majority (71.8%), Canadian-born Indigenous (individuals who self-identify as First Nations, Inuit or Métis) followed (17.4%) and Canadian-born non-Indigenous the minority (7.0%) (2). The World Health Organization (WHO) End TB strategy aims to reduce the number of deaths from TB by 95% and the TB incidence rate by 90% by the year 2035 (3).

Two clinical phenotypes result from infection with *M. tuberculosis* – latent TB infection (LTBI), in which individuals exposed to *M. tuberculosis* develop immune memory in response to stimulation with bacillary antigens but remain asymptomatic, and ATB, in which patients present with symptoms (4). The previous model of TB as a dichotomy, existing either as LTBI or ATB, has been revised over the years and is now considered a continuum of heterogenous states, the TB spectrum (4–7). While identification and treatment of ATB is a widely used approach for elimination of TB, another key approach of WHO End TB is the identification of individuals with LTBI at high risk of reactivation and treatment with preventive therapy (8–10). The global prevalence of LTBI is approximately 20-25% of the global population, an estimated two billion people (11,12). Individuals with LTBI have the potential to develop reactivation TB that is transmissible and therefore represent a pool in the population with the potential to progress to ATB. An estimated 10% of otherwise healthy individuals with LTBI progress to active disease in

their lifetime; of these, 5% develop ATB within the first two years of acquiring *M. tuberculosis* infection (13).

Multiple factors drive the spread of TB, including the HIV pandemic, the development of multi-drug resistant strains, and weak public health systems, particularly in TB-endemic countries (14). Other factors include TB stigma, which causes delays in patients seeking treatment and low treatment compliance, and inequities in the healthcare provision (15–17).

Thus, TB remains a significant health threat worldwide, especially in resource-limited settings and some at-risk and marginalized populations in developed countries such as Canada.

1.1.2 Characteristics of *Mycobacterium tuberculosis*

The bacterium is an aerobic, slow-growing, intracellular microorganism, which, under optimal conditions, doubles every 15 to 20 hours. It is a non-motile, non-spore-forming bacterium with a complex cell wall of waxy high lipid coating (primarily mycolic acid). The high lipid content cell wall has low permeability and cannot take up the aqueous-based Gram stain commonly used in microbiology. Instead, a differential staining method, Ziehl Neelsen staining, is used; the lipid layer stains with the carbol-fuchsin stain but prevents acid decolorization. Therefore, the bacteria are described as acid-fast bacilli (18).

1.1.2.1 Classification of *M. tuberculosis*

M. tuberculosis belongs to the family Mycobacteriaceae, order Actinomycetales, and is a member of the *M. tuberculosis* complex (MTBC) of bacteria that cause TB disease in humans. The mycobacteria in this complex share a common ancestor and are genetically similar. The main strains that cause disease in humans are *M. tuberculosis sensu stricto* and *M. africanum*. Other members of the MTBC cause disease primarily in animals but may also cause disease in humans: *M. bovis* and *M. caprae* in cattle and goats, respectively, *M. microti* in voles, and *M. pinnipedii* in seals and sea lions, among others (Figure 1) (19–22).

Genomic assessment of these species uses various regions within the bacterial genome, including 1) Regions of Difference (RD), 2) H37Rv (Classic Reference Strain) deletion 1 to 5 (RvD1-5), and 3) *M. tuberculosis*-specific deletion 1 (TbD1) (Figure 1). For example, the *M. bovis*

Bacillus Calmette–Guérin (BCG) strain lacks the RDs, *M. tuberculosis* H37Rv lacks RvD1-5 and TbD1, while *M. canettii* contains the three regions (22,23). Human-adapted strains are further classified into seven MTBC phylogenetic lineages: *M. tuberculosis sensu stricto* (Lineage 1 [L1] to L4, L7) and *M. africanum* (L5 and L6) (24,25). Lineages 1 (L1), L5 and L6 are known as "ancient" lineages; L2, L3 and L4 as "modern"; and lineage 7 as "intermediate" lineage (Figure 1). The hyper-virulent HN878 strain and the reference H37Rv strain commonly used in *in vitro* studies belong to the "modern lineages L2 and L4, respectively (26,27).

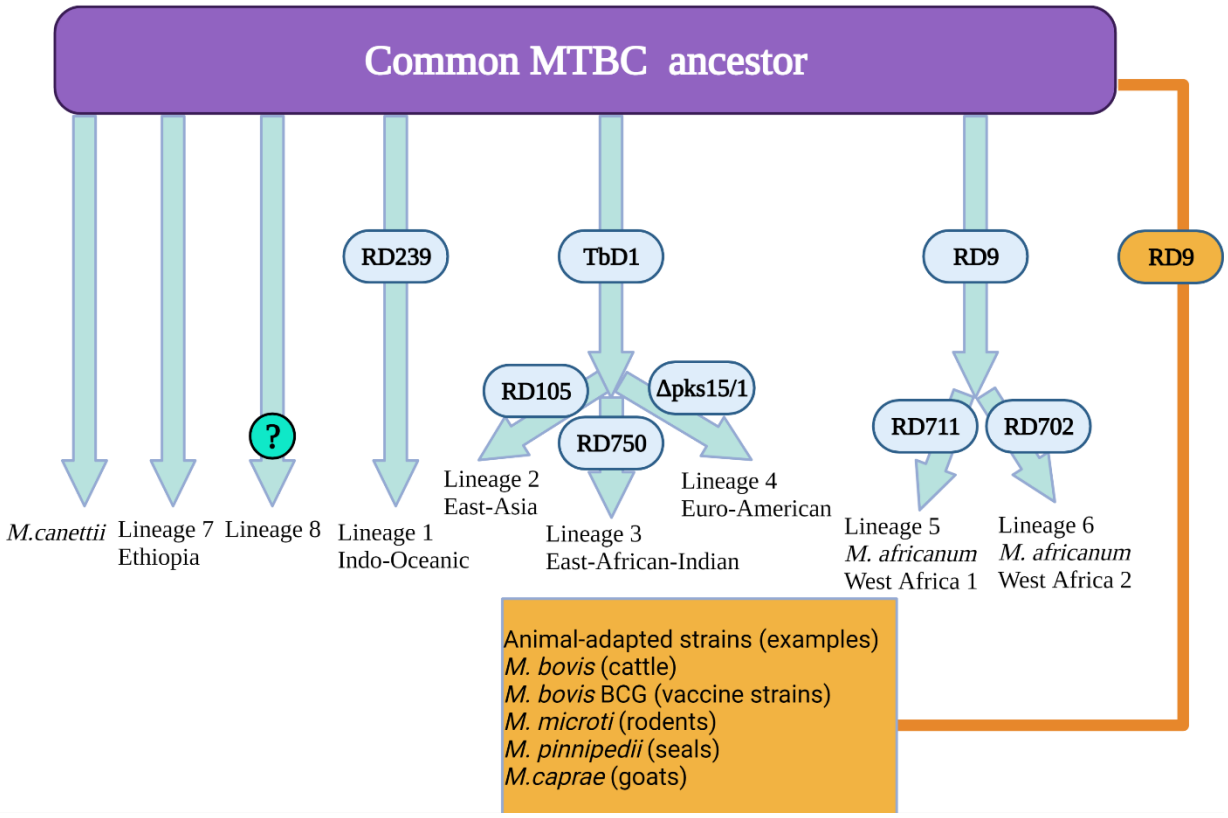

Figure 1. **Mycobacterial speciation and strain differentiation**.

RD's and deletions responsible for genotyping the various mycobacteria species and lineages are listed. These genetic determinants segregate these into the human-adapted (green arrows) and animal-adapted strains (brown) (22,28). Created with BioRender.com

Lineages differ in virulence, transmissibility, induction of the host immune response, clinical presentation, and the ability to develop drug resistance. For example, "modern" lineages

generally demonstrate a faster replication rate and higher virulence but a slower induction of pro-inflammatory cytokines than "ancient" lineages (29–32). However, these differences in the immune responses observed within groups are thought to result from differences in induction of the immune response by sub-lineages or by individual strains within lineages (30). For instance, in a mouse model of infection with the hypervirulent Beijing strain, L2 lineage, high type I IFN mRNA was induced compared to the less virulent CD1551 strain (33). These immune response variations are attributed to differences in pathogen-associated molecular patterns (PAMPs) between lineages, influencing their interaction with the pattern recognition receptors (PRRs) and immune cells (22).

The global distribution of *M. tuberculosis* lineages differs with some, L2 and L4, being more widely distributed, while others are restricted to specific locations – L5 and L6 to West Africa, and L7 to Ethiopia (34). A more recent addition to the lineages, L8, appears to be limited to the African Great Lakes region (35). Lineage distribution is likely the cause of founder effects and differences in transmissibility (36). Understanding the factors that lead to the success *of M. tuberculosis* may lead to a better understanding of TB pathogenesis and novel approaches to control TB disease.

1.1.2.2 *M. tuberculosis* genome and virulence factors

The genome of *M. tuberculosis* is 4.41 million base pairs in length with approximately 4000 genes (37). Clinical isolates of *M. tuberculosis*, the virulent reference strain of *M. tuberculosis*, H37Rv, and virulent strains of *M. bovis* contain the region of difference 1 (RD1), which is associated with pathogenicity and is absent in the BCG vaccine strains (38,39).

In *M. tuberculosis*, the RD1 genes *esxB* (Rv3874) and *esxA* (Rv3875) code for the secreted proteins culture filtrate protein 10 (CFP-10) and early secretory antigenic target protein 6 (ESAT-6), respectively; RD1 genes also code for the ESAT-6 secretion system-1 (ESX-1) required for the secretion of the heterodimeric ESAT-6:CFP-10 complex (39,40). In *M. tuberculosis*, ESAT-6 is a virulence factor that functions through various mechanisms. In THP-1 cells and dendritic cells (DCs), ESAT-6 has a pore-forming role that aids in the intracellular trafficking of the bacillus and translocation from the phagosome to the cytosol (41–43). In vitro assessment of neutrophils stimulated with the ESAT-6:CFP-10 complex or its components shows that CFP-10 also caused pore-formation in the absence of cellular disintegration. This protein was also observed to

stimulate the recruitment and activation of neutrophils and the production of reactive oxygen species (ROS) (44). Aside from ESAT-6 and CFP-10, various other *M. tuberculosis* virulence factors have been described. These include the TB7.7 (Rv2652) used in the QuantiFERON-TB (QFT) immunodiagnostic test, the Antigen 85 (Ag85) complex that prevents phagolysosome formation, the "latency antigens" that are gene products of the dormancy regulon or DosR, and the resuscitation promoting factors (Rpf) that show the ability to induce replication in "quiescent" bacilli (45–47).

1.1.3 *M. tuberculosis* transmission

The respiratory tract serves as the main portal of entry for *M. tuberculosis*. The proposed transmission flow starts with a patient with ATB - pulmonary TB (PTB) or laryngeal TB aerosolizing *M. tuberculosis*-laden particles into the air through cough and other respiratory activities (48,49). In the air, evaporation of the respiratory droplets leads to the formation of infectious droplet nuclei, measuring one to five microns that can remain suspended in air for hours depending on the airflow and, if inhaled by a susceptible host, may lead to infection (48,50,51). The transmission of *M. tuberculosis*, risk of infection and progression to disease are influenced by various factors.

1.1.3.1 Risk factors for infection

Risk factors associated with the infected individual include the source's bacillary load in the lung, proximity to and duration of exposure to the infected individual (14,52,53). Risk factors in the exposed individual include immunosuppressive conditions such as human immunodeficiency virus (HIV) and anti-tumor necrosis factor-α therapy for autoimmune disorders such as rheumatoid arthritis (54–56). Other high-risk groups include patients with diabetes (57–60) and malnourished individuals (61–63). Diabetes and malnutrition, including protein-energy malnutrition and micronutrient deficiency, interfere with the immune homeostasis, impairing the immune response and increasing susceptibility to infection and risk of disease progression (14,62,64,65). Individuals with obesity or increased body mass index (BMI) are less susceptible to infection (66).

Socioeconomic and behavioural factors may also exacerbate the aforementioned risk factors; for example, low socioeconomic status (SES) is associated with poverty, increasing the likelihood of malnutrition, and overcrowding in houses with poor ventilation. In addition, poor ventilation enhances proximity to the infected individual and duration of exposure and air pollution due to solid fuels indoors. Other factors include smoking which impairs mucous secretion and removal, bacterial phagocytosis, and the immune response; and alcohol which impairs cytokine production (67–70). Furthermore, age is associated with disease development, with infants and children less than five years of age and the elderly at higher risk due to dampened immune responses in these age groups. Gender is also associated with an increased risk of TB, affecting more males than females. Indeed, 56% of the TB cases reported in 2019 were males (71). The increased risk in males is related to behavioural factors (travel, smoking, alcohol) or physiological factors related to genetic differences in the immune responses between males and females (72).

Host genetic factors linked to race are associated with an increased risk of TB acquisition and have been described in some countries (73–76). For example, Indigenous persons in Canada and Australia have a higher risk of acquiring TB than the rest of the population. They also have higher rates of underlying factors that predispose them to TB, such as diabetes and renal failure (77). However, it has not been established which factors account for this increased risk for TB – host genetics or underlying epidemiological factors.

1.1.4 Outcomes of *M. tuberculosis* infection and diverse spectrum of disease

Exposure to *M. tuberculosis* leads to several potential outcomes: 1) Infection clearance - the initial bacterial invasion induces an effective innate immune response that kills and clears the bacilli leaving no clinical, radiological, or immunological indication of infection; 2) LTBI - controlled infection where the bacteria are “walled off” in a dormant form within a granuloma, individuals with LTBI present with no symptoms; and, 3) ATB - disease resulting from uncontrolled bacterial replication that starts either immediately after initial infection (primary TB), or from reactivation of LTBI (postprimary TB); (4–6) (Figure 2). Following the establishment of a productive infection with *M. tuberculosis*, two distinct clinical states were previously described – LTBI or ATB. This paradigm has evolved and is now described as a spectrum of states that displays heterogeneity in immune responses and clinical and pathological outcomes (5,7).

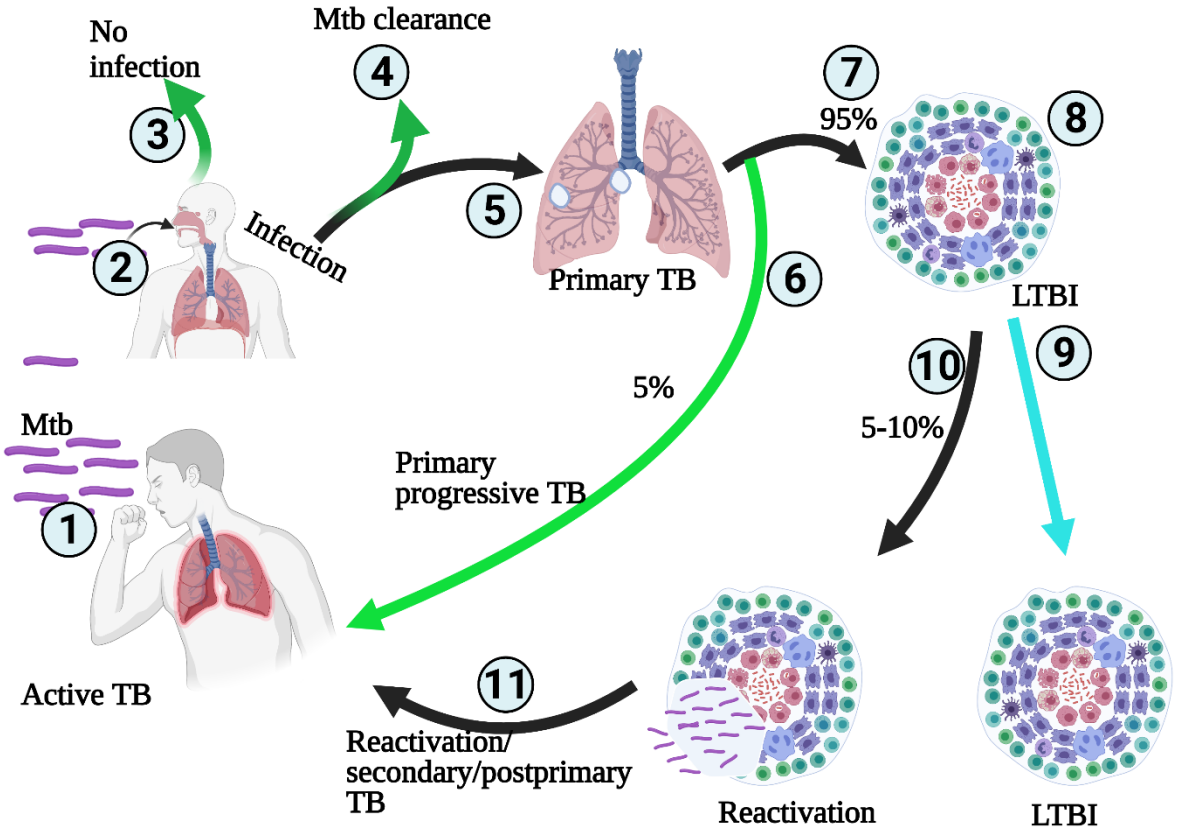

Figure 2. **Overview of *M. tuberculosis* infection outcomes**.

1: ATB patient expectorates *M. tuberculosis* (Mtb) bacilli, 2: Mtb bacilli inhaled, 3: Exposure may result in no infection, or 4: Infection develops and is cleared by the immune response, or 5: Initial infection in lung and draining hilar lymph nodes (primary TB), which can progress to 6: ATB directly (primary progressive TB), or 7: in 95% of infections, a well-structured granuloma forms leading to 8: (LTBI), 9: 90% of individuals maintain latent infection, while 10: in 5-10% of individuals reactivation of LTBI leads to 11: ATB (reactivation/ secondary/ postprimary TB) (78,79). Created with BioRender.com

1.1.4.1 Spectrum of disease states

1.1.4.1.1 Latent TB infection

In the natural cycle of *M. tuberculosis*, nine out of 10 individuals that acquire *M. tuberculosis* demonstrate the ability to control the infection in a latent form, latent TB infection (LTBI), a form in which individuals remain asymptomatic (6) (Figure 2). LTBI is the result of effective infection containment by the host immune response, a phase in which bacteria remain dormant within an immune cell enclosure known as the granuloma (discussed in section 1.2.1.3).

This phase of infection is defined as a state in which stimulation with *M. tuberculosis* antigen induces a persistent host immune response without clinical and radiological evidence of ATB disease (7). Mathematical modelling and a meta-analysis of immunological tests for LTBI estimated that about 20 to 25% of the world's population has LTBI (11,12). Thus, the immune system maintains the LTBI or dormant state for most individuals, and an individual can maintain this state for their lifetime without ever knowing they were infected. Importantly though, anyone with LTBI has the possibility of reactivation, which means their infection comes out of dormancy and bacteria begin replicating again, resulting in reactivation/ secondary/ postprimary TB (5,6). This process is thought to be the primary source of ATB cases in countries with low prevalence (80,81) where community transmission is undetectable.

1.1.4.1.2 Active TB disease

ATB commonly presents with lung disease known as pulmonary TB (PTB). From the natural history of the disease (Figure 2), TB can be divided into three disease phenotypes – primary, progressive primary TB, and postprimary TB. The first infection with *M. tuberculosis* occurs more commonly in infants and children under five years of age and is known as primary TB. The infection localizes in the mid or lower lobe of the lung (the Ghon focus) and, together with accompanying hilar lymphadenopathy, forms the Ghon complex. This phase of the disease is often subclinical but may present as a unilateral pneumonic process indistinguishable radiographically from other bacterial types of pneumonia (82). Thus, primary TB has two potential outcomes depending on whether the immune response contains or fails to contain the infection.

Failure of infection containment by the immune system results in progressive primary TB. This clinical phenotype commonly develops one to two years after the initial infection in children less than five years of age and immunosuppressed individuals (including HIV). The disease commonly involves the lower lobes of the lungs and usually has an extrapulmonary component (82).

Postprimary TB, also known as reactivation TB or secondary TB, results when the successful containment of infection following primary infection fails. The granuloma that serves to "wall off" the *M. tuberculosis*-infected macrophages in layers of immune cells breaks down with the reactivation of dormant bacilli from within this structure. Breakdown in this containment of latent infection occurs in both immunocompetent and immunocompromised individuals. In

immunocompromised individuals, conditions such as HIV infection, uncontrolled diabetes, renal failure, chemotherapy, and organ transplantation increase the risk for reactivation (83,84). A more significant proportion (90%) of immunocompetent individuals infected with *M. tuberculosis* contain the bacilli in the latent form (Figure 2). In comparison, 5% to 10% have a lifetime risk of reactivation to active disease. Thus, reactivation can happen any time after the establishment of the granuloma.

While these outcomes mainly depend on the host immune response to the infection (discussed in section 1.2), the precise correlates of protection in *M. tuberculosis* are unknown. The immune factors, including those that determine outcome after exposure, maintaining latent infection in the absence of immunosuppression or leading to the reactivation of latent infection to active disease, remain largely unknown.

1.1.5 Clinical presentation of TB

Individuals with LTBI are asymptomatic and non-contagious unless they reactivate to an ATB state. Patients with PTB present with chronic cough, defined as a cough for more than two weeks, chest pain, and hemoptysis, as well as systemic symptoms: night sweats, fever, chills, weight loss, and fatigue (85).

1.1.6 Laboratory diagnostics in *M. tuberculosis* infection and disease

1.1.6.1 Laboratory diagnosis of LTBI

LTBI diagnosis is not based on isolation of the bacilli in culture mainly because the state and location of the bacillus in this stage remain unknown. Tests currently used for LTBI diagnosis are the Tuberculin skin test (TST) and the interferon-γ release assays (IGRA) that measure T cell-mediated responses against *M. tuberculosis* antigens. Available IGRA tests include the enzyme-linked immunosorbent assay (ELISA), QuantiFERON-TB test (QFT) and the enzyme-linked immunosorbent spot (ELISPOT) assay T-SPOT.TB test (86,87)

Active or latent infection with mycobacteria leads to immune cell proliferation and primes T lymphocytes that enter the circulation. The TST measures the host response to a subcutaneous

injection of the *M. tuberculosis* antigen purified protein derivative (PPD), which stimulates the primed T lymphocytes that act with antigen-presenting cells to produce cytokines. These cytokines induce a local inflammatory response in individuals previously exposed to *M. tuberculosis*. The inflammatory response is a delayed-type hypersensitivity response that takes 48 to 72 hours to develop. The results are interpreted by the size of induration measured in millimetres 72 hours later. However, a positive test result does not differentiate between latent infection and active disease. For TST, testing before the development of cell-mediated immunity gives false-negative results either due to the absence of a functional immune system to induce a response to the injected protein or anergy resulting from immunosuppression (88). Infection with non-tuberculous mycobacteria (NTMs) and BCG vaccination also give false-positive TST results due to the genetic similarity of NTM and the BCG vaccine strain immune antigens to those of *M. tuberculosis*. This similarity leads to immunological cross-reactions (89).

The IGRAs also identify an individual's prior exposure to *M. tuberculosis* by measuring IFN-γ released by circulating T cells in an individual's whole blood stimulated with *M. tuberculosis*-specific antigens - ESAT-6, CFP-10 and TB7.7 (88,90). However, similar to TST, IGRAs do not discriminate between LTBI and ATB. Notably, the antigens used in IGRA tests are absent in the BCG vaccine; thus, previous BCG vaccination does not affect IGRA results because the test is specific for *M. tuberculosis*. In addition, for the IGRAs, conditions associated with low peripheral lymphocyte counts, such as HIV and advanced age, can lead to false-negative results (91–94). Thus none of the currently available tests is helpful as a gold standard diagnostic test for benchmarking the diagnosis of LTBI due to their limitations (89,95).

1.1.6.2 Laboratory diagnosis of active TB

Several laboratory tests are available for the diagnosis of ATB, including microscopy, bacterial culture, and molecular diagnostic tests. Light microscopy is more widely accessible for diagnosis, particularly in low- and medium-economic TB-endemic countries (90). This test has a high specificity with variable sensitivity (20–80%). Improvements to light microscopy include fluorescent microscopy (FM) and light-emitting diode (LED) microscopy, which increase sensitivity by 5% and 6%, respectively (96–98).

Culture-based diagnosis is the gold standard of ATB diagnosis (99). *M. tuberculosis* is a slow-growing microorganism and takes 3-8 weeks to grow on solid media and an average of 10

and 20 days in liquid media for smear-positive and smear-negative samples, respectively (18). Other culture techniques, such as the BACTEC Mycobacterial Growth Indicator Tube (MGIT) system, a commercial automated culture system that uses a fluorometric technique to detect carbon dioxide production, take approximately 1-3 weeks for a positive result. The Microscopic observation susceptibility (MODS) technique that identifies the characteristic serpentine cording growth of *M. tuberculosis* in liquid broth takes 7-10 days for a positive result (100).

Molecular techniques available for DNA detection or nucleic acid amplification testing (NAAT) include both the quantitative polymerase chain reaction (PCR) and reverse transcription PCR (RT-PCR) methods. The WHO endorsed the line probe assays like Cepheid Xpert MTB/RIF (GeneXpert) and Xpert MTB/RIF Ultra assays to detect *M. tuberculosis* and identify drug resistance mutations (101–103). These molecular methods provide a more rapid diagnosis of TB and have reduced the turn-around time to a few hours (104). Emerging diagnostic tests focus on modifications of currently available NAAT techniques, the potential use of next-generation sequencing for detection of *M. tuberculosis* and drug susceptibility testing, and host transcriptomics to identify transcript signatures for TB diagnosis (105,106).

Despite the number of diagnostic tests available for TB, the disease spreads undetected in many parts of the world, particularly in low-income TB-endemic areas. Even with its variable sensitivity, the affordability of smear microscopy for the diagnosis of TB makes it widely available in most low-income countries (97,107). The roll-out of high throughput, low-cost molecular tests faces challenges with the lack of appropriate infrastructure and health systems, particularly in low-income countries (108).

1.1.7 Treatment of *M. tuberculosis* infection and disease

A systematic review of studies carried out in the period before the widespread use of antibiotics in TB determined a mean 10-year case-fatality rate of 70% in untreated HIV-negative sputum smear-positive TB patients and 20% in sputum smear-negative patients (109). These findings suggest that even without the impact of HIV, untreated TB is associated with high mortality.

Treatment of LTBI prevents progression to ATB disease. Treatment options utilize isoniazid and rifampicin or rifapentine, either as monotherapy or combination therapy. WHO recommends LTBI treatment for individuals at risk of reactivation, including HIV-positive individuals, children under the age of five, patients on dialysis, patients undergoing transplantation, and individuals on anti-TNF therapy (110). Early detection of individuals with ATB and their contacts, and individuals with LTBI at risk of reactivation, combined with appropriate treatment, therefore, breaks the transmission chain and is critical in controlling TB (110,111). Early detection follows two pathways: the patient-initiated pathway in which the patient seeks treatment and the screening pathway in which individuals with suspected TB and treatment defaulters who do not seek care are actively identified through screening (112).

The treatment of ATB combines rifampicin, isoniazid, ethambutol and pyrazinamide (113). Treatment in the initial two-month intensive phase of treatment uses rifampicin and isoniazid plus one or two other treatment options, followed by a four-month continuation phase of rifampicin and isoniazid, adding up to a total of six months of treatment. Although the treatment regimens are lengthy and complicated, they are lifesaving. In addition, combination therapy is also beneficial for the prevention of drug resistance emergence.

The treatment of ATB caused by drug-resistant strains of *M. tuberculosis* utilizes a second line of treatment that include: Fluoroquinolones (levofloxacin, moxifloxacin, ofloxacin, and gatifloxacin); injectable drugs (amikacin, kanamycin, streptomycin, and capreomycin); and oral bacteriostatic agents (ethionamide, prothionamide, cycloserine, and *p*-aminosalicylic acid). More recently approved agents include bedaquiline, delamanid, and linezolid (114). Treatment of drug-resistant TB presents challenges as treatment duration is much longer and takes up to 24 months, is more expensive, and uses more toxic drugs with more severe side effects (115).

Several types of drug-resistant TB have been identified. Multidrug-resistant TB (MDR-TB) defined as TB caused by *M. tuberculosis* strains resistant to at least both rifampicin and isoniazid. Extensively drug-resistant TB (XDR-TB) is caused by MDR-TB strains resistant to a fluoroquinolone such as moxifloxacin, levofloxacin and gatifloxacin, and one second-line injectable drug such as amikacin, kanamycin, and capreomycin. WHO recently updated the definition of XDR-TB to a disease caused by MDR-TB strains resistant to a fluoroquinolone and either linezolid or bedaquiline (116,117). Other types of resistance include mono-resistance, which

is defined as resistance to one of the first-line drugs, and poly-resistance, which is defined as resistance to more than one of the first-line drugs other than both isoniazid and rifampicin (114). Approximately 465 000 incident cases of rifampicin-resistant TB (RR-TB) were reported worldwide in 2019, of which 78% were MDR-TB (71).

The preventive measures work towards the WHO End TB strategy that aims to reduce the number of new TB cases by 90%, deaths from TB by 95%, and reduce poverty that results from TB costs by 100% by the year 2035 (3). However, given the current challenges in identifying an effective vaccine, treatment, and diagnosis, it is crucial to improve our understanding of the immune response to *M. tuberculosis* and define the parameters of a good immune response to *M. tuberculosis*.

1.1.8 TB prevention and control

The main preventive measures against TB include early diagnosis and effective treatment of TB cases, vaccination, and control of the LTBI reservoir, which is a constant source of ATB cases. Without proper targeting of the LTBI pool, ending TB is not possible.

As with other infectious diseases, vaccination presents the most efficient prevention strategy against TB. *M. bovis* Bacillus Calmette–Guérin (BCG) is the only approved vaccine against TB and one of the most widely administered vaccines worldwide. Although the vaccine protects children against disseminated forms of the disease, it demonstrates variable protection against PTB, the most common clinical presentation of the disease (118). There are also contrasting results on the protection conferred by the vaccine in adults. A 15-year follow-up study in India reported a BCG vaccine efficacy of 0% (119). After excluding the study from India, a review of prospective studies determined a vaccine efficacy ranging from 52% to 83% (120). The follow-up in these protective studies ranged from 11 to 50 years, but the findings vary widely geographically.

Besides the BCG vaccine, numerous other vaccine candidates are at various clinical trial stages (Figure 3) (121–123). These include inactivated vaccines (live attenuated vaccines and whole-cell mycobacteria), subunit/adjuvant vaccines, and recombinant vaccines. Live-attenuated vaccines aim to elicit *M. tuberculosis*-specific immune responses in the host similar to that induced

by infection but without leading to disease (124). Vaccines in this group include: MTVAC that contains all *M. tuberculosis* antigens including those in the RD1 region; VPM1002, a recombinant *M. bovis* BCG vaccine administered intradermally; and intradermal BCG revaccination using BCG and fusion proteins from TB 10.4, Ag85B. Most of the vaccines from inactivated whole-cell mycobacteria are intended for use as "therapeutic" agents either for LTBI or to reduce disease recurrence (125). These include DAR-901, a heat-inactivated non-tuberculous (NTM) vaccine; RUTI, a cell-wall fragmentation formulation produced from bacilli cultured under stress-inducing latency antigens; and MIP/ Immuvac, which is currently approved as immunotherapy and immune-prophylaxis for leprosy and is made from heat-killed *M. indicus pranii*. Subunit vaccines are classified as either viral vector vaccines or adjuvant vaccines. Viral-vector vaccines in clinical trials against *M. tuberculosis* include: Ad5Ag85A a recombinant replication-deficient human adenoviral (serotype 5) TB vaccine containing the immunodominant Ag85A, ChAdOx85A/MVA85A containing a simian adenovirus expressing the immunodominant Ag85A, and TB/FLU-04L, an attenuated replication-deficient influenza virus containing both ESAT-6 and Ag85A. Adjuvanted vaccines are administered intramuscularly and include: ID93:GLA-SE, a recombinant protein (ID93) of four *M. tuberculosis* antigens Rv1813, Rv2606, RV3619, and Rv3620 with the adjuvant GLA-SE, a synthetic TLR4 agonist, M72/ASO1E a recombinant fusion protein M72 made up of two antigens MTB32A and MTB39A with the ASO1E adjuvant system, H56:IC31 a fusion protein of three mycobacterial antigens ESAT-6, Ag85B, and Rv2660c with the IC31 adjuvant, and GamTBvac a fusion protein of two antigens AG85A, and ESAT-6-CFP10 with a dextran domain on dextran.

However, the correlates of protection in TB are largely unknown, presenting a challenge in the identification of an effective vaccine (126). Protection in *M. tuberculosis* infection may differ based on whether vaccine-induced versus natural infection-induced; in the different stages of the natural cycle of *M. tuberculosis* infection spanning from infection and progression to active disease; and in reactivation versus reinfection (126).

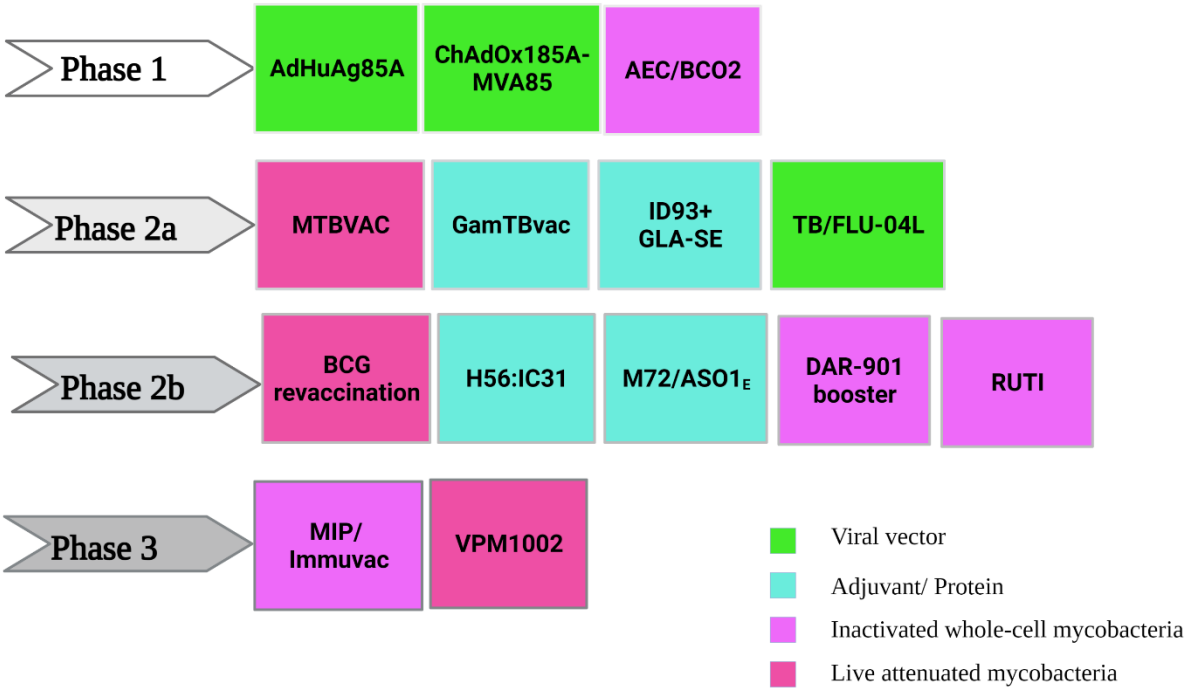

Figure 3. **TB vaccines in clinical trials**.

The pipeline shows the vaccines in phase 1 (safety and dosage), phase 2 (efficacy and side effects), and phase 3 (efficacy, effectiveness, and safety) (71). Created with BioRender.com

1.2 Human immune responses to *Mycobacterium tuberculosis*

1.2.1 Innate immune responses against *M. tuberculosis*

1.2.1.1 Uptake and recognition of *M. tuberculosis*

Once the inhaled *M. tuberculosis*-containing droplets traverse the upper respiratory tract and get deposited in the lung alveoli, one of the first interactions of the bacilli with the immune system is with the alveolar macrophages. *M. tuberculosis* is a facultative intracellular pathogen that requires intracellular localization within the phagosome for replication. Uptake of the bacilli through phagocytosis is mainly receptor-mediated, requiring surface receptors for its spread. Opsonized bacilli utilize complement receptors (CRs) and Fcγ receptors (FcγR), while non-opsonized bacilli utilize mannose receptors (MRs) and scavenger receptors (SRs) (127,128). The binding of the complement fragment C3b on the surface of *M. tuberculosis* enhances its binding to complement receptors, particularly CR1, CR3 and CR4, boosting its uptake by the macrophage. Complement receptor blockade has been shown to inhibit phagocytosis (129). The FcγRs recognize immunoglobulin G-coated *M. tuberculosis*. The uptake of opsonized bacilli benefits the host by promoting phagosome-lysosome fusion (127). Mannose receptors are expressed on tissue macrophages and monocyte-derived macrophages and bind mannose residues in the lipoarabinomannan layer of the *M. tuberculosis* cell wall, facilitating bacterial uptake into macrophages. However, uptake using these receptors inhibits the phagosome-lysosome fusion driving bacterial survival and may promote infection (130,131). The role of scavenger receptors (SR) – the macrophage receptor with collagenous (MARCO) structure, macrophage scavenger receptor 1 (MSR1), and CD36 – in the phagocytosis of *M. tuberculosis* is not well-defined. These receptors are expressed largely on monocytes and macrophages and recognize lipids. Scavenger receptor class A (SR-A) shows low expression in alveolar macrophages. In vitro studies suggest that SRs are important in phagocytosis when CRs are blocked (132).

Non-phagocytic pattern recognition receptors (PRRs) such as Toll-like receptors (TLRs), C-type lectin receptors (CLRs), and cytosolic DNA sensors are also involved in the interaction between these phagocytic cells and pathogens (Figure 4) (127,128,133). Toll-like receptors are a family of 10 receptors in humans, TLR1-TLR10. TLR1, 2, 4,5, and 6 are expressed on the cell surface, while TLR 3, 7, 8, and 9 are expressed in endosomal vesicles in the cytoplasm. Surface TLR4 and TLR2 recognize *M. tuberculosis* PAMPs with TLR2 forming heterodimers with TLR1

and TLR6 (Figure 4) (134–137). TLR4 binds lipids and glycoproteins in the bacillary cell wall and secreted proteins. Ligands for TLR2 include lipoarabinomannan, mannosylated phosphatidylinositol, lipomannan and secreted proteins, such as heat shock proteins and ESAT-6. Heterodimeric TLR2/6 and TLR1/2 bind to diacylated and triacylated lipoproteins, respectively (133,138). Ligand binding triggers a signaling cascade in which the adaptor molecule myeloid differentiation primary response 88 (MyD88) protein is recruited to the intracellular portion of the TLR. Subsequently, IL-1 receptor-associated kinases (IRAK), mitogen-activated protein (MAP) kinases, and TGF-β activated protein kinase 1 (TAK1) are recruited into the signaling cascade leading to activation of NFκB in the nucleus. This NFκB activation signaling pathway results in the gene transcription and production of IL-1β, IL-12, TNF, and nitric oxide (133).

TLR4 gets internalized into endosomes inducing a signaling cascade independent of MyD88. This cascade involves the adaptors Toll-interleukin-1 receptor containing adaptor inducing IFN-β (TRIF) and translocation chain-associated membrane (TRAM) proteins with downstream activation of interferon (IFN) regulatory factor 3 (IRF3) leading to **IFN-β** production. The ligands for the other endosomal TLRs involved in the detection of *M. tuberculosis* are single-stranded RNA (ssRNA) for TLR7 and TLR8, and CpG (5'-cytosine-phosphodiester bond-guanine-3') DNA for TLR9 (138,139). TLRs signal either through a MyD88-dependent pathway with pro-inflammatory cytokines production or through IRF7 with the production of **IFN-α** (138).

C-type lectin receptors (CLRs) are also found on the cell surface and include Macrophage-inducible C-type lectin (Mincle) and Dendritic cell-associated C-type lectin (Dectin-1). Mincle binds trehalose-6,6'-dimycolate, a glycolipid in the cell wall of *M. tuberculosis* (140), while the ligand for Dectin-1 has not been identified. CLRs signal through the Syk/CARD9 signaling pathway leading to the production of **pro-inflammatory cytokines** (138,141).

Cytosolic receptors, including nucleotide-binding oligomerization domain (NOD)-like receptors (NLRs), cyclic guanosine monophosphate–adenosine monophosphate (GMP-AMP) synthase (cGAS), and the inflammasomes that bind to muramyl dipeptide (for NLRs) and cytosolic *M. tuberculosis* DNA (for cGAS and inflammasomes) recognize *M. tuberculosis* DNA and RNA. The bacterial nucleic acids access the cytosol through ESX-1-mediated phagosomal membrane perforations. These receptors signal through the stimulator of IFN genes (STING)-TBK1-IRF3 pathway leading to the production of **IFN-β** (142–144).

It remains unclear how the simultaneous binding of multiple *M. tuberculosis* PAMPs and cellular PRRs affects the immune response. In addition, the contribution of each PRR in *M. tuberculosis* uptake and their effect on outcome is also not established.

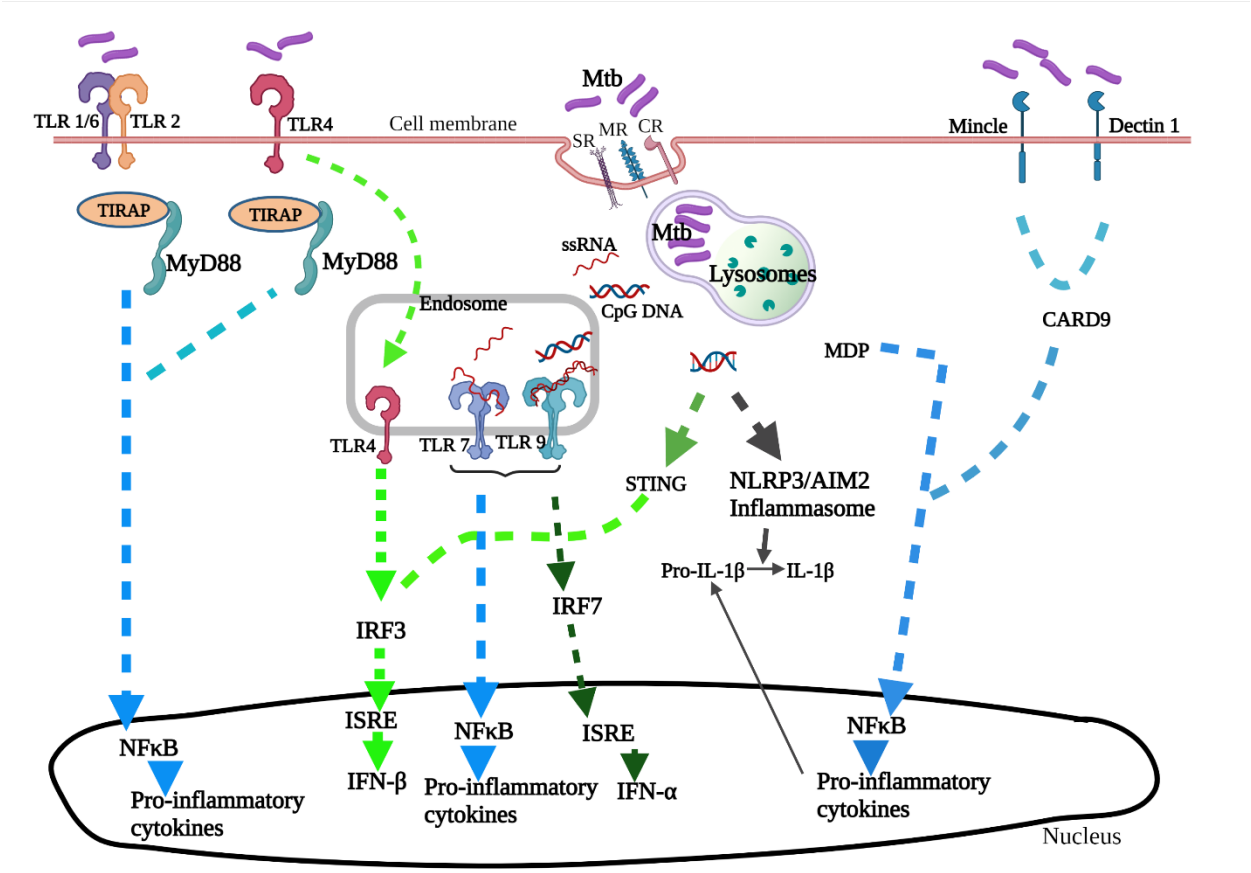

Figure 4.**Signaling pathways of pattern recognition receptors in *M. tuberculosis* infections.**
M. tuberculosis ligands bind to either TLR1/2 or to TLR6/2 or to TLR4, inducing MyD88 signaling and activating NFκB with production of **pro-inflammatory cytokines.** TLR4 binding also acts through the endosome with IRF3 secretion and downstream production of **type I IFNs**. Scavenger receptors, mannose receptors, and complement receptors bind to and phagocytose *M. tuberculosis* into the phagolysosome within which the bacilli are degraded releasing ssRNA and CpG DNA. In the endosome, ssRNA and CpG DNA are recognized by TLR7 and TLR9 respectively, activating NFκB with the production of **pro-inflammatory cytokines,** and through IRF7 with the production of **IFN-α**. C-type receptors, Mincle and Dectin 1 recognize *M. tuberculosis* ligands leading to CARD-mediated activation of NFκB with the production of **pro-inflammatory cytokines**. Mycobacterial DNA in the cytosol act on IRF3 through cGAS/STRING pathway, inducing **IFN-β** production. The DNA also activates the NLRP3/AIM2 inflammasome, which drives the maturation of IL-1β (138,145). Created with BioRender.com

1.2.1.2 Phagocytosis

In macrophages, the recognition of *M. tuberculosis* PAMPs by PRRs initiates the bacillary engulfment by the macrophage plasma membrane. *M. tuberculosis* gets internalized into a phagosome which fuses with an endosome to form a phagolysosome. The phagolysosome is the compartment within which *M. tuberculosis* gets degraded. The fusion of the two vesicles leads to the release of lysosomal hydrolases and the synthesis of reactive oxygen intermediates, which acidify the phagosome. However, *M. tuberculosis* can inhibit this fusion via the production of numerous bacterial proteins that allow its survival. Phagocytosis also initiates cytokines and chemokines production through the recognition of ssRNA and CpG DNA by TLR7 and TLR9, resulting in NFκB-mediated production of pro-inflammatory cytokines (Figure 4) (128,138). Chemokines recruit other immune cells to the infection site forming a layer around a center core of macrophages with ingested dormant *M. tuberculosis* to form a granuloma in the lung.

1.2.1.3 The granuloma

The granuloma consists of multiple immune cell types (Figure 5). Macrophages are central to this formation that involves different macrophage phenotypes such as foamy macrophages, epithelioid histiocytes, and Langerhans' cells (146–148). Foamy macrophages are macrophages loaded with lipids that are thought to provide nutrition for the bacterium that undergoes changes to utilize fatty acids within the granuloma (149). Histiocytes are macrophages located within granuloma in which they resemble epithelioid cells hence the name epithelioid histiocytes. Macrophages also fuse to form multinucleated giant cells known as Langerhan's cells (150,151). Other cells recruited to this forming structure include neutrophils, natural killer (NK) cells, dendritic cells (DCs), CD4+ T cells, CD8+ T cells, and B cells (147,152).

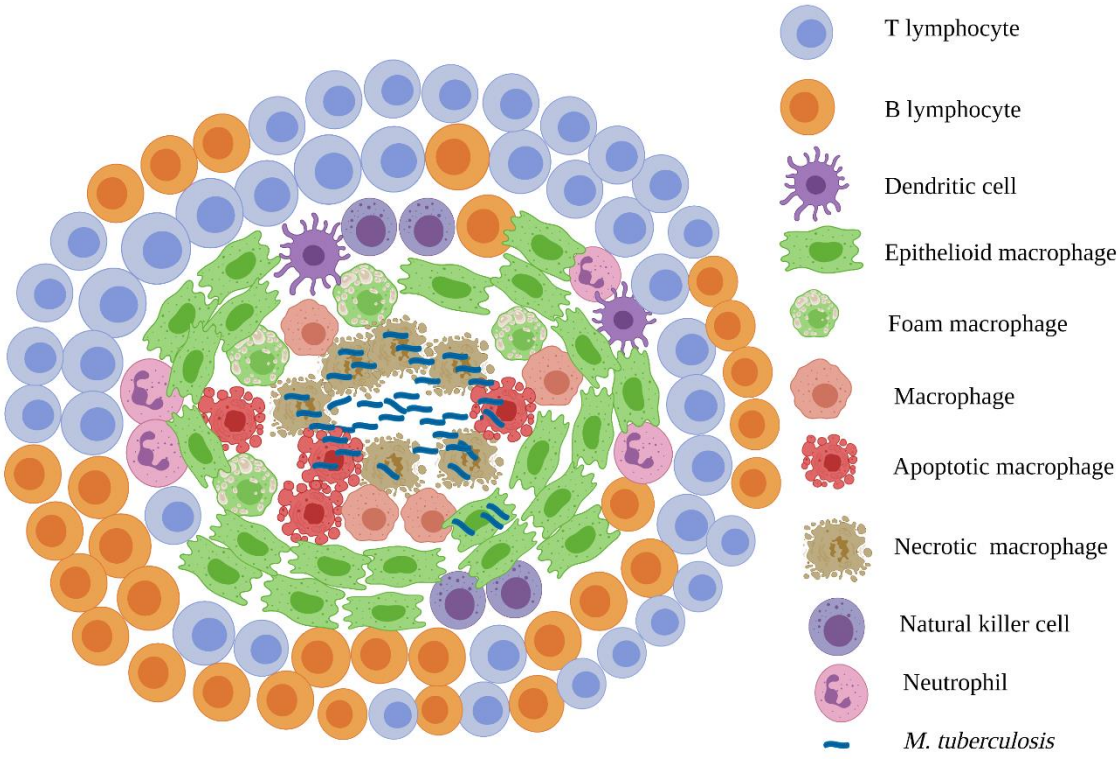

Figure 5. **The basic structure of the tuberculous granuloma.**

The basic tuberculous granuloma consists of multi-layers of immune cells surrounding a central area of free *M. tuberculosis* and necrotic macrophages containing *M. tuberculosis*. The layer of dead or dying macrophages is surrounded by different types of transformed macrophages such as epithelioid macrophages with interlinked cell membranes, Langerhans' cells which are multinucleated giant cells, or foamy macrophages that contain lipids. Other immune cells include dendritic cells, neutrophils, and an outer layer of T and B lymphocytes (153). Created with BioRender.com

Three types of granulomas have been described. The solid granuloma is a feature of LTBI containing a low bacillary load. The bacilli in this granuloma are either non-replicating or replicating at a low rate, reducing their metabolic activity and leading to dormancy (154,155). The necrotic granuloma is a feature of early ATB. This granuloma retains the outer structure, but the hypoxia in the central area leads to cellular necrosis. The bacilli remain viable and, in the presence of adequate oxygen and nutrients, can be resuscitated. The third type, caseous granulomas, is present in severe TB. The material in the central area undergoes caseous necrosis forming a cheese-like material that then liquifies. The liquefied necrotic material may be expelled into the bronchus

or blood vessel, leaving a cavity and disseminating infection. The caseous material also provides nutrients to the *M. tuberculosis* bacilli, while the presence of the cavitary lesions allows for oxygenation leading to bacterial replication (154). The process by which the granuloma develops is not well established (156). For a long time, the granuloma was viewed as a protective structure, "walling off" dormant bacteria within macrophages, therefore, containing and limiting the growth of *M. tuberculosis* and its spread to immune-privileged sites such as the brain (157). However, it also provides a niche where the bacteria survive and can disseminate in the event of TB reactivation (151). The formation of a granuloma may therefore signify an adequate protective immune response to *M. tuberculosis* infection. The production of Th1 cytokines by T lymphocytes induced by *M. tuberculosis* antigens sustains the granuloma. These cytokines also activate the phagocytic cells, induce the antimicrobial activity of the macrophages, and induce inflammation. If the antimicrobial activity is adequate, there is a reduction in the size of the granuloma and its cellular "wall", and, where inadequate, the granuloma becomes a source of infection to other parts of the body and dissemination to the air (154,155).

1.2.2 Cellular components of the innate immune response against *M. tuberculosis*

1.2.2.1 Macrophages

Within inactivated macrophages, bacilli block the fusion of the phagosome with the lysosome preventing exposure to the bactericidal effects of the phagolysosome, which include reactive oxygen intermediates (ROIs), reactive nitrogen intermediates (RNIs), and low pH (127). Macrophages also present *M. tuberculosis* antigens to T helper cells (Th0) using MHC class II molecules, leading to the production of cytokines such as IL-12, IL-1, and TNF. However, when the *M. tuberculosis* bacilli escape from the phagosome or when its antigens are translocated to the cytosol, these antigens are recognized by CD8+ T cells when presented in association with MHC class 1 molecules (43). Macrophage activation is induced by IFN-γ, produced in early infection by NK cells or in the adaptive response by CD4+ T cells and CD8+ T cells. Macrophages activated by IFN-γ are known as classically activated or M1 macrophages which are essential for the control of *M. tuberculosis* (158,159). Activation by IFN-γ produces phagocytic cells with the ability to produce high levels of reactive oxygen intermediates (ROIs), reactive nitrogen intermediates (RNIs), inducible nitric oxide synthase (iNOS), antimicrobial peptides, pro-inflammatory

cytokines (IL-1β, TNF-α, IL-6, and IL-12) and chemokines. These cells also demonstrate increased capacity to act as antigen-presenting cells (160)]. They induce Th17 lymphocyte expansion with increased release of IL-17 capable of recruiting neutrophils. M1 macrophages also up-regulate the expression of suppressor of cytokine signaling 3 (SOCS3), a negative regulator of type I IFN signaling.

M2 or alternatively activated macrophages are induced by IL-4 and IL-13 and express scavenger receptors and mannose receptors (158). These cells perform an anti-inflammatory role and produce IL-10 and transforming growth factor-beta (TGF-β) (161). In a murine model of *M. tuberculosis* infection, M2 macrophages increase in chronic infection and are associated with bacterial persistence (162,163). In vitro modeling of the granuloma in tuberculosis showed M1 macrophages predominating in the early granuloma formation stage and transforming to the M2 phenotype in the later stages of formation, resulting in an M2 phenotype predominance (164).

Macrophage polarization is related to the macrophage scavenger receptor, SR-A, also known as macrophage scavenger receptor 1 (MSR1) or CD204. In an *M. tuberculosis* infection murine model, this receptor inhibits polarization to the M1 phenotype while driving the M2 anti-inflammatory phenotype (165). M1 macrophages drive the granuloma formation, whereas M2 macrophages inhibit the formation of the same. Recent in vitro studies have also demonstrated a role for type I IFNs in regulating macrophage polarization in *M. tuberculosis* infection. In mice, type I IFNs, in the absence of IFN-γ, maintain macrophages in the M1 phenotype and therefore play a protective role (166,167).

Various mechanisms by which *M. tuberculosis* hijacks the immune system and counteracts the innate immune response have been described. The *M. tuberculosis* bacillus has developed the ability to obstruct the mycobactericidal function of macrophages by preventing phagosome maturation, blocking the fusion of the phagosome with lysosomes, and preventing the acidification of the phagosome. Virulent strains of *M. tuberculosis* also prevent eradication by inhibiting macrophage apoptosis and driving cellular necrosis resulting in evasion of the host defenses and dissemination (168–170).

1.2.2.2 Other innate immune cells against *M. tuberculosis*

Airway epithelial cells (AECs) form the largest cell population in the lungs, but their role in *M. tuberculosis* infection is not well defined. In in vitro models of *M. tuberculosis* infection, primary bronchial epithelial cells are unresponsive to infection, whereas alveolar epithelial cells are susceptible (171,172). These cells participate in the recognition and internalization of *M. tuberculosis*, induction of cytokines and chemokine production, production of antimicrobial peptides such as β-defensins and LL-37, and interaction with other immune cells, including alveolar macrophages and neutrophils (171,173,174). A study of *M. tuberculosis* infected A549 cells, a cell line from human type II AEC carcinoma cells, revealed a bacterial transcriptome that favored bacillary replication and dissemination distinct from that in the macrophage which favored transition to a dormant state (175). This suggests *M. tuberculosis* uses AECs as a niche for replication and evasion of the innate immune response. AECs are the main source of IFN-lambda (IFN-λ) which shows crosstalk with IFN-α/β in viral infections (176). Type I IFNs have been shown to inhibit the growth of AECs in culture, although in a mouse model of pneumococcal pneumonia they are protective for AECs (177,178). The role of these cells in shaping the alveolar microenvironment in *M. tuberculosis* infection remains an understudied area.

Dendritic cells (DCs) also phagocytose *M. tuberculosis* with high efficacy. Resident immature DCs in the alveoli phagocytose the bacilli leading to DC maturation with enhanced surface expression of MHC class I molecules and T cell co-stimulatory molecules- CD80, CD86, and CD40 (179,180). As DCs mature, their phagocytic function declines while their antigen presentation function increases. Mature DCs migrate to secondary draining LNs and present antigens to naïve T cells in association with either MHC class I or class II molecules (181,182). Therefore, DCs act as a link between the innate and the adaptive immune responses to *M. tuberculosis* infection. However, *M. tuberculosis* can evade the function of the DCs and demonstrates the ability to sabotage the maturation of DCs, both phenotypically and functionally, in their activation of naïve T cells, thereby inhibiting the capacity of the DCs to control the infection (183).

The role of neutrophils in TB is not well-defined. Neutrophils recruitment to the site of infection is an early event resulting in phagocytosis of *M. tuberculosis* (184). Uptake of the bacteria activates the mycobactericidal activity in neutrophils with degranulation, production of reactive

oxygen intermediates (ROIs), and neutrophil extracellular traps (NETs) formation thought to provide a hidden niche for *M. tuberculosis* growth extracellularly (185). This activity appears to be driven by TNF-α and not by IFN-γ, as seen in macrophages (186,187). In *M. tuberculosis*-infected mice, type I IFN signaling in neutrophils has been shown to enhance NETosis and induce neutrophil necrosis resulting in uncontrolled growth of the bacteria and promoting disease progression (188). In addition, a neutrophil-driven IFN-inducible blood transcriptional profile has been identified in ATB patients (189).

Natural killer cells recognize *M. tuberculosis* cell wall components through TLR2 and other NK receptors leading to the release of IFN-γ and IL-22, increasing the bactericidal activity of infected phagocytic cells and enhancing the cytotoxic function of infected cells. Through the production of granulysin and perforin, NK cells can kill extracellular bacilli. In *M. tuberculosis*-infected *Rag1*$^{-}$ deficient mice, which lack T- and B-cells, NK cells become the predominant IFN-γ-producing cells, which may be of significance in T cell dysfunction in HIV. NK cells are also involved in regulating CD8 T cells responses to *M. tuberculosis* and their ability to lyse infected macrophages (190–192).

Innate T lymphocytes, the invariant natural killer T (iNKT) cells, Mucosal-associated invariant T (MAIT), and gamma-delta (γδ) T cells are also components of the innate response against *M. tuberculosis*. iNKT cells are a subset of T cells that is a component of the innate immune response and forms a link between innate and adaptive immunity. iNKT cells are activated by *M. tuberculosis*-infected macrophages expressing CD1d alongside IL-12/ IL-8. Stimulation of the T-cell receptor (TCR) of iNKT cells induces the production of pro-inflammatory cytokines, IFN-γ and TNF-α, cytokines that are protective against *M. tuberculosis* infection (193,194). MAIT cells are predominantly CD8+ T cells that detect *M. tuberculosis* through an MHC-like molecule, the MHC-related protein 1 (MR1) and are activated by metabolic derivatives such as riboflavin and IL-12/IL-18 (195–197). Studies investigating MAIT cell functions in the different *M. tuberculosis* infection states show contrasting findings. Some studies observed a lower frequency of MAIT cells in TB patients compared to LTBI and healthy individuals (198–200), whereas others observed similar frequencies in TB, LTBI, and healthy controls (201). MAIT cells are involved in cytotoxic activity in *M. tuberculosis* infection through the production of granulysin, IFN-γ and TNF-α (195,202). γδ T cells recognize *M. tuberculosis*-derived phosphoantigens independent of MHC

(203,204). γδ cells are also cytotoxic through the production of granulysin and perforin and induce the production of IFN-γ and TNF-α in non-severe TB resulting in inhibition of bacillary growth. The cells also induce the production of IL-10 in severe TB, an immunoregulatory cytokine that may reverse their protective roles (195,204). γδ T cell frequencies are reduced in patients with severe TB pathology compared to LTBI and healthy donors.

Taken together, both conventional and non-conventional innate immune cells play a role in the immune response to *M. tuberculosis* infection. In some cases, the innate response is sufficient to contain bacterial growth and stop a productive infection before inducing the adaptive immune response. However, if a productive infection is not curtailed, persistent bacterial replication leads to the induction of adaptive responses.

1.2.3 Components of the adaptive immune responses against *M. tuberculosis*

1.2.3.1 T cells against *M. tuberculosis* infection

The interaction between *M. tuberculosis* and T lymphocytes starts when the bacteria reach the antigen-presenting cells in mediastinal lymph nodes (205). Within the lymph nodes, DCs containing bacteria present the bacterial antigens and prime naïve T cells. Macrophages and DCs activate T cells through the action of secreted IL-12 and IL-18. Activated CD4+ T lymphocytes, CD8+T cells and γδ T cells produce IFN-γ, which is required for phagosome maturation (206–208). The absence of both CD4+ T cells and CD8+ T cells, therefore, increases susceptibility to *M. tuberculosis* infection and progression to disease. In the mouse model of infection, the development of TB occurred earlier with CD4+ T cell depletion and later with CD8+ T cell depletion (209).

Subsets of CD4+ T cells such as Th17 cells, T regulatory cells (Tregs), and T follicular helper (Tfh) cells are also involved in the immune response to *M. tuberculosis*. Th17 cells produce IL-17 that drives the production of the pro-inflammatory cytokines IL-6 and G-CSF, and the chemokines CXCL9, CXCL10, and CXCL11 that drive the recruitment of neutrophils involved in the development of the granuloma and cells producing IFN-γ. The production of excessive amounts of IL-17 implicates these cells in neutrophil-associated inflammation and tissue damage (210–212). T regulatory cells (Tregs) are involved in immune homeostasis and regulate the balance

between the pro-and anti-inflammatory responses in *M. tuberculosis* infection (213). Peripheral blood mononuclear cells (PBMCs) from ATB patients have a higher Tregs frequency than LTBI or healthy controls (210,214). In addition, pulmonary TB patients have a lower frequency of T follicular helper than individuals with LTBI (215). In *M. tuberculosis*-infected mice, the reduced frequency of Tfh cells results in a loss of IL-21 signaling associated with lower production of IFN-γ and TNF-α and increased expression of T cell inhibitory molecules, increasing susceptibility to infection (216). *M. tuberculosis* antigen recognition by CD8+ T cells is in association with MHC class I. CD8+ T cells are involved in the control of *M. tuberculosis* through the production of IFN-γ, IL-2, and TNF-α and through the cytotoxic effects of granulysin and perforin (217,218). However, CD8+ T cells also produce IL-10 and TGF-β, which drive infection. T cell subsets play different roles in *M. tuberculosis* infection, some resulting in protection against infection while others lead to increased pathology. The balance between the cellular frequencies and cytokine profile may therefore determine infection outcome.

1.2.3.2 B cells and antibodies against *M. tuberculosis* infection

The presence of B cells in the granuloma, as shown in Figure 5, suggests that B cells participate in the immune response against *M. tuberculosis*, a role that is not fully understood. *M. tuberculosis* antigens activate naïve B cells, which develop into plasma cells that produce antibodies (219). B cells also present antigens to CD4+ T cells leading to their activation (220). For a long time, the perceived concept that intracellular pathogens require cell-mediated immunity for clearance while extracellular pathogens require humoral immunity has been upheld (221). Due to this property of *M. tuberculosis* as a facultative intracellular organism, most immunology research in TB was focused on the cell-mediated immune response. This resulted in the role of antibodies in *M. tuberculosis* remaining largely understudied (222). However, studies in murine models of *M. tuberculosis* infection have revealed that antibodies play an immune-modulatory and a protective role in TB (221,223–225). Mice treated with monoclonal antibodies to either the capsular *M. tuberculosis* antigen, arabinomannan, or to a glycolipid found in the cell wall, lipoarabinomannan, showed reduced bacterial burden and improved survival linked to enhanced cellular immune response (224,225). The protection conferred by monoclonal antibodies against *M. tuberculosis* is thought to occur through four mechanisms: monoclonal antibodies enhance antigen presentation that drives cell-mediated immunity; antibodies also bind extracellular bacteria

preventing cell entry; antibody-dependent cellular cytotoxicity (ADCC) eliminates both infected cells and bacteria; antibody-dependent cellular phagocytosis increases bacterial killing (226).

In humans, an antibody-profiling study revealed differences in the humoral response between LTBI and ATB (227). In this study, antibody responses in LTBI were associated with activation of the inflammasome, maturation of the phagolysosome, and enhanced ability of macrophages to kill the pathogen (227). It is hypothesized that the induction of antibody responses are essential in vaccine-induced protection against pathogens (228). However, the immune responses targeted by vaccines in development against *M. tuberculosis* have mainly focused on cell-mediated immunity. In a study using the TB vaccine candidate MVA85A (Modified Vaccinia virus Ankara expressing Ag85A from *M. tuberculosis*) in infants vaccinated with BCG in the Western Cape province in South Africa, no additional protection was noted despite induction of Ag85-specific T-cell response (229,230). However, post hoc data analysis revealed an association between the presence of Ag85A-specific IgG antibodies and a reduction in the risk for TB on day 28 post-vaccination (231). A better understanding of the function of B cells and antibodies in *M. tuberculosis* infection is necessary. Gene profiling studies revealed that the expression of the *FCGR1A* gene that encodes the FcγR1 is significantly increased in ATB compared to LTBI and healthy control (232–234).

1.2.4 Cytokine and chemokine responses in *M. tuberculosis* infection

The immune response to *M. tuberculosis* infection is complex and involves both pro-inflammatory and anti-inflammatory cytokines. The pro-inflammatory response is required for the control of infection, while the anti-inflammatory response prevents excessive pathology at the site of infection (235).

1.2.4.1 Tumor necrosis factor-alpha (TNF-α)

Initial interaction between *M. tuberculosis* and the immune system leads to the production of TNF-α. Although macrophages are the primary sources of this pro-inflammatory cytokine, TNF-α, other cells, such as lymphocytes, fibroblasts, endothelial cells and mast cells, also secrete this cytokine on activation (236).

TNF-α is essential in the formation of granuloma. Mouse models of TB with TNF-α deficiency fail to form granulomas even with the trafficking of inflammatory cells to the site of infection (237–239). The TNF-α deficient mice also demonstrate increased susceptibility to TB, increased bacterial burden and lower survival rates. In vivo TNF-α plays a role in *M. tuberculosis*-infected mice in induction and maintenance of the granuloma in the presence of type 1 cytokines – IL-1α, IFN-γ, and inducible nitric oxide synthase (iNOS) (240). TNF-α is also required in the maintenance of the granuloma and induces the expression of CXCL10, CCL2, CCL5, and CCL9 chemokines that aid in T cell recruitment necessary for granuloma formation (241–243). Neutralization of phagocytosis and phagocytic killing activity TNF-α in a murine model of LTBI resulted in a lower granuloma formation and reactivation of TB (244). Clinical studies also support these findings showing reactivation of LTBI in patients with autoimmune disorders and chronic diseases receiving treatment with anti-TNF-α agents such as the monoclonal antibodies (adalimumab, infliximab, and certolizumab) or the soluble TNF receptor (etanercept) (245–247). Monoclonal antibodies show a higher risk of reactivation than etanercept (247). Therapy with anti-TNF-α increases the relative risk for TB reactivation 1.6-25.1 times (245). In *M. tuberculosis* infection, TNF-α also acts on macrophages enhancing the killing activity and inducing cellular apoptosis (248). Apoptosis has a protective role in infection by destroying the bacterial intracellular niche. However, not all the effects of TNF-α are beneficial. In progressive disease, excessive production of TNF-α leads to tissue damage and necrosis, resulting in disseminated infection (249). The induction of TNF-α differs between *M. tuberculosis* strains in infected mice and monocyte-derived macrophages (26,250).

1.2.4.2 Interleukin 12 (IL-12)

Interleukin 12 is a family made up of several heterodimeric cytokines that are members of the IL-6 superfamily. These include IL-12p70 made up of the subunits p35 and p40, IL-23 made up of the subunits p19 and p40, IL-27 composed of the IL-27 p28 and the Epstein-Barr virus-induced molecule 3, and IL-35 made up of the p35 subunit and EBI-3 (251). The p40 subunit is shared by IL12-p70 and IL-23. In *M. tuberculosis*, IL-12 is produced by monocytes/ macrophages, DCs and B cells and acts as a link between innate and adaptive immunity, and is essential in reducing the bacillary burden during infection (252). In vivo *M. tuberculosis*-infected mouse model, the presence of IL-12 reduced the bacterial burden while its blockade with antibodies

increased bacterial load (253,254). IL-12 is also involved in granuloma formation. Granulomas in *M. tuberculosis*-infected mice treated with anti-IL-12 antibodies were poorly formed and diffuse, whereas those in IL-12-treated mice were well-formed (254,255). In *M. tuberculosis* infection, the migration of DCs requires IL-12p40 (256). IL-12 treatment of mice also induces and maintains the production of IFN-γ from CD4 T cells but not from NK cells (254). Continuous production of IL-12p40 is required for antimycobacterial immune responses, including the maintenance of the granuloma, induction and maintenance of Th1 responses, activation and expansion of CD4+ T cells and cellular effector function (257).

1.2.4.3 IL-18

IL-18 is a macrophage and DC-derived cytokine that induces NK cell activation and the production of IFN-γ driving a Th1 immune response. Although the IL-18 receptor (IL-18R) shares the MyD88 signaling pathway with IL-1R, studies in a MyD88-deficient mouse model of *M. tuberculosis* infection demonstrated the importance of IL-1R in protection while IL-18R was not crucial for protection (258). Studies in IL-18 knock-out mice show a high susceptibility to *M. tuberculosis* infection similar to that observed in MyD88 knock-out mice and IL-1β/IL-18 double deficiency mice (259).

1.2.4.4 IL-10

IL-10 is one of the members of the IL-10 family. This cytokine is produced by macrophages, neutrophils, some subsets of DCs, Th1, Th2 and Th17 cells, and B cells (260). In macrophages, *M. tuberculosis* induces the production of IL-10 through the TLR2-dependent extracellular signal-regulated kinase (TLR2-ERK) and the PI3K/AKT signaling pathways (261,262). In addition, induction of IL-10 by IFNα/β has also been demonstrated in *M. tuberculosis*-infected macrophages (263). IL-10 is an anti-inflammatory cytokine that counters the effect of pro-inflammatory cytokines (IFN-γ, IL-12, and TNF-α), thereby preventing damage to tissues (264). Although impaired IL-10 production in acute infection is beneficial for pathogen clearance, prolonged deficiency of IL-10 would result in an unbalanced and exaggerated pro-inflammatory response causing immune-mediated pathology and damage to tissues.

1.2.4.5 IL-1α and IL-1β

IL-1α and IL-1β are members of the IL-1 family comprising 11 cytokines with pro-and anti-inflammatory functions (265). Cellular sources of IL-1 include mononuclear phagocytes, T and B lymphocytes, fibroblasts and keratinocytes (266). IL-1α is a cytokine with dual functionality and binds to its cell membrane receptor, inducing signal transduction. In contrast, when located in the nucleus, it functions as a transcription factor for pro-inflammatory cytokines such as IL-8 (267). In IL-1α or IL-1β antibody-depleted wild-type mice, increased susceptibility to *M. tuberculosis* appears to be linked to IL-1α, not IL-1β (268). IL-1α-and IL-1 β-deficient mice also show increased susceptibility to infection compared to wild-type mice (269,270).

1.2.4.6 Chemokines

Chemokines play both protective and detrimental roles in *M. tuberculosis* infection. In LTBI, chemokines are involved in recruiting cells to the site of infection and in granuloma development and maintenance (271,272). However, in excessive amounts of some cytokines, the increased cellular infiltration, particularly with monocytes and neutrophils, may drive pathology (273,274). In a murine model of *M. tuberculosis* infection, upregulation of chemokines involved in cell recruitment to the lungs early in infection was observed. These included CCL3 (Macrophage inflammatory protein 1-alpha), CCL4 (Macrophage inflammatory protein-1β), CCL5 (Regulated on Activation, Normal T Expressed and Secreted-RANTES), CCL8 (Monocyte chemoattractant protein 2), CXCL9, CXCL10 (Interferon gamma-induced protein 10 [IP-10] or small-inducible cytokine B10), and CXCL11 (274,275). The levels of some of these chemokines (CCL3, CXCL9, and CXCL11), as well as of CCL1, CXCL1, and CXCL2, are elevated in the plasma of pulmonary TB patients (276). CXCL9 and CXCL10 have been identified as potential biomarkers that differentiate ATB from LTBI and decline with anti-tuberculous therapy (277–279). In addition, CXCL11, CXCL2, CCL1 and CCL2 (monocyte chemoattractant protein 1) have also shown potential for use in treatment monitoring (276).

In summary, despite these seemingly effective immune responses, *M. tuberculosis* remains one of the most successful pathogens in causing human disease. The immune response against *M. tuberculosis* is a complex interaction of multiple players that are not entirely understood. The pro-inflammatory responses associated with the production of IFN-γ, IL-12 and TNF-α aim to control infection, while the anti-inflammatory responses aim to prevent uncontrollable pathology. The

outcome of infection is, therefore, a result of the maintenance or disruption of this balance. (235,280). Studies in mice revealed the production of type I IFNs in response to *M. tuberculosis* infection with induction of high levels of the IFN in infection with hypervirulent strains of the bacilli (26,33).

1.2.5 Interferons in *M. tuberculosis* infection

The word "interferons" was coined from the viral "interference" observed in the presence of these substances (281). The classification of interferons is based on the cell surface receptor they bind to and signal through. Type I IFNs comprise 13 IFN-α subtypes, IFN-β, IFN-κ, -ε, and IFN-ω that bind to the IFN-α receptor (IFNAR) (282,283) (described in section 1.3). Type II IFN (IFN-γ) binds to the IFN-γ receptor (IFNGR) (284), and type III IFNs-IFN-λ1, IFN-λ2 and IFN-λ3- through a receptor composed of the IFN-lambda receptor (IFNLR1) and IL-10R2 subunit (285,286).

1.2.5.1 Interferon gamma (IFN-γ)

In *M. tuberculosis* infection, the production of IFN-γ by innate immune cells results in pro-inflammatory responses. The increased susceptibility to mycobacterial diseases in patients with Mendelian Susceptibility to Mycobacterial Disease (MSMD) supports the importance of IFN-γ in TB. MSMD is a primary immunodeficiency disease characterized by multiple mutations, including IFN-γR deficiency (287,288). In the innate immune phase, IFN-γ activates phagocytes resulting in the killing of intracellular bacteria, but in its absence, lysosome-phagosome fusion is inhibited, and there is minimal production of ROIs and RNIs. In a mouse model of *M. tuberculosis* infection, macrophages treated with IFN-γ alone showed higher inducible NO synthase 2 (*Nos2*) mRNA expression and NO production, whereas when treated with IFN-γ and IFN-β together, a significant reduction in NO production was observed (166). Nevertheless, the production of IFN-γ in the innate immune response may be inadequate to control infection. In most cases, IFN-γ is required together with *M. tuberculosis* antigen-specific T cells to control TB (289). IFN- γ also functions alongside IL-1, IL-6, and TNF-α to control *M. tuberculosis* infection.

1.2.5.2 Interferon lambda (IFN-λ)

IFN-λ, the newest addition to the IFN family, was first described in 2003 (285,286). The effects of IFN-λ in infection are not well characterized and are thought to result from their overlapping function with IFN-α/β (290). Unlike the ubiquitous production of IFN-α/β, IFN-λ is produced at mucosal surfaces, and its receptor is found mainly in epithelial surface barriers such as the respiratory tract. Its effects are, therefore, more specific to epithelial surfaces. In *M. tuberculosis* infection, higher levels of IFN-λ2 have been detected in the sputum of active PTB patients compared to healthy controls (291). Studies on *M. tuberculosis*-infected cynomolgus macaques observed the expression of IFN-λ in normal lung tissue and tuberculous granuloma (292). A study of macrophages from cynomolgus macaques observed differences in the expression of IFN stimulated genes (ISGs) induced by IFN-λ and IFN-α/β, with most genes upregulated after IFN-α/β stimulation. The study also observed differences between responses to stimulation with different IFN-λ subtypes with more genes upregulated after IFN-λ1 stimulation compared to IFN-λ4 stimulation which had negligible effects (293). IFN-λ1 stimulation upregulated the expression of pro-inflammatory genes such as TLR1, IL-1β, IL-8, and BATF while IFN-α/β downregulated TLR1and IL-1β genes. *M. tuberculosis*-infected A549 lung epithelial cells also express IFN-λ (294). Although the function of IFN-λs more closely resembles that of type I IFNs, their structure resembles that of IL-10 and its related cytokines (285,286). The impact of these similarities to cytokines that play a role in the pathogenesis of *M. tuberculosis* has not been defined.

1.3 Type I Interferons

Type I IFNs are a family of cytokines encoded by multiple genes (283). They induce a wide range of effects on immune cells during infection. Although type I IFNs are best characterized for their role in viral infections, they are also involved in the immune response to bacterial, fungal, and parasitic infections (295–300). IFN-α and IFN-β are the best-characterized type I IFNs.

1.3.1 IFN-α/β

In 1957, Isaacs and Lindenmann first described the antiviral function of IFN-α/β (281). In humans, IFN-α consists of 13 subtypes - IFN-α1, α2, α4, α5, α6, α7, α8, α10, α13, α14, α16, α17, and α21- that are encoded by multiple genes while IFN-β is encoded by a single gene, all located

on chromosome 9 (283). Plasmacytoid DCs (pDCs) and hematopoietic cells, primarily leukocytes, are the primary producers of IFN-α, while nucleated cells, DCs, epithelial cells and fibroblasts are the primary producers of IFN-β (301). In viral infections, pDCs produce about 1000-fold more IFN-α/β than the other cell types (302). All type I IFNs bind to the same receptor, the IFNAR, a heterodimeric structure consisting of the transmembrane proteins IFNAR1 and IFNAR2, expressed ubiquitously; therefore, type I IFNs act on almost all cells. The receptor has conserved residues that serve as "anchor" points necessary for binding these IFNs. However, differences have been observed within these binding sites that confer specificity in binding and function (303). The affinity of the IFNs for the receptor also varies. IFN-β has a 20 to 30-fold higher affinity for the IFNAR1 and IFNAR2 subunits and a slower dissociation rate than IFN-α subtypes that demonstrate different affinities to the IFNAR subunits. This results in prolonged effects of IFN-β and is associated with a reduction of ubiquitin-specific protease-18 (USP18)-mediated negative feedback regulation of IFN signaling (304,305). The binding affinity also strongly correlates with the antiproliferative activity of these IFNs on immune cells, which is regulated by the expression of the IFNAR (305–308).

Studies in mouse fibroblasts demonstrate a hierarchical production of IFN-α and IFN-β (309,310). Low circulating levels of IFN-β are detected in non-inflammatory states; in influenza A virus infection, these low circulating levels prime the immune cells leading to a more rapid immune response early in infection (311,312). In a mouse model of HSV-2, the production of type I IFNs was observed in two waves with IFN-β produced first post-infection, binding to IFNAR and inducing the second wave of both IFN-α and IFN-β (313,314). Therefore, IFN-β regulates the type I IFN signaling pathway and the subsequent production of IFN-α (309,311). In vitro studies using cell lines have also demonstrated the preferential induction of type I IFNs by IFN regulatory factors (IRFs). All cell types constitutively express IRF3, which preferentially activates the *IFN-A1* and *IFN-B* genes. In contrast, IRF7, induced through the IFN signaling pathways and encoded by an ISG, activates several *IFN-A* genes. Furthermore, since IRF3 is constitutively expressed, the induction of IFN-β following PRR activation occurs earlier than that of IFN-α (315).

1.3.2 Type I IFN induction in *M. tuberculosis* infection

M. tuberculosis is an intracellular bacterium that localizes within the phagolysosome of phagocytic cells. Like other intracellular pathogens such as *Listeria monocytogenes* that also

occupy an intracellular vacuole (316), this location provides a niche within which the bacteria evades the immune system and its effectors, enabling bacterial survival and replication (317,318). In vitro studies of *L. monocytogenes* infection of primary bone-marrow-derived macrophages observed that the presence of bacterial products in the cytosol induced type I IFNs production (317). Similarly, bacterial translocation into the cytosol was also observed in *M. tuberculosis*-infected human monocyte-derived DCs and macrophages and murine macrophages; only a proportion of the bacilli get translocated to the cytosol in macrophages, with most remaining within the phagolysosome (43,319). Studies on murine macrophages show that the TLR2-MyD88 signaling pathway confines the bacilli inside the phagolysosome. Therefore, bacillary interference with this signaling pathway allows for its translocation to the cytosol (319).

Translocation is dependent on ESAT-6 and CFP-10, proteins that play a role in the virulence of this pathogen and are essential for its release from infected cells and spread to adjacent cells (320). Virulent *M. tuberculosis* strains also possess an active type VII secretion system, ESX-1 secretion system, through which the bacterial proteins ESAT-6 and CFP-10 get secreted. Two potential theories have been proposed in driving *M. tuberculosis* translocation: 1) ESAT-6 secreted through the ESX-1 secretion system has pore-forming activity and causes lysis of the phagosome membrane leading to translocation (321), and 2) ESX-1 mediates cell lysis by causing membrane disruptions at points of contact with the bacteria allowing for the translocation of the bacterial products of the phagosome to the cytoplasm (41,142,322). Both ESX-1-dependent and -independent mechanisms of type I IFN induction have been described. Induction of IFN-β requires a functional ESX-1 secretion system and *M. tuberculosis* translocation (41–43,319,323). However, the full extent of the importance of ESX-1 in the induction of IFN-α/β production is not fully understood. The *M. bovis* BCG strain, although it does not possess the ESX-1, also induces type I IFN, albeit to a lesser extent than that by virulent strains of *M. tuberculosis* (324).

M. tuberculosis is also known to passively induce IFN-α/β production independent of ESX-1 through secretion of type I IFN-inducing molecules. These include double-stranded DNA (dsDNA) and cyclic-di-AMP (c-di-AMP), a second messenger (324) recognized by cytosolic PRRs such as cyclic GMP-AMP synthase (cGAS) (143) and AIM2 (325), resulting in activation of STING which complexes with the TANK (TRAF-associated NFκB activator) -binding kinase (TBK-1) (142,144). The complex formed is involved in the activation of IRF3 and IRF5, resulting

in the production of IFN-β in both humans (326) and mice (327,328). Some of the PRRs that interact with *M. tuberculosis* – endosomal TLR4, TLR7, and TLR9, result in the production of IFN-α and IFN-β (Figure 6). The IFN-α/β then acts through several signaling pathways to produce their downstream effector molecules, the ISGs, as described in section 1.3.3.

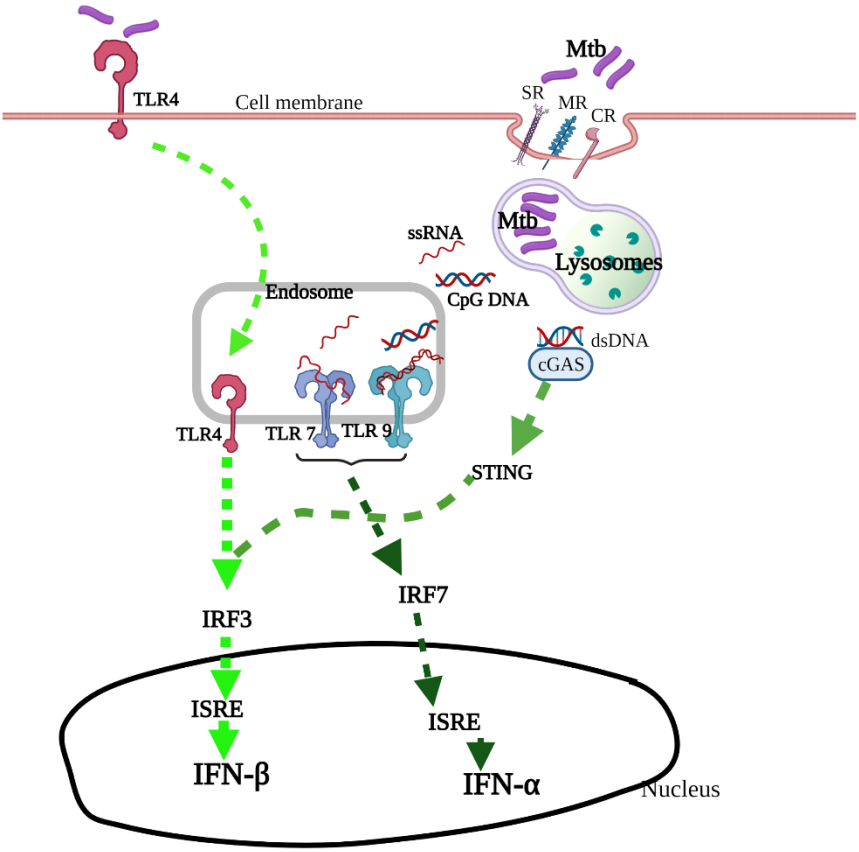

Figure 6. **Induction of IFN-α and IFN-β production in M. tuberculosis infection.**
M. tuberculosis bacilli bind to cell surface receptors- complement receptors (CR), mannose receptors (MR), and scavenger receptors (SR) - and are phagocytosed into the cell. Pathogen-associated molecular patterns (PAMPs) bind to and activate surface TLR4 and endosomal TLR7 and TLR9. Internalized endosomal TLR4, and both endosomal TLRs (TLR7 and TLR9) signal through IRF3 and IRF7 respectively, with the production of **IFN-β** and **IFN-α,** respectively (138). Created with BioRender.com

1.3.3 IFN-α/β signaling and ISG production

The canonical pathway of IFN-α/β signaling signals through the IFNAR, a heterodimeric structure consisting of the transmembrane proteins IFNAR1 and IFNAR2, surface receptors, expressed on all nucleated cells, that are associated with tyrosine kinase 2 (TYK2) and Janus kinase 1 (JAK1), respectively, on their cytoplasmic part (282) (Figure 7). The binding of IFN-α/β to the cognate receptor causes transphosphorylation of the kinases resulting in phosphorylation of conserved tyrosine residues located in the receptor's cytoplasmic tails. The Signal Transducer and Activator of Transcription 1 (STAT1) and STAT2 molecules attach to these residues, get phosphorylated by the JAK1 and TYK2 and dimerize. The resulting STAT1-STAT2 dimer trimerizes with IRF9 to form the IFN-stimulated gene factor 3 (ISGF3), a transcription factor complex. The complex translocates into the nucleus, where it binds to the IFN-stimulated response elements (ISRE) in the ISG promoter leading to ISG transcription, the effector molecules of IFNs (282,329).

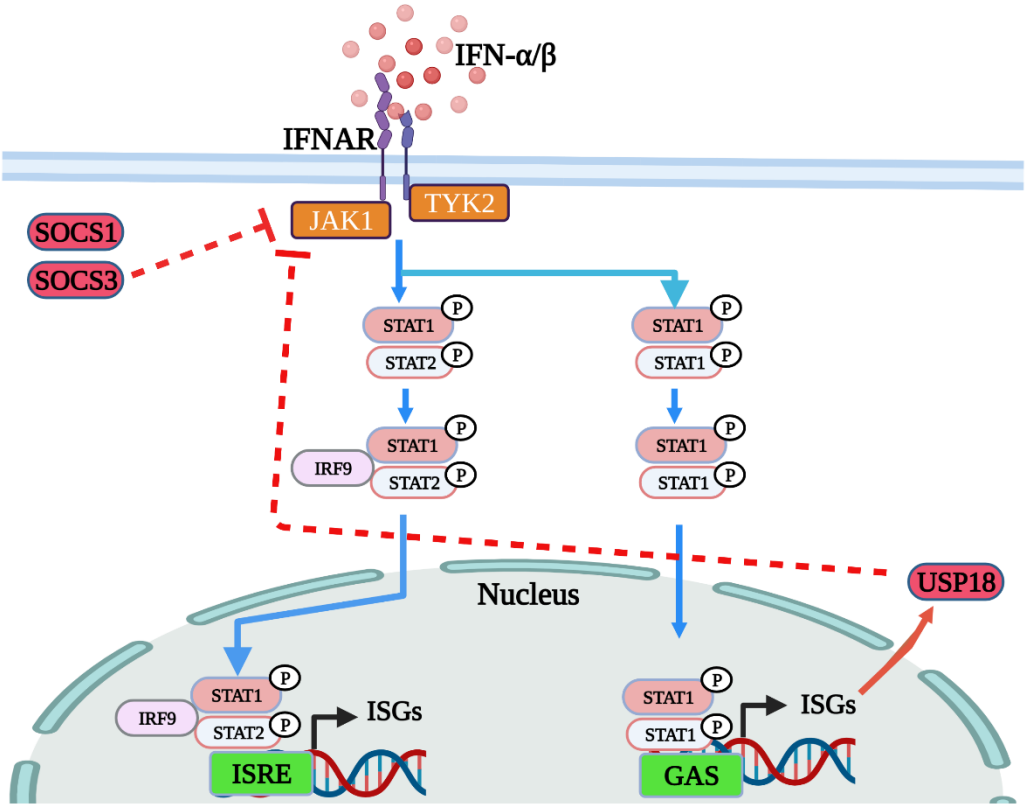

Figure 7. **The type I interferon signaling pathway**.

The binding of interferon-α/β (IFN-α/β) to the IFN-α receptor (IFNAR) activates the kinases, Janus kinase 1 (JAK1) and tyrosine kinase 2 (TYK2). The activation recruits the signal transducer and activator of transcription (STAT) molecules that get phosphorylated by the kinases and dimerize. STAT1-STAT2 dimer trimerizes with IFN regulatory factor 9 (IRF9) to form the IFN-stimulated gene factor 3 (ISF3) which is translocated into the nucleus. The complex binds the IFN-stimulated response elements (ISRE), resulting in IFN-stimulated gene (ISG) transcription. STAT1 homodimers are also translocated into the nucleus and bind to gamma-activated sequences with transcription of ISGs. The suppressor of cytokine signaling proteins (SOCS1 and SOCS3) and the Ubiquitin Specific Peptidase 18 (USP18), an ISG, inhibit the type I IF signaling pathway (329–331). Created with BioRender.com

IFN-α/β can also induce ISG transcription through other pathways, such as through interaction with STAT3, STAT4, and STAT5, or through activation of the phosphoinositide 3-kinase (PI3K)-mammalian target of rapamycin (mTOR), and the multiple mitogen-activated protein kinase (MAPK) pathways (329). IFN-α/β signaling through these diverse pathways results in the transcription of ISGs and genes that encode cytokines, chemokines, and pro-apoptotic and anti-apoptotic molecules (329).

The simple description of an ISG is a gene whose expression is induced in type I, II, or III IFN responses (332). However, not all ISGs fit into this simple definition. Some ISGs are constitutively expressed at low levels prior to induction of the IFN signaling pathway, but their expression is enhanced once IFN signaling commences; some are only induced by IFN responses; and some are induced in the absence of IFN signaling through IRFs (IRF1, IRF3, and IRF7) activation downstream of PAMP-PRR signaling (332–334). Some of the IRFs are also IFN-inducible.

In viral infections, the production and signaling of IFN-α/β result in the activation of ISGs, driving an antiviral response both in the infected cells and neighboring uninfected cells, limiting the spread of infection (335). Besides this well-established effect of IFN-α/β, these cytokines cause a broader range of effects determined by the specific pathogen and the pathways activated downstream of the IFNAR. Furthermore, the activated pathways regulate the specific ISG responses through alternate ISG activation or suppression (298). Therefore, the specific ISG response may influence infection and lead to either protective or detrimental effects on the host.

1.3.3.1 IFN-α/β in viral infections

IFN-α/β demonstrate the ability to 'interfere' with viral replication and induce an antiviral state in cells neighboring infected cells mainly through the induction of IFN-stimulated genes (ISGs), a group of antiviral factors ultimately leading to a reduction in the spread of infection (335). The importance of IFN-α/β in host-mediated cellular protection against viral infections is demonstrated by the various strategies employed by viruses to circumvent its effects by targeting either IFN-α/β production or its signaling (336). Although the mechanisms of ISGs in limiting viral infections are not fully understood and vary between viruses, they have been shown to act at several stages in the viral life cycle. For example, the IFN-induced transmembrane (IFITM) protein members either block viral entry or interfere with the endocytosis-fusion stage; the myxoma resistance proteins, Mx1 and Mx2, block transcription and replication; and the FN-induced protein with tetratricopeptide repeats (IFIT) family inhibits viral translation [reviewed in (334,335)]. Human and murine studies have described various immunomodulatory mechanisms of action of IFN-α/β in viral infections. These include activation of immature DCs, increased expression of MHC molecules and co-stimulatory molecules, trafficking of DCs to local lymph nodes and subsequent activation of T cells, among other mechanisms (298). IFN-α/β also show detrimental effects in viral infections by causing tissue damage through induction of inflammation and IL-10 and other immunosuppressive molecules, leading to disease exacerbation and viral persistence (337–340).

1.3.3.2 IFN-α/β in bacterial infections

In bacterial infections, the role of IFN-α/β varies with species and appears to be protective in infection with extracellular bacteria but detrimental in infections with intracellular bacteria (295,298). In vitro studies on mouse macrophages infected with extracellular bacteria, including Group B Streptococci (GBS), *Streptococcus pneumoniae,* and *Escherichia coli,* demonstrate the protective role of IFN-α/β in extracellular bacteria (341–343). In vitro cellular models of intracellular bacterial infections treated with IFN-α/β inhibited the replication of *Chlamydia* species, *Shigella* species, and *Legionella pneumophila* (343–347). In contrast, IFN-α/β inhibits host resistance to other intracellular bacteria such as *Francisella tularensis*, *Listeria monocytogenes,* and *Mycobacteria tuberculosis* with detrimental effects (299,343,348).

In summary, IFN-α/β show both protective and detrimental effects in infection with microbes. The mechanisms vary with the species of the pathogens. However, there is a paucity of studies on humans; hence, it is unclear how these findings translate to human disease.

1.3.4 Regulation of the type I interferon response

Regulation of type I IFN signaling involves various mechanisms (329) (Figure 3). Basal low-level type I IFN signaling in the absence of infection maintains the expression of components of the signaling pathway in cells. This constitutive expression of low IFN levels enables rapid response to low levels of the IFN in early infection (349). Factors that induce the expression of STAT1 and IRF9 also enhance type I IFN signaling. These include type I IFNs in a positive feedback mechanism, IFN-γ, TNF, and IL-6. In early infection, low-level type I IFNs, through STAT1 induction, lead to macrophage priming, increasing cellular response to these IFNs, and promoting their pro-inflammatory and antimicrobial roles (329). However, suppression of this signaling is necessary to prevent the persistent type I IFN signaling either due to its detrimental effect or after the infection resolution. Mechanisms that suppress type I IFN signaling include 1) downregulation of IFNAR expression on cell surfaces –receptor degradation by viruses and tumor cells as an evasion tactic; IFNAR internalization; and dephosphorylation of signaling intermediates; 2) induction of negative regulators such as suppressor of cytokine signaling (SOCS) proteins (SOCS1 and SOCS3), which competes with STAT1 for its binding site on IFNAR; and Ubiquitin Specific Peptidase 18 (USP18), which displaces JAK from its binding site on IFNAR; and 3) MicroRNA induction: for example, miR-146a negatively regulates STAT1 expression on Th1 cells (350); Tumor necrosis factor receptor (TNFR)-associated factor 6 (TRAF6), Interleukin 1 Receptor Associated Kinase 1 (IRAK1) and IRAK2 on macrophages (351).

1.3.5 Effects of the type I interferons in *M. tuberculosis* infection

Transcriptional profiling studies have revealed an overrepresentation of genes induced by type I and II IFNs, the IFN signature, in the blood of ATB patients suggesting a possible role in the pathogenesis of TB (26,189,233,352–354). The IFN signature observed in ATB correlates with disease severity and diminishes with treatment (189,355,356). More recently, an RNA signature

described among individuals with LTBI was predictive of the risk of developing ATB or reactivation (357). An IFN response was also over-represented in this signature, supporting a previous finding by Berry and colleagues that a proportion of patients with LTBI had a signature similar to that of ATB patients (189,357).

Type I IFNs appear to enhance susceptibility to *M. tuberculosis* infection and subsequent development of active disease (358,359). For instance, murine studies demonstrate that infection with the hypervirulent HN878strain induces higher levels of IFN-α mRNA, positively correlating with virulence and the ability of *M. tuberculosis* to induce a type I IFN response (33). A similar correlation was observed in infections with *Staphylococcus aureus*, a facultative intracellular bacterium (360).

Intranasal administration of exogenous type I IFNs was associated with a lower bacterial burden in *M. tuberculosis*-infected IFNAR-deficient mice than in wild-type mice that showed increased bacterial burden and reduced survival (26). Moreover, mice treated with type I IFN inducers also showed an increased bacterial burden with exacerbated lung pathology (353). Wild-type mice infected with *M. africanum*, part of the MTBC, resulted in a higher bacterial burden, increased severity of inflammation and reduced survival compared to infected IFNAR -/- mice (361). These findings suggest a similar pathogenic role for the IFNs in mycobacterial species. However, murine studies also demonstrate that type I IFNs in early *M. tuberculosis* infection play a potential protective role (167). The studies demonstrated that both type I IFNs and IFN-γ are required in equal concentrations in the lungs for the synergistic activity that induces optimal immune responses during the innate immune phase of *M. tuberculosis* infection. These findings support the concurrent increase in type I and II IFN-inducible genes observed in TB (189). The balanced concentrations drive the recruitment, differentiation, and survival of DCs and macrophages within the lungs. Thus, increased target cells promote cellular *M. tuberculosis* infection and lower bacterial load in the lungs. However, murine studies also revealed a dual role for type I IFNs, demonstrating pro-inflammatory and anti-inflammatory properties in TB, roles that appeared to be influenced by IFN-γ (167). In the absence of IFN-γ, type I IFNs appear to play a protective role in *M. tuberculosis* infection in mice, a characteristic that was also observed in a patient with *M. avium* infection (167,362). In contrast, in high IFN-γ concentrations, type I IFNs switch to an anti-inflammatory role, evidenced by a decrease in recruitment, differentiation, and

survival of myeloid cell subsets (167). This switch in roles suggests that the balance between induction of type I and type II IFN signaling pathways may consequently be an essential component in determining the outcome of LTBI but has not been established in human TB.

The protective role of type I IFNs also depends on the TLR activated, with most *M. tuberculosis* strains activating TLR2, but some strains, particularly hypervirulent strains, activate TLR4 (363). *M. tuberculosis*-induced activation of TLR4 drives type I IFN production, as shown in Figure 4. Type I IFN production suppresses arginase 1 (*Arg1)* gene expression and protein activity in *M. tuberculosis*-infected mice and bone-marrow-derived macrophages in the absence of IFN-γ, driving macrophage polarization to the protective classically activated or M1 phenotype (166). The induction of type I IFN production in a murine model of *M. tuberculosis* infection resulted in the production of chemokine (C-C motif) ligand 2 (CCL2) and C-C chemokine receptor type 2 (CCR2). The chemokines caused the recruitment of monocytes permissive to *M. tuberculosis* infection to the inflammation site in the lungs, exacerbating infection (353).

The onset of the adaptive immune response leads to increased production of IFN-γ by CD4+ and CD8+ T cells; IFN-γ then becomes the primary regulator of T cell recruitment, antigen presenting cell (APC) activation, and controlling growth of *M. tuberculosis*. In this phase, type I IFNs limit the abundance of myeloid DCs and macrophages in the lungs reducing the number of target cells (167).

Various other mechanisms by which type I IFNs are involved in TB pathogenesis are shown in Figure 7(298,364). In mice infected with *M. tuberculosis* strain HN878, type I IFNs suppressed the Th1 response with reduced activity of IFN-γ and TNF-α; they also observed reduced IL-6, IL-12, and IL-10. In contrast, treatment of *M. tuberculosis*-infected macrophages with IFN-β enhances the production of IL-10; this treatment inhibited IL-12 and TNF-α production and impaired the responsiveness of IFN-γ receptor to IFN-γ, thereby blocking the activation of macrophages by Th1 cells (365). However, a study of a murine model of *M. tuberculosis* observed an initial strong Th1 response with a rapid influx of IFN-γ-secreting CD4+ and CD8+ T cells into the lungs, followed by a decline in the Th1 response as IL-10-secreting CD4+ T cells increased in the lungs (354). An increase in type I IFN levels was also shown to suppress IL-12p40 expression and reduce IL-12p70 production (366,367). IL-12p40 is required for activation of DCs and

migration to the lymph nodes, while IL-12p70 induces the Th1 response (251,256,368). Inhibition of these protective cytokines, IL-12, IFN-γ, and TNF-α, could reactivate latent infection (369).

The interaction between type I IFN, IL-1, and eicosanoids and the role of this interaction in controlling the intracellular growth of *M. tuberculosis* has also previously been described (370). IL-1 plays a role in the development of host resistance against *M. tuberculosis*. The interleukin also induces the production of eicosanoids which control the production of IFN-α/β, resulting in the containment of bacterial growth (371). LTBI is characterized by a prostaglandin E2-mediated balance between IL-1 and type I IFNs that is crucial in preventing the uncontrolled inflammation associated with pathology in ATB. In ATB, the imbalance in eicosanoid production tips the balance to favor type I IFNs with suppression of IL-1α and IL-1β responses mediated by IL-1 and IL-10 receptor agonist activity. Virulent *M. tuberculosis* strains also induce the production of IL-1β, which is negatively regulated by type I IFNs (372).

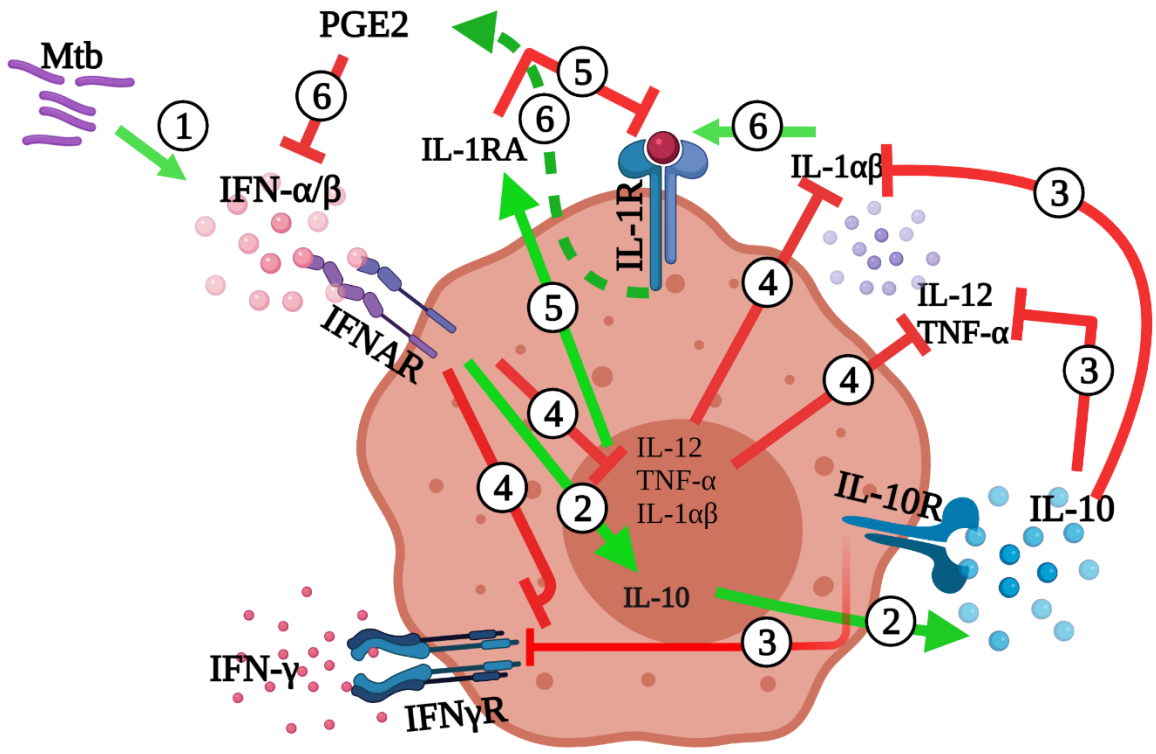

Figure 8. **Effects of type I IFNs in *M. tuberculosis* infection**.

1. Infection with *M. tuberculosis* induces the production of IFN-α/β. 2. IFN-α/β induces the production of IL-10, which,3. suppresses the production of the pro-inflammatory cytokines IL-12, TNF-α, IL-1α, and IL-1β, and inhibits the IFN-γ receptor. 4. IFN-α/β also directly suppresses the production of IL-12, TNF-α, IL-1α, and IL-1β, and inhibits IFNγR. 5. IFN-α/β also induces the production of IL-1RA, which inhibits the IL-1R. 6. IL-1α and IL-1β signal through IL-1R, inducing the production of prostaglandin E2, which suppresses the production of IFN-α/β (298,373). Created with BioRender.com

In summary, IFN-α/β involvement in the pathogenesis of *M. tuberculosis* infection results from its interaction with previously described immune responses, both cellular and cytokine. These interactions determine whether the downstream effects of the IFN-α/β are protective or detrimental. The functions of IFN-α/β are achieved through IFN-inducible transcripts, the ISGs, which are produced downstream of the IFNAR in response to IFN-α/β signaling.

1.4 Transcriptional profiling in TB

The transcriptome is the entire collection of RNA transcripts expressed by a tissue or cell in a given timeframe and includes coding RNA and non-coding RNA. Transcriptional or gene expression profiling assesses mRNA expression levels or a transcript profile in a cell population at a given time. Techniques used for transcriptional profiling include RT-qPCR, RNA-Seq, microarray technology, and tag-based technology. More recently, studies assessing the use of host transcriptomics in the diagnosis of TB aim to identify specific transcripts or transcriptional signatures that discriminate *M. tuberculosis* infection states (106,374). A number of these studies have defined a signature enriched for genes downstream of the type I IFN signaling pathway in ATB that show potential to 1) discriminate *M. tuberculosis*-infected from the uninfected and ATB from LTBI or other diseases, 2) identify those at risk of LTBI reactivation to ATB, and 3) for treatment monitoring (189,352,356,357,375–377).

Assessment of genome-wide transcriptional profiles in whole blood from 54 individuals with ATB (culture positive), 69 with LTBI (positive TST and/ or QFT), and 24 healthy controls (TST and QFT negative) recruited from South Africa and the UK (189) revealed a 393-transcript signature in ATB patients with enrichment of genes in type I and II IFN signaling pathways. Correlation of disease severity with overrepresentation of type I IFN-inducible genes was

observed. Some genes in the transcript signature were overexpressed in neutrophils from ATB patients than in healthy controls suggesting that neutrophils were driving the transcriptional signature.

A genome-wide transcriptional profiling study in Indonesia assessed PBMCs from 23 new HIV-negative PTB patients and 23 healthy controls recruited from a longitudinal cohort at three timepoints - week 0 (pre-treatment stage), week 8 (treatment stage), and week 28 (convalescent stage) (352). The study also assessed the transcriptional profile in a human macrophage cell line, BCG-infected THP-1, and a mouse model of acute TB. Biological processes common to the three study models included immunity and defense, and IFN-mediated immunity. Three IFN-α pathway genes–*GBP4*, *IL15RA* and *UBE2L6*- were upregulated in the three models while IFN-γ was downregulated; the expression of the genes normalized with treatment.

A pre-and post-TB treatment study recruited 29 ATB cases and 38 controls (LTBI with positive QFT result) from South Africa and 8 ATB cases from the UK (356). ATB cases were sampled at different timepoints – week 0 (pre-treatment), week 2, week 8, week 16, and week 24. Whole blood was processed through RNASeq. This study also described the overrepresentation of genes in type I and II IFN signaling pathways in ATB, with significant changes in the transcriptional response observed two weeks after commencement of treatment.

A study from multiple European facilities compared the transcriptional profile in whole blood and leukocytes from patients with PTB or active sarcoidosis to healthy controls and patients with primary lung cancer and community-acquired pneumonia. Pre-and post-treatment samples revealed the overexpression of genes enriched for IFN signaling and immune responses (375).

A study from Singapore compared transcriptional profiles from 5 healthy controls (no recent history of exposure, no ATB), 26 household contacts (contact with smear-positive TB cases), and 14 ATB cases and identified a 186-gene exposure signature for recent TB exposure (376). Biological processes for these genes included the type I IFN signaling pathway, inflammatory response, and neutrophil-mediated immune responses. In addition, the exposure signature included genes previously identified for LTBI *(SOCS3*, *DUSP2*, *OSM*) (378), incipient TB in individuals with LTBI (*ANKRD22*, *SCARF1*, *BATF2* and *SERPING1*) (357), and incipient TB in individuals with a history of exposure to an ATB case (*SCARF1*, and *BATF2*) (379).

A longitudinal study from India evaluated the transcriptional profile of 30 healthy controls, 30 ATB (TB), 30 diabetic patients (DM) and 30 diabetic patients with ATB (TBDM) in India and identified genes involved in type I and II IFN responses in TB patients (380).

The detection of transcript signatures enriched for type I IFNs signaling in ATB suggests that type I IFNs levels are elevated in TB. For instance, a study on ATB patients from India found higher expression of IFN-α mRNA in peripheral blood than IFN-β and IFN-γ (381). However, a study from South Africa found undetectable plasma IFN-β levels and low plasma IFN-α levels (below 100 fg/mL) with no differences between individuals with LTBI and ATB patients (382). These findings contrast findings from similar studies with influenza virus where serum or plasma levels of IFN-α protein are elevated alongside the ISG signatures (382,383).

These studies show that induction of type I IFN-inducible genes is observed in whole blood and PBMCs from TB patients without stimulation. In contrast, type I IFN-inducible genes are not predominant following stimulation with *M. tuberculosis*-specific antigens, which appears to diminish these responses (384,385). Although type I IFN-inducible genes have been identified in multiple studies, the individual genes in the IFN signatures appear to vary between studies. Moreover, these responses have not been evaluated to determine the responses of individual genes and their behavior in the different clinical phenotypes of *M. tuberculosis* infection with or without *M. tuberculosis* antigen-specific stimulation.

1.5 Rationale

More than 150 years after *M. tuberculosis* was identified as the causative agent of TB, currently infecting a quarter of the world's population, causing more than 10 million active disease cases and more than one million deaths annually, the human host immune response is still incompletely understood. Although various components of the immune system are described, the more recent discovery of a role for type I IFNs in TB pathogenesis presents a new dimension in this host immune response.

Studies on unstimulated ex-vivo whole blood or PBMCs from both human ATB patients and mouse-models of *M. tuberculosis* infection reveal the dominance of genes linked to the type I IFN pathway, the type I IFN signature (189,352,386–389). The genes showed higher expression

in ATB than in LTBI or controls in these studies. However, in PBMCs stimulated with ESAT-6 or CFP-10 (384) or PPD (385), the stimulation appears to diminish the overrepresentation of genes in the type I IFN pathway; the IFN signature is not predominant. **It, therefore, remains unclear what drives or induces the higher expression of the genes in the IFN signature in ATB.** Knowledge of these drivers would inform the development of tools for identifying individuals at risk of disease progression for targeted preventive therapy and new treatment options to improve LTBI prevention treatment.

The similarity in gene expression responses to IFN-α and IFN-β stimulation has been observed in PBMCs from healthy individuals (390). However, the responses to these IFNs, both their effect on gene expression and cytokine responses, have not been elucidated in *M. tuberculosis* infection. With the application of IFN-α and IFN-β as therapeutic agents in various clinical conditions, including chronic hepatitis, cancers and multiple sclerosis (391–394), and reports of therapy with IFN-α causing LTBI reactivation (395), it is crucial to address the effect of IFN-α and IFN-β on the immune responses in *M. tuberculosis* infection and understand how each IFN subtype contributes to maintaining or possibly promoting disease pathology or reactivation.

1.6 Hypotheses and objectives

The central hypothesis of this thesis is **IFN-α- and/or IFN-β-driven transcriptomic signatures and cytokine responses can distinguish clinical TB states**

Three objectives were proposed to test this hypothesis:

1. To explore the expression of selected interferon-stimulated genes in unstimulated, IFN-α or IFNβ-, or *M. tuberculosis* whole cell lysate (WCL)-stimulation of PBMCs in clinical phenotypes of *M. tuberculosis* infection.

   Sub-hypotheses:

   Compared to LTBI, ISG expression in ATB is higher following IFN-α/β stimulation and lower following Mtb WCL stimulation and expression does not differ between IFN-α and IFN-β

2. To quantify cytokine response profiles to IFN-α or IFNβ-, and *M. tuberculosis* whole cell lysate (WCL)-stimulation of PBMCs in clinical phenotypes of *M. tuberculosis* infection.

   Sub-hypotheses:

   Compared to LTBI, pro-inflammatory cytokine responses in ATB are suppressed by IFN-α/β and increased by Mtb WCL stimulation and do not differ between IFN-αand IFN-β

3. To evaluate the relationship between gene expression levels and cytokine expression levels in *M. tuberculosis* infection to determine whether there are associations between cytokine expression and gene expression levels in specific TB infection states.

   Sub-hypothesis: There is an association between gene expression levels and cytokine expression levels in TB infection states.

To characterize type I IFN responses in *M. tuberculosis* infection, this thesis assessed the responses of selected ISGs to stimulation with IFN-α, IFN-β, and *M. tuberculosis* whole cell lysate in PBMCs from healthy controls (HC), TST reactive (TST), LTBI, and ATB patients. In addition, Gene expression analysis was conducted in parallel with cytokine responses to assess the effect of IFN-α and IFN-β on the immune response. The findings from this thesis will add to our understanding of the role of IFN signaling and dichotomous IFN-α/ IFN-β responses in patients with TB to determine whether there are specific signatures associated with ATB and LTBI profiles.

CHAPTER 2: MATERIALS AND METHODS

2.1 Study participants

Study participants were recruited from several clinics within the Health Sciences Centre in Winnipeg, Manitoba, Canada, between 2013 and 2017. PBMCs were isolated from heparinized whole blood collected from each participant and cryopreserved. Each participant was also subjected to a QFT test to identify LTBI cases. Using this available PBMC catalogue, we selected cryopreserved PBMCs from HIV-negative participants for this thesis research, excluding individuals identified with diabetes, end-stage renal disease (ESRD), post-transplantation, or undergoing treatment with immunosuppressive agents. All participants were 18+ years.

2.1.1 Study participants for optimization experiments

Blood samples for optimization experiments were obtained from volunteers at the JC Wilt Infectious Diseases Research Centre in Winnipeg, Manitoba, Canada

2.2 Case definitions

Healthy controls (HC): individuals with no clinical, radiological, or laboratory evidence of ATB, TST- and QFT-negative.

Latent TB (LTBI): individuals with no clinical signs and symptoms of ATB but were QFT-positive.

Tuberculin skin test-reactive (TST): QFT-negative individuals who had previously been TST-positive as indicated by historical chart confirmation, not a recent test. For the analysis, these participants were classified as TST "reactive" (TST-positive, QFT-negative).

Active TB (ATB): patients with microbiologically confirmed presence of *M. tuberculosis* by microscopy or culture and additional clinical or radiological evidence of active disease.

2.3 Ethics statement

The University of Manitoba Health Research Ethics Board approved this study [Protocol #s: HS11849 (H2008:300) and HS11850 (H2008:301)].

2.4 General reagents

2.4.1 Stimulants

Three stimulants were used in these experiments:

- *Mycobacterium tuberculosis* whole cell lysate (Mtb WCL) (strain H37Rv) (BEI Resources, NIAID) at a concentration of 50µg/ml. The lysate contains proteins, lipids and carbohydrates present within the bacterial cell.
- Recombinant human IFN-α2a (PBL Assay Science) at a concentration of 500IU/ml was combined with recombinant human IFN-α2b (PBL Assay Science) at a concentration of 500IU/ml. According to the manufacturer's insert, IFN-α2a and IFN-α 2b were sourced from human leukocyte interferon cDNA expressed in Escherichia coli, had >95% purity, and endotoxin levels <1 endotoxin unit/µg.
- Recombinant human IFN-β (PeproTech) at a concentration of 10ng/µl. According to the manufacturer's insert, IFN-β was sourced from CHO cells, had >95% purity, and endotoxin levels <1 endotoxin unit/µg.

2.4.2 Media and buffers

R10 culture media was prepared using RPMI 1640 supplemented with 2% of 100x Penicillin/Streptomycin solution and 10% heat-inactivated fetal bovine serum (FBS) (all from Gibco Life Technologies, Thermo Fisher Scientific, Ontario, Canada)

Phosphate buffered saline (PBS) solution, pH 7.4, with 2% heat-inactivated fetal bovine serum (FBS)

Freezing media was prepared using 10% Dimethyl sulphoxide (DMSO) and 90% heat-inactivated fetal bovine serum (FBS) (Sigma-Aldrich, St Louis-USA)

2.4.3 RNA processing reagents and kits

RNeasy Plus Mini kit® (Qiagen) was used for RNA extraction from cultured PBMCs according to the manufacturer's instructions. The kit contents include Buffer RLT Plus, Buffer RW1, Buffer RPE, gDNA eliminator spin columns, RNeasy Mini spin columns, and collection tubes.

RNA concentration kits: RNA concentration was done using GeneJET RNA cleanup and concentration micro kit (Thermo Fisher Scientific™) according to manufacturer's instructions.

SuperScript™ VILO™ cDNA synthesis kit (Thermo Fisher Scientific®) was used for reverse transcription. The kit contains 10X SuperScript™ enzyme mix, and 5X VILO™ reaction mix.

TaqMan OpenArray Real-Time PCR plates, TaqMan OpenArray Real-Time PCR Master mix (Thermo Fisher Scientific™) were used for quantitative PCR run on the QuantStudio platform.

Diethyl pyrocarbonate (DEPC)-treated water that is nuclease-free.

2.4.4 Milliplex assay reagents and kits

MILLIPLEX MAP Human Cytokine/Chemokine Magnetic Bead Panel - 33 Plex (HCYTOMAG-60K- 33, Human Cytokine MAGNETIC Kit, EMD-Millipore, USA)

2.5 Sample processing

2.5.1 PBMC isolation and thawing

2.5.1.1 PBMC isolation and storage

Using the Ficoll-Histopaque density centrifugation technique, PBMCs were isolated from 30ml of heparinized whole blood obtained from three volunteer blood donors. Briefly, whole blood was centrifuged at 1500 rpm for 7 minutes to separate the plasma, which was then aspirated and stored. The blood was then diluted with sterile PBS with 2% FBS in a 1:1 volume ratio and mixed with a pipette. The blood-PBS mixture was carefully layered on Lymphoprep (StemCell Technologies, Vancouver, Canada), a density gradient medium and centrifuged at 1600 rpm for 10 minutes to separate the PBMCs. PBMCs were collected from the interface using a pipette into a fresh tube, washed twice with PBS containing 2% FBS, and resuspended in R10 media. Cell counting and viability testing were performed using Trypan Blue (Sigma-Aldrich, St. Louis, USA) and a haemocytometer (Neubauer-Neutec, California, USA). For freezing, 1 x 10^7 cells were resuspended in 1ml of freezing media in a vial. The vials were then placed into Mr. Frosty™ containers (Thermo Fisher Scientific, USA) filled with 100% isopropyl alcohol and frozen to -80°C. The PBMCs were kept at -80°C overnight and then transferred to liquid nitrogen tanks for

long-term storage. Mr. Frosty™ containers cool at a rate of approximately -1°C/minute, which has been found to be an optimum rate for preserving cells and successful recovery of cells (396)

2.5.1.2 Thawing of PBMCs

1 x 10^7 PBMCs was used for each participant. PBMC vials from liquid nitrogen were placed on dry ice and thawed in a water bath at 37°C, one tube at a time, for about 30 seconds to thaw the cells. Thawed cells were immediately transferred into 10ml R10 media in a 15ml conical tube using a transfer pipette. Cells were washed twice by centrifuging at 1200 rpm for 8 minutes with media, decanted, and the pellet re-suspended in 3ml R10 media. Cell viability testing was done using Trypan Blue viability testing technique. Cells were counted in 50 µl of the suspension in a haemocytometer, and only samples with >80% viability were processed further. Cells were made up to a concentration of approximately 2 million cells per ml and then rested for one hour at 37°C in 5% CO_2 prior to stimulation.

2.5.2 PBMC culture

The concentrations of IFN-α and IFN-β used to stimulate PBMCs were determined in optimization experiments. PBMCs from healthy donors were each tested at three different concentrations used for each stimulant, as outlined in Table 1.

Table 1. Stimulation concentrations for optimization experiments

Stimulant	**Concentration**		
IFN-α*	100 U/ml	500 U/ml	1000 U/ml
IFN-β	1 ng/ml	10 ng/ml	50 ng/ml

* For IFNα, half the concentration was used for each isoform (IFNα2 and IFNαA)

Optimized quantities of 1000 U/ml of IFN-α and 10ng/ml of IFN-β were then used for PBMC stimulation experiments at 37°C in 5% CO_2 for 4 hours for gene expression studies and overnight for cytokine assays. For IFN-α, recombinant human IFN-α2 (IFN-α2b) (500IU/ml) was mixed with recombinant human IFN-αA (IFN-α2a) (500IU/ml) for each sample. For IFN-β,

10ng/ml of recombinant human IFN-β was used for each sample. *M. tuberculosis*, strain H37Rv whole cell lysates. Previously optimized concentration of 50ug/ml *M. tuberculosis* strain H37Rv whole cell lysate was used for stimulation. This concentration was used because there is a quantity order restriction for the lysate to two per year. The PBMCs were then processed using RT-qPCR for the genes listed in Table 4.

Time-course experiments were done at three different time points – 1 hour (T_1), 4 hours (T_4), and overnight ($T_{o/n}$) stimulation with 1000 U/ml of IFN-α and 10ng/ml of IFN-β. The PBMCs were then processed using RT-qPCR for the genes listed in Table 4.

2.5.3 IFN-α, IFN-β, and *M. tuberculosis* whole-cell lysate stimulation of PBMCs

Appropriately labelled polypropylene tubes and 24-well plates for unstimulated control, IFN-α-stimulated, IFN-β-stimulated or *M. tuberculosis* whole-cell lysate-stimulated were used for PBMC stimulation for PCR and cytokine analysis, respectively. The optimal amount of each stimulant was added into the appropriate tube or well containing 1 x 10^6 PBMCs in 500 µl, then mixed thoroughly by vortexing and incubated at 37°C in 5% CO_2 for 4 hours for gene expression analysis and18 hours for cytokine/ chemokine assays. Identical samples were set up for each stimulation condition, one set of tubes for 4 hours for PCR experiments, and one set of 24-well plates stimulated overnight for cytokine/ chemokine assays.

2.5.4 Gene expression studies

Following the 4-hour incubation period, the PBMCs were counted before harvesting the cells. The contents of the polypropylene tubes were transferred into labelled Eppendorf tubes and then centrifuged at 300 x g for 5 minutes to pellet the cells. Transfer pipettes were used to remove the supernatant without touching the pellet. The pellet was washed twice with cold PBS centrifuging at 300 x g for 5 minutes and decanting the supernatant. The cell pellet was dislodged by flicking the tube, and 350µl of RLT Plus buffer with β-mercaptoethanol (β-ME) was added. The tube was vortexed for 30 seconds to homogenize the lysate, then stored at -80°C for future RNA extraction.

2.5.4.1 RNA extraction, purification, and concentration

2.5.4.1.1 RNA extraction

RNA extraction was done using RNeasy Plus Mini kit® (Qiagen) according to the manufacturer's instructions. Briefly, the lysed cell pellet was thawed at room temperature and then vortexed for 30 seconds. The homogenized cell lysate was transferred to a gDNA eliminator spin column placed in a collection tube and centrifuged at 8000 *x g* for 30 seconds. The column was discarded, and 350 µl of freshly prepared 70% ethanol was added to the flow-through. After pipetting to mix, 700 µl was transferred to a RNeasy spin column in a collection tube. The closed tube was centrifuged at 8000 *x g* for 15 seconds, and the flow-through was discarded. 700 µl of RW1 buffer was added, and centrifugation was repeated, followed by two washes using 500 µl of RPE buffer centrifuged for 15 seconds for the first wash and 2 minutes for the second wash. After decanting the RPE buffer, the spin column was centrifuged for one minute in a new collection tube at full speed to dry the column membrane. In a 1.5 ml collection tube, 40 µl RNase-free water was added to the column membrane, and the closed tube was centrifuged at 8000 x g for one minute. The RNA elute was then concentrated and purified.

2.5.4.1.2 RNA concentration and purification

The GeneJET RNA cleanup and concentration micro kit (Thermo Fisher Scientific™) was used to concentrate and purify the RNA elute according to the manufacturer's instructions. Briefly, the reaction mixture was adjusted to 200 µl with nuclease-free water and 100 µl binding buffer added and mixed. 300 µl of absolute ethanol was added and mixed. The mixture was transferred to the GeneJET RNA Purification Micro column in a collection tube and centrifuged at 14,000 *x g* for 60 seconds. The flow-through was discarded, 700 µl of wash buffer 1 was added to the column, and centrifugation was repeated. The process was repeated with 700 µl wash buffer 2. The flow-through was discarded, and the column was placed back into the tube and centrifuged at 14,000 *x g* for 60 seconds. The column was transferred into a clean collection tube, 10 µl nuclease-free water added and centrifuged at 14,000 *x g* for 60 seconds. RNA eluted was then quantified.

2.5.4.1.3 RNA quantification

RNA from each sample was quantified on the BioTek™ Take3™ Plate using Synergy™ H1 Hybrid Multi-Mode Microplate Reader. Samples with 260/280 values of ≈ 2.0 were processed further for RT-qPCR.

2.5.4.2 cDNA synthesis

A total of 50ng RNA was used for cDNA synthesis using the SuperScriptTM VILO™ cDNA synthesis kit (Thermo Fisher Scientific®) as per the manufacturer's instructions. For each tube, 4µl of 5X VILO™ reaction mix, 2µl 10X SuperScript enzyme mix, a volume equivalent to 50ng extracted RNA, were added and topped up to a total of 20µl with Diethyl pyrocarbonate (DEPC)-treated water. Tube contents were mixed and incubated for 10 minutes at 25°C, then for 60 minutes at 42°C, followed by 5 minutes at 85°C to terminate the reaction. The cDNA was stored at -80°C.

2.5.4.3 RT-qPCR for optimization experiments

The PCR was performed using the QuantiFast® SYBR® Green PCR Master Mix (Qiagen) kit per the manufacturer's instructions. Each reaction mix contained 12.5µl of 2X QuantiFast SYBR Green PCR Master Mix, primers (at a final concentration of 1µM), 50ng cDNA, and RNAse-free water to make up a total volume of 25µl. The mixture was run on the LightCycler® 96 system using cycling conditions outlined in Table 2.

Table 2. PCR cycling conditions for IFN kinetics study.

Step	**Temperature**	**Time**
Initial heat activation	95°C	5 minutes
2-step cycling:		
Denaturation	95°C	10 seconds
Annealing/ extension	60°C	30 seconds
Number of cycles	40	

2.5.4.3.1 Genes selection for optimization of stimulation conditions

RNA seq data from PBMCs stimulated with PPD previously assessed in our laboratory from two ATB patients and two healthy controls were used to identify responsive genes for optimizing the stimulation kinetics and ideal concentrations of IFN-α2 (IFN-α2b), IFN-αA (IFN-

α2a), and IFN-β stimulation. From this data 15 differentially expressed genes were selected for the optimization experiments. The genes and their primer sequences are listed in Table 3.

Table 3. Primer sequences of genes used for optimization experiments.

Gene	**Primer sequence: Forward**	**Primer sequence: Reverse**
ANKRD22	CCCCCTTTGAGTATTGAGCA	CACACTCACCGCTGACACTT
BATF2	AGACCCCAAGGAGCAACA	CTTTTTCCAGAGACTCGTGCT
CCL8	AATGTCCCAAGGAAGCTGTG	GGGAGGTTGGGGAAAATAAA
CXCL9	ACTATCCACCTACAATCCTTGAAAGAC	TCACATCTGCTGAATCTGGGTTTAG
CXCL10	AGCAAGGAAAGGTCTAAAAGATCTCC	GGCTTGACATATACTCCATGTAGGG
CXCL11	TGCTACAGTTGTTCAAGGCTTCC	GGTACATTATGGAGGCTTTCTCAATATC
ETV7	AATGGGCTCGCCAGACTCT	CAGGGCACGAGACATCTTCTC
FCGR1A	AAGCGCAGCCCTGAGTTG	TGCCAGATAGAAAAGGACATGAAA
IFIT3	TCCACACCAAACAATGGCTA	TGTTGCTTTTCAGCATCAGG
IFI44L	GGTGGGTCCAGTTGGGTCTGGA	GCACAGTCCTGCTCCTTCTGCC
ISG15	AGCTCCATGTCGGTGTCAG	GAAGGTCAGCCAGAACAGGT
MSR1	TCCCACTGGAGAAGTGGTC	CTCCCCGATCACCTTTAAGAC
MX1	GGTGTCGACATACCGGAAGA	CTCCTTGCATGAGAGCAGTG
SECTM1	AGAGCGACCAAGAGGATGAA	CCCATGTCAACATCAAGCTG
SOCS1	TTTTCGCCCTTAGCGTGAAG	CATCCAGGTGAAAGCGGC

2.5.4.4 PCR for clinical samples

The QuantStudio^{TM}OpenArray® system (ThermoFisher Scientific®) was used for PCR. Three of this system's four components were used: the TaqMan® OpenArray plate, the Accufill and the Real-time PCR instrument. Inventoried TaqMan® OpenArray Real-Time PCR plates (Thermo Fisher Scientific®) in the 56-plate format were used to test gene expression. The array plate contained gene primers and probes listed in Table 4 that included three reference genes- 18S ribosomal RNA (*18S rRNA*), β-actin (*ACTB*) and hypoxanthine phosphoribosyltransferase1 (*HPRT1*). These genes comprised the 15 genes from the optimization panel compiled from our previous RNA Seq data from two ATB patients and two healthy controls, and an additional 38 genes from some of the ISGs identified in other transcriptional profiling studies in TB (189,352,356,357,377,397–401).

Table 4. Candidate genes for RT-qPCR.

Gene symbol	**Gene name**	**Assay ID, Applied Biosystems**
ANKRD22	Ankyrin Repeat Domain 22	Hs00944018_m1
APOL1	Apolipoprotein L1	Hs01066280_m1
BATF2	Basic Leucine Zipper ATF-Like Transcription Factor 2	Hs00912737_m1
CAMP	Cathelicidin Antimicrobial Peptide	Hs00189038_m1
CCL8	C-C Motif Chemokine Ligand 8	Hs04187715_m1
CXCL10	C-X-C Motif Chemokine Ligand 10	Hs00171042_m1
CXCL11	C-X-C Motif Chemokine Ligand 11	Hs00171138_m1
CXCL9	C-X-C Motif Chemokine Ligand 9	Hs00171065_m1
ETV7	ETS Variant Transcription Factor 7	Hs00903229_m1
FAM26F	Family with Sequence Similarity 26 Member F	Hs01383017_m1
FCGR1A	Fc Fragment of IgG Receptor Ia	Hs00174081_m1
FCGR1B	Fc Fragment of IgG Receptor Ib	Hs02341825_m1
GBP1	Guanylate Binding Protein 1	Hs00977005_m1
GBP2	Guanylate Binding Protein 2	Hs00894837_m1
GBP4	Guanylate Binding Protein 4	Hs00925073_m1
GBP5	Guanylate Binding Protein 5	Hs00369472_m1
IFI35	Interferon Induced Protein 35	Hs00413458_m1
IFI44	Interferon Induced Protein 44	Hs00197427_m1
IFI44L	Interferon Induced Protein 44 Like	Hs00915292_m1
IFIT1	Interferon Induced Protein with Tetratricopeptide Repeats 1	Hs03027069_s1
IFIT2	Interferon Induced Protein with Tetratricopeptide Repeats 2	Hs01922738_s1
IFIT3	Interferon Induced Protein with Tetratricopeptide Repeats 3	Hs01922752_s1
IFITM1	Interferon Induced Transmembrane Protein 1	Hs00705137_s1
IFITM2	Interferon Induced Transmembrane Protein 2	Hs00829485_sH

Table 4: continued

Gene symbol	**Gene name**	**Assay ID, Applied Biosystems**
IFITM3	Interferon Induced Transmembrane Protein 3	Hs03057129_s1
IL10	Interleukin 10	Hs00961622_m1
IL12B	Interleukin 12B	Hs01011518_m1
IL1A	Interleukin 1 Alpha	Hs00174092_m1
IL1B	Interleukin 1 Beta	Hs01555410_m1
IRF1	Interferon Regulatory Factor 1	Hs00971965_m1
IRF7	Interferon Regulatory Factor 7	Hs01014809_g1
IRF9	Interferon Regulatory Factor 9	Hs00196051_m1
ISG15	ISG15 Ubiquitin Like Modifier	Hs01921425_s1
LAG3	Lymphocyte Activating 3	Hs00958444_g1
MSR1	Macrophage Scavenger Receptor 1	Hs00234007_m1
MX1	MX Dynamin-Like GTPase 1	Hs00895608_m1
MX2	MX Dynamin-Like GTPase 2	Hs01550814_m1
OAS1	2'-5'-Oligoadenylate Synthetase 1	Hs00973635_m1
OAS3	2'-5'-Oligoadenylate Synthetase 3	Hs00196324_m1
OASL	2'-5'-Oligoadenylate Synthetase Like	Hs00984387_m1
PSMB8	Proteasome Subunit Beta 8	Hs00544758_m1
SCARF1	Scavenger Receptor Class F Member 1	Hs01092477_m1
SECTM1	Secreted and Transmembrane 1	Hs00356334_m1
SEPT4	Septin 4	Hs00365352_m1
SERPING1	Serpin Family G Member 1	Hs00163781_m1
SOCS1	Suppressor Of Cytokine Signaling 1	Hs00705164_s1
SOCS3	Suppressor Of Cytokine Signaling 3	Hs02330328_s1
STAT1	Signal Transducer and Activator of Transcription 1	Hs01013996_m1
TAP1	Transporter 1, ATP Binding Cassette Subfamily B Member	Hs00388675_m1

Table 4: continued

Gene symbol	**Gene name**	**Assay ID, Applied Biosystems**
TNFSF10	TNF Superfamily Member 10	Hs00921974_m1
TRAFD1	TRAF-Type Zinc Finger Domain Containing 1	Hs00198630_m1
UBE2L6	Ubiquitin Conjugating Enzyme E2 L6	Hs01125548_m1
USP18	Ubiquitin Specific Peptidase 18	Hs00276441_m1
ACTB	Beta-actin	Hs01060665_g1
18S rRNA	18S ribosomal RNA	Hs99999901_s1
HPRT1	Hypoxanthine phosphoribosyltransferase 1	Hs02800695_m1

The TaqMan OpenArray plates are high throughput PCR plates that use small volumes for PCR. The steel plates contain 48 subarrays in a 4 X 12 layout; each subarray has 8 X 8 through-holes (wells) spotted with the primer and probe set, giving 3,072 through-holes per plate. Sample files for the 96-well plate were created in Excel and uploaded onto the OpenArray sample tracker software as comma-separated values (.csv) files, then mapped to the 384-well plate format. The .csv files were uploaded into the sample folder. For each well, 5.0 µl TaqMan OpenArray Master Mix was mixed with 2.6 µl of nuclease-free water and 2.4 µl cDNA, making a final volume of 10.0 µl in each well. The mixture was centrifuged at 1000 rpm for one minute to remove bubbles. Next, 10.0 µl of the mixture was transferred to the 384-well plate using a fixed 8-channel pipette; the plate was sealed with a foil seal and centrifuged for one minute at 1000 rpm to remove bubbles. Finally, the OpenArray plate was loaded with 5.0 µl using the Accufill using the plate .csv and .tpf files, sealed with the provided lids and sealed with immersion fluid, then run on the QuantStudio using the manufacturer's settings.

Data management:

Results were downloaded from the Quantstudio equipment as an Excel file. The OpenArray technology uses the Crt or relative threshold method in which the threshold set for each curve depends on the shape of the amplification curve. The Crt method differs from the traditional Ct technology that sets the threshold based on all the amplification curves for each gene target (402).

2.5.4.5 Data analysis

Crt values of unstimulated, IFN-α-stimulated, IFN-β-stimulated, and *M. tuberculosis* WCL-stimulated samples were exported into an Excel worksheet to create a result database for data analysis. Genes with less than 60% detectability of expression data in any clinical phenotype group or stimulation were excluded from further overall analysis or analysis that focused on the specific groupings in which the gene had a low detectability rate.

Calculations for PCR experiments:

Normalized relative expression, in which the relative expression of the target gene is normalized to the relative expression of the three reference genes (18S rRNA, β-actin, and HPRT1 genes) in each sample, was calculated using the formula

Relative expression = $2^{-\Delta Crt}$, where

Delta Crt (ΔCrt) = $Crt_{\text{target gene}} - Crt_{\text{reference gene}}$(403).

This calculation does not consider the basal expression (unstimulated samples) and, therefore, can be used to identify distinct gene expression patterns after stimulation.

Fold change was then calculated, which is the fold difference between a control sample used as a reference and another sample. The gene expression data were then assessed against the three stimulation conditions (IFN-α, IFN-β, and Mtb WCL) with the unstimulated condition as the control sample.

Fold change was calculated using the formula

Fold change = $2^{-\Delta\Delta Crt}$, where

Delta delta Crt ($\Delta\Delta Crt$) = $\Delta Crt_{\text{stimulated}} - \Delta Crt_{\text{unstimulated}}$

Unlike the previous calculation, fold change considers the basal gene expression and is, therefore, a measure of both the change in gene expression levels and the directionality of that change. The fold change calculation gives an expression of 1 (one) for the control group (unstimulated condition) and, for the stimulated conditions, demonstrates either a fold increase (upregulation) or a fold decrease (downregulation) relative to the control sample (403). Significant differentially

expressed genes were defined using an adjusted p-value < 0.05, with $log_2FC \geq 1.0$ being upregulated and $log_2FC \leq 1.0$ downregulated. (404,405).

2.5.5 Cytokine/ chemokine assays

Each sample set up for PCR had a parallel set up for cytokine/ chemokine assays incubated overnight at 37°C in 5% CO_2. Following the 16 to18-hour incubation period, the contents of each of the 24 wells were transferred into appropriately labelled Eppendorf tubes. Each well was rinsed with 500µl R-10, and the contents were transferred to the respective tubes. The tubes containing the stimulated or unstimulated PBMCs were spun at 300 *x g* for 5 minutes, and the culture supernatant was transferred to labelled tubes and stored at -80°Cuntil further processing.

Milliplex assays were done using Milliplex® MAP Human Cytokine / Chemokine kits (EMD Millipore, USA) were used to quantify selected cytokines and chemokines. The first kit was used to assess the detectability of the following 41 human protein analytes in a number of the samples: EGF, Eotaxin, G-CSF, GM-CSF, IFNα2, IFN-γ, IL-1α, IL-1β, IL-10, IL-12P40, IL-12P70, IL-13, IL-15, IL-17A, IL1RA, IL-2, IL-3, IL-4, IL-5, IL-6, IL-7, IL-8, IL-9, IP-10, MCP-1, MCP-3,MIP-1α, MIP-1β, RANTES, TNFα, TNFβ, VEGF,FGF-2, TGF-α, FIT-3L, Fractalkine, GRO, MDC, PDGF-AA, PDGF-AB/BB, and.sCD40L. Based on previous optimization experiments, proteins with less than 15% detectability were excluded narrowing the cytokine panel to 33 protein analytes. FLT-3L, IL-3, IL-5, IL-9, IL-15, IL-17A, TGF-α, and TNF-β were excluded from subsequent kits leaving the analytes listed in Table 5.

Table 5. Cytokines in the MILLIPLEX MAP Human Cytokine/Chemokine Magnetic Bead Panel – 33-Plex assay.

Symbol	**Name**	**Aliases**
EGF	Epidermal growth factor	
FGF-2	Fibroblast growth factor 2	
Eotaxin	Eotaxin	CCL11
G-GSF	Granulocyte colony-stimulating factor	
GM-CSF	Granulocyte-macrophage colony-stimulating factor	
Fractalkine	Fractalkine	CX3CL1
IFN-α2	Interferon-alpha2	IFN-α 2b
IFN-γ	Interferon gamma	
GRO	Growth-regulated protein	CXCL1
IL-10	Interleukin 10	
MCP-3	Monocyte-chemotactic protein 3	CCL7
IL-12p40	Interleukin 12 beta	IL-12B
MDC	Macrophage-derived chemokine	CCL22
IL-12p70	Interleukin 12 subunit alpha	IL-12A
PDGF-AA	Platelet Derived Growth Factor-AA	
IL-13	Interleukin 13	
PDGF-AB/BB	Platelet-Derived Growth Factor-AB/BB	
sCD40L	Soluble CD40 ligand	CD154, TRAP
IL-1RA	Interleukin 1 receptor antagonist	
IL-1α	Interleukin 1α	
IL-1β	Interleukin 1β	
IL-2	Interleukin 2	
IL-4	Interleukin 4	
IL-6	Interleukin 6	
IL-7	Interleukin 7	
IL-8	Interleukin 8	CXCL8
IP-10	Interferon gamma-induced protein 10	CXCL10
MCP-1	Monocyte chemoattractant protein1	CCL2
MIP-1α	Macrophage inflammatory protein 1 alpha	CCL3
MIP-1β	Macrophage inflammatory protein-1 beta	CCL4
RANTES	Regulated on Activation, Normal T Expressed and Secreted	CCL5
TNF-α	Tumor necrosis factor-alpha	
VEGF	Vascular endothelial growth factor	

Milliplex assays were processed according to the manufacturer's instructions. Wash buffer (200 µl) was added to each well, the plate seal and mixed for 10 minutes on a plate shaker at 20 to 25°C, then decanted. 25 µl of samples, standards, and QC controls were pipetted into the respective 24-wells and assay buffer into the background and the sample wells. An equal volume of R10 culture medium was added to the background, standard and QC control wells, and culture supernatant was added to the respective wells, followed by 25 µl of the beads to all wells. The sealed plate was incubated overnight on a shaker at 4°C. Following overnight incubation, the plate was washed twice with 200 µl wash buffer, 25 µl of detection antibodies added to each well, and the sealed plate was incubated on a shaker for 1hr at room temperature. An equal volume of streptavidin-phycoerythrin was added to each well, and the sealed plate was incubated at room temperature for 30 minutes on a shaker. The plate was washed twice on the magnetic plate washer, and 150µl of sheath fluid was added to each well and shaken for a further 5 minutes to re-suspend the beads. The plate was run on Luminex® 200, and data were acquired using Bioplex data Pro software (Bio-Rad, USA).

2.5.5.1 Data analysis

Cytokines with less than 60% detectability in any clinical phenotype group or with any stimulation were excluded from further overall analysis or analysis that focused on the specific groupings in which the cytokine had a low detectability rate.

Comparisons were made between groups for cytokine concentrations. Fold change was calculated using the concentration of cytokine after stimulation/ concentration with no stimulation. Significant differentially expressed cytokines were defined using an adjusted p-value < 0.05, with $\log_2 FC \geq 1.0$ being upregulated and $\log_2 FC \leq 1.0$ downregulated. (404,405).

2.6 Statistical analyses

Data were analysed using IBM SPSS® version 20 (IBM Corp. Released 2011. IBM SPSS Statistics for Windows, Version 20.0. Armonk, NY: IBM Corp.) and GraphPad Prism® version 8.00 for Windows (GraphPad Software, La Jolla California USA, www.graphpad.com)software.

For continuous data, the Shapiro-Wilk normality test was conducted to assess the normality of distribution in each group based on the p-value. Normally distributed data ($p \leq 0.05$) were presented as means and analysed using parametric tests, while non-normally distributed data ($p>0.05$) were presented as medians and analysed using non-parametric tests. The characteristics of participants were summarized as frequencies or means with standard deviation (SD). For participant characteristics with less than five individuals, comparisons between groups and within groups were made using the Fisher-Freeman-Halton Exact test with a p-value <0.05 considered significant. The test is an extension of Fisher's exact test that can be used for contingency tables greater than 2x2 (406).

Data visualization using Principal Component Analysis (PCA) and hierarchical clustering was carried out using Clustvis software (http://biit.cs.ut.ee/clustvis/). PCA was performed to identify gene and cytokine profiles associated with the four clinical phenotypes for the different stimulations. Hierarchical clustering on heatmaps was used to assess genes and cytokines clustering.

For the clinical sample analysis, the data showed non-normal distribution and was analysed using non-parametric tests. Comparisons of quantitative variables between clinical phenotypes with each stimulation condition were made using Kruskal-Wallis test and a post hoc Dunn's test with Bonferroni multiple comparison test. The use of multiple comparisons increases the type I error, increasing the probability of getting a significant test. The Bonferroni multiple comparisons test, therefore, modifies the level for rejection of the null hypothesis by dividing the α (0.05) by the total number of comparisons; therefore, rejection of the null hypothesis is reset at a smaller p-value (407). A p-value <0.05 was considered statistically significant.

For comparisons between IFN-α and IFN-β gene and cytokine responses we used the Wilcoxon signed rank test which tests the difference of repeated measurements done on a single sample.

Correlation analyses between gene expression and the participants' demographic data for each stimulation condition - age, sex, BCG status, TST results, QFT results, and chest X-ray results and between fold changes of genes and cytokines were done using Spearman's rank-order correlation. Spearman' correlation is a non-parametric test that measures the association's strength between the two variables tested and the association's direction using the correlation coefficient

(r_s). The strength of the association was classified as strong positive (negative) correlation [r_s > 0.7 (< -0.7)], moderate positive (negative) correlation [r_s 0.5 to 0.7 (-0.7 to -0.5)], low positive (negative) correlation [r_s 0.3 to 0.5 (-0.5 to -0.3)] or negligible correlation [r_s 0.0 to 0.3 (-0.3 to 0.0)] (408).

CHAPTER 3: RESULTS

3.1 Demographic and clinical characteristics of study participants

The demographic and clinical characteristics of the study participants are outlined in Table 6. Samples from 61 participants were included in this study. The overall mean age of the study groups was 35.90 years (± 11.32). Participants were categorized into healthy controls (HC) (n=11), tuberculin skin test reactive (TST) (n=12), latent TB infection (LTBI) (n=19) and active tuberculosis (ATB) (n=19), and there was no statistically significant difference between infection states by age as assessed by the Fisher Exact test (p= 0.722). Overall, the study population was predominantly female (70.5% vs 29.5%), with the HC and TST groups having higher female representation even though there was no statistically significant difference between infection states (HC, TST, LTBI, and ATB) by sex as assessed by the Fisher Exact test (p = 0.112). The overall study group comprised individuals who self-identified as foreign-born or born outside of Canada (all were reported to be of Filipino heritage) 44.26%, Canadian-born non-Indigenous making up 19.67%, and Canadian-born Indigenous (First Nations, Inuit, and Métis) 36.07%. The Foreign-born and Canadian-born Indigenous made up the majority of the LTBI (78.9%) and the ATB groups (78.9%), respectively. A statistically significant difference was observed between the infection states by ethnicity as assessed by the Fisher Exact test (p< 0.001). Most study participants had received the BCG vaccine (75.4%), while 19.7% had not, and the BCG status for 4.9% of the participants was unknown. The largest proportion of individuals who had received the BCG vaccine was in the TST group (100%) who were reactive to TST, followed by the LTBI group (89.5%) and ATB group (68.4%). There was no significant difference between the infection states by BCG status (p= 0.064). Participants with a previously reported TST positive test made up the bulk of enrollees in the study population (55.7% vs 9.8% TST-negative). By definition, all the participants in the TST group were TST-positive and 73.7% of the LTBI group. A statistically significant difference was observed between the infection states by the reported TST status as assessed by the Fisher Exact test (p< 0.001).

Table 6. Demographic and clinical characteristics of study participants.

Characteristics	**HC (N=11)**	**TST (N=12)**	**LTBI (N=19)**	**ATB (N=19)**	**p-value between groups**
Age (mean years) (SD) [range]	34.73 (12.0) [19-59]	33.58 (11.7) [20-51]	37.89 (9.1) [22-53]	36.05 (13.1) [20-64]	0.722
Sex - **no. (%)**					0.112
Male	2 (18.2)	1 (8.3)	6 (31.6)	9 (47.4)	
Female	9 (81.8)	11 (91.7)	13 (68.4)	10 (52.6)	
Ethnicity - **no. (%)**					**< 0.001**
Foreign-born	2 (18.2)	8 (66.7)	15 (78.9)	2 (10.5)	
Canadian-born non-Indigenous	5 (45.5)	2 (16. 7)	3 (15.8)	2 (10.5)	
Canadian-born Indigenous	4 (36.4)	2 (16.7)	1 (5.3)	15 (78.9)	
BCG - **no. (%)**					0.064
Yes	4 (36.4)	12 (100.0)	17 (89.5)	13 (68.4)	
No	6 (54.5)	0 (0.0)	2 (10.5)	4 (21.1)	
Not known	1 (9.1)	-	0 (0.0)	2 (10.5)	
TST - **no. (%)**					**< 0.001**
Positive	0 (0.0)	12 (100.0)	14 (73.7)	8 (42.1)	
Negative	3 (27.3)	0 (0.0)	1 (5.3)	2 (10.5)	
Not known	8 (72.7)	-	4 (21.1)	9 (47.4)	
Chest X-ray- **no. (%)**					**< 0.001**
Normal	4 (36.4)	10 (83.3)	11 (57.9)	4 (21.1)	
Abnormal	0 (0.0)	0 (0.0)	2 (10.5)	9 (47.4)	
Not known	7 (63.6)	2 (16.7)	6 (31.6)	6 (31.6)	
QFT - **no. (%)**					**< 0.001**
Positive	0 (0.0)	0 (0.0)	19 (100.0)	15 (78.9)	
Negative	11 (100.0)	12 (100.0)	0 (0.0)	3 (15.8)	
Not known	-	-	-	1 (5.3)	

HC: healthy controls, TST: tuberculin skin test, LTBI: latent TB infection, ATB: active TB. Data for age expressed as mean (standard deviation) [range]. Data for sex, ethnicity, BCG, TST, chest X-ray, and QFT expressed as no. (%). p-values determined using Chi-square test between study groups p-value. **Bolded** p-values are significant ($p<0.05$).

Overall, most of the study participants (47.5%) had a normal chest X-rays, while 34.4% had no recorded results. Most of the previous abnormal chest X-ray reports were from ATB patients (47.4%); two individuals with LTBI had previous abnormal chest X-rays. Chest X-ray

findings showed a significant difference between infection states ($p<0.001$). More than half of the study participants were QFT-positive (55.7% vs 42.6% QFT-negative). All the study participants in the HC and TST groups were QFT-negative, and all in the LTBI group were QFT-positive. Most of the ATB patients were QFT-positive (78.9%) which was statistically significant ($p<0.001$). The Fisher Exact test assessed a significant association between QFT results and clinical phenotype ($p< 0.001$).

3.1.1 Summary

Significant differences in the study population were observed between clinical groups in ethnicity (which were more Foreign-born in the TST group and more Canadian-born Indigenous in the ATB group), in the immunological diagnostic assays (TST and QFT) and, as expected, in the chest X-ray findings as these were criteria used to largely define the study groups. However, contrary to the global picture, most of our participants were female, although this difference was not statistically significant. This difference may have been due to the method of participant selection, which was based on the availability of adequate samples, not randomized selection.

3.2 Optimization of stimulation conditions using IFN-α and IFN-β

3.2.1 Determination of IFN-α/β duration and concentration kinetics

To determine the stimulation kinetics for IFN-α (IFN-α2 and IFN-αA) and IFN-β, we selected 15 differentially expressed genes that showed distinct differences in RNA seq experiments previously performed in the lab on PBMCs isolated from two participants with ATB patients and two uninfected controls. Primers listed in Table 3 for the 15 genes *ANKRD22, BATF2, CCL8, CXCL9, CXCL10, CXCL11, ETV7, FCGR1A, IFIT3, IFI44L, ISG15, MSR1, Mx1, SECTM1*, and *SOCS1* were used for the optimization experiments. The PBMCs isolated from healthy donors were stored in liquid nitrogen for at least seven days prior to their use in the stimulation kinetics experiments to replicate the conditions of our clinical samples. Each stimulation kinetics experiment was used to identify the stimulation concentration and kinetics that resulted in the largest change in gene expression.

For optimization experiments, frozen PBMCs from three healthy donors were thawed and rested for one hour at 37°C in 5% CO_2, as outlined in section 2.5 above. Approximately one million

PBMCs were stimulated with three different concentrations of IFN-α (100 IU/ml, 500 IU/ml, and 1000 IU/ml; IFN-αA and IFN-α2 in a 1:1 concentration) and IFN-β (1 ng/ml, 10 ng/ml, and 50 ng/ml), using concentrations identified from previous studies (409–413), and an unstimulated control. The stimulation of PBMC was performed for 4 hours, and RT-qPCR was carried out on the genes listed in Table 3. Gene expression was calculated using the $2^{-\Delta\Delta Ct}$ method (414).

After stimulation with the three concentrations, most of the 15 optimization genes listed in Table 3 showed the highest fold change with 1000 IU/ml IFN-α except IFI44L, which was highest with 500 IU/ml (Figure 9). The combined mean expression for the genes was higher when the cells were stimulated at a concentration of 1000IU/ml IFN-α compared to 500IU/ml and 100IU/ml with fold changes of 14.68±3.266 at 1000IU/ml versus 9.279±1.808 (p=0.0529) at 500IU/ml and versus 3.782±0.7273 (p< 0.0001) at 100IU/ml. After stimulation with IFN-β, most of the genes showed the highest fold change with 10ng/ml except for *FCGR1A*, *BATF2*, and *ETV7*, which were highest with 50ng/ml (Figure 9). The combined mean expression was also higher when cells were stimulated at a concentration of 10ng/ml IFN-β compared to 50ng/ml and 1ng/ml with fold changes of 99.29±28.82 at 10ng/ml versus 91.40±26.27 (p=0.4324) at 50ng/ml and versus 44.91±11.96 (p<0.0001) at 1ng/ml. Based on these findings, the concentrations, 1000IU/ml for IFN-α and 10ng/ml for IFN-β, were selected for subsequent sample stimulations.

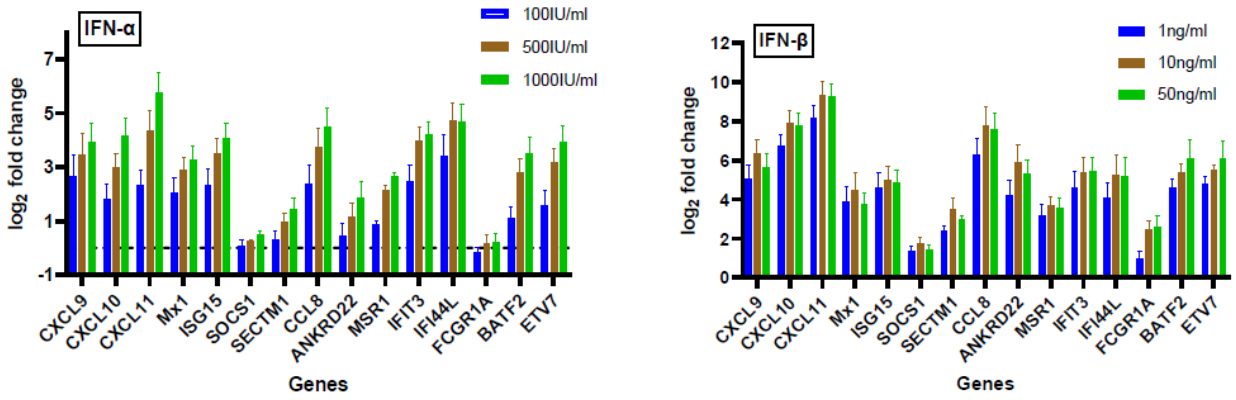

Figure 9. **Concentration titration of gene expression responses of PBMCs to IFN-α or IFN-β stimulation**. PBMCs from three healthy donors were stimulated for 4 hours with IFN-α (100 IU/ml, 500 IU/ml, and 1000 IU/ml) and IFN-β (1 ng/ml, 10 ng/ml, and 50 ng/ml), and an unstimulated control followed by RNA extraction and RT-qPCR assay of the optimization genes listed in Table 3. Fold change in gene expression was calculated using the formula $2^{-\Delta\Delta Ct}$. Data are presented as mean with SEM.

The concentrations of IFN-α and IFN-β selected from the optimization experiments were used to assess the kinetics of the stimulation with 1000 IU IFN-α and 10ng/ml IFN-β in PBMCs from three healthy donors at three timepoints- 1 hour (T_{1hr}), 4 hours (T_{4hr}), and overnight stimulation (16-18 hours) ($T_{o/n}$). Most of the 15 optimization genes listed in Table 3 showed the highest fold change with IFN-α at T_4 except *SOCS1*, *CXCL10*, *BATF2* and *ANKRD22*, which had the highest expression at T_1 (figure 10). The combined mean expression for all the genes was higher when the cells were stimulated for 4 hours compared to the 1 hour and overnight stimulation (Fold change 30.31±7.765 versus 17.62±4.492 (p> 0.999) at T_{1hr} and versus 3.992±0.637 (p=0.0024) at $T_{o/n}$) (Figure 10). The highest fold change after stimulation with 10ng/ml IFN-β was at T_4 for most optimization genes except for *FCGR1A*, *SOCS1*, *CXCL10*, *BATF2*, *IFI44L*, and *ANKRD22*, with expression highest at T_1, and *MSR1* at $T_{o/n}$ (Figure 10). The combined mean fold change for IFN-β was highest at T_{4hr} (Fold change 214.7±87.86 versus 142.4±34.72 (p> 0.999) at T_{1hr} and 23.82±7.527 (p=0.0179) at $T_{o/n}$). Based on these findings, the 4-hour duration of stimulation was used for subsequent experiments. For Mtb WCL, a concentration previously determined by our group (50ug/ml) was used, and PBMCs were stimulated for 4 hours as described in previous studies (415,416).

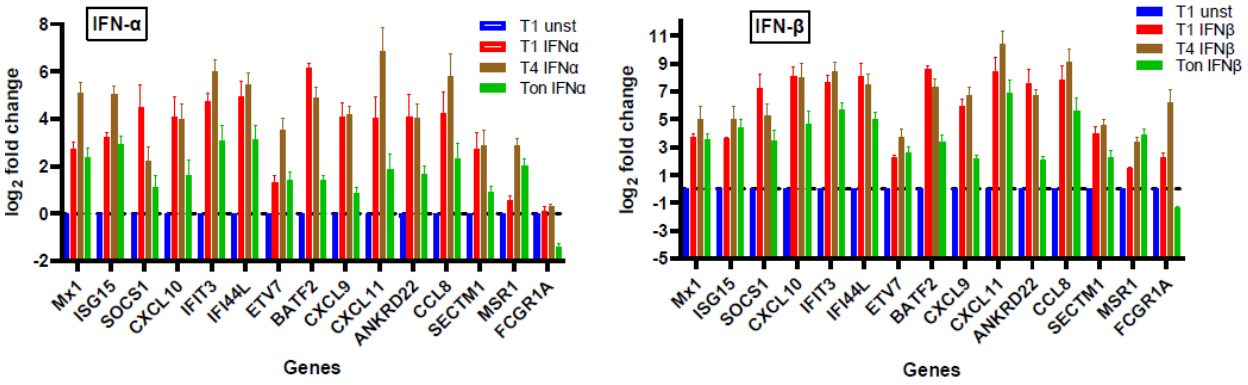

Figure 10. **Kinetics of gene expression responses by PBMCs to IFN-α and IFN-β stimulation**.
PBMCs from three healthy donors were stimulated with IFN-α or IFN-β for 1 hour (T_1), 4 hours (T_4), and overnight ($T_{o/n}$) and an unstimulated control, followed by RNA extraction and RT-qPCR assay of the optimization genes listed in Table 3. Fold change in gene expression was calculated using the $2^{-\Delta\Delta Ct}$ method. Data are presented as mean with SEM.

3.3 Analysis of gene expression in clinical samples

After determining the optimized conditions, clinical samples were tested using OpenArray chips as described in the Methods section to assess 53 ISGs and 3 reference genes listed in Table 4 from study groups – HC, TST, LTBI and ATB. PBMCs from each study participant were divided into four parts, each with one million cells. The cells were stimulated with 1000IU/ml IFN-α, 10ng/ml IFN-β, 50μg/ml Mtb WCL, and an unstimulated sample for 4 hours. RNA was extracted from the PBMCs and RT qPCR using the OpenArray plate on the Quantstudio platform to get Crt values.

3.3.1 Comparison of relative ISG expression between clinical groups in baseline samples

Previous transcriptional profiling studies have described an increased expression of IFN stimulated genes (ISGs) in ATB compared to controls in baseline blood samples ex-vivo (189,352,376). To explore whether a similar transcriptional profile would be observed in PBMCs from our dataset, the expression of each gene was first evaluated at baseline in the four study groups and compared to that of the control group (HC). PBMCs isolated from study participants were cultured for 4 hours with no stimulation, RNA was isolated, and RT-qPCR was carried out. The Crt results acquired on the Quantstudio platform were used to calculate the relative expression using the ΔCt method for each gene normalized to the reference genes.

3.3.1.1 Clustering analysis of relative expression in unstimulated samples

To get a general overview of the data, the relative expression at the specific gene level was evaluated. The mean ISG expression of HC was compared to the expression of each of the other *M. tuberculosis* infection groups (Figure 11). There was no statistically significant difference between the groups as determined using the Mann-Whitney test.

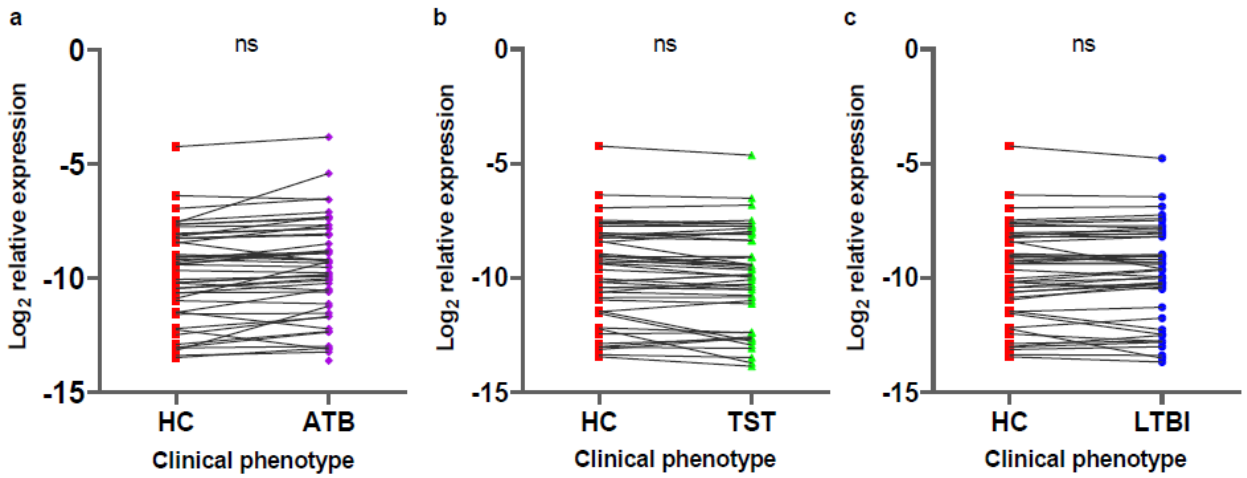

Figure 11. **Relative ISG expression in ATB, TST and LTBI compared to HC**.
Unstimulated PBMCs from ATB (n=19), HC (n=11), LTBI (n=19), and TST (n=12) were incubated for 4 hours, RNA extracted and processed using RT-qPCR for detection of selected ISGs. Relative expression was calculated using the formula $2^{-\Delta Ct}$. Each dot represents the mean relative expression of each ISG; each line connects the mean relative expression of an ISG in HC to that of the same ISG in a) ATB, b) TST, and c) LTBI. Mann-Whitney test was used for comparisons of relative expression between HC and the other study groups. ns – not significant, $p<0.05$

To better understand individual ISG differences at baseline, hierarchical clustering was used to explore whether relative gene expression of the genes would cluster by clinical groups using Clustvis (http://biit.cs.ut.ee/clustvis/). Hierarchical clustering is a method used to identify genes that are similar together in groups known as clusters and was used to find out whether relative expression of unstimulated samples would cluster the genes by clinical phenotype. The data was uploaded into Clustvis to visualize gene expression profiles in baseline samples from the four clinical phenotypes. As per the recommendations on Clustvis for data with values between 0 and 1, data was log-transformed to reduce the skewness of the data. Cluster analysis using principal component analysis (PCA) did not cluster genes by infection state (Figure 12).

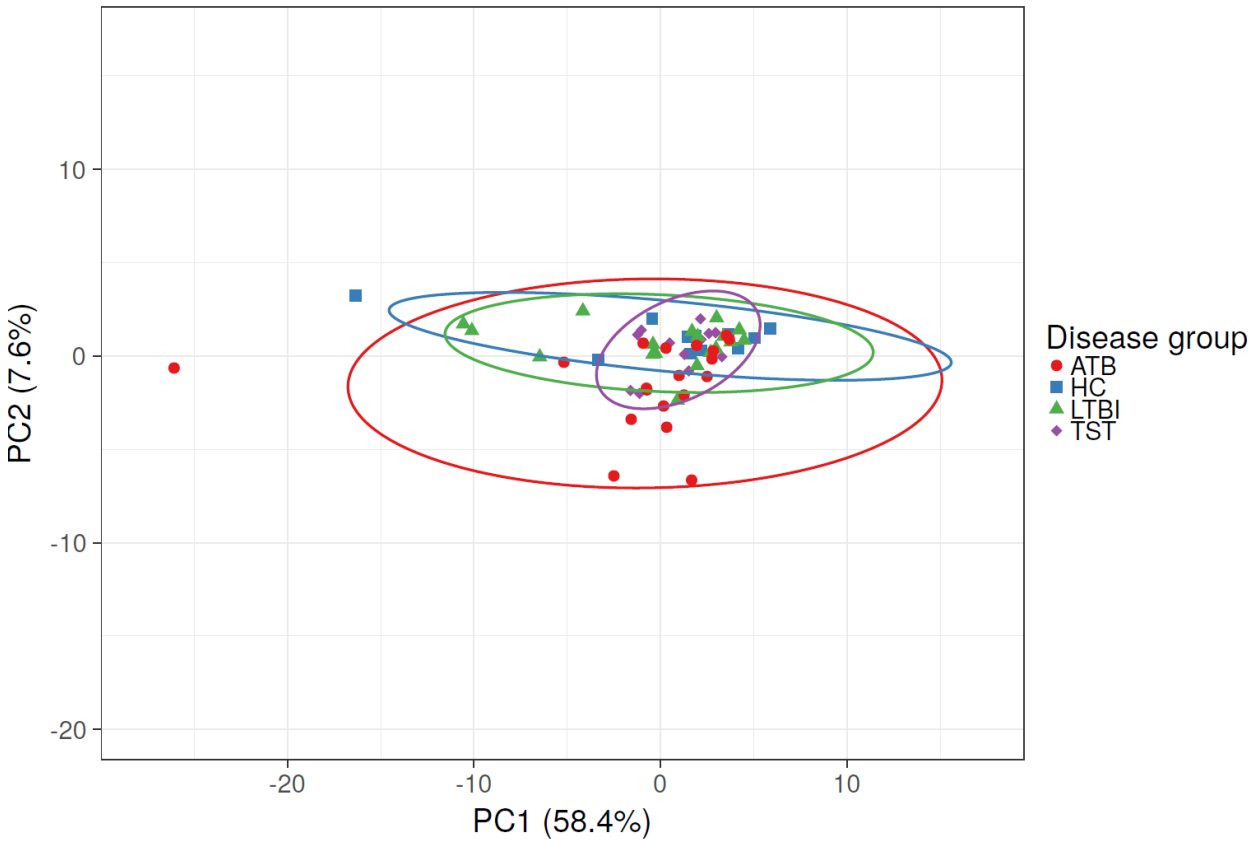

Figure 12. Principal component analysis of relative ISG expression with no stimulation.

Unstimulated PBMCs from ATB, HC, LTBI, and TST were incubated for 4 hours, RNA extracted and processed using RT-qPCR for detection of 53 ISGs. Relative expression was calculated using the formula $2^{-\Delta Ct}$. The original values for 52 genes were uploaded into Clutvis (http://biit.cs.ut.ee/clustvis/) and log transformed. The clinical groups are represented by shapes – red circle=ATB, blue square=HC, green triangle=LTBI, purple rhombus=TST.

Cluster analysis was also assessed using a heatmap. The *CAMP* gene was excluded from the analysis since the gene was undetectable in most samples. As can be seen in Figure 13, the expression pattern of the 52 ISGs varies considerably between individuals, but there was no clustering of the ISGs by clinical groups, which were equally distributed by the clustering algorithm. The columns show the clinical phenotypes; the rows list the genes on the right, while the left axis shows genes that cluster together.

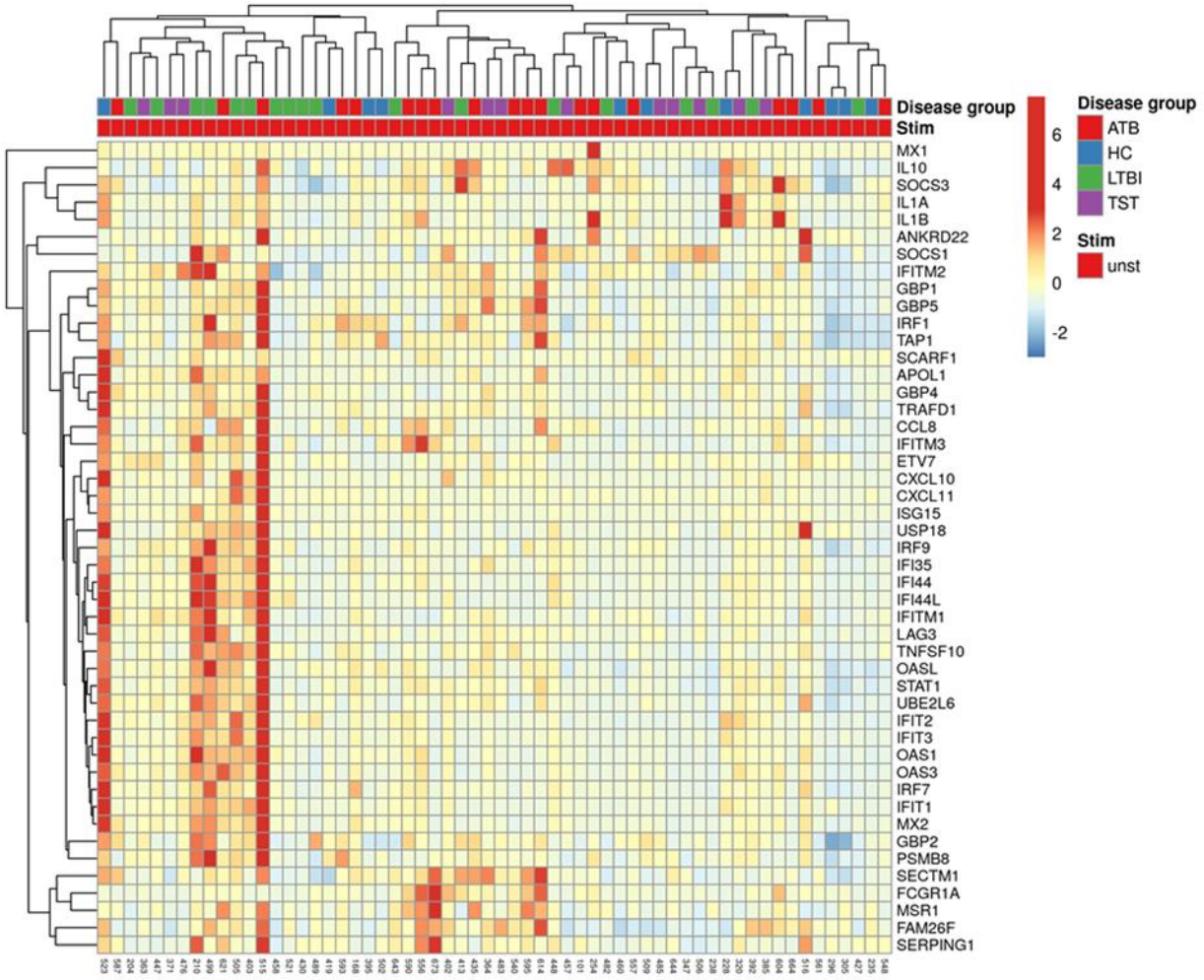

Figure 13. Heatmap showing unsupervised clustering of 52 ISGs in baseline samples.

Baseline PBMCs from study participants in ATB, HC, LTBI, and TST groups were thawed and incubated for 4 hours, RNA extracted and processed using RT-qPCR for detection of 53 genes. Relative expression was calculated using the formula $2^{-\Delta Ct}$. The original values for 52 genes were uploaded into Clutvis (http://biit.cs.ut.ee/clustvis/) and log-transformed. The rows show the genes – blue color indicates low expression; red color indicates high expression). Columns show the clinical phenotypes (red=ATB; blue=HC; green= LTBI; purple=TST).

3.3.1.2 Comparison of relative ISG expression across clinical groups at baseline.

To examine the baseline levels of expression at the single gene level, the individual relative expression of the ISGs was then assessed in unstimulated samples. The detection rate for each gene was determined and, using a cut-off of 60% detection in the samples, excluded *BATF2*, *CAMP*, *CXCL9*, *FCGR1B*, *IL-12B*, and *SEPT4* from further statistical analysis in baseline samples. First, we conducted a pathway analysis to identify the signaling pathways in which the genes were

involved to better group the results. Using REACTOME enrichment analysis from STRING analysis (https://string-db.org/), we identified genes involved in signaling pathways. The genes were enriched in IFN signaling (28 genes), of which 12 genes were specific to type I IFN signaling, five (5) to the IFN-γ signaling pathway, 10 were common to the type I and IFN-γ signaling pathways, with one gene not grouped to any specific IFN pathway (Figure 14). In addition, four genes were enriched for IL-10 signaling. The remaining genes were not enriched for any signaling pathway and were grouped together.

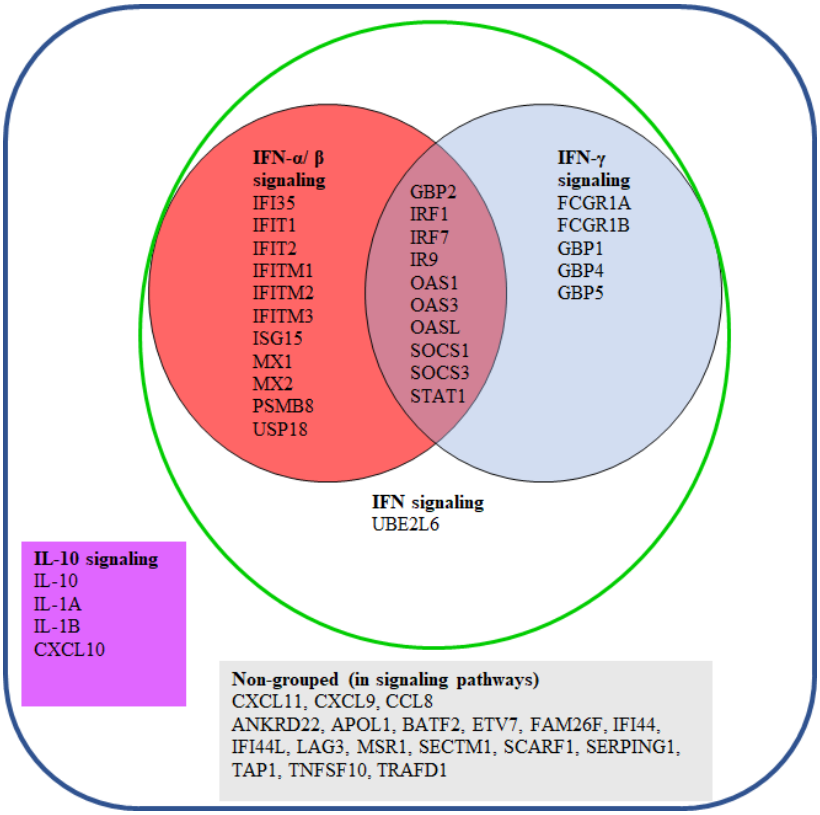

Figure 14. Venn diagram demonstrating the relationship of genes in dataset.

Genes were entered into https://string-db.org/ for analysis. The results represent the Reactome enrichment analysis. Genes in the green open circle were enriched for IFN signaling, the red filled circle for IFN-α/β signaling, the blue filled circle for IFN-γ signaling, with overlapping genes in both pathways. Genes in the purple filled square were enriched for IL-10 signaling; genes in the light gray rectangle were not enriched for any signaling pathway.

Using the relative expression of the 47 genes with a greater than 60% detection rate, each gene's median expression was determined for each clinical phenotype shown in Figure 15. Overall, more than half the genes tested (59.2%) showed higher expression in ATB than in LTBI; 40.2% showed higher expression in LTBI than in ATB (Table S1).

Kruskal-Wallis test was conducted to determine statistically significant differences between the median relative expression values of these measured genes across the four clinical phenotypes. A significant p-value indicates that the median value of at least one clinical phenotype differs from that of another. Three of the 47 genes interrogated showed differences among the groups - *FCGR1A*, *MSR1*, and *SECTM1*. The expression of *FCGR1A* gene was highest in ATB followed by TST, HC, and lowest in LTBI groups (median for HC, TST, LTBI, ATB: 0.000108, 0.000116, 0.000078, 0.000239; p=0.001) (Figure 15). The expression of the *MSR1* gene was highest in ATB, with a potential stepwise decrease in expression from LTBI to TST to HC (median for HC, TST, LTBI, ATB: 0.000406, 0.000575, 0.000809, 0.001292; p=0.002). Similarly, the expression of *SECTM1* gene was also highest in ATB followed by TST, LTBI, with the lowest expression in HC (median for HC, TST, LTBI, ATB: 0.000293, 0.000413, 0.000356, 0.000587; p=0.002).

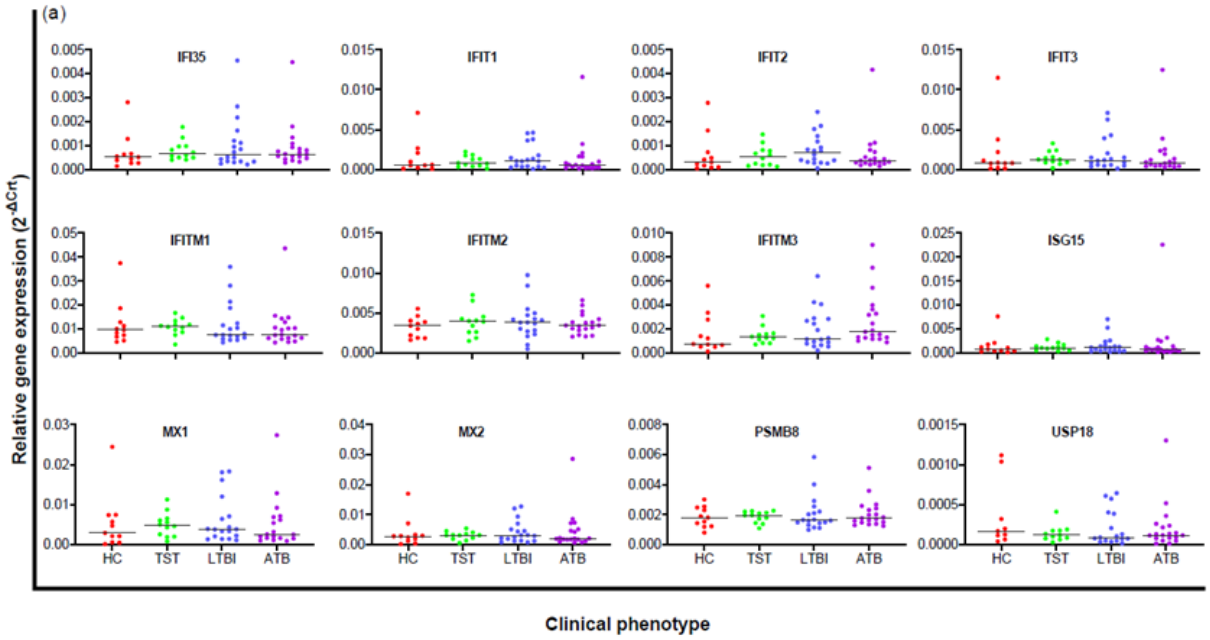

Figure 15: Relative ISG expression in baseline samples.

Genes enriched for (a) IFN-α/β signaling pathway, (b) IFN-γ signaling pathway, (c) IFN-α/β and IFN-γ signaling pathways, (d) IFN signaling, (e) IL-10 signaling pathway, and (f) Not classified. RT qPCR analysis of mRNA expression of ISGs in baseline PBMCs from study participants in HC, TST, LTBI, and ATB groups was normalized to 18S rRNA, β-actin and HPRT1(ΔCt). Relative gene expression was calculated as $2^{-\Delta Ct}$. Data are presented as median. Each dot represents one participant. Kruskal-Wallis test was performed to assess differences between clinical phenotypes. A significant p-value indicates that the median value of at least one clinical phenotype differs from that of another clinical phenotype. * $p< 0.05$, ** $p< 0.01$, ***$p\leq 0.001$. Genes were listed according to Figure 14. Symbol color: red=HC, green=TST, blue=LTBI, purple=ATB. x-axis = clinical phenotype; y-axis= relative expression.

Figure 15: continued

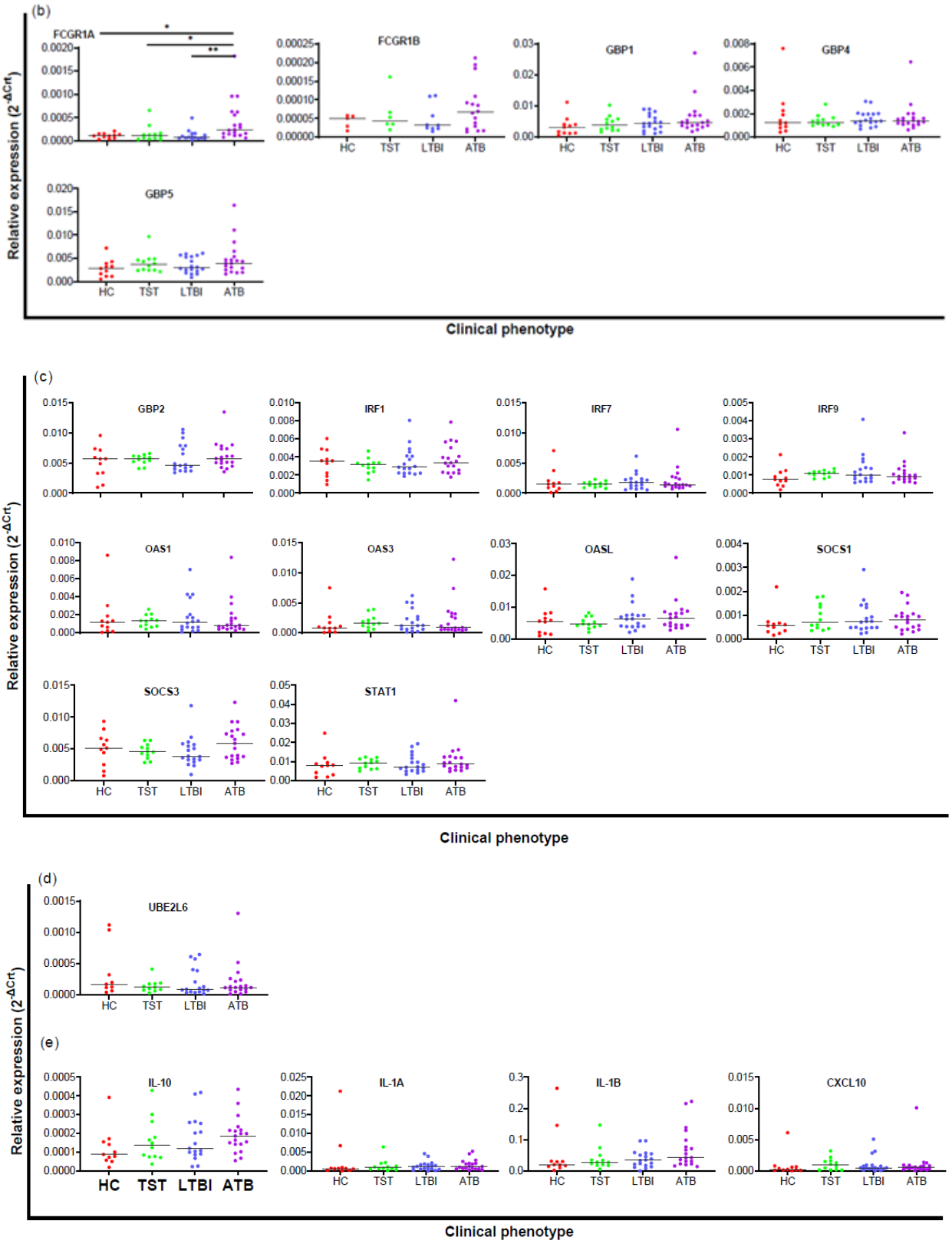

Figure 15: continued

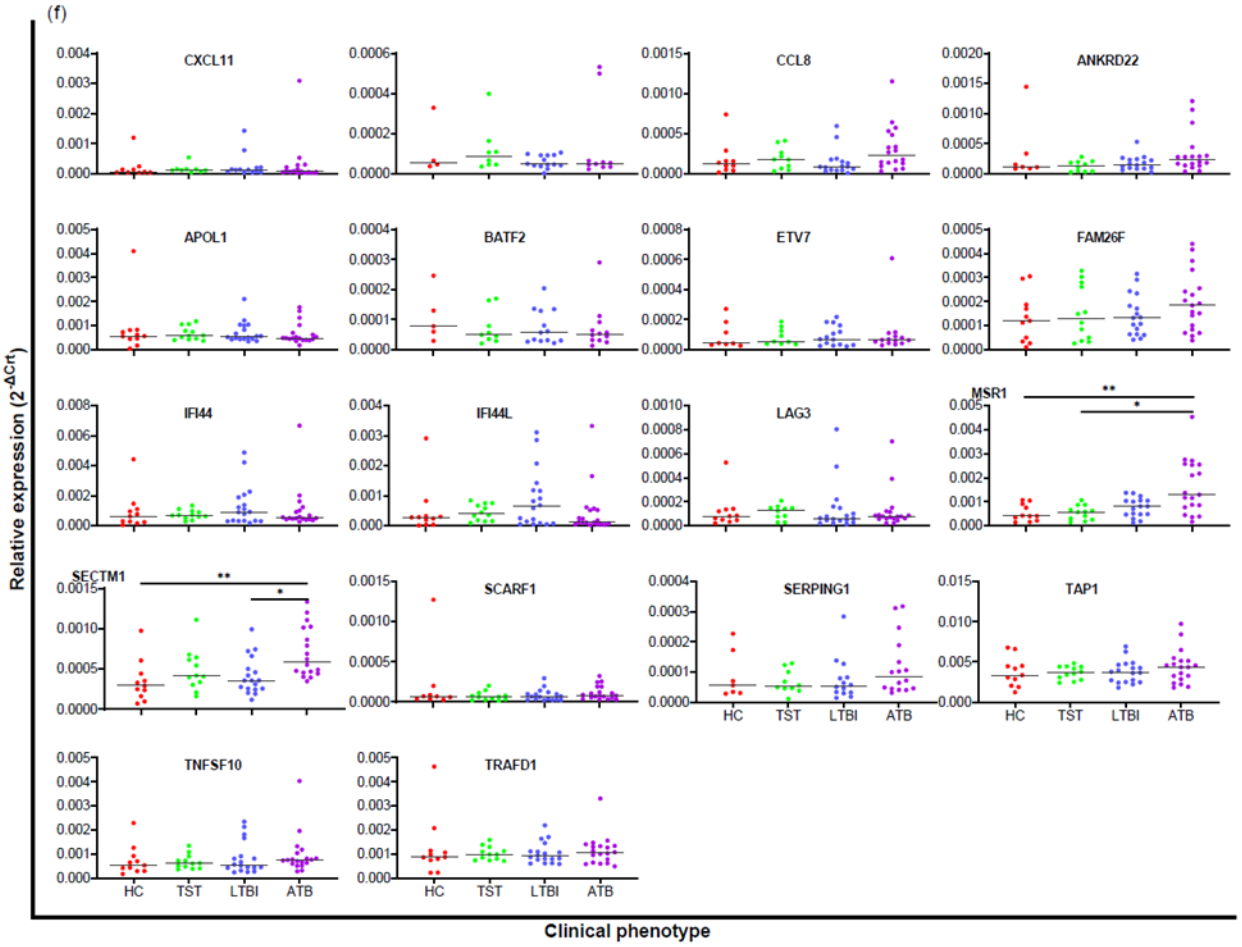

3.3.1.3 Comparison of relative ISG expression between clinical groups at baseline.

For the expression of *FCGR1A*, *MSR1*, and *SECTM1* genes that were differentially expressed across the four study groups identified using the Kruskal-Wallis test, pairwise comparisons using Dunn's procedure were subsequently performed to identify the specific pairs of medians that differed significantly, followed by post hoc analysis using Bonferroni correction for multiple comparisons. Dunn's procedure compares the medians of all pairs to identify those that differ significantly- ATB vs HC, ATB vs TST, ATB vs LTBI, TST vs HC, TST vs LTBI, and LTBI vs HC. Pairwise comparison outlined in Table 7 revealed significant differences in *FCGR1A* gene expression median between the ATB and HC groups (median: 0.000239 vs 0.000108; p=0.003), the ATB and TST groups (median: 0.000239 vs 0.000116; p=0.004), and the ATB and LTBI groups (median: 0.000239 vs 0.000078; p<0.001). Differences were also identified in the expression of the *MSR1* gene between the ATB and HC groups (median: 0.001292 vs 0.000406; p=0.001) and between the ATB and TST groups (median: 0.001292 vs 0.000575; p=0.002); and for *SECTM1* gene between the ATB and HC (median: 0.000587 vs 0.000293; p<0.001) and between the ATB and LTBI groups (median: 0.000587 vs 0.000356; p=0.003). However, the use of multiple comparisons increases the type I error, increasing the probability of getting a significant test. The Bonferroni adjustment, therefore, modifies the level for rejection of the null hypothesis by dividing the α (0.05) by the total number of comparisons; therefore, rejection of the null hypothesis is reset at a smaller p-value (407). For the adjusted p-value, a strict Bonferroni threshold would be a $p < 0.0083$ (0.05 ÷ number of comparisons); a less stringent significance p-value of p<0.05 was set. Statistically significant differences were identified in the expression of the *FCGR1A* gene between the ATB and HC groups (p=0.018), the ATB and TST groups (p=0.027), and the ATB and LTBI groups (p=0.003) (Table 7). Differences in expression of *SECTM1* gene between the ATB and HC (p=0.002) and between the ATB and LTBI groups (p=0.016); and of *MSR1* gene between the ATB and HC groups (p=0.009) and between the ATB and TST groups (p=0.012). For the three differentially expressed genes, higher expression was observed in ATB for all significant comparisons.

Table 7. Genes differentially expressed in unstimulated samples between clinical groups (relative expression).

					Post hoc analysis	
Gene	**N**	**Chi-square (χ2)**	**p-value[a]**	**Comparison[b]**	**p-value[c]**	**adjusted p-value[d]**
FCGR1A	57	16.479	0.001	ATB-LTBI	< 0.001	**0.003**
				ATB-HC	0.003	**0.018**
				ATB-TST	0.004	**0.027**
SECTM1	59	15.206	0.002	ATB-LTBI	0.003	**0.016**
				ATB-HC	< 0.001	**0.002**
MSR1	59	14.348	0.002	ATB-HC	0.001	**0.009**
				ATB-TST	0.002	**0.012**

ATB-active tuberculosis; TST- Tuberculin skin test positive; LTBI-latent tuberculosis infection; HC-healthy controls. N: total number of individuals in whom gene is detected. Comparisons of relative expression data between clinical groups using Kruskal-Wallis test with post hoc pairwise comparisons and Bonferroni correction for multiple comparisons. **Bolded** and yellow highlighted p-values are significant after Bonferroni correction ($p<0.05$). Chi square (χ^2) is the square of the difference between the observed values and the expected values. p-values: [a] – across groups p-value; [c]–pairwise comparison (between groups) p-value; [d]–adjusted p-value using Bonferroni correction for multiple comparisons; [b] – the order in the comparison shows the direction of the difference with the higher expression listed first.

3.3.1.4 Summary

This study sought to determine the baseline expression of ISGs in TB. The sub-hypothesis tested was that ISGs expression would be higher in ATB patients compared to LTBI and healthy individuals. The expression of a panel of ISG genes was assessed in baseline PBMCs from study participants in ATB, individuals who were TST reactive, LTBI and HC. Overall, about half the genes tested supported the sub-hypothesis with the highest expression in ATB, although only three of the genes- *FCGR1A*, *MSR1*, and *SECTM1*- were differentially expressed between ATB and LTBI (*FCGR1A* and *SECTM1*), ATB and TST (*FCGR1*A, and *MSR1*), and ATB and HC (*FCGR1A*, *MSR1*, and *SECTM1*).

3.3.2 Comparison of ISG expression genes between clinical groups following IFN-α and IFN-β stimulation

Increased levels of type I IFNs in murine models of *M. tuberculosis* infection and the overrepresentation of type I IFN stimulated genes in patients with ATB suggest that type I IFNs are linked to TB pathogenesis (33,189,352). This enrichment of type I IFN stimulated genes has been described from ex-vivo unstimulated whole blood or PBMCs (189,352,376). However, this was not observed in our study with the exception of the differentially expressed genes - *FCGR1A*, *MSR1*, and *SECTM1* genes. The three genes also showed their highest expression in unstimulated PBMCs from ATB patients. Although *M. tuberculosis* infection induces the production of type I IFNs (33,372), studies that assessed the effect of *M. tuberculosis*-specific antigen stimulation-ESAT-6 and CFP-10 (384) and PPD (385) in TB did not show a similar induction of type I IFN stimulated genes.

IFN-α and IFN-β are key drivers of the innate and acquired immunity, and stimulation with these factors results in important downstream effects. Therefore, it is important to understand the potential effects of these IFN subtypes on gene expression in *M. tuberculosis* infection phenotypes and their potential role in TB pathogenesis. We, therefore, set out to interrogate the potential drivers or inducers of the type I IFN signature observed in ATB by assessing the specificity of IFN-α and IFN-β on the expression of genes and the potential differences between the expression of these genes.

To study these effects, PBMCs from study participants classified as HC (n=11), TST (n=12), LTBI (n=19) and ATB (n=19) were stimulated with either 1000 IU/ml or 10ng/ml IFN-β or left unstimulated as a control. RNA was extracted from the PBMCs pellet, and RT qPCR was carried out on the Quantstudio platform to assess 53 ISGs and 3 reference genes listed in Table 5. Using the Crt results acquired, the relative expression of the 53 ISGs was calculated using the $2^{-\Delta Ct}$ method, where Delta Crt (ΔCrt) = $Crt_{target\ gene} - Crt_{reference\ gene}$.

3.3.2.1 Clustering analysis of relative expression in unstimulated-, IFN-α-, or IFN-β- stimulated samples

First, cluster analysis was conducted to evaluate the differences in gene expression following stimulation among the various *M. tuberculosis* infection states. For this analysis, the unstimulated, IFN-α- and IFN-β-induced relative expression data was uploaded into Clustvis

(http://biit.cs.ut.ee/clustvis/), log-transformed the data to visualize gene expression profiles in unstimulated, IFN-α and IFN-β-stimulated samples from the four clinical phenotypes. Cluster analysis using principal component analysis (PCA) separated the genes into two clusters – one cluster comprised genes from the unstimulated samples, the other formed an overlap of expression of genes after stimulation with IFN-α and IFN-β – but failed to pick differences between infection states (Figure 16).

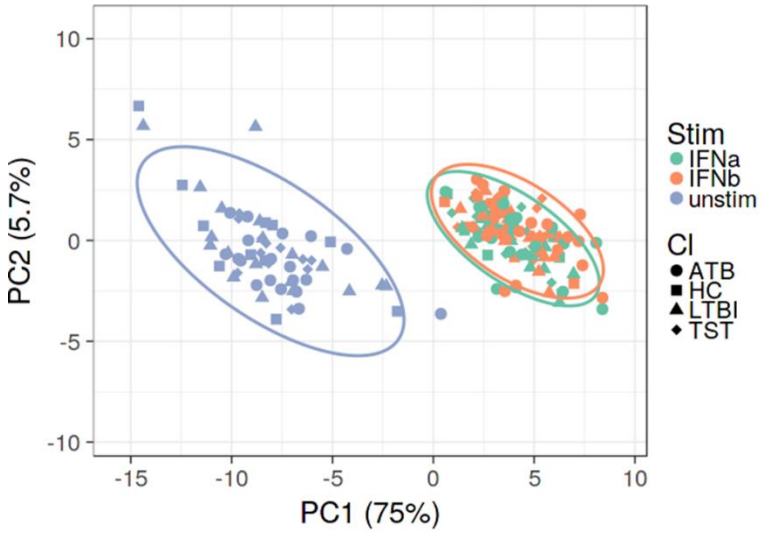

Figure 16. **Principal component analysis of relative ISG expression with no stimulation and in response to IFN-α and IFN-β.**

Unstimulated or IFN-α/β-stimulated PBMCs from ATB, HC, LTBI, and TST were incubated for 4 hours, RNA extracted and processed using RT-qPCR for detection of 53 genes. Relative expression was calculated using the formula $2^{-\Delta Ct}$. The original values for 52 genes were uploaded into Clutvis (http://biit.cs.ut.ee/clustvis/) and log transformed. The stimulations are represented in color by green= IFN-α, orange=IFN-β, and blue=unstimulated. The clinical groups are represented by shapes - circle=ATB, square=HC, triangle=LTBI, rhombus=TST.

Further to this, hierarchical clustering of the relative ISG expression was assessed by using heatmap analysis using the Clustvis software. As expected, most of the ISGs showed increased expression with both the IFN-α- and IFN-β stimulations compared to that observed in baseline samples (Figure 17). The exception to this finding was the expression of IL-1A and IL-1B genes that appear to show reduced expression with the IFN-α- and IFN-β-stimulation relative to no stimulation. There was a clear distinction between the unstimulated gene expression and that of the IFN-stimulated conditions, but no clear distinction between the IFN-α- and IFN-β-stimulation

clustering profile similar to what was observed with the PCA analysis. Similarly, we failed to see any obvious clustering by *M. tuberculosis* infection groups as groups were equally distributed by the clustering algorithm. The columns show the *M. tuberculosis* infection groups; the rows list the genes on the right, while the left axis shows genes that cluster together.

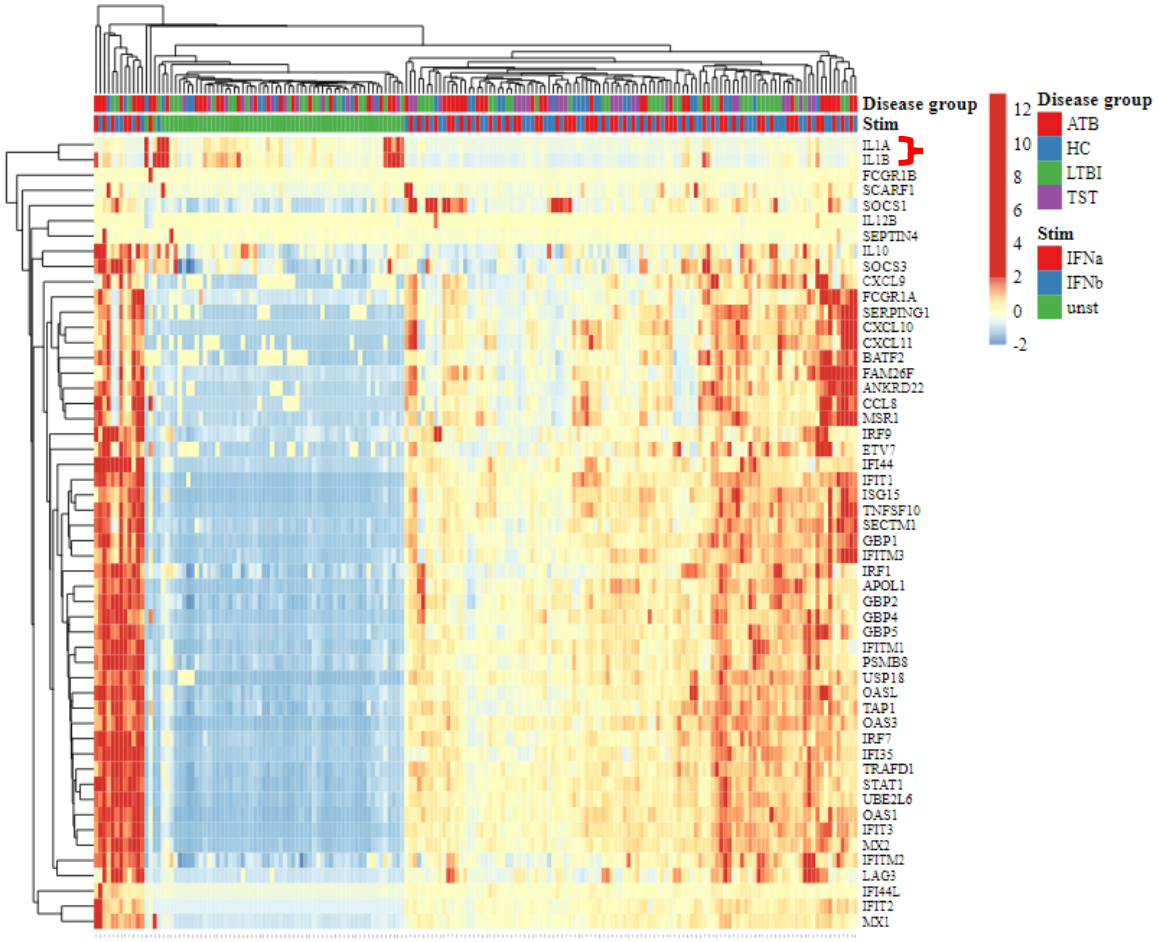

Figure 17. **Heatmap of relative ISG expression of in unstimulated, or IFN-α- or IFN-β -stimulated PBMCs**. PBMCs from ATB, HC, LTBI, and TST groups were unstimulated or IFN-α/β-stimulated for 4 hours, RNA extracted and processed using RT-qPCR for detection of 53 ISGs. Relative expression was calculated using the formula $2^{-\Delta Ct}$. The original values for 52 genes were uploaded into Clutvis (http://biit.cs.ut.ee/clustvis/) and log transformed. The rows show the genes – blue color indicates low expression; red color indicates high expression). Columns show the clinical phenotypes (red=ATB; blue=HC; green= LTBI; purple=TST). Red and blue indicate higher and lower relative gene expression, respectively. Both rows and columns are clustered using correlation distance and average linkage.

3.3.2.2 Comparison of the relative ISG expression of across clinical groups following IFN-α or IFN-β stimulation.

After data visualization using PCA and the heatmap, the data was interrogated at the individual gene level. The median relative expression values for each gene in the IFN-stimulated samples were tested using the Kruskal-Wallis test to assess for statistically significant differences across the median of the relative expression values from IFN-stimulation between clinical groups. The relative expression was calculated using the ΔCt method gene expression and assessed for distinct gene expression patterns with stimulation irrespective of the baseline levels. As can be seen in Figure 18, a trend of increased expression was observed for most genes with IFN-α and IFN-β stimulation except for *IL-1A* and *IL-1B* genes.

Using the relative expression method, less than half of the ISGs (45.1%) had higher expression in ATB compared to LTBI after stimulation with IFN-α; 54.9% had a higher expression in LTBI than in ATB (Table S1). With IFN-α stimulation significant differences were identified in expression across clinical groups for several ISGs that had higher expression in ATB compared to the other clinical groups - *ANKRD22*, *CCL8*, *FCGR1A*, *FCGR1B*, and *MSR1* (Figure 18). The expression of *ANKRD22* gene was highest in ATB followed by HC, LTBI and TST (median for HC, TST, LTBI, ATB: 0.002588, 0.002376, 0.002482, 0.003765; p=0.019); *CCL8* gene in ATB followed by HC, TST and LTBI (median for HC, TST, LTBI, ATB: 0.15753, 0.14111, 0.013818, 0.022401; p=0.046); *FCGR1A* gene in ATB followed by HC, TST and LTBI (median for HC, TST, LTBI, ATB: 0.000742, 0.000700, 0.000604, 0.001381; p=0.008); *FCGR1B* gene in ATB followed by LTBI, TST, and HC (median for HC, TST, LTBI, ATB: 0.000090, 0.000114, 0.000122, 0.000305; p=0.0013); and *MSR1* gene in ATB followed by HC, LTBI and TST (median for HC, TST, LTBI, ATB: 0.008749, 0.007011, 0.008058, 0.011690; p=0.039).

Following IFN-β stimulation, less than half the ISGs (41.2%), had higher expression in ATB compared to LTBI after IFN-β stimulation whereas 58.8% had higher expression in LTBI than in ATB (Table S1). Significant differences were identified in the expression of a similar ISG profile as with IFN-α stimulation - *ANKRD22*, *CCL8*, *FCGR1A*, *FCGR1B*, and *MSR1*, and in addition in *FAM26F*, with higher expression in ATB (Figure 18). *ANKRD22* gene expression was highest in ATB followed by LTBI, HC and TST (median for HC, TST, LTBI, ATB: 0.002630, 0.002131, 0.002805, 0.004685; p=0.024); *CCL8* gene was highest in ATB followed by HC, TST,

and LTBI (median for HC, TST, LTBI, ATB: 0.020688, 0.016840, 0.016775, 0.028615; p=0.045); *FCGR1A* gene in ATB then LTBI, HC and TST (median for HC, TST, LTBI, ATB: 0.000628, 0.000554, 0.000847, 0.001573; p=0.001); *FCGR1B* in ATB, LTBI, TST then HC (median for HC, TST, LTBI, ATB: 0.000078, 0.000093, 0.000161; 0.000318; p=0.001); and *MSR1* in ATB then LTBI, HC and TST (median for HC, TST, LTBI, ATB: 0.008663, 0.007266, 0.009928, 0.013216; p=0.041). *FAM26F* gene expression was elevated only with IFN-β stimulation with the highest expression in ATB, then LTBI, TST and HC (median for HC, TST, LTBI, ATB: 0.001232, 0.001306, 0.001518, 0.002338; p=0.035).

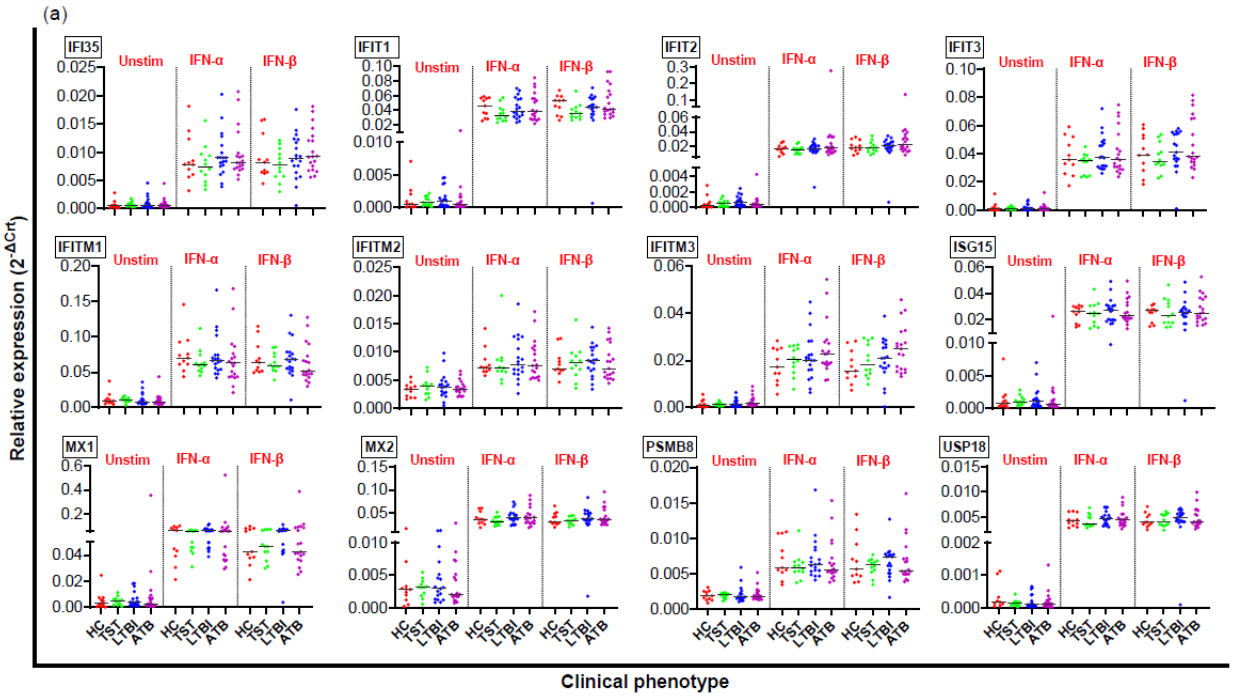

Figure 18. Relative ISG expression in unstimulated, IFN-α, or IFN-β-stimulated samples.

Genes enriched for (a) IFN-α/β signaling pathway, (b) IFN-γ signaling pathway, (c) IFN-α/β and IFN-γ signaling pathways, (d) IFN signaling, (e) IL-10 signaling pathway, and (f) Not classified. RT qPCR analysis of mRNA expression of ISGs in unstimulated PBMCs was normalized to 18S rRNA, β-actin and HPRT1(ΔCt). Relative gene expression was calculated as $2^{-\Delta Ct}$. Data are presented as median; each circle represents one participant. Kruskal-Wallis test was performed to assess differences between clinical phenotypes, * $p< 0.05$, ** $p< 0.01$, ***$p\leq 0.001$. Genes were listed according to Figure 14. Symbol color: red=HC, green=TST, blue=LTBI, purple=ATB. x-axis= Clinical phenotype and stimulation; y-axis= relative expression.

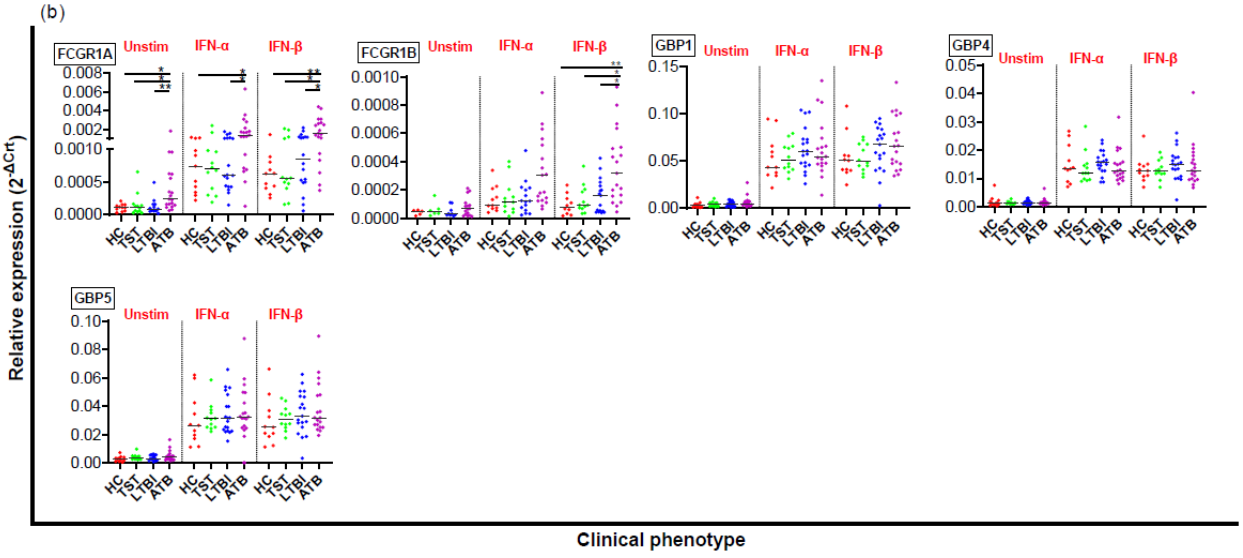

Figure 18: continued

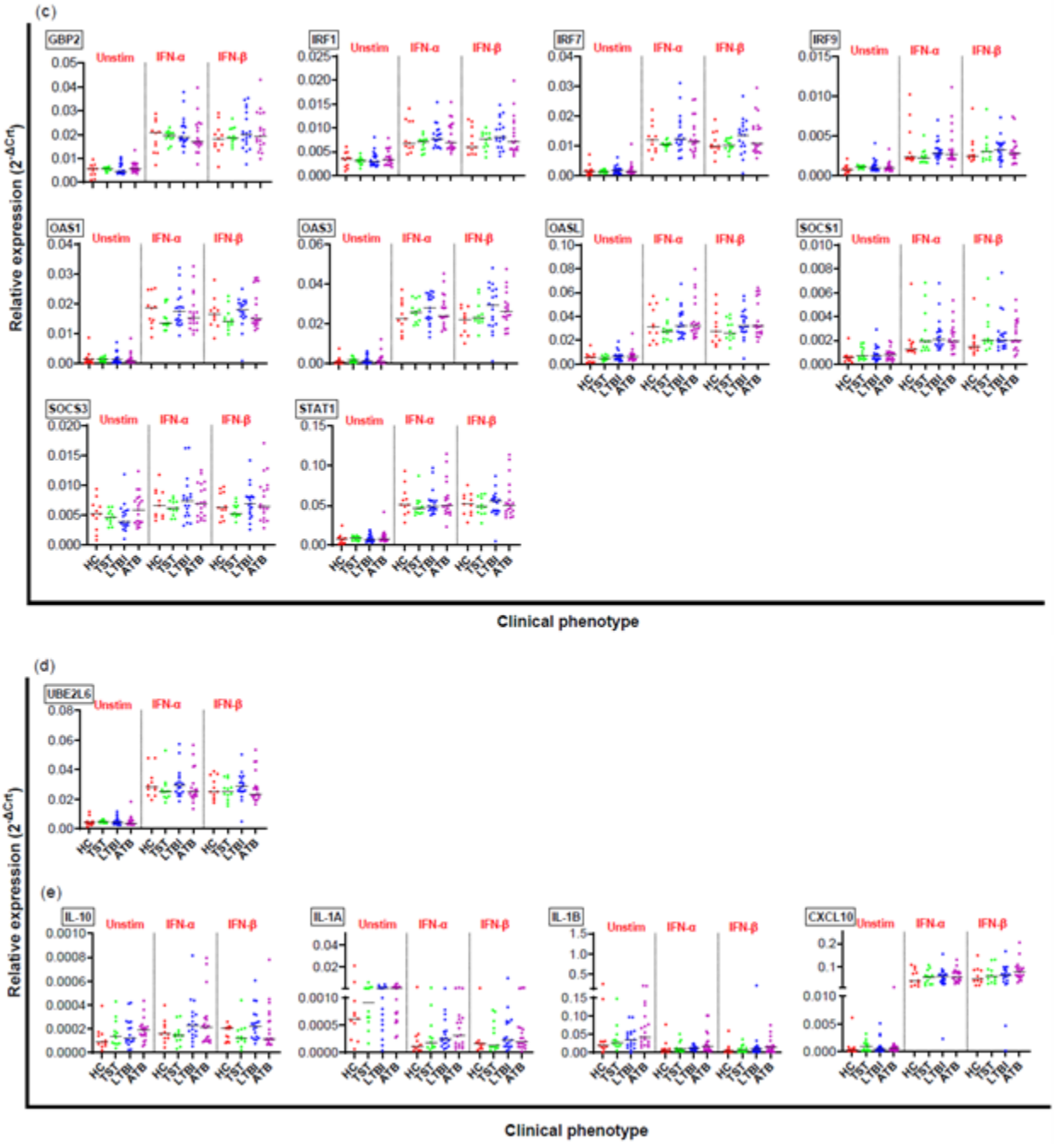

Figure 18: continued

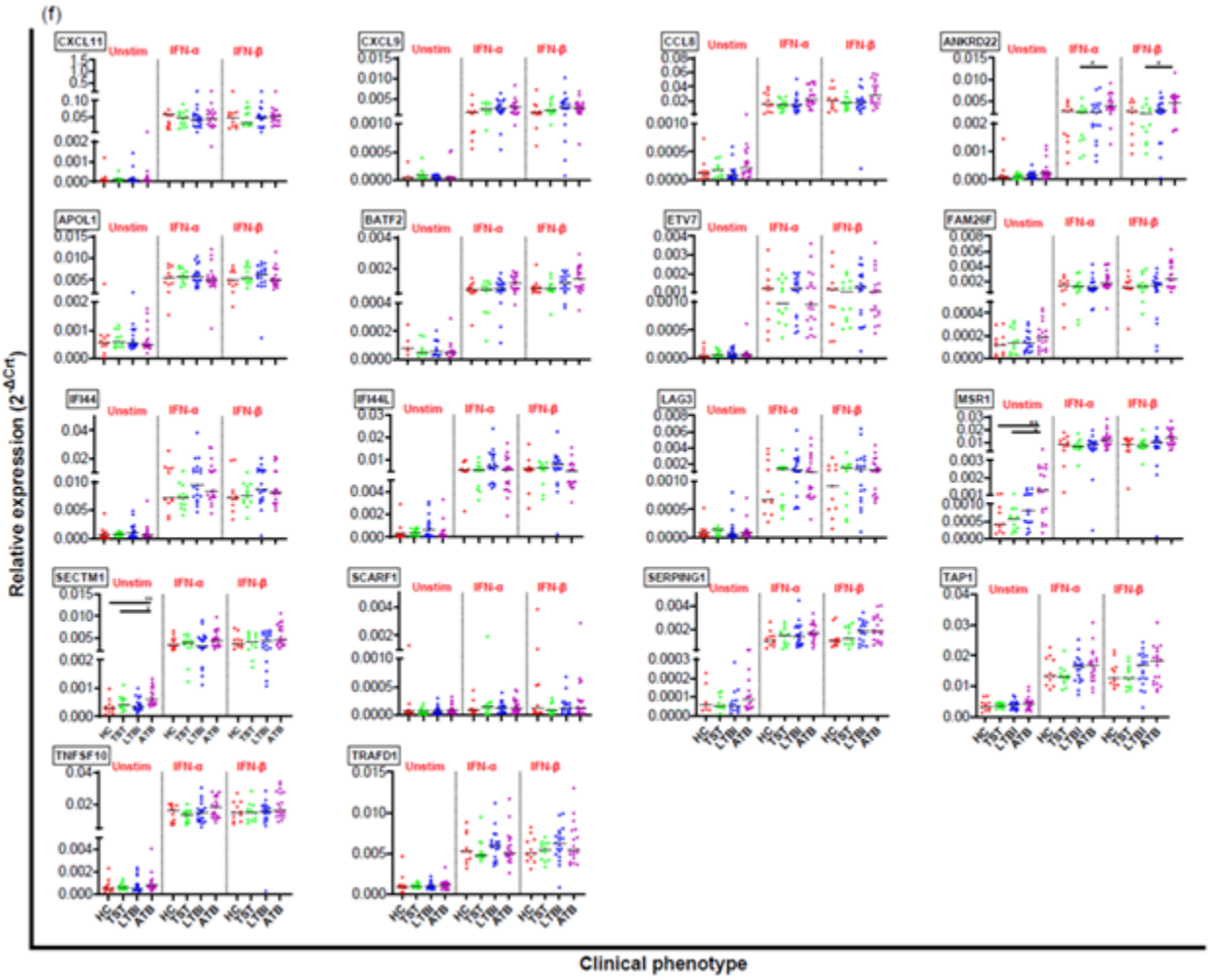

3.3.2.3 Comparison of relative ISG expression between clinical groups following IFN-α or IFN-β stimulation

For the expression of *ANKRD22*, *CCL8*, *FCGR1A*, *FCGR1B*, *MSR1*, and *FAM26F* genes that were differentially expressed across the four study groups identified using the Kruskal-Wallis test, pairwise comparisons using Dunn's procedure were subsequently performed to identify the specific pairs of medians that differed significantly, followed by post hoc analysis using Bonferroni correction for multiple comparisons with statistical significance set at $p< 0.05$.

3.3.2.3.1 IFN-α stimulation

Pairwise comparisons identified significant differences in the median IFN-α induced relative gene expression response of *ANKRD22* between ATB and TST (median: 0.003765 vs 0.002376; p=0.007); *CCL8* between ATB and LTBI(median: 0.022401 vs 0.013818; p=0.014), and ATB and TST (median: 0.022401 vs 0.014111; p=0.020); *FCGR1A* between ATB and LTBI (median: 0.001381 vs 0.000604; p=0.006), and ATB and HC (median: 0.001381 vs 0.000742; p=0.007); *FCGR1B* between ATB and LTBI (median: 0.000305 vs 0.000122; p=0.011), ATB and TST (median: 0.000305 vs 0.000114; p=0.009), and ATB and HC (median: 0.000305 vs 0.00009; p=0.013); and for *MSR1* between ATB and LTBI (median: 0.011690 vs 0.008058; p=0.015) and ATB and TST (median: 0.011690 vs 0.007011; p=0.014) as listed in Table 8. With Bonferroni correction, the median relative expression levels were differentially expressed for *ANKRD22* gene between ATB and TST (median: 0.003765 vs 0.002376; p=0.042); *FCGR1A* gene between ATB and HC (median: 0.001381 vs 0.000742; p=0.039), and between ATB and LTBI (median: 0.001381 vs 0.000604; p=0.034) with IFN-α stimulation.

3.3.2.3.2 IFN-β stimulation

Pairwise comparisons identified differences significant differences in the median IFN-β induced relative gene expression response of *ANKRD22* between ATB and LTBI (median: 0.004685 vs 0.002805; p=0.042), ATB and TST (median: 0.004685 vs 0.002131; p=0.006), and ATB and HC (median: 0.004685 vs 0.002630; p=0.032); *CCL8* between ATB and LTBI (median: 0.028615 vs 0.016775; p=0.015), and ATB and TST (median: 0.028615 vs 0.016840; p=0.019); *FAM26F* between ATB and LTBI (median: 0.002338 vs 0.001518; p=0.010), ATB and TST (median: 0.002338 vs 0.001306; p=0.031), and, ATB and HC (median: 0.002338 vs 0.001232; p=0.040); *FCGR1A* between ATB and LTBI (median: 0.001573 vs 0.000847; p=0.007), ATB and TST (median: 0.001573 vs 0.000554; p=0.002), and ATB and HC (median: 0.001573 vs 0.000628; p=0.001); *FCGR1B* between ATB and LTBI (median: 0.000318 vs 0.000161; p=0.007), ATB and TST (median: 0.000318 vs 0.000093; p=0.006), and ATB and HC (median: 0.000318 vs 0.000078; p<0.001); and *MSR1* between ATB and LTBI (median: 0.013216 vs 0.009928; p=0.025) and ATB and TST (median: 0.013216 vs 0.007266; p=0.014) as listed in Table 8. With Bonferroni correction, the median relative expression levels were differentially expressed for *ANKRD22* gene between ATB and TST (median: 0.004685 vs 0.002131; p=0.034); for *FCGR1A* gene between

ATB and HC (median: 0.001573 vs 0.000628; 0.003), ATB and TST (median: 0.001573 vs 0.000554; p=0.013), and ATB and LTBI (median: 0.001573 vs 0.000847; p=0.041); and for *FCGR1B* gene between ATB and HC (median: 0.000318 vs 0.000078; p=0.002), ATB and TST (median: 0.000318 vs 0.000093; p=0.038), and ATB and LTBI (median: 0.000318 vs 0.000161; p=0.043) with IFN-β stimulation (Table 8).

Table 8. Genes differentially expressed in IFN-α and IFN-β-stimulated samples between clinical groups (relative expression).

						Post hoc analysis	
Stimulation	**Gene**	**N**	**χ2**	**p-value[a]**	**Comparison[b]**	**p-value[c]**	**adjusted p-value[d]**
IFN-α	*ANKRD22*	60	9.964	0.019	ATB-TST	0.007	**0.042**
	CCL8	60	8.016	0.046	ATB-LTBI	0.014	0.083
					ATB-TST	0.02	0.122
	FCGR1A	60	11.935	0.008	ATB-HC	0.007	**0.039**
					ATB-LTBI	0.006	**0.034**
	FCGR1B	57	10.841	0.013	ATB-HC	0.013	0.076
					ATB-LTBI	0.011	0.067
					ATB-TST	0.009	0.055
	MSR1	61	8.38	0.039	ATB-LTBI	0.015	0.09
					ATB-TST	0.014	0.086
IFN-β	*ANKRD22*	60	9.401	0.024	ATB-HC	0.032	0.194
					ATB-LTBI	0.042	0.254
					ATB-TST	0.006	**0.034**
	CCL8	60	8.05	0.045	ATB-LTBI	0.015	0.093
					ATB-TST	0.019	0.114
	FAM26F	61	8.599	0.035	ATB-HC	0.04	0.241
					ATB-LTBI	0.01	0.06
					ATB-TST	0.031	0.184
	FCGR1A	60	16.257	0.001	ATB-HC	0.001	**0.003**
					ATB-LTBI	0.007	**0.041**
					ATB-TST	0.002	**0.013**
	FCGR1B	58	15.806	0.001	ATB-HC	< .001	**0.002**
					ATB-LTBI	0.007	**0.043**
					ATB-TST	0.006	**0.038**
	MSR1	60	8.283	0.041	ATB-LTBI	0.025	0.149
					ATB-TST	0.014	0.084

ATB-active tuberculosis; TST- Tuberculin skin test positive; LTBI-latent tuberculosis infection; HC-healthy controls. N: total number of individuals in whom gene is detected. Comparisons of relative expression data between clinical groups using Kruskal-Wallis test with post hoc pairwise comparisons and Bonferroni correction for multiple comparisons. **Bolded** and yellow highlighted p-values are significant after Bonferroni correction. Chi square (χ^2) is the square of the difference between the observed values and the expected values. p-values: [a] – across groups p-value; [c] – pairwise comparison (between groups) p-value; [d] – adjusted p-value using Bonferroni correction for multiple comparisons.[b] – the order in the comparison shows the direction of the difference with the higher expression listed first.

3.3.2.4 Summary

This study aimed to quantify gene expression responses of selected ISGs to stimulation with IFN-α and IFN-β in *M. tuberculosis* infection states. We hypothesized that stimulation with IFN-α or IFN-β would upregulate the expression of distinct ISGs in ATB compared to LTBI. To test this hypothesis, the expression of selected genes was assessed in PBMCs from healthy controls, TST-reactive and individuals from the *M. tuberculosis* infection states (LTBI and ATB) stimulated with IFN-α or IFN-β. Overall, using the relative expression method, most genes had higher expression following IFN-α or IFN-β compared to no stimulation, except for *IL-1A* and *IL-1B* genes that had lower expression following stimulation. About half the genes had higher expression in ATB compared to LTBI and supported the sub-hypothesis; the rest showed higher expression in LTBI compared to ATB and did not support the sub-hypothesis. Following IFN-α stimulation *FCGR1A* gene was differentially expressed between ATB and both LTBI and HC, and *ANKRD22* between ATB and TST. After IFN-β stimulation, both *FCGR1A* and *FCGR1B* genes were differentially expressed between ATB and LTBI, HC, and TST.

3.3.3 Comparison of ISG expression between clinical groups following IFN-α and IFN-β stimulated samples

Relative expression calculated using the formula $2^{-\Delta Crt}$ allows for assessment of normalized gene expression, which includes the normalized expression of the unstimulated samples. However, this calculation does not show the induction of gene regulation, whether upregulated or downregulated. To assess this, the fold was calculated change using the $2^{-\Delta\Delta Crt}$ method. This represents the expression of the target gene in treated samples normalized to a reference gene and relative to the unstimulated sample (unstimulated control). Fold change gives directionality to gene expression - whether upregulated or down-regulated as compared to the unstimulated control. The unstimulated control is therefore not a stimulation group of its own in these calculations but is rather used as the reference to which the stimulated conditions are compared. Fold change was calculated as:

Delta deltaCrt ($\Delta\Delta Crt$) = $\Delta Crt_{stimulated} - \Delta Crt_{unstimulated}$(414,417).

3.3.3.1 Clustering analysis of fold changes in IFN-α and IFN-β- stimulated samples

To visualize whether the fold change data clusters by clinical groups, the gene expression fold changes from IFN-α- and IFN-β-stimulated samples were uploaded into Clustvis, and log-transformed the data. In Figure 19, as we observed for the relative gene expression analysis (Figure 16), there was no clear distinction between IFN-α and IFN-β-induced gene expression (fold change) by study groups; IFN-α- and IFN-β-induced genes clustered together.

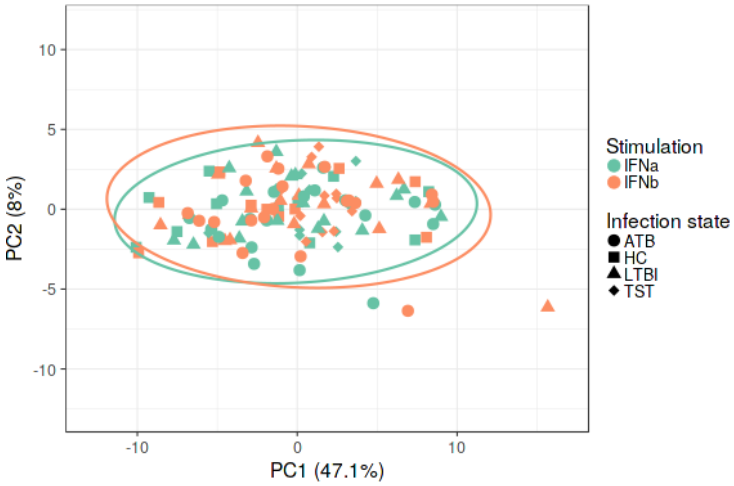

Figure 19. **Principal component analysis of ISG expression in fold changes in response to IFN-α or IFN-β stimulation.**

IFN-α or IFN-β -stimulated PBMCs from ATB, HC, LTBI, and TST were incubated for 4 hours, RNA extracted and processed using RT-qPCR for detection of 53 genes. Fold changes were calculated using the formula $2^{-\Delta\Delta Ct}$. The original values for 52 genes were uploaded into Clutvis (http://biit.cs.ut.ee/clustvis/) and log transformed. The stimulations are represented in color by green= IFN-α, and orange= IFN-. The clinical groups are represented by shapes - circle=ATB, square=HC, triangle=LTBI, rhombus=TST.

In addition to the PCA, cluster analysis was also assessed using a heatmap. Most of the genes appeared to be upregulated (red) after IFN-α and IFN-β stimulation, although some genes appeared to be downregulated (blue) (Figure 20). There was no apparent clustering of specific gene patterns or clinical groups after IFN-α and IFN-β stimulation.

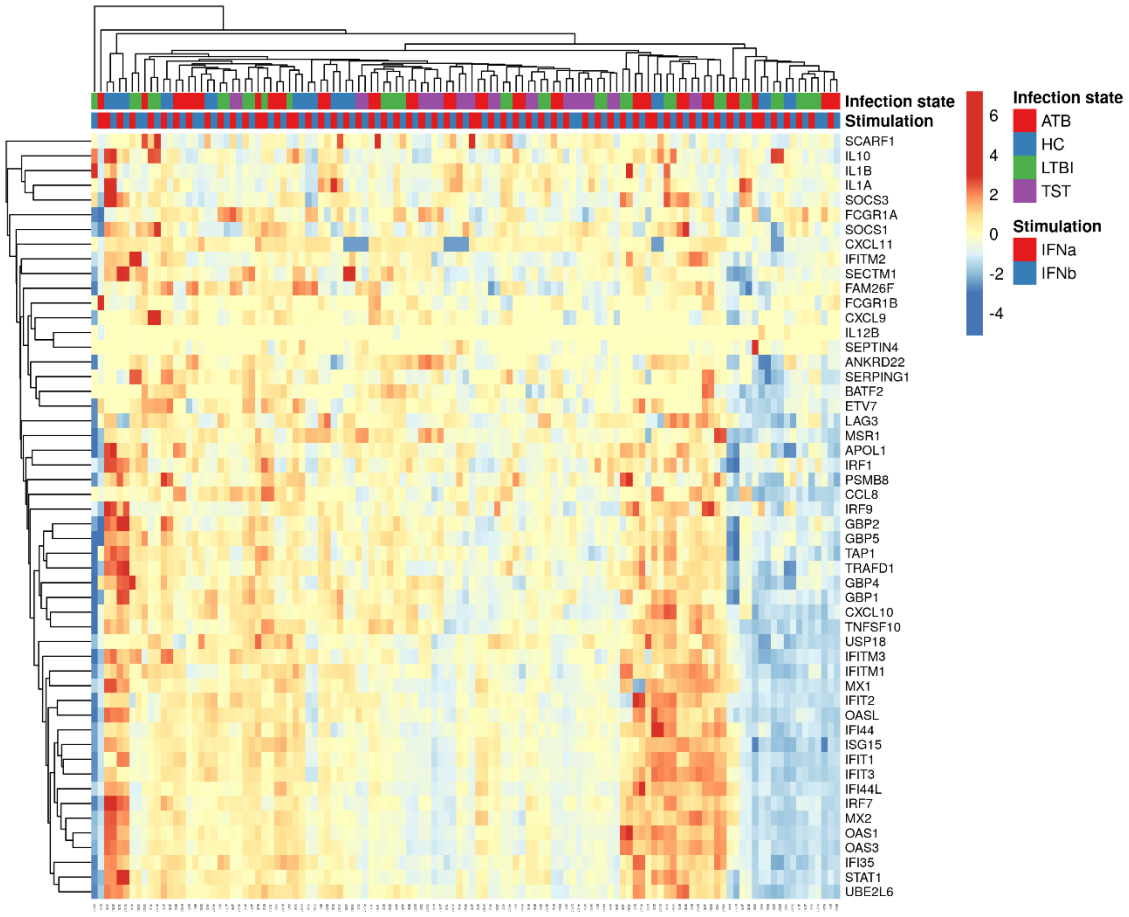

Figure 20. **Heatmap showing the unsupervised clustering of fold changes for ISGs in IFN-α- or IFN-βstimulated samples**.

Peripheral blood mononuclear cells (PBMCs) from ATB, HC, LTBI, and TST were incubated for 4 hours with IFN-α orIFN-β, with an unstimulated control, RNA extracted and processed using RT-qPCR for detection of 53 genes. Fold change was calculated using the formula $2^{-\Delta\Delta Crt}$. The original values for 52 genes were uploaded into Clutvis (http://biit.cs.ut.ee/clustvis/) and log-transformed. The rows show the genes – blue color indicates downregulation; red color indicates upregulation. Columns show the clinical phenotypes (red=ATB; blue=HC; green= LTBI; purple=TST).

3.3.3.2 Comparison of ISG expression across clinical groups following IFN-α or IFN β stimulation

After data visualization using PCA and the heatmap, the data was interrogated at the individual gene level. The median $\log_2$ fold changes (FC) for each gene in the IFN-stimulated samples were tested using the Kruskal-Wallis test to assess for statistically significant differences across the median of the $\log_2$ FC values from IFN-α and IFN β stimulation between clinical groups.

As can be seen in Figure 21 (presented as $\log_2$ of fold change) and Table S2 using a cut-off of absolute ($\log_2$FC) of |1|; with $\log_2$ FC ≥1 being upregulated and ≤ -1 downregulated. Log_2fold change values in-between showed no regulation. Most genes were upregulated after IFN-α and IFN-β stimulation in HC (77.4% of 53 genes), TST (79.2%), LTBI (83.0%), and ATB (83.0%) as shown in Table S2. With IFN-α stimulation 47.9% of genes had a larger fold change in ATB compared to 52.1% in LTBI. Upregulated genes included *ANKRD22* gene expression was highest in HC then TST, ATB, and LTBI ($\log_2$ of median FC for HC, TST, LTBI, ATB: 4.75, 4.38, 4.17, 4.23); *FCGR1A* gene expression was highest in LTBI followed by HC, TST, and ATB ($\log_2$FCfor HC, TST, LTBI, ATB: 2.77,2.72, 2.96,2.59); *MSR1* gene expression showed the largest change in HC, followed by TST, LTBI, and lowest in ATB ($\log_2$FC for HC, TST, LTBI, ATB: 4.09, 3.59, 3.38, 3.36); and, *IRF9* gene expression was highest in HC, then in ATB, LTBI, and TST ($\log_2$FC for HC, TST, LTBI, ATB: 2.22, 1.09, 1.27, 1.58). The expression of two genes was downregulated after IFN-α stimulation: *IL-1A* gene which showed the largest downregulation in LTBI followed by HC, TST, and ATB ($\log_2$FC for HC, TST, LTBI, ATB: -2.25, -2.12, -2.40, -1.69), and *IL-1B* gene with the largest change in LTBI & TST followed by HC, and ATB ($\log_2$FCfor HC, TST, LTBI, ATB: -1.51, -1.69, -1.69, -1.32). Some genes showed no regulation for all groups: IL-10 gene had the highest expression in HC then LTBI, ATB, and TST ($\log_2$FCfor HC, TST, LTBI, ATB: 0.77, 0.23, 0.58, 0.37), *SOCS3* expression – in LTBI, followed by HC, TST, and ATB ($\log_2$FC for HC, TST, LTBI, ATB: 0.63, 0.44, 0.68, 0.40), and *SCARF1* gene expression –highest in TST then LTBI, ATB, and HC ($\log_2$FC for HC, TST, LTBI, ATB: 0.21, 0.94, 0.90, 0.29).

Similarly, most genes were upregulated after IFN-β stimulation. in HC (83.0% of genes), TST (83.0%), LTBI (83.0%), and ATB (86.8%) (Figure 20, Table S2). Of these 52.1% had a larger expression in ATB compared to 47.9% in LTBI. Upregulated genes included *ANKRD22* gene expression – highest in HC then ATB, TST, and LTBI ($\log_2$FC for HC, TST, LTBI, ATB: 4.66, 4.39, 4.18, 4.44); *FCGR1A* expression – highest in LTBI, ATB, HC, and TST ($\log_2$FC for HC, TST, LTBI, ATB: 2.39, 2.19, 3.08, 2.62); *MSR1* expression – highest in HC, then TST, LTBI, and ATB ($\log_2$FC for HC, TST, LTBI, ATB: 4.08, 3.84, 3.62, 3.39); IRF9 expression – highest in HC, followed by ATB, TST, and lowest in LTBI ($\log_2$FC for HC, TST, LTBI, ATB: 1.95, 1.44, 1.33, 1.47). Some of the genes showed mixed responses with upregulation in some groups and no regulation in other groups. For example, *SCARF1* gene was upregulated in HC and ATB but showed no regulation in TST and LTBI ($\log_2$FC for HC, TST, LTBI, ATB: 1.11, 0.79, 0.69, 1.28);

IL-10 gene expression was upregulated for HC but showed no regulation for the other clinical phenotypes (log_2FC for HC, TST, LTBI, ATB: 1.01, -0.07, 0.28, -0.04). Downregulated gene expression was observed for *IL-1A* –with the largest change in LTBI, followed by TST, HC, and ATB (log_2FC for HC, TST, LTBI, ATB: -2.40, -2.47, -2.64, -2.06), and *IL-1B* – in HC, followed by ATB, TST, and LTBI (log_2FC for HC, TST, LTBI, ATB: -2.25, -2.00, -1.84, -2.12). Similar to the response to stimulation with IFN-α, *SOCS3* gene showed no regulation for all groups – (log_2FC for HC, TST, LTBI, ATB: 0.66, 0.26, 0.90, 0.19).

IRF9 and *MSR1* genes were differentially expressed across clinical groups with IFN-α-stimulation, as shown in Figure 21, but not after IFN-β stimulation. Following IFN-α-stimulation, *IRF9* fold expression was highest in HC, followed by ATB, LTBI, and lowest in TST (log_2FC for HC, TST, LTBI, ATB: 2.22, 1.58, 1.27, 1.09 respectively; p=0.002); *MSR1* fold expression was highest in HC, with stepwise decrease in expression from TST to LTB, to ATB (log_2FC for HC, TST, LTBI, ATB: 4.09, 3.59, 3.38, 3.36; p=0.013). With IFN-β stimulation, *SOCS3* gene fold expression was highest in LTBI with stepwise decrease in expression from HC, TST to ATB (log_2FC for HC, TST, LTBI, ATB: 0.66, 0.26, 0.90, 0.19; p=0.043). However, the fold changes of the *SOCS3* gene in TST and ATB were below the absolute(log_2FC) cut-off of |1|.

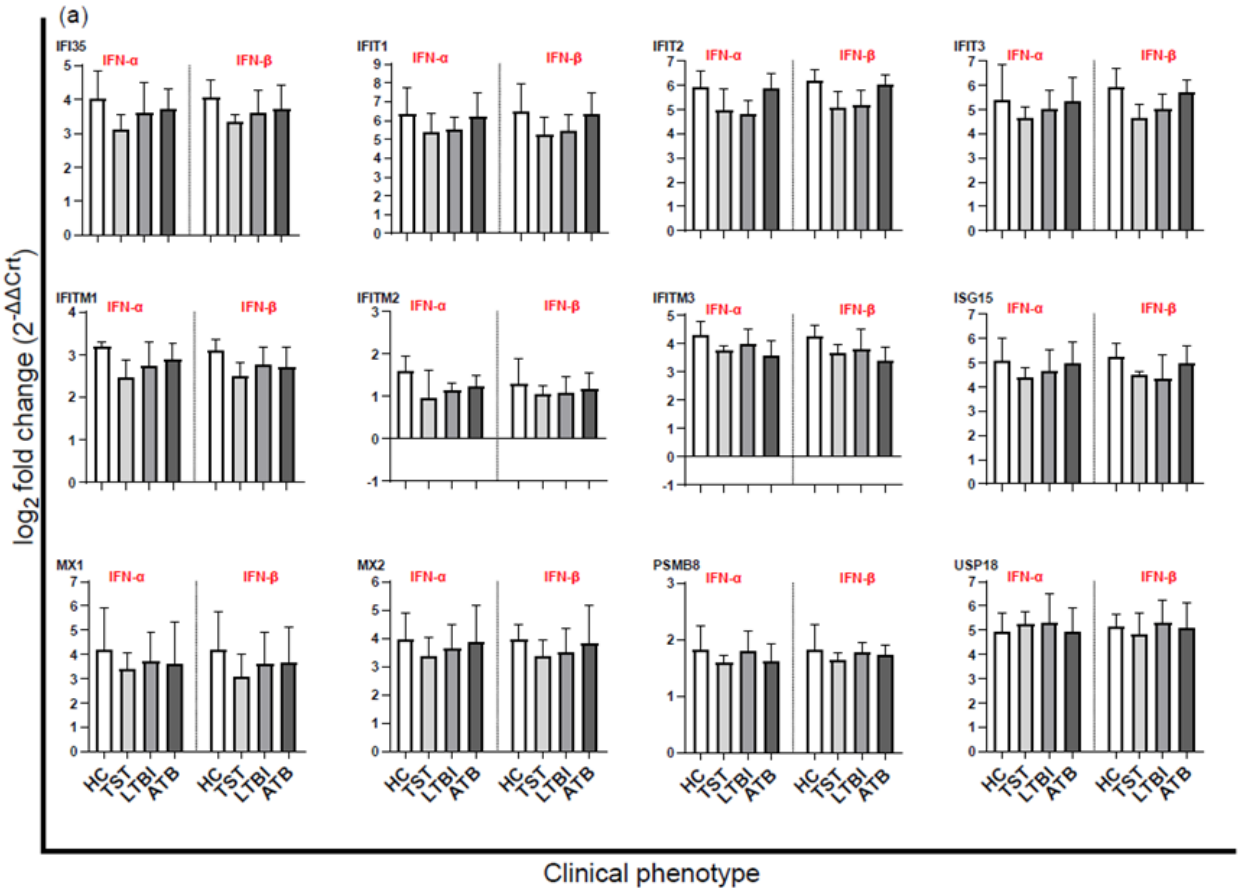

Figure 21. ISG expression (fold changes) in IFN-α- and IFN-β stimulated samples.

Genes enriched for (a) IFN-α/β signaling pathway, (b) IFN-γ signaling pathway, (c) IFN-α/β and IFN-γ signaling pathways, (d) IFN signaling, (e) IL-10 signaling pathway, and (f) Not classified. RT qPCR analysis of mRNA expression of ISGs in PBMCs with no stimulation or stimulated with IFN-α or IFN-β were normalized to *18S rRNA, ACTB* and *HPRT1* (ΔCrt). Fold changes was calculated as $2^{-\Delta\Delta Crt}$ and presented in a $\log_2$ format. Data are presented as bars with median and IQR. Kruskal-Wallis test was performed to assess differences between clinical phenotypes, * $p< 0.05$, ** $p< 0.01$, ***$p\leq 0.001$. Genes were listed according to Figure 14. The bars in each section are labelled in the order HC (white), TST, LTBI, and ATB (dark gray). x-axis=clinical phenotype; y-axis= $\log_2$ fold change.

Figure 21: continued

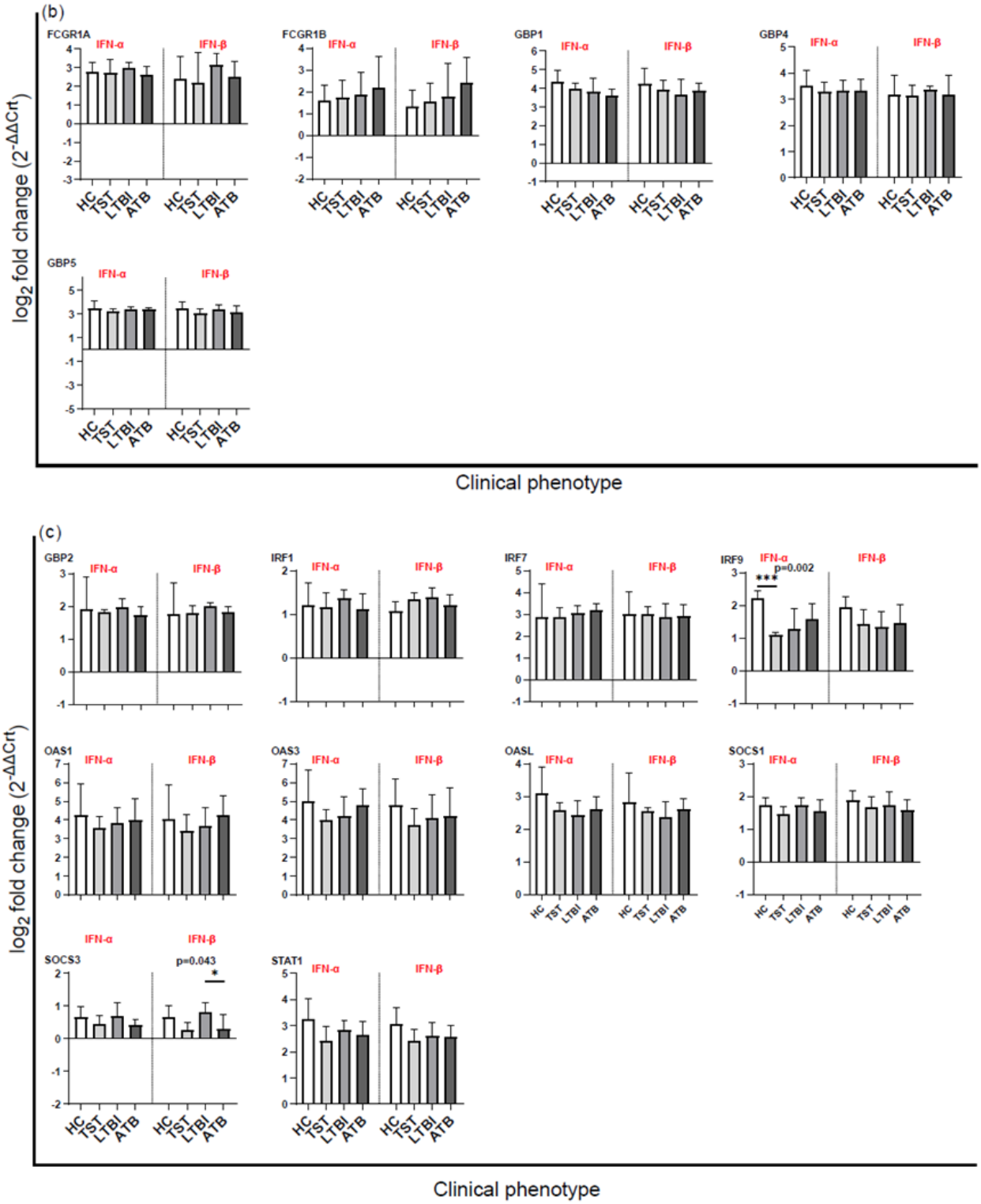

Figure 21: continued

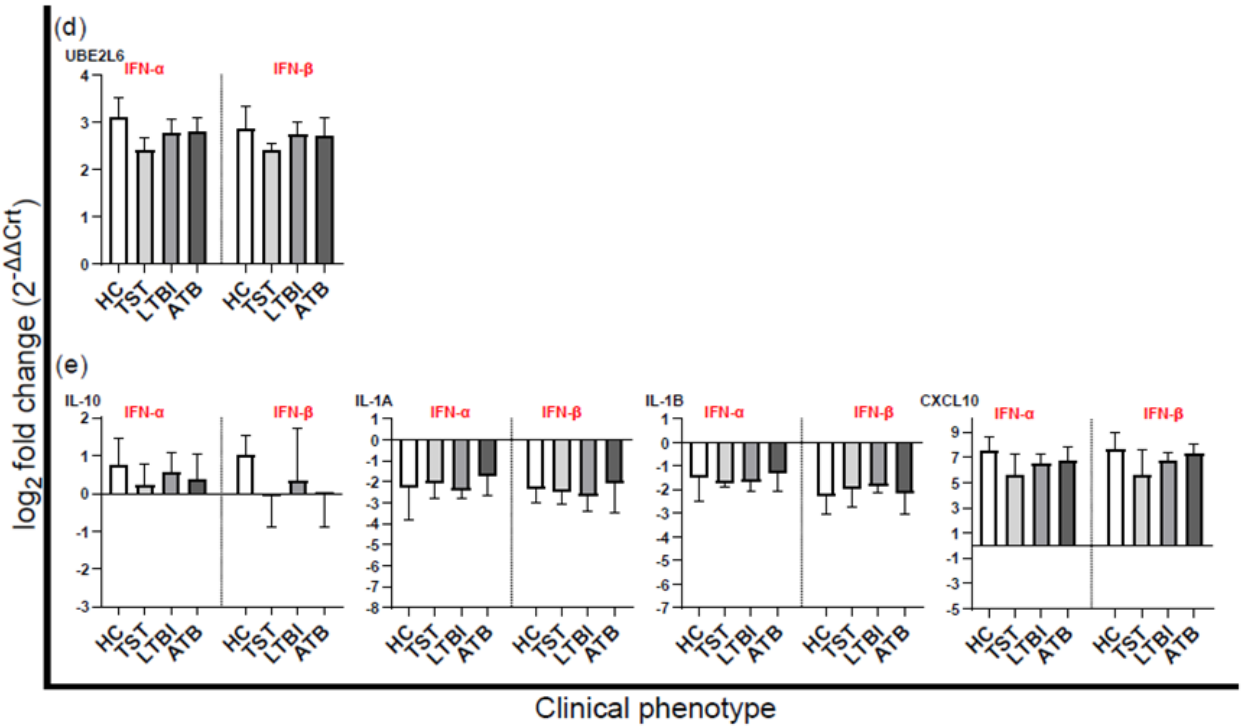

Figure 21: continued

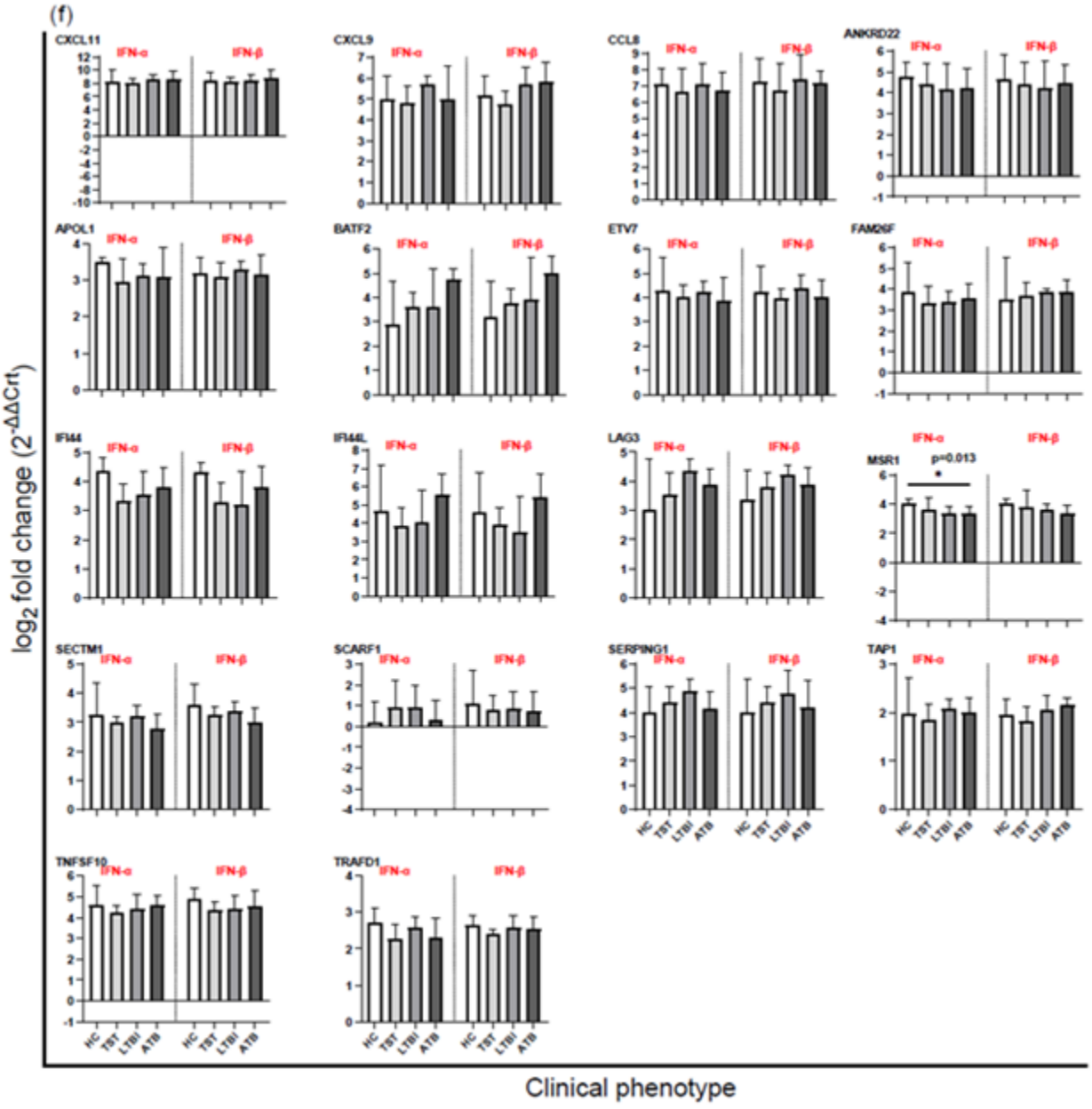

3.3.3.3 Comparison of ISG expression between clinical groups following IFN-α or IFN-β stimulation

For the differentially expressed genes identified following IFN- α and IFN-β stimulation – *IRF9, MSR1,* and *SOCS3* genes, pairwise comparisons using Dunn's procedure were subsequently performed to identify the specific pairs of medians that differed significantly, followed by post hoc analysis using Bonferroni correction for multiple comparisons with statistical significance set at $p<0.05$. Dunn's procedure compares the medians of all pairs to identify those that differ significantly- ATB vs HC, ATB vs TST, ATB vs LTBI, TST vs HC, TST vs LTBI, and LTBI vs HC.

3.3.3.3.1 IFN-α stimulation

Pairwise comparisons identified significant differences in the IFN-α-induced fold changes in *IRF9* gene between ATB and TST (log_2FC: 1.58 vs 1.09; p=0.009), HC and LTBI (2.22 vs 1.27; p=0.013), and HC and TST (2.22 vs 1.09; p< 0.001); and in *MSR1* gene between HC and ATB (4.09 vs 3.36; p=0.005), TST and ATB (3.59 vs 3.36; p=0.024), and HC and LTBI (4.09 vs 3.38; p=0.025). Bonferroni correction at a threshold of p< 0.05 revealed statistically significant differences in median fold changes with IFN-α stimulation for *IRF9* gene expression between HC and TST (2.22 vs 1.09; p= 0.001), and for *MSR1* gene expression between HC and ATB (4.09 vs 3.36; p=0.029) as can be seen in Table 9.

3.3.3.3.2 IFN-β stimulation

Pairwise comparisons identified significant differences in IFN-β -induced fold changes in the *SOCS3* gene between LTBI and ATB (0.90 vs 0.19; p=0.007), and between LTBI and TST (10.90 vs 0.26; p=0.039) as can be seen in Table 9. Following correction for multiple comparisons, the *SOCS3* gene was differentially expressed between LTBI and ATB with IFN-β stimulation (0.90 vs 0.19; p=0.043) (Table 9). Although the expression of the *SOCS3* gene was statistically significant between LTBI and ATB, it did not meet the absolute(log_2FC) cut-off of |1|.

Table 9. Differentially expressed genes with IFN-α and- IFN-β stimulation between clinical groups (fold change).

						Post hoc analysis	
Stimulation	**Gene**	**N**	**χ2**	**p-value[a]**	**Comparison[b]**	**p-value[c]**	**adjusted p-value[d]**
IFNα	*IRF9*	60	14.858	0.002	ATB-TST	0.009	0.054
				0.002	HC-LTBI	0.013	0.076
				0.002	HC-TST	< 0.001	**0.001**
	MSR1	59	10.821	0.013	HC-ATB	0.005	**0.029**
				0.013	TST-ATB	0.024	0.143
				0.013	HC-LTBI	0.025	0.151
IFNβ	*SOCS3*	59	8.137	0.043	LTBI-ATB	0.007	**0.043**
				0.043	LTBI-TST	0.039	0.236

ATB-active tuberculosis; TST- Tuberculin skin test positive; LTBI-latent tuberculosis infection; HC-healthy controls. N: total number of individuals in whom gene is detected. Comparisons of fold changes between clinical groups using Kruskal-Wallis test with post hoc pairwise comparisons and Bonferroni correction for multiple comparisons. **Bolded** and yellow highlighted p-values are significant after Bonferroni correction. Chi square (χ^2) is the square of the difference between the observed values and the expected values. p-values: [a] – across groups p-value; [c] – pairwise comparison (between groups) p-value; [d] – adjusted p-value using Bonferroni correction for multiple comparisons. [b] – the order in the comparison shows the direction of the difference with the higher expression listed first.

3.3.3.4 Summary

The experiments in this section aimed to compare gene regulation in response to stimulation with IFN-α or IFN-β in distinct *M. tuberculosis* infection states. We hypothesized that stimulation of PBMCs with IFN-α or IFN-β would result in upregulation of ISGs in ATB compared to LTBI. As expected, stimulation with IFN-α or IFN-β upregulated the expression of most genes, except for *IL-1A* and *IL-1B* genes that were downregulated. About half the gens had a larger fold change in ATB than LTBI with both IFN stimulations supporting the sub-hypothesis. With IFN-α stimulation, the *IRF9* gene was differentially expressed between HC and TST, the *MSR1* gene between HC and ATB, and after IFN-β, the *SOCS3* gene between LTBI and ATB.

3.3.4 Comparison of relative ISG expression in Mtb WCL stimulated samples versus unstimulated samples between clinical groups

In previous transcriptional profiling studies, gene expression from PBMCs stimulated with ESAT-6/CFP-10 and with PPD did not reveal enrichment for IFN-inducible genes (384,385). In addition to understanding the differences in genes expression responses to the type I IFNs, we therefore also studied the *M. tuberculosis*-specific gene expression responses relative to unstimulated responses on PBMCs from our study participants to explore whether *M. tuberculosis* WCL would elicit differential responses between the *M. tuberculosis* infection states, and whether this response would be suppressed compared to responses elicited by IFN-α or IFN-β.

For these experiments, frozen PBMCs from the study participants classified as HC (n=11), TST (n=12), LTBI (n=19) and ATB (n=19) were thawed, and approximately one million cells were cultured with 50μg/ml of Mtb WCL for four hours alongside an unstimulated control. Thereafter, RNA was extracted from the washed cell pellet and processed through RT-qPCR for analysis of the 53 genes listed in Table 5. Crt values of the target genes were normalized using the reference genes *18S rRNA*, *ACTB*, and *HPRT1*, and the relative expression was calculated using the $2^{-\Delta Ct}$ method.

3.3.4.1 Clustering analysis of relative expression in unstimulated and Mtb WCL stimulated samples

The relative expression data for unstimulated and Mtb WCL-stimulated samples were uploaded into Clustvis, and the data were log-transformed as described in section 3.3.1. As can be seen in Figure 22, cluster analysis using principal component analysis (PCA) partially separates the expression of genes in unstimulated samples from the Mtb WCL-stimulated samples. However, the stimulation does not cluster the genes by the clinical groups.

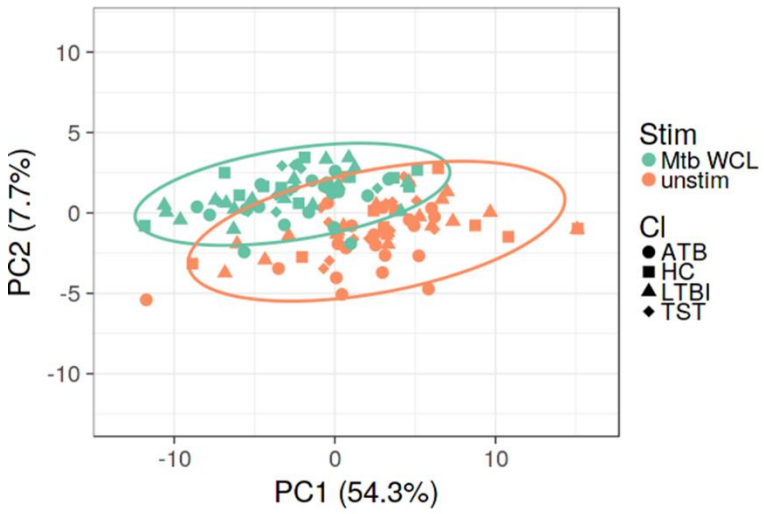

Figure 22. **Principal component analysis of relative ISG expression with no stimulation and in response to Mtb WCL**.

Unstimulated or Mtb WCL-stimulated PBMCs from ATB, HC, LTBI, and TST were incubated for 4 hours, RNA extracted and processed using RT-qPCR for detection of 53 ISGs. Relative expression was calculated using the formula $2^{-\Delta Crt}$. The original values for 52 genes were uploaded into Clutvis and log transformed. The stimulations are represented in color by green=Mtb WCL, and orange=unstimulated. The clinical groups are represented by shapes - circle=ATB, square=HC, triangle=LTBI, rhombus=TST.

Gene clustering was then assessed using a heatmap. As can be seen in Figure 23, stimulation with Mtb WCL induced a higher expression of most ISGs compared to expression at baseline, although some of the ISGs also showed lower expression with stimulation in some of the study participants. However, there was no distinct clustering of gene expression by the clinical groups.

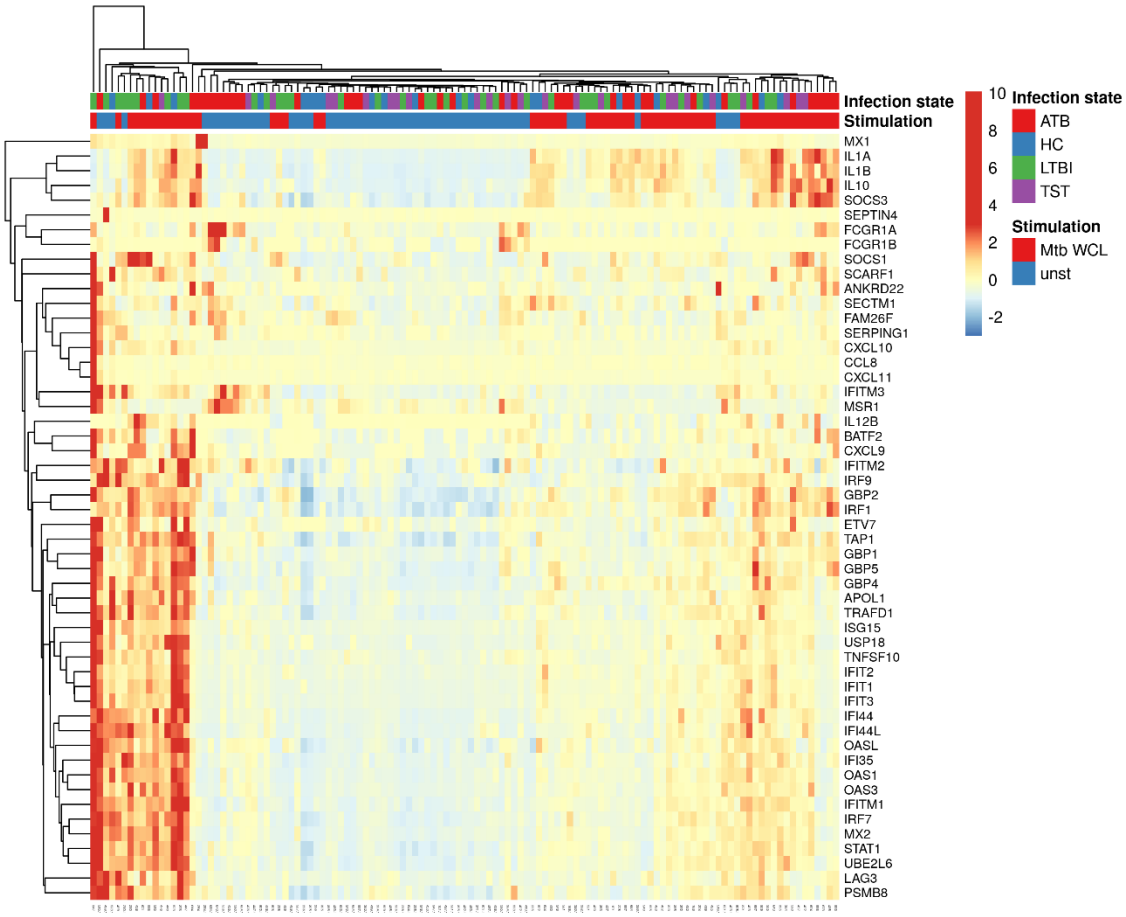

Figure 23.**Heatmap showing the unsupervised clustering of ISGs in unstimulated and Mtb WCL stimulated samples**.

Peripheral blood mononuclear cells (PBMCs) from ATB, HC, LTBI, and TST were incubated with Mtb WCL or unstimulated for 4 hours, RNA extracted and processed using RT-qPCR for detection of 53 ISGs. Relative expression was calculated using the formula $2^{-\Delta Crt}$. The original values for 52 genes were uploaded into Clutvis (http://biit.cs.ut.ee/clustvis/) and log-transformed. The rows show the genes – blue color indicates low expression; red color indicates high expression. Columns show the clinical phenotypes (red=ATB; blue=HC; green= LTBI; purple=TST).

3.3.4.2 Comparison of relative ISG expression across clinical groups following Mtb WCL stimulation

After data visualization using PCA and the heatmap the data was assessed at the individual gene level. The median relative expression values for each gene in the Mtb WCL-stimulated

samples were analysed using the Kruskal-Wallis test to assess for statistically significant differences across the median of the relative expression values from IFN-stimulation between clinical groups. In agreement with the findings of the heatmap in Figure 23, most genes demonstrated a higher expression with Mtb WCL-stimulation than in the unstimulated samples (Figure 24); the expression of most ISGs following stimulation with Mtb WCL was lower than that following IFN stimulation (Table S1). *FCGR1B* gene expression was not induced by Mtb WCL while it was observed in unstimulated samples (Figure 15) and with both IFN stimulations (Figure 18).

Overall, 29.4% of ISGs had higher expression in ATB compared to LTBI after Mtb WCL stimulation; 70.6% had higher expression in LTBI than in ATB (Table S1). Significant differences in expression were observed across clinical groups for several ISGs – *FCGR1A* and *MSR1* with the highest expression in ATB; *IFI44*, *IFI44L*, and *IFIT1*, with the highest expression in LTBI; and *SECTM1* with the highest expression in HC. The median relative expression of the *FCGR1A* gene was highest in ATB, followed by LTBI and TST, and was lowest in HC (median for HC, TST, LTBI, ATB: 0.000045, 0.000049, 0.000127, 0.000161; p=0.001) as can be seen in Figure 24. The expression of *MSR1* was highest in ATB followed a decrease in expression in LTBI, and HC, with the lowest expression in TST (median for HC, TST, LTBI, ATB: 0.000135, 0.000081, 0.000140, 0.000180; p=0.012). *IFI44* had the highest expression in LTBI, with stepwise decrease from TST to HC, to the lowest expression in ATB (median for HC, TST, LTBI, ATB: 0.001467, 0.001702, 0.002338, 0.0001072; p=0.030). *IFI44L* gene also showed the highest expression in LTBI, with stepwise decrease from TST to HC, to the lowest expression in ATB (median for HC, TST, LTBI, ATB: 0.000718, 0.000922, 0.001605, 0.000489; p=0.015). The expression of the *IFIT* gene was also highest in LTBI, followed by a decrease in expression in TST and HC, to the lowest expression in ATB (median for HC, TST, LTBI, ATB: 0.003048, 0.003080, 0.004762, 0.001528; p=0.036). The relative expression of *SECTM1* was highest in HC followed by a reduction in gene expression in ATB, TST, and LTBI (median for HC, TST, LTBI, ATB: 0.000886, 0.000566, 0.000544, 0.000734; p=0.006).

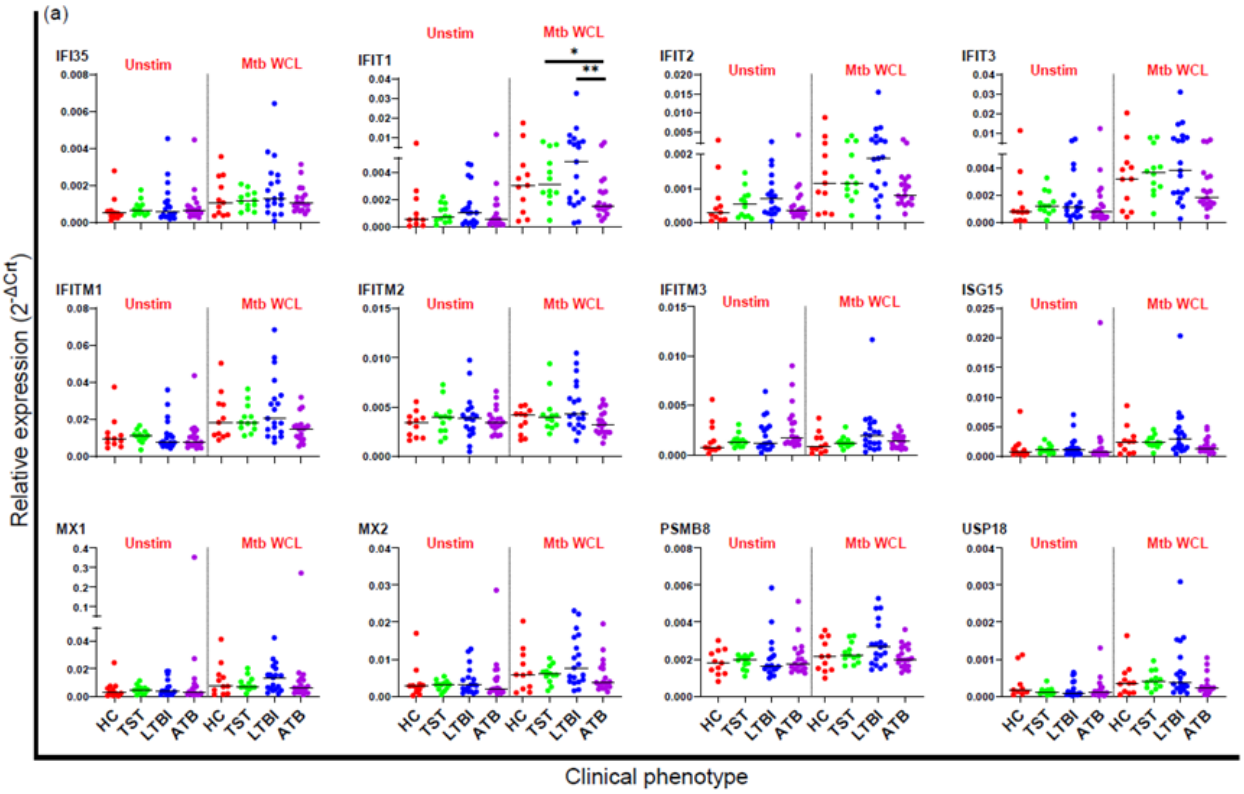

Figure 24. Relative ISG expression in unstimulated and Mtb WCL-stimulated samples.

Genes enriched for (a) IFN-α/β signaling pathway, (b) IFN-γ signaling pathway, (c) IFN-α/β and IFN-γ signaling pathways, (d) IFN signaling, (e) IL-10 signaling pathway, and (f) Not classified. RT qPCR analysis of mRNA expression of ISGs in unstimulated and Mtb WCL-stimulated PBMCs were normalized to *18S rRNA*, *ACTB* and *HPRT1*(ΔCrt). Relative gene expression was calculated as $2^{-\Delta Crt}$. Data are presented as median; each circle represents one participant. Kruskal-Wallis test was performed to assess differences between clinical phenotypes, * $p < 0.05$, ** $p < 0.01$, *** $p \leq 0.001$. Genes were listed according to Figure 14. Symbol color: red=HC, green=TST, blue=LTBI, purple=ATB. x-axis=clinical phenotype; y-axis=relative expression.

Figure 24: continued

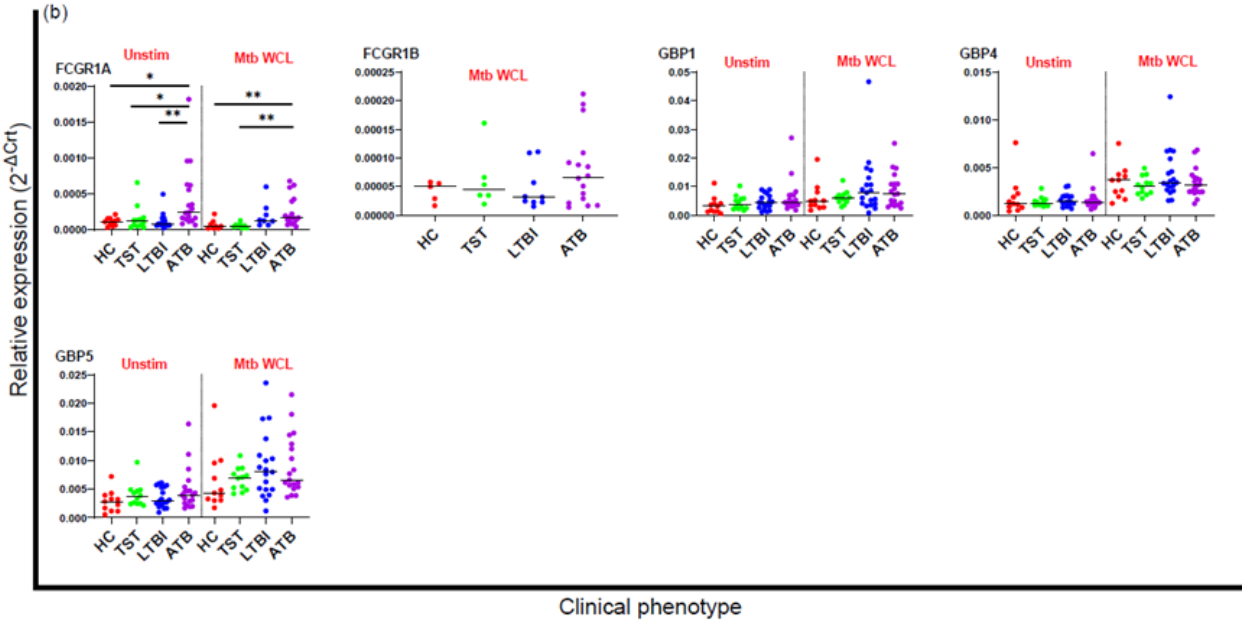

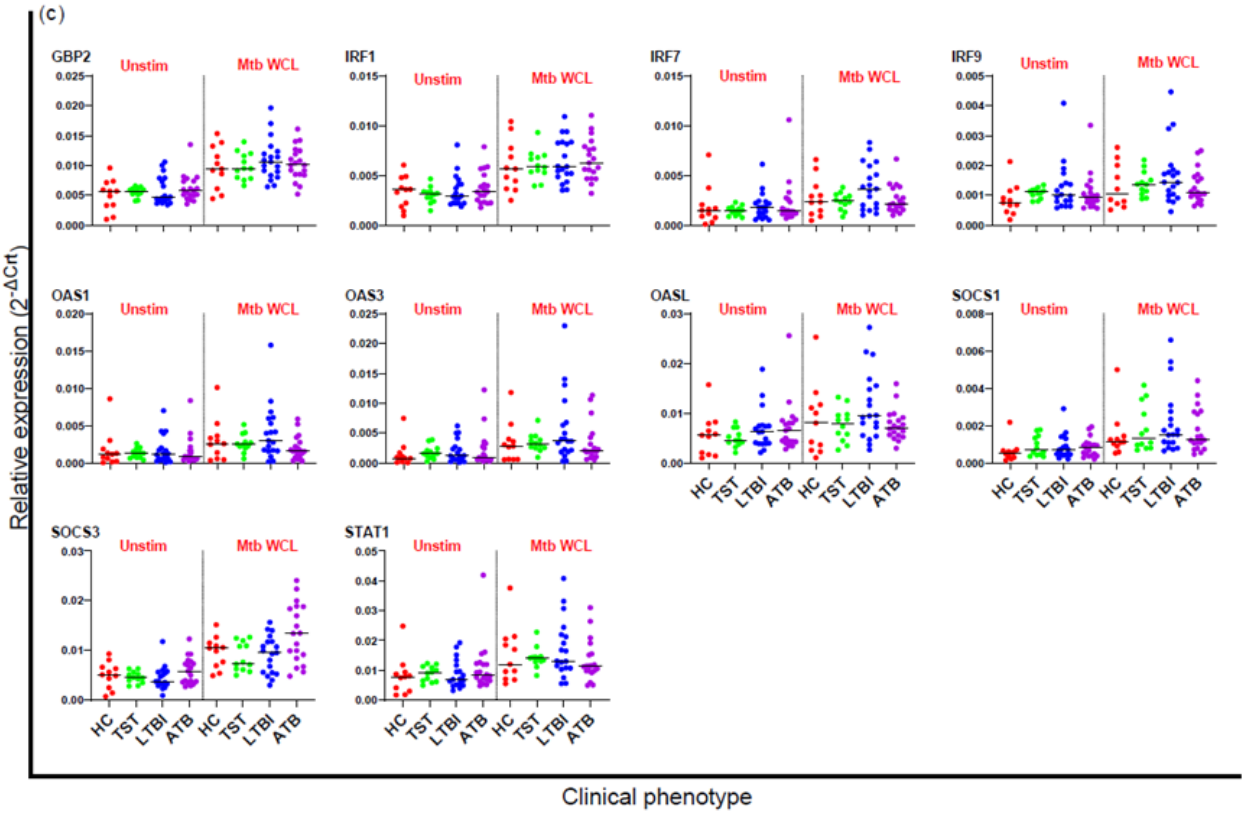

Figure 24: continued

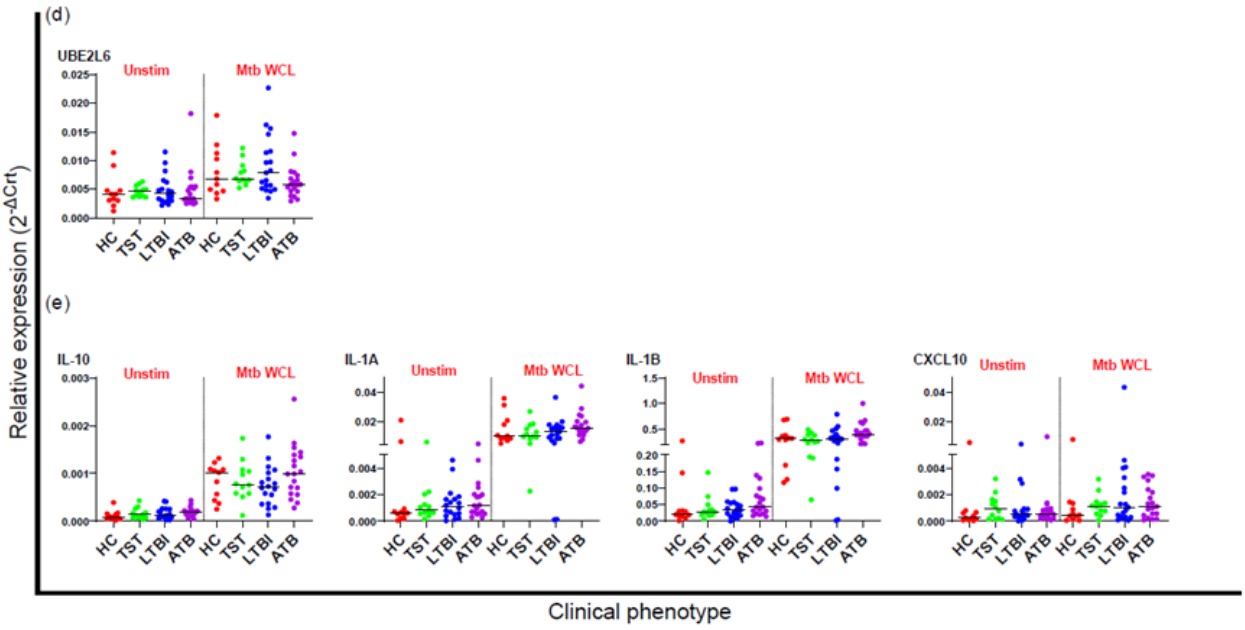

Figure 24: continued

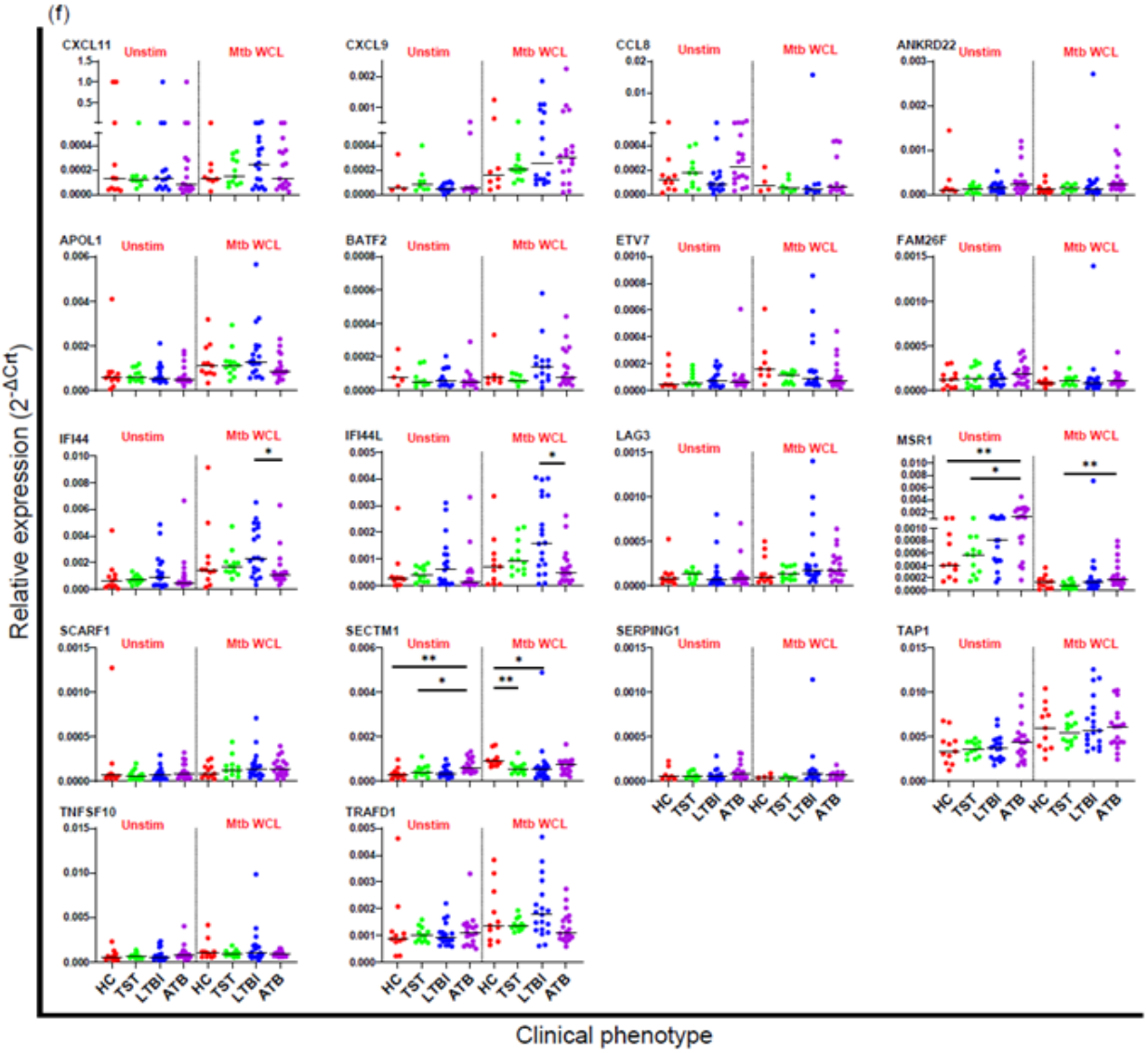

3.3.4.3 Comparison of relative ISG expression between clinical groups following Mtb WCL stimulation

For the expression of *FCGR1A*, *IFI44*, *IFI44L*, *IFIT1*, *MSR1*, and *SECTM1* genes identified as differentially expressed across the four study groups using the Kruskal-Wallis test, pairwise comparisons using Dunn's procedure were subsequently performed to identify the specific pairs of medians that differed significantly, followed by post hoc analysis using Bonferroni correction for multiple comparisons with statistical significance set at $p< 0.05$.

Pairwise comparisons identified significant differences in *FCGR1A* between HC and both ATB (median: 0.000045 vs 0.000161; p=0.001), and LTBI (median: 0.000045 vs 0.000127; p=0.028); TST and both ATB (median: 0.000049 vs 0.000161; p=0.001) and LTBI (median: 0.000049 vs 0.000127; p=0.019); and *MSR1* between ATB and TST (median: 0.000180 vs 0.000081; p=0.001); as shown in Table 10. *IFI44* showed significant difference between LTBI and ATB (median: 0.002338 vs 0.001072; p=0.003); *IFI44L* between LTBI and both ATB (median: 0.001605 vs 0.000489; p=0.003) HC (median: 0.001605 vs 0.000718; p=0.022); *IFIT1* between ATB and both LTBI (median: 0.001528 vs 0.004762; p=0.005) and TST (median: 0.001528 vs 0.003080; p=0.048); and *SECTM1* between HC and ATB (median: 0.000886 vs 0.000734; p=0.031), LTBI (median: 0.000886 vs 0.000544; p=0.001) and TST (median: 0.000886 vs 0.000566; p=0.007).

Post hoc analysis at a threshold of $p< 0.05$ revealed statistically significant differences in median gene expression fold changes of *FCGR1A* between ATB and HC (0.000161 vs 0.000045; p=0.009) and between ATB and TST (0.000161 vs 0.000049; p=0.005); and of *MSR1* between ATB and TST (0.000180 vs 0.000081; p=0.007) – both genes showed higher expression in ATB as can be seen in Figure 24 and Table S1. Significant differences were also found in the expression of *IFI44* between LTBI and ATB (median: 0.002338 vs 0.001072; p=0.02); *IFI44L* between LTBI and ATB (median: 0.001605 vs 0.000489; p=0.016); and *IFIT1* between LTBI and ATB (median: 0.004762 vs 0.001528; p=0.031); - all with higher expression in LTBI. Significant differences were also observed in the expression of *SECTM1* gene between HC and LTBI (median: 0.000886 vs 0.000544; p=0.004) and between HC and TST (median: 0.000886 vs 0.000566; p=0.041) with higher expression in HC.

Table 10. Genes differentially expressed between clinical groups with Mtb WCL stimulation (relative expression).

						Post hoc analysis	
Stimulation	**Gene**	**N**	**χ2**	**p-value[a]**	**Comparison[b]**	**p-value[c]**	**adjusted p-value[d]**
Mtb WCL	*FCGR1A*	42	17.323	0.001	ATB-HC	0.001	**0.009**
					LTBI-HC	0.028	0.166
					ATB-TST	0.001	**0.005**
					LTBI-TST	0.019	0.115
	IFI44	61	8.92	0.03	LTBI-ATB	0.003	**0.02**
	IFI44L	61	10.476	0.015	LTBI-ATB	0.003	**0.016**
					LTBI-HC	0.022	0.134
	IFIT1	61	8.539	0.036	LTBI-ATB	0.005	**0.031**
					TST-ATB	0.048	0.29
	MSR1	59	10.983	0.012	ATB-TST	0.001	**0.007**
	SECTM1	61	12.407	0.006	ATB-HC	0.031	0.187
					HC- LTBI	0.001	**0.004**
					HC-TST	0.007	**0.041**

ATB-active tuberculosis; TST- Tuberculin skin test positive; LTBI-latent tuberculosis infection; HC-healthy controls. N: total number of individuals in whom gene is detected. Comparisons of relative expression data between clinical groups using Kruskal-Wallis test with post hoc pairwise comparisons and Bonferroni correction for multiple comparisons. **Bolded** and yellow highlighted p-values are significant after Bonferroni correction. Chi square (χ^2) is the square of the difference between the observed values and the expected values. p-values: [a] – across groups p-value; [c] – pairwise comparison (between groups) p-value; [d] – adjusted p-value using Bonferroni correction for multiple comparisons.[b] – the order in the comparison shows the direction of the difference with the higher expression listed first.

3.3.4.4 Summary

The objective in this section aimed to assess gene expression responses to stimulation with Mtb WCL in various *M. tuberculosis* infection states. We hypothesized that stimulation with Mtb WCL would suppress the expression of ISGs compared to that observed with stimulation with IFN-α and IFN-β. Mtb WCL contains proteins, lipids and carbohydrates present within *M. tuberculosis* H37Rv bacterial cell. PBMCs from healthy controls and individuals identified as TST, LTBI, and ATB were stimulated with Mtb WCL with an unstimulated control and then tested

using RT qPCR for the expression of selected ISG genes relative to the unstimulated control. The gene expression induced by Mtb WCL was higher than that at baseline but lower compared to that observed with IFN-α and IFN-β stimulation. Most of the genes tested demonstrated higher expression in LTBI than in ATB, supporting the sub-hypothesis of suppression of ISG expression in ATB. Genes differentially expressed between LTBI and ATB were *IFI44*, *IFI44L*, and *IFIT1*, with higher expression in LTBI; between ATB and TST, *FCGR1A* and *MSR1* with higher expression in ATB; and between ATB and HC, *FCGR1A*, with higher expression in ATB. *SECTM1* gene was differentially expressed between HC and LTBI, and HC and TST, with higher expression in HC. The *FCGR1B* gene was not induced in PBMCs stimulated with Mtb WCL.

3.3.5 Comparison of ISG expression between clinical groups following Mtb WCL stimulation

Following the assessment of relative gene expression responses (normalized gene expression) to Mtb WCL, fold changes were calculated using the $2^{-\Delta\Delta Crt}$ method. This method represents the expression of a gene of interest in a treated sample (in this section, samples treated with Mtb WCL) normalized to reference genes (18S rRNA, β-actin, and HPRT-1) and relative to an untreated control sample. Fold change indicates whether a gene is up-regulated or down-regulated. Fold change was calculated as:

Delta Crt (ΔCrt) = $Crt_{target\ gene} - Crt_{reference\ gene}$

Delta delta Crt ($\Delta\Delta Crt$) = $\Delta Crt_{stimulated} - \Delta Crt_{unstimulated}$(414,417).

3.3.5.1 Clustering analysis of gene expression fold changes in unstimulated and Mtb WCL stimulated samples

To visualize whether the fold change data clusters by clinical groups, the gene expression data from Mtb WCL-stimulated samples were uploaded into Clustvis and log-transformed data. As can be seen in Figure 25, cluster analysis using PCA did not cluster genes stimulated with Mtb WCL by the clinical groups.

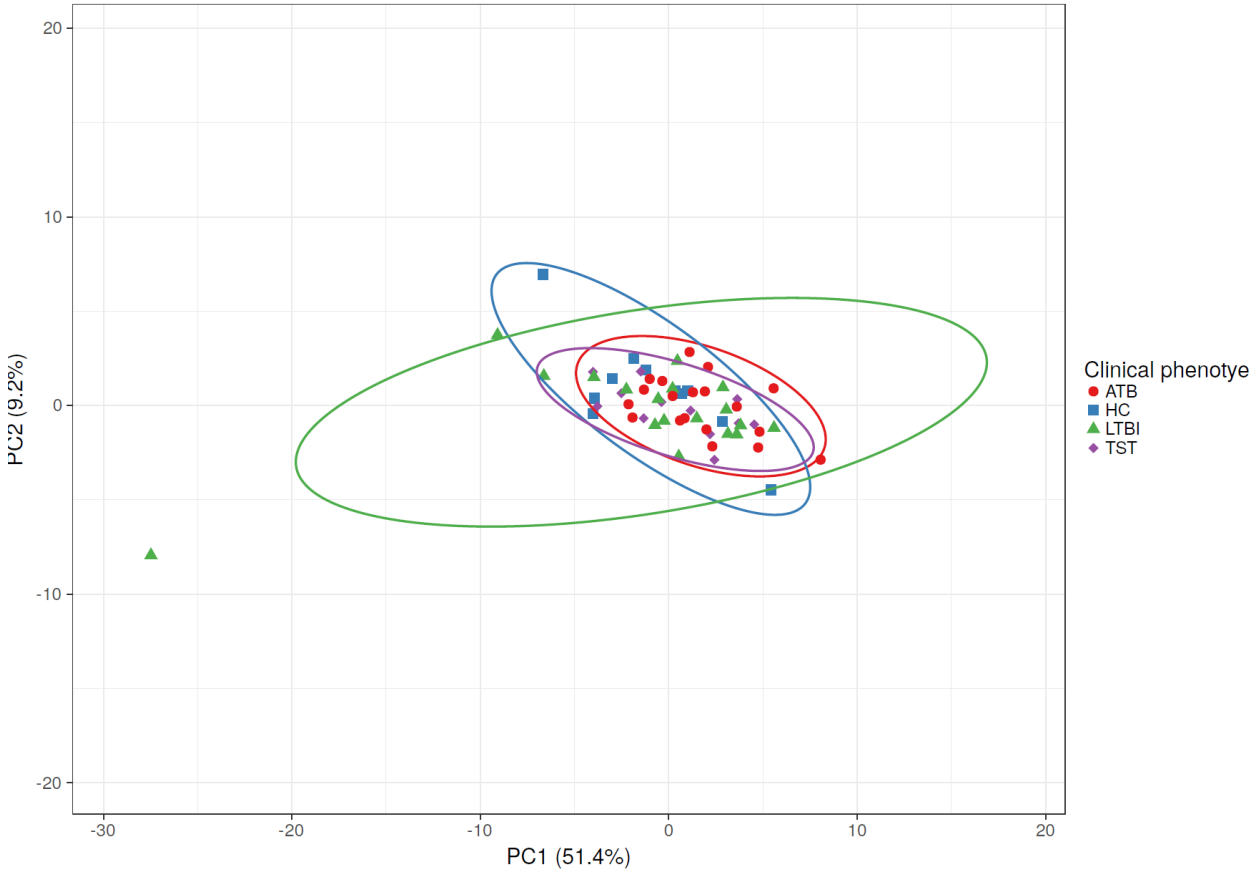

Figure 25. Principal component analysis of ISG expression fold changes in response to Mtb WCL.

Mtb WCL-stimulated PBMCs from ATB, HC, LTBI, and TST were incubated for 4 hours, RNA extracted and processed using RT-qPCR for detection of 53 genes. Gene expression fold changes was calculated using the formula $2^{-\Delta\Delta Ct}$. The original values for 52 genes were uploaded into Clutvis (http://biit.cs.ut.ee/clustvis/) and log transformed. The clinical groups are represented by shapes – red circle=ATB, blue square=HC, green triangle=LTBI, purple rhombus=TST.

In addition to the PCS, gene clustering was also assessed using a heatmap. As can be seen in Figure 26, the pattern of gene expression varies considerably by individuals, with some showing strong responses but, similar to the relative expression data in Figure 23, there was no clustering of gene expression by clinical phenotypes after Mtb WCL stimulation.

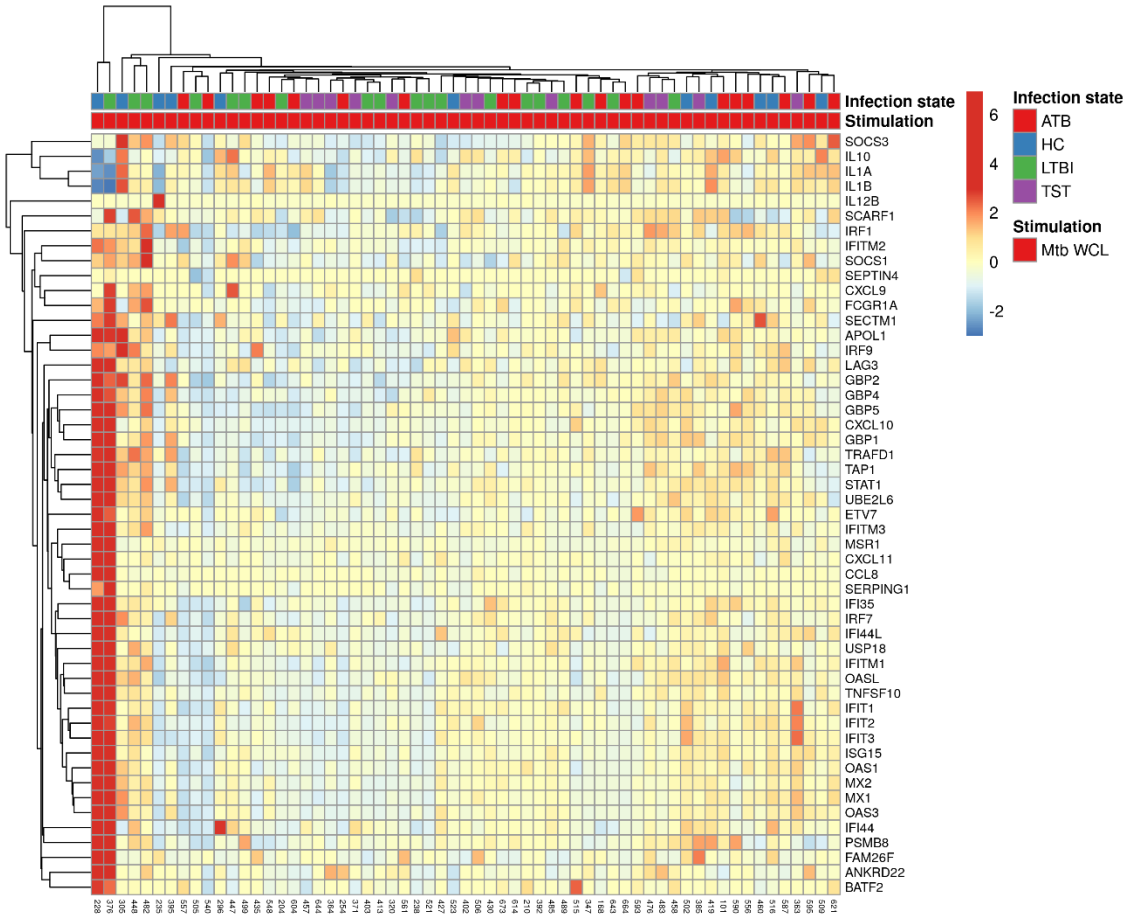

Figure 26. Heatmap showing the unsupervised clustering of ISG expression fold changes in Mtb WCL stimulated samples.

Peripheral blood mononuclear cells (PBMCs) from ATB, HC, LTBI, and TST were incubated with Mtb WCL or unstimulated for 4 hours, RNA extracted and processed using RT-qPCR for detection of 53 ISGs. Relative expression was calculated using the formula $2^{-\Delta\Delta Crt}$. The original values for 52 ISGs were uploaded into Clutvis (http://biit.cs.ut.ee/clustvis/) and log-transformed. The rows show the genes – blue color indicates low expression; red color indicates high expression). Columns show the clinical phenotypes (red=ATB; blue=HC; green= LTBI; purple=TST).

3.3.5.2 Comparison of ISG expression across clinical groups following Mtb WCL stimulation

Following data visualization using PCA and the heatmap the data was interrogated at the individual gene level. The median $\log_2$ fold changes (FC) for each gene in the IFN-stimulated samples were tested using the Kruskal-Wallis test to assess for statistically significant differences across the median of the $\log_2$ FC values from Mtb WCL stimulation between clinical groups.

As can be seen in Figure 27 (presented as log_2FC) and Table S2, using an absolute(log_2FC) of |1| cut-off with $log_2FC \geq 1.0$ being upregulated, and ≤ -1.0 being downregulated, less than half the genes were upregulated in most of the clinical groups after Mtb WCL stimulation in contrast to the findings after IFN-α/β stimulation (HC-50.9%, TST-32.1%, LTBI-24.5%, ATB-26.4%). Most of the genes showed no regulation (HC-30.2%, TST-50.9%, LTBI-62.3%, ATB-60.4%).

Only seven genes were upregulated in all clinical phenotypes: *GBP4* gene had the largest upregulation in HC, then LTBI, ATB and TST [log_2FC HC, TST, LTBI, ATB: 1.59, 1.13, 1.21, 1.18 respectively], *IFI44L* gene in ATB then TST, HC, and LTBI [1.22, 1.36, 1.15, 1.89], *IFIT1* gene in HC, TST, LTBI, and ATB [2.45, 2.16, 1.88, 1.66], *IFIT3* gene in HC, TST, ATB, and LTBI [2.34, 1.43, 1.14, 1.35], *IL-10* gene in HC, ATB, TST, and LTBI [2.85, 2.54, 1.98, 2.79], *IL-1A* gene in HC, ATB, LTBI, and TST [4.02, 3.50, 3.61, 3.86], and *IL-1B* gene in HC, LTBI, ATB, and TST [3.65, 2.95, 3.13, 2.98]. *MSR1* gene was downregulated in all groups with the largest change in LTBI, then in ATB, TST, and HC [-1.51, -2.32, -2.47, -2.40]. More than half of the genes tested exhibited mixed responses of up- or down-regulated genes with expression in some groups showing no regulation, these included *FCGR1A* [-1.06, -1.36, 0.23, -0.51]; *SOCS3* [1.10, 0.86, 0.85, 1.07]; SECTM1 [1.99, 0.49, 0.53, 0.06]; and *IFI44* [1.16, 1.44, 1.24, 0.82]. Others showed no change after Mtb WCL stimulation for all clinical phenotypes such as *IRF9* [log_2FC HC, TST, LTBI, ATB – 0.87, 0.34, 0.28, 0.23 respectively], *TNFSF10* [0.96, 0.70, 0.30, -0.07]. *FCGR1B* gene was not detected in TST, LTBI, and ATB, and was only detected in one individual in HC after Mtb WCL stimulation making it ineligible for analysis.

IFITM3, *OAS3*, *SECTM1*, *STAT1*, and *TNFSF10* genes were being differentially expressed after Mtb WCL stimulation. The largest change in the expression of *IFITM3* gene was in in ATB then LTBI, HC and TST (log_2FC HC, TST, LTBI, ATB: -0.22, -0.18, -0.29, -0.86; p=0.019); that for *OAS3* was largest in HC, followed by LTBI, ATB, and TST (log_2FC HC, TST, LTBI, ATB: 1.91, 0.87, 1.31, 0.91; p=0.045); for *SECTM1* gene in HC, LTBI, TST, and lowest in ATB (log_2FC HC, TST, LTBI, ATB: 1.99, 0.49, 0.53, 0.06; $p< 0.001$), as can be seen in Figure 27. The change in expression of *STAT1* gene was largest in HC then TST, LTBI, and ATB (1.44, 0.69, 0.62, 0.49; p=0.024); and for *TNFSF10* gene in HC, TST, LTBI, ATB (log_2FC HC, TST, LTBI, ATB: 0.96,

0.70, 0.30, -0.07; p=0.044). The log_2FC levels of *IFITM3* and *TNFSF10* genes were outside the cut-off of 1; those of *SECTM1* and *STAT1* genes were upregulated in HC only.

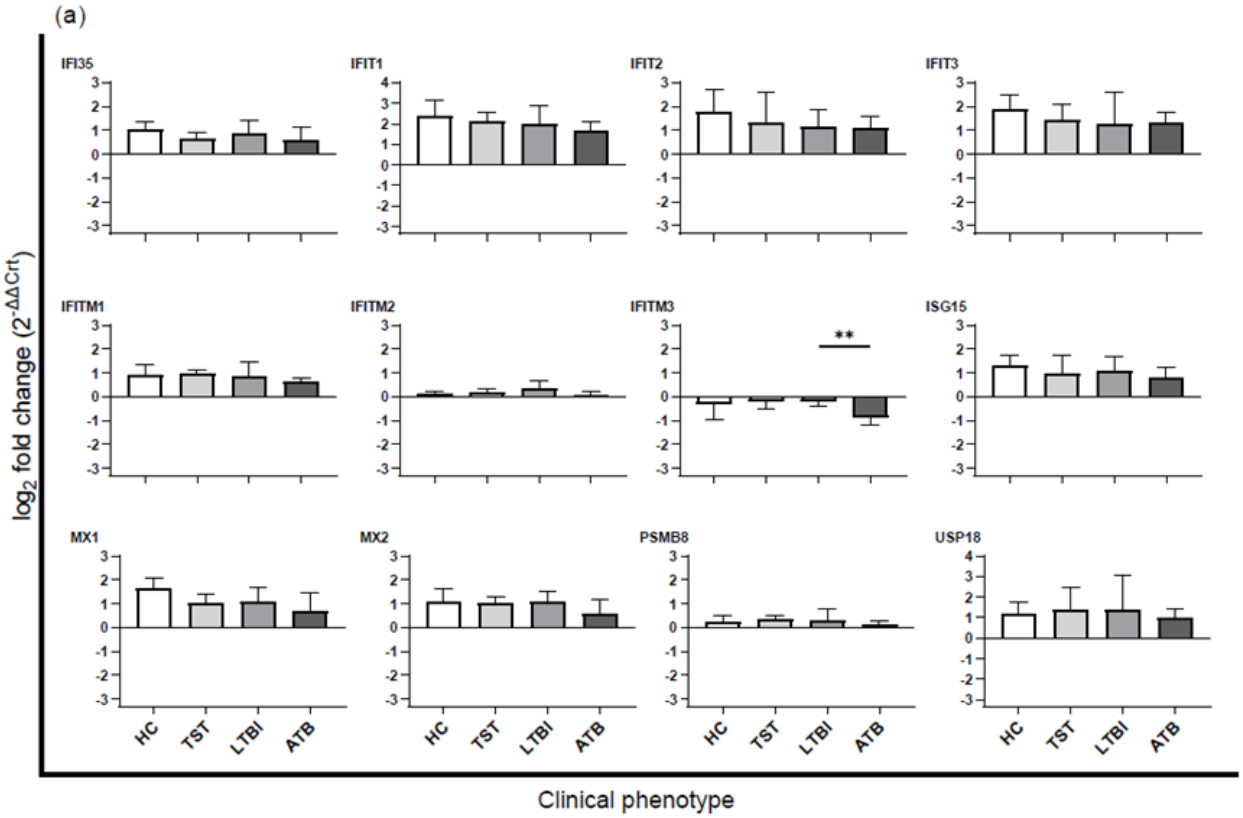

Figure 27. Gene expression (fold changes) in Mtb WCL- stimulated samples.

Genes enriched for (a) IFN-α/β signaling pathway, (b) IFN-γ signaling pathway, (c) IFN-α/β and IFN-γ signaling pathways, (d) IFN signaling, (e) IL-10 signaling pathway, and (f) Not classified. RT qPCR analysis of mRNA expression of ISGs in PBMCs with no stimulation or stimulated with Mtb WCL were normalized to 18S rRNA, β-actin and HPRT1 (ΔCt). Fold change was calculated as $2^{-\Delta\Delta Crt}$ and presented in a log_2 format. Data are presented as median; each circle represents one participant. Kruskal-Wallis test was performed to assess differences between clinical phenotypes, * $p< 0.05$, ** $p< 0.01$, *** $p\leq 0.001$. Genes were listed according to Figure 14. Bars in each section are labelled in the order HC (white), TST, LTBI, and ATB (dark gray). x-axis=clinical phenotype; y-axis= log_2 fold change.

Figure 27: continued

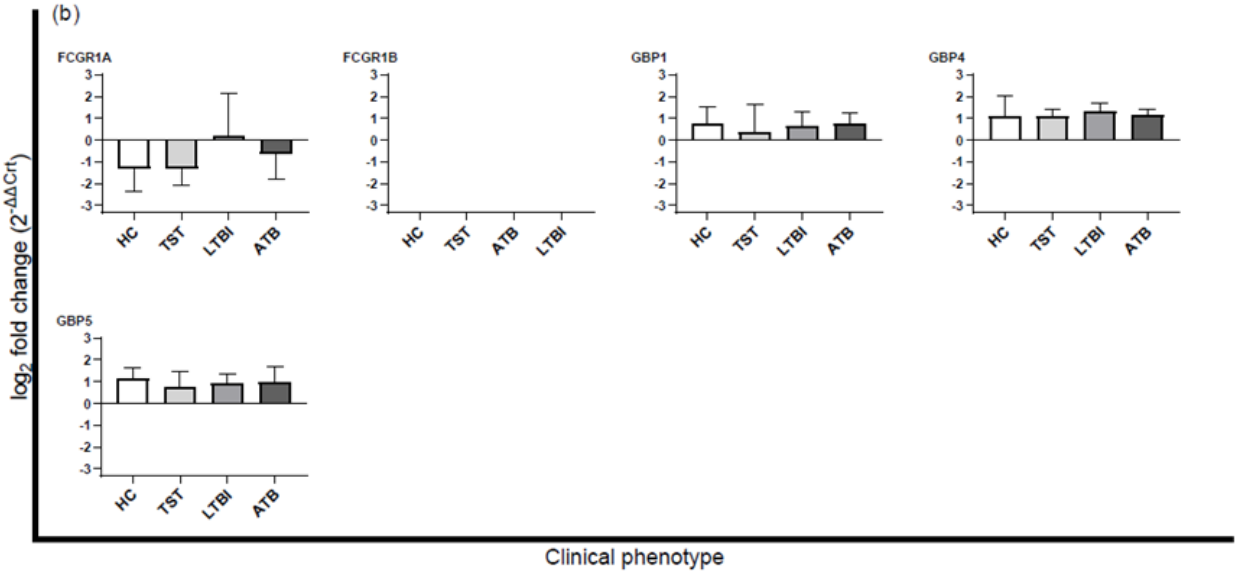

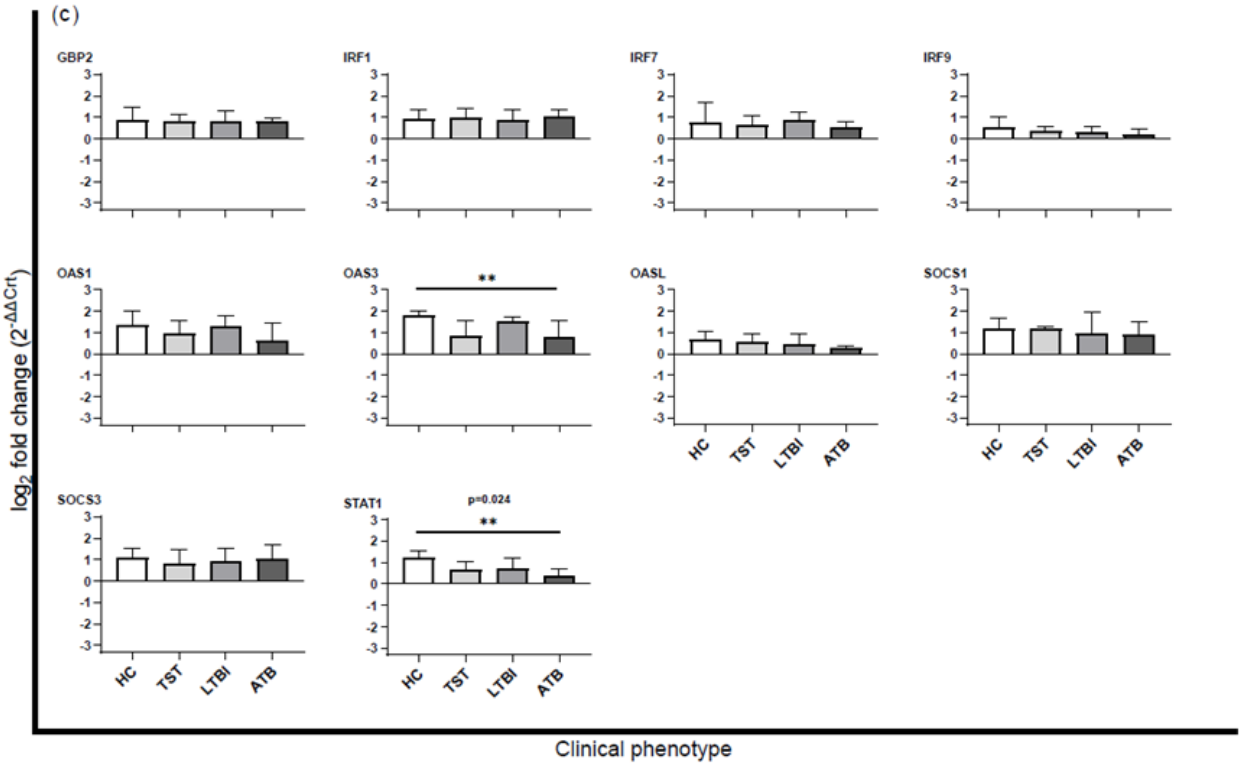

Figure 27: continued

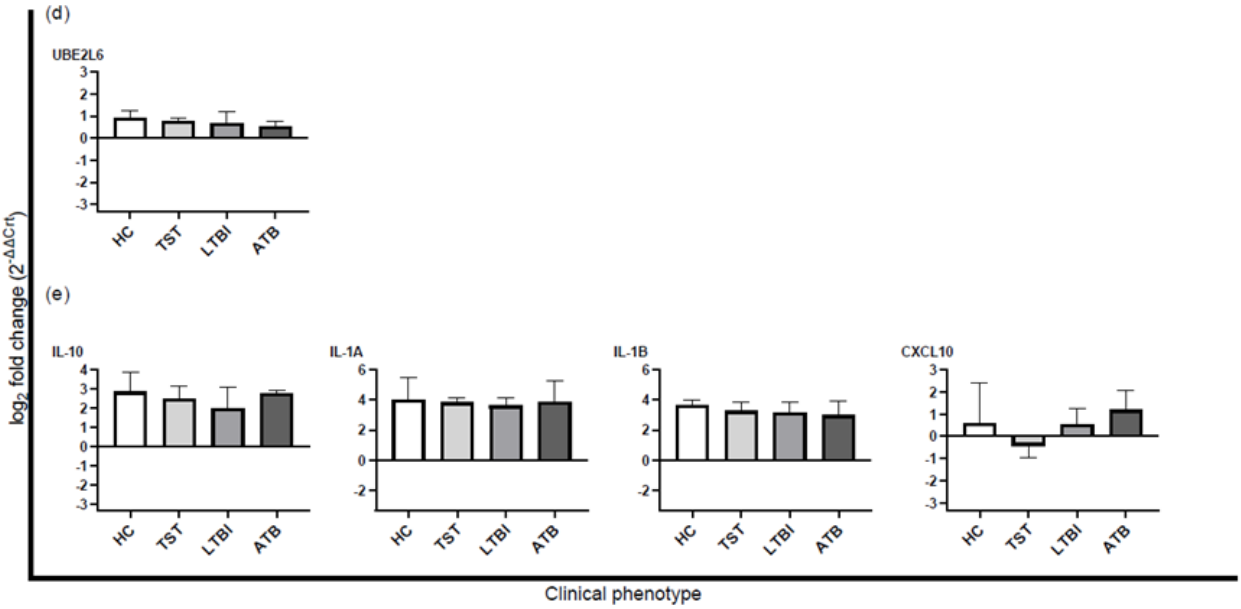

Figure 27: continued

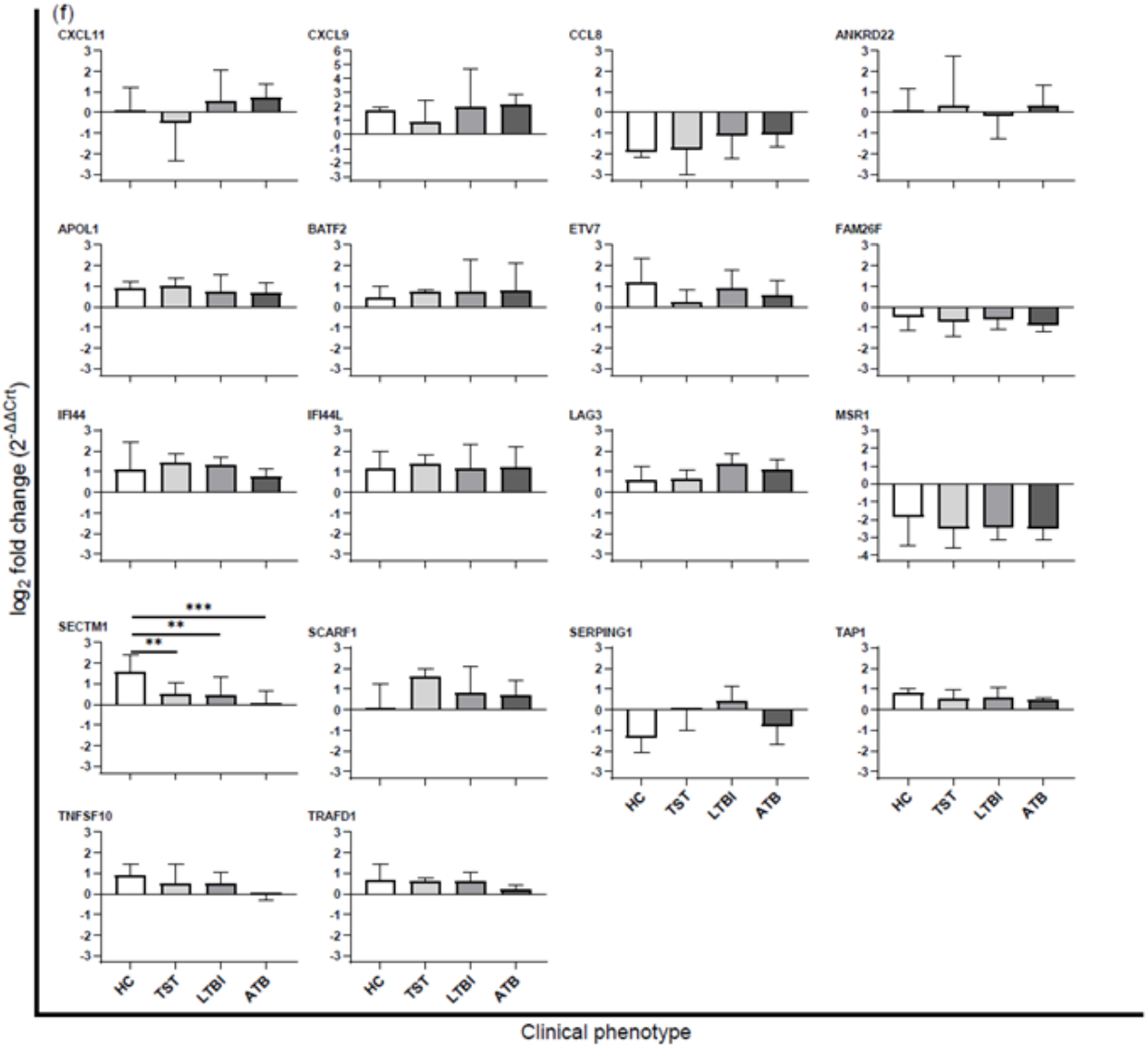

3.3.5.3 Comparison of ISG expression between clinical groups following Mtb WCL stimulation

For the expression of *IFITM3*, *OAS3*, *SECTM1*, *STAT1*, and *TNFSF10* genes following Mtb WCL stimulation that were differentially expressed across the four study groups identified using the Kruskal-Wallis test, pairwise comparisons using Dunn's procedure were subsequently performed to identify the specific pairs of medians that differed significantly, followed by post hoc analysis using Bonferroni correction for multiple comparisons with statistical significance set at $p< 0.05$.

Pairwise comparisons identified significant differences in the Mtb WCL-induced fold changes in *IFITM3* gene between ATB and LTBI (log_2FC: -0.86 vs -0.29; p=0.005), and ATB and TST (log_2FC: -0.86 vs -0.18; p=0.024); in *OAS3* gene between HC and ATB (log_2FC: 1.91 vs 0.91; p=0.007), and HC and TST (log_2FC: 1.91 vs 0.87; p=0026); in *SECTM1* gene between HC and ATB (log_2FC: 1.99 vs 0.06; p<0.001), HC and LTBI (log_2FC: 1.99 vs 0.53; p=0.002), and HC and TST(log_2FC: 1.99 vs 0.49; p=0.001); in *STAT1* between HC and ATB (log_2FC: 1.44 vs 0.49; p=0.002); and in *TNFSF10* between HC and ATB (log_2FC: 0.96 vs -0.07), and HC and LTBI (log_2FC: 0.96 vs 0.30) with larger fold change in HC. (Table 11).

Following corrections for multiple comparisons statistically significant differences in median fold changes were observed in the expressions of *IFITM3* between ATB and LTBI with larger fold changes in ATB; *OAS3* between HC and ATB, *SECTM1* gene between HC and ATB, HC and LTBI, and HC and TST, and *STAT1* between HC and ATB with higher fold changes in HC after Mtb WCL stimulation as shown in Table 11.

Table 11. Differentially expressed genes with Mtb WCL stimulation between clinical groups (fold change).

						Post hoc analysis	
Stimulation	**Gene**	**N**	**χ2**	**p-value[a]**	**Comparison[b]**	**p-value[c]**	**adjusted p-value[d]**
Mtb WCL	*IFITM3*	60	9.937	0.019	ATB-LTBI	0.005	**0.03**
					ATB-TST	0.024	0.142
	OAS3	60	8.033	0.045	HC-ATB	0.007	**0.04**
					HC-TST	0.026	0.154
	SECTM1	59	21.056	< 0.001	HC-ATB	< 0.001	**< 0.001**
					HC-LTBI	0.002	**0.012**
					HC-TST	0.001	**0.007**
	STAT1	60	9.48	0.024	HC-ATB	0.002	**0.013**
	TNFSF10	60	8.108	0.044	HC-ATB	0.009	0.053
					HC-LTBI	0.026	0.155

ATB-active tuberculosis; TST- Tuberculin skin test positive; LTBI-latent tuberculosis infection; HC-healthy controls
N: total number of individuals in whom gene is detected. Comparisons of fold changes between clinical groups using Kruskal-Wallis test with post hoc pairwise comparisons and Bonferroni correction for multiple comparisons. **Bolded** and yellow highlighted p-values are significant after Bonferroni correction. Chi square (χ^2) is the square of the difference between the observed values and the expected values. p-values: [a] – across groups p-value; [c] – pairwise comparison (between groups) p-value; [d] – adjusted p-value using Bonferroni correction for multiple comparisons.[b] – the order in the comparison shows the direction of the difference with the higher expression listed first.

3.3.5.4 Summary

The experiments in this section aimed to compare gene regulation responses to stimulation with Mtb WCL in different *M. tuberculosis* infection states. We hypothesized that stimulation of PBMCs with Mtb WCL would result in suppression of ISGs in ATB compared to LTBI. Stimulation with Mtb WCL resulted in upregulation of slightly over half the genes tested, with about a third of the genes showing little effect in LTBI and ATB. Even for the genes that were upregulated after stimulation, the induction was markedly reduced compared to that induced after IFN-α/β stimulation except for *IL-1A* and *IL-1B* genes that were upregulated after Mtb WCL stimulation but downregulated with IFN-α/β. For differentially expressed genes –*OAS3*, *SECTM1*,

and *STAT1* - fold changes were highest in HC and higher LTBI than in ATB. The downregulation of *IFITM3* expression was highest in ATB compared to the other groups.

3.3.6 Comparison of ISG expression with IFN-α stimulation versus IFN-β stimulation within clinical groups

IFN-α and IFN-β both signal through the IFN-α receptor (IFNAR). Differences in the binding affinities of these IFNs to the receptor have been observed. IFN-β shows a 20 to 30-fold higher affinity and lower dissociation rate for IFNAR and hence prolonged effects than IFN-α (303,305). A transcriptional profiling study of PBMCs extracted from healthy individuals and stimulated with type I IFNs observed similar expression of genes induced by IFN-α and IFN-β (390). Here differences in gene expression induced by IFN-α and IFN-β were assessed, as each PBMC sample from the participant groups HCs, TST, LTBI, and ATB were stimulated with either IFN-α or IFN-β.

3.3.6.1 Comparison of the relative ISG expression following IFN-α versus IFN-β stimulation within clinical groups

The relative expression for each ISG was calculated using the formula, Relative expression = $2^{-\Delta Crt}$ and the ISG responses induced by IFN-α compared with those induced by IFN-β within each clinical group using a Wilcoxon signed-rank test which tests whether a set of pairs (repeated measures on a single sample) differs significantly.

Statistically significant differences were observed with the relative expression of several genes shown in Figure 28. Most genes showed higher expression with IFN-β than with IFN-α stimulation. The median values are presented as relative expression in IFN-α vs IFN-β.This was observed in the expression of *BATF2* gene in LTBI (0.000768vs 0.001099;17 pairs; p< 0.0001)and in ATB (0.001109 VS 0.001343;18 pairs; p= 0.0483); *CCL8* gene in LTBI (0.013818 vs 0.016775; 17 pairs; p= 0.0013) and in ATB (0.022401 vs 0.028615; 19 pairs; p= 0.0005); *CXCL10* gene in TST (0.055564 vs 0.056384; 12 pairs; p=0.0425), LTBI (0.057678 vs 0.062898; 17 pairs; p=0.0258)and in ATB (0.054174vs 0.076740; 18 pairs; p= 0.0095); *FAM26F* gene in ATB only (0.001771 vs 0.002338; 19 pairs; p= 0.0138); *FCGR1A* gene in LTBI only (0.000604 vs 0.000847; 18 pairs; p= 0.0375); *IFI44L* gene in LTBI only (0.007206 vs 0.008172; 19 pairs; p=0.0258); *IFIT1*

gene in ATB only (0.038357 vs 0.041119; 19 pairs; p= 0.0230); *IFIT2* gene in HC(0.016122 vs 0.018386; 11 pairs; p=0.0137), TST (0.015750 vs 0.017674; 12 pairs; p= 0.0122), LTBI (0.016811 vs 0.020819; 19 pairs; p= 0.0020) and ATB (0.017696 vs 0.021977; 19 pairs; p= 0.0204). Similar observations were made in the expression of *IFIT3* gene in TST (0.034889 vs 0.034438; 12 pairs; p=0.0425); *IRF9* gene in TST (0.002255 vs 0.002992; 12 pairs; p= 0.0425), and *SERPING1* gene in ATB (0.001703 vs 0.001854; 19 pairs; p= 0.0401).

Genes with higher expression with IFN-α than with IFN-β stimulation were *IRF1* (0.006818 vs 0.005943; 11 pairs; p= 0.0098), *MX1* (0.057390 vs 0.042507; 11 pairs; p=0.0323), and *OAS3* gene (0.022520 vs 0.022360; 11 pairs; p= 0.0137) in HC; and, *IL-1A* gene (0.000318 vs 0.000203; 19 pairs; p= 0.0361), and *IL-1B* gene (0.017254 vs 0.013663; 19 pairs; p= 0.0046) in ATB (Figure 28).

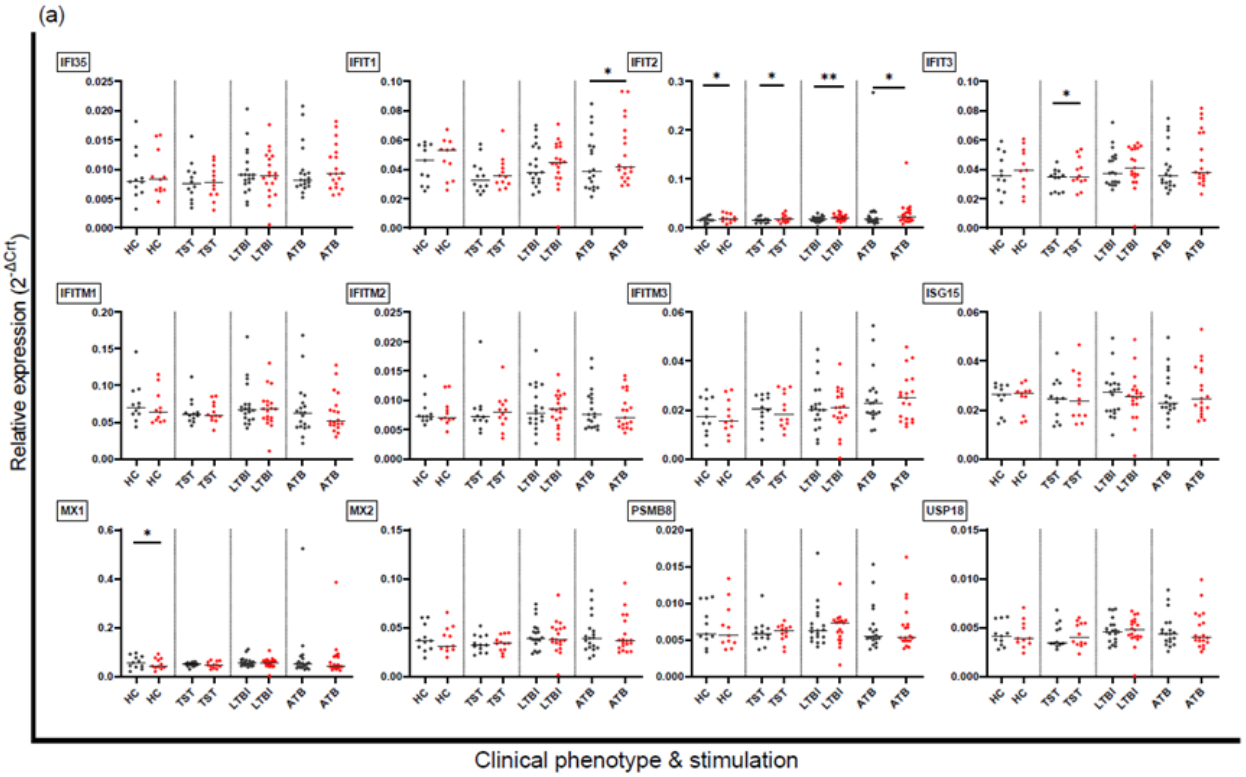

Figure 28. Relative ISG expression of IFN-α versus IFN-β stimulation of PBMCs within clinical groups.

Genes enriched for (a) IFN-α/β signaling pathway, (b) IFN-γ signaling pathway, (c) IFN-α/β and IFN-γ signaling pathways, (d) IFN signaling, (e) IL-10 signaling pathway, and (f) Not classified. Peripheral blood mononuclear cells (PBMCs) from 11 HC, 12 TST, 19 LTBI, and 19 ATB were cultured with IFN-α in parallel with IFN-β for 4 fours. RNA was extracted from the PBMC pellets and processed through RT-qPCR on the Quantstudio platform acquiring Crt values. Fold changes were calculated for each gene using the $2^{-\Delta Crt}$ method and comparisons between IFN-α and IFN-β responses done using the Wilcoxon signed-rank test. Data are presented as median values. p-value: * < 0.05; ** ≤ 0.01; *** ≤ 0.001. IFN-α responses are represented by black symbols and IFN-β responses by red symbols.

Figure 28: continued

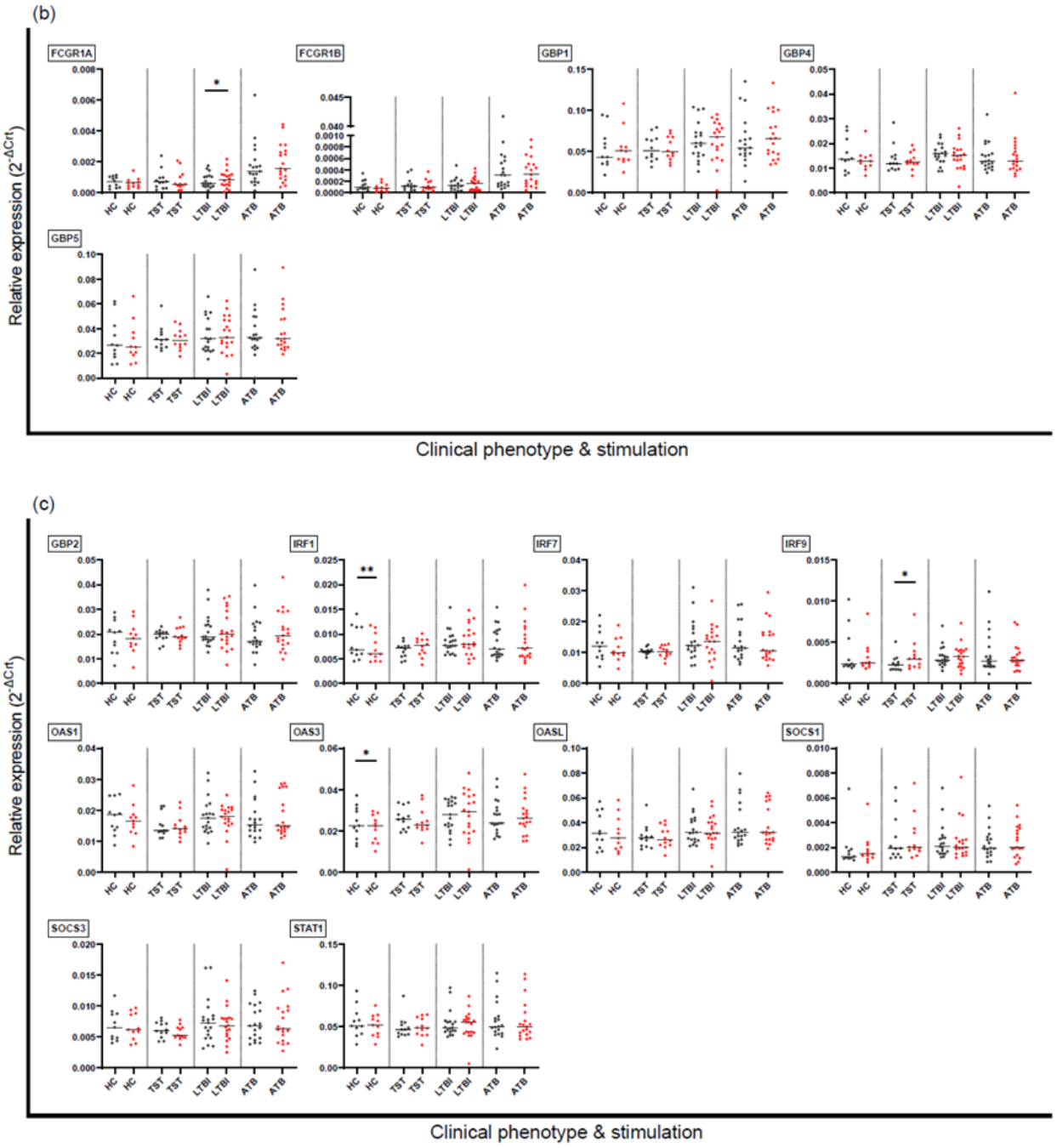

Figure 28: continued

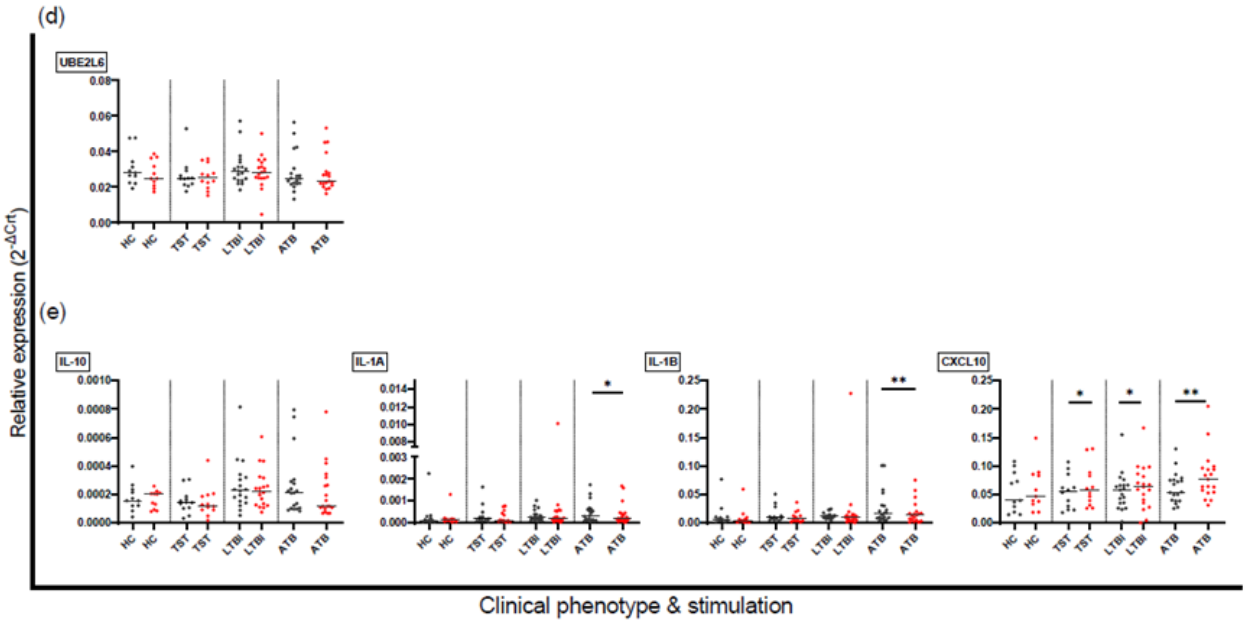

Figure 28: continued

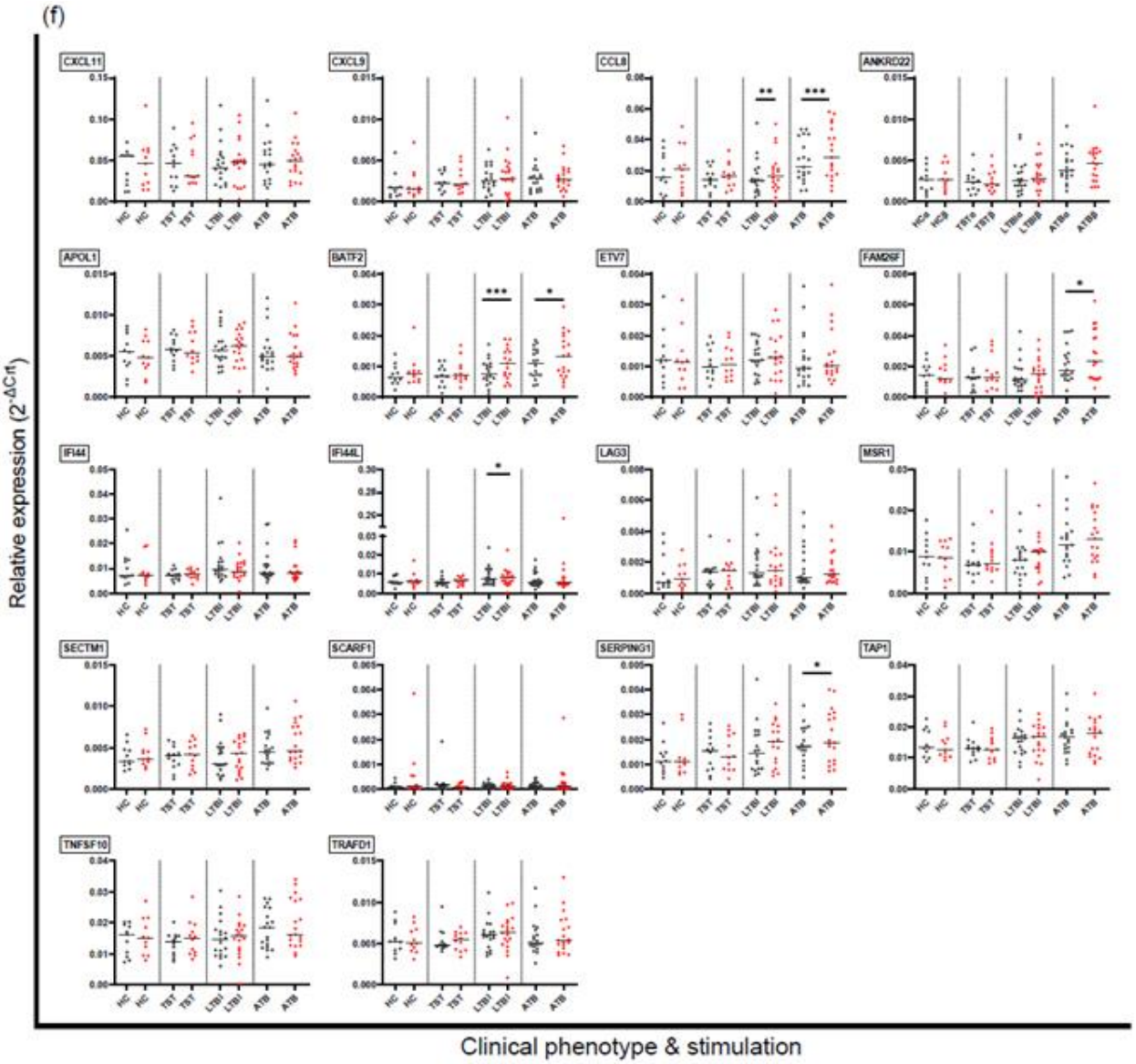

3.3.6.2 Comparison of ISG fold changes following IFN-α versus IFN-β stimulation within clinical groups

The fold change for each ISG was calculated using the formula, Fold change = $2^{-\Delta\Delta Crt,}$ and the ISG responses induced by IFN-α compared with those induced by IFN-β within each clinical phenotype using a Wilcoxon signed-rank test which tests whether a set of pairs (repeated measures on a single sample) differs significantly.

Significant differences were observed between IFN-α- and IFN-β- inducedexpression of several genes shown in Figure 29. Most genes showed higher expression with IFN-β than with IFN-α stimulation. The values are presented as log_2FC in IFN-α vs IFN-β. This was observed in the expression of *BATF2* gene in LTBI (3.62 vs 3.86; 12 pairs; p= 0.0005); *CCL8* gene in LTBI (7.13 vs 7.37; 15 pairs; p= 0.0054) and in ATB (6.70 vs 7.19; 18 pairs; p= 0.0034); *CXCL10* gene in ATB (6.71 vs 7.28; 19 pairs; p= 0.0095); *CXCL11* gene in TST only (8.09 vs 8.25; 11 pairs; p=0.0322); *FAM26F* gene in ATB only (3.58 vs 3.89; 19 pairs; p= 0.0204); *FCGR1A* gene in LTBI only (2.96 vs 3.08; 15 pairs; p= 0.0413); *IFIT1* gene in ATB only (6.21 vs 6.10; 19 pairs; p= 0.0361); *IFIT2* gene in TST (5.00 vs 5.07; 12 pairs; p= 0.0269), LTBI (4.84 vs 4.99; 18 pairs; p= 0.0028) and ATB (5.86 vs 5.97; 19 pairs; p= 0.0323). Similar observations were made in the expression of *IRF9* gene in TST (1.09 vs 1.44; 12 pairs; p= 0.0425). The expression of *IL-1A* gene (-1.69 vs -2.06; 19 pairs; p= 0.0483), and *IL-1B* gene (-1.32 vs -2.12; 19 pairs; p= 0.0004) in ATB showed higher downregulation with IFN-β stimulation than with IFN-α.

Gene differentially expressed between IFN-α and IFN-β with higher expression after IFN-α stimulation than after IFN-β stimulation were *CXCL10* gene (5.59 vs 5.58; 12 pairs; p= 0.0342) and *SOCS3* gene (0.44 vs 0.26; 12 pairs; p=0.0342) in TST; and *IRF1* (1.22 vs 1.06; 11 pairs; p= 0.0049), and *OAS3* gene (4.99 vs 4.78; 11 pairs; p= 0.0420) in HC.

Most genes showed similar trends between IFN-α and IFN-β induced gene expression with both relative expression and fold change calculations. These were observed in HC – *IRF1* and *OAS3* gene expression; in TST – *CXCL10*, *IFIT2*, and *IRF9* gene expression; in LTBI – *BATF2*, *CCL8*, *FCGR1A*, and *IFIT2* gene expression; and in ATB - *CCL8*, *CXCL10*, *FAM26F*, *IFIT1*, and *IFIT2* gene expression.

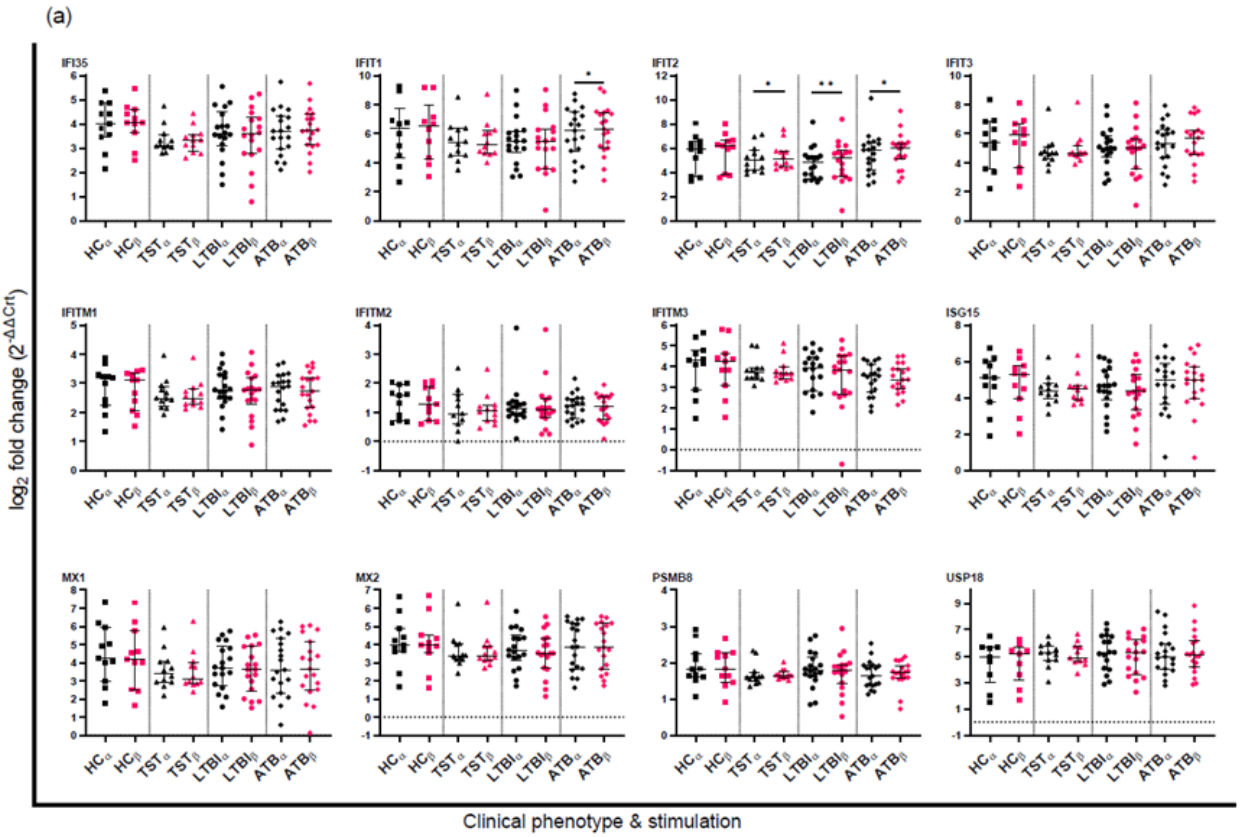

Figure 29. Gene expression (fold changes) of IFN-α versus IFN-β stimulation of PBMCs within clinical groups.

Genes enriched for (a) IFN-α/β signaling pathway, (b) IFN-γ signaling pathway, (c) IFN-α/β and IFN-γ signaling pathways, (d) IFN signaling, (e) IL-10 signaling pathway, and (f) Not classified. Peripheral blood mononuclear cells (PBMCs) from 11 HC, 12 TST, 19 LTBI, and 19 ATB were cultured with IFN-α in parallel with IFN-β for 4 fours. RNA was extracted from the PBMC pellets and processed through RT-qPCR on the Quantstudio platform acquiring Crt values. Fold changes were calculated for each gene using the $2^{-\Delta\Delta Crt}$ method and comparisons between IFN-α and IFN-β responses done using the Wilcoxon signed-rank test. Data are presented as median values. p-value: * < 0.05; ** ≤ 0.01; *** ≤ 0.001. IFN-α responses are represented by black symbols and IFN-β responses by pink symbols.

Figure 29: continued

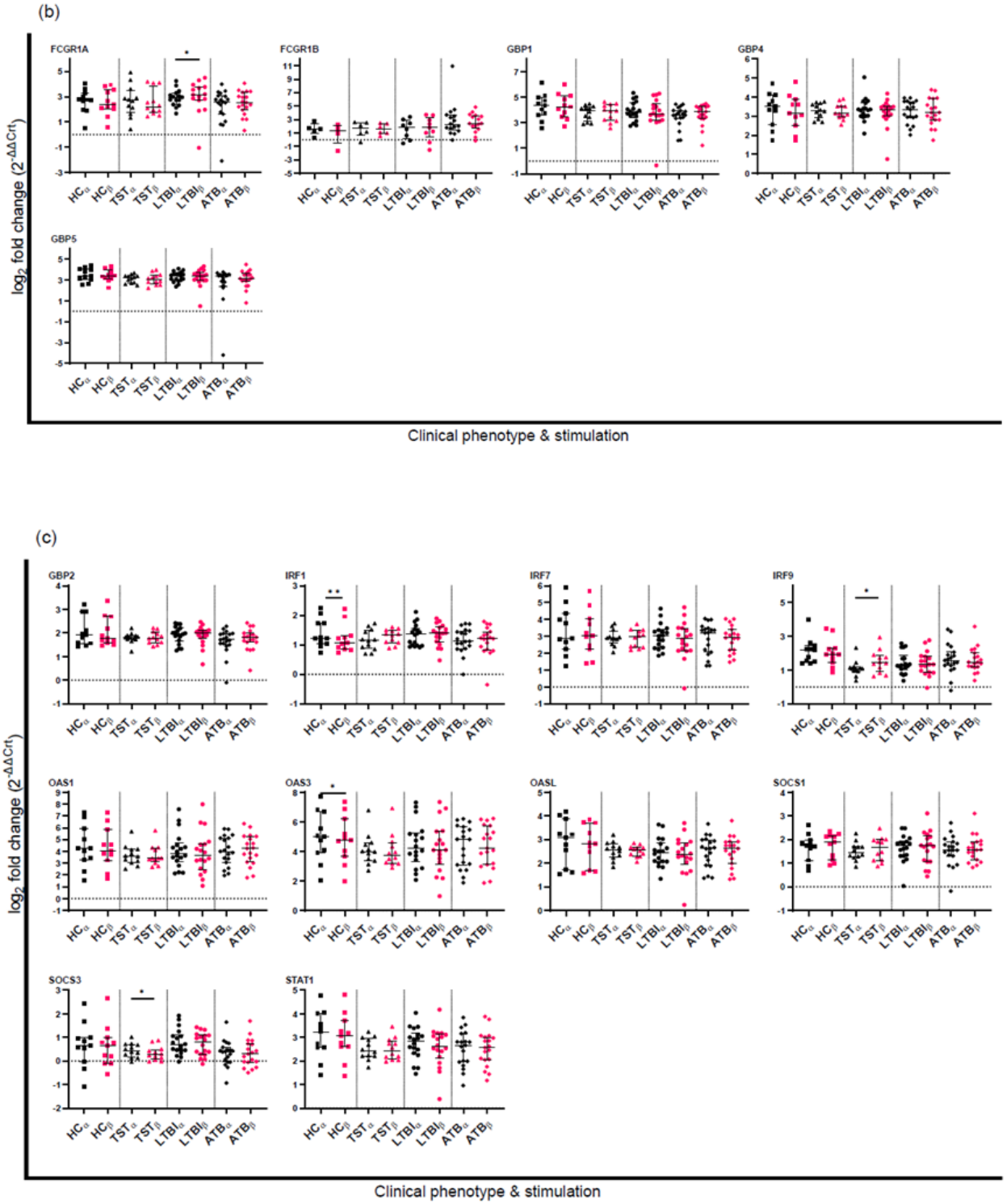

Figure 29: continued

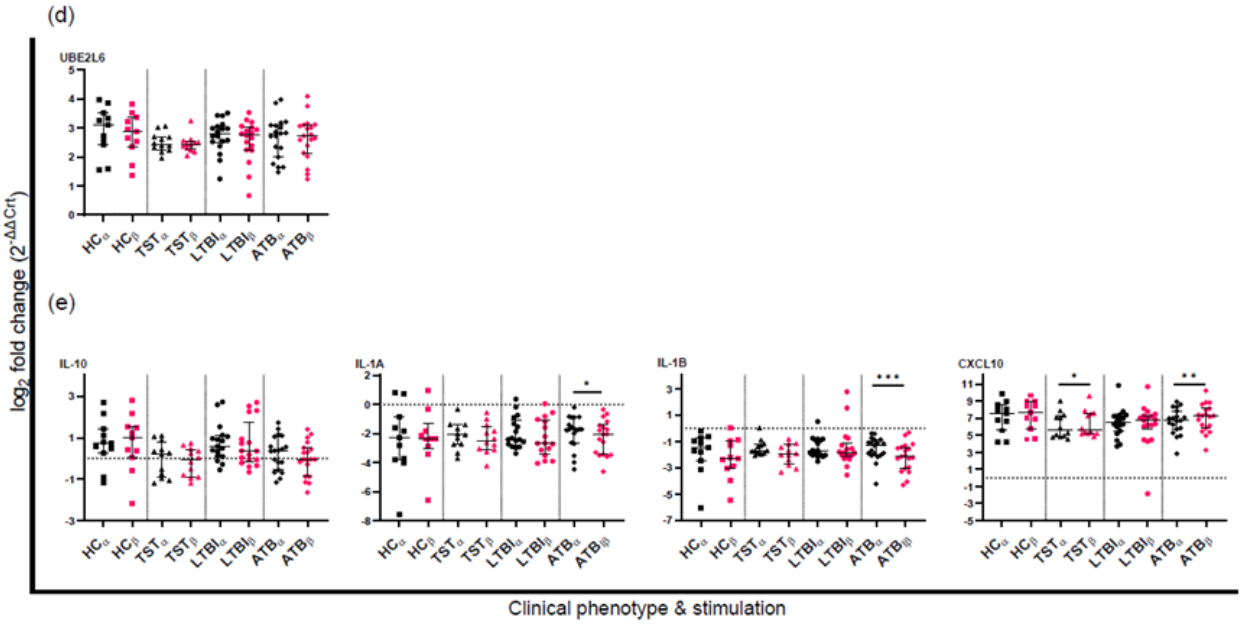

Figure 29: continued

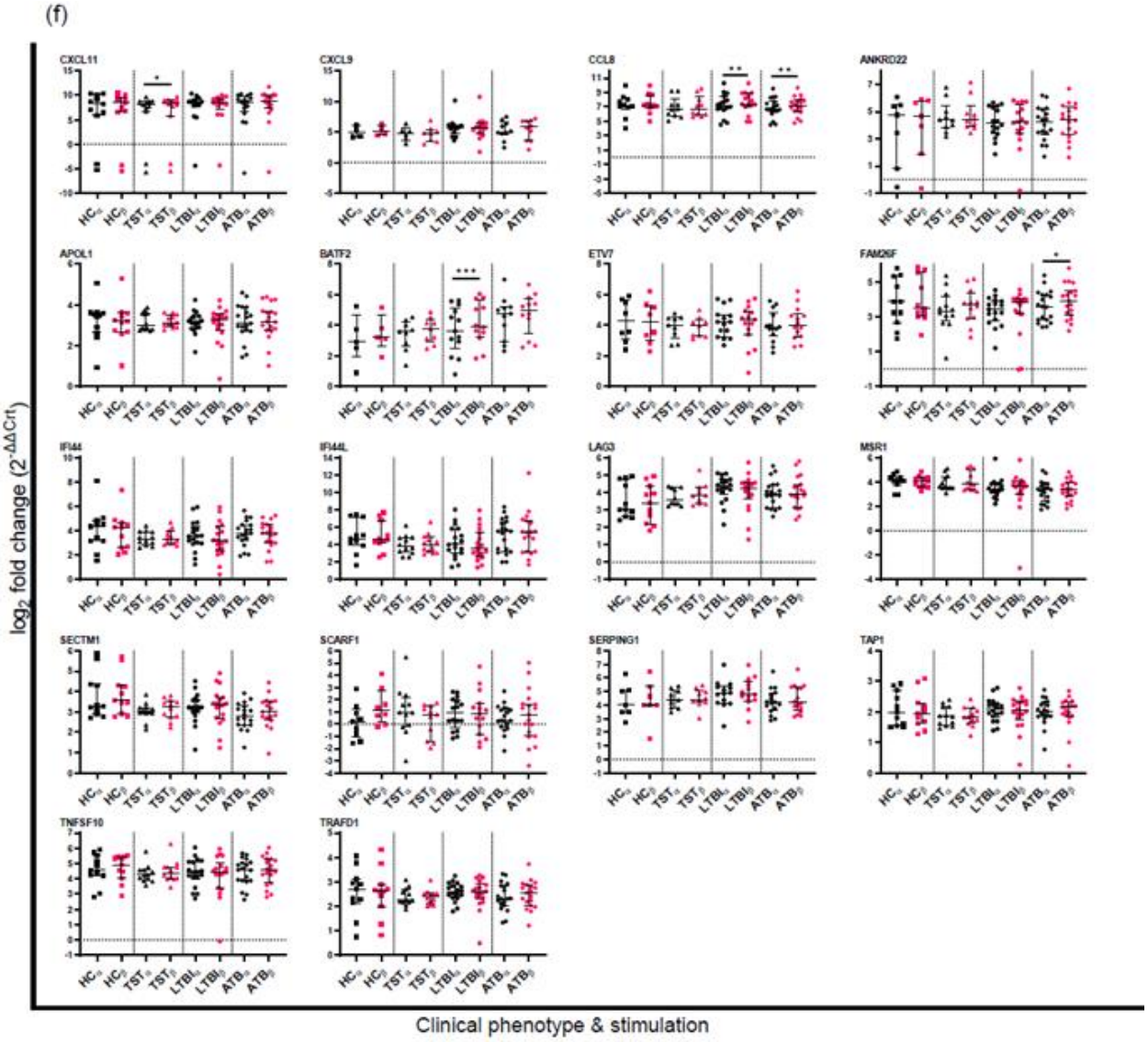

3.3.6.3 Summary

The experiments in this section aimed to compare gene expression induced by IFN-α and IFN-β. We, therefore, hypothesized that stimulation with IFN-α and IFN-β would drive similar transcriptional profiles in the *M. tuberculosis* infection states. PBMC samples from each study participant were tested in parallel, with one tube of PBMCs stimulated with IFN-α and the other with IFN-β. RT qPCR was run, and data was analysed using both the ΔCt and the ΔΔCt methods.

IFN-α and IFN-β signal through the same receptor, IFNAR, but show differences in binding affinities and in their binding sites on the receptor.

Although the expression of the ISGs followed similar trends with IFN-α and IFN-β stimulation, statistically significant differences were observed in some of the ISGs between the responses induced by the IFNs in the four clinical groups. Most of the differentially expressed ISGs following IFN-α and IFN-β stimulation were common to both relative expression and fold change analyses with similar directionality. Most of the ISG responses were higher with IFN-β than with IFN-α when assessed with both relative expression and fold change except for *IRF1, IL-1A* and *IL-1B* genes, which showed higher expression with IFN-α with both analyses. Although most of the genes supported the sub-hypothesis that stimulation with IFN-α and IFN-β would drive similar transcriptional profiles in the *M. tuberculosis* infection states, a number of genes showed differences in the expression levels between the stimulations in the infection states.

3.4 Analysis of cytokines in clinical samples

The interaction between the production of type I IFNs and cytokines in the immune response to *M. tuberculosis* infection has been studied both in vivo in mouse-models of infection and in in vitro cell cultures. These studies have shown that type I IFNs suppress Th1 responses in *M. tuberculosis* infection with reduced activity of TNF-α, IFN-γ, IL-12, IL-1α, IL-1β and IL-6 (26,366,367,372,418–420). In these studies, the immunoregulatory cytokine, IL-10, shows contrasting effects; some studies demonstrate increased IL-10 production induced by type I IFNs, while others show reduced IL-10 production.

To better understand the effect of IFN-α and IFN-β on the immune response in different *M. tuberculosis* infection phenotypes, in addition to the gene expression analysis, we also characterized the cytokine profile in cultures of unstimulated PBMCs from 10 HC, 12 TST, 18 LTBI, and 16 ATB. The PBMCs were cultured unstimulated for 16 to 18 hours as described in section 2.6.5. Supernatants from the cultured PBMCs were analysed for 33 cytokines, listed in Table 5, using Milliplex® MAP Human Cytokine / Chemokine kits (EMD Millipore, USA).

3.4.1 Comparison of cytokine levels between clinical groups at baseline

A total of 23 cytokines that had at least 60% detectability were analysed, excluding the remaining nine cytokines – FGF-1, GM-CSF, IL-1α, IFN-γ, IL-12p40, IL-12p70, IL-13, IL-2, IL-4, VEGF -from further analysis in all samples, and IFN-γ from further analysis in the unstimulated samples. Using REACTOME enrichment analysis from STRING analysis (https://string-db.org/), we identified cytokines involved in signaling pathways. 15 of the tested cytokines were involved in "Signaling by ILs" with most of the 15 overlapping with other signaling pathways – "Cytokine signaling in immune system", "IL-10 signaling", "IL-4 and IL-13 signaling" pathways. The cytokines that did not overlap with other pathways included fractalkine and EGF in "Signal transduction, IFN-α2 and sCD40L in "Cytokine signaling in immune system" and MDC that was not involved in any signaling pathway.

The median levels for each cytokine at baseline for the four study groups are shown in Table S3 and in Figure 30. Higher cytokine level in ATB compared to HC was observed for eotaxin (median level for ATB vs HC: 7.56pg/ml vs 6.65pg/ml), fractalkine (31.14pg/ml vs 23.98pg/ml), MCP-3 (298.36pg/ml vs 119.53pg/ml), MCP-1 (3233.34pg/ml vs 1743.05pg/ml), IL-8 (5157.91pg/ml vs 2915.97pg/ml), and RANTES (568.39pg/ml vs 453.30pg/ml), PDGF-AA (49.37pg/ml vs 25.33pg/ml), PDGF-AB/BB (140.18pg/ml vs 93.18pg/ml), IL-1β (34.99pg/ml vs 28.80pg/ml), IL-6 (100.69pg/ml vs 70.20pg/ml), sCD40L (15.78pg/ml vs 9.90pg/ml), and IL-1RA (195.41pg/ml vs 189.64pg/ml); the remaining cytokines were higher in HC. Cytokine levels were higher in ATB compared to LTBI for GRO (1769.38pg/ml vs 1567.68pg/ml), IL-8 (5157.91pg/ml vs 4057.15pg/ml), PDGF-AA (49.37pg/ml vs 37.68pg/ml), PDGF-AB/BB (140.18pg/ml vs 112.10pg/ml), and sCD40L (15.78pg/ml vs 12.50pg/ml); the remaining cytokines were higher in LTBI.

A Kruskal Wallis test conducted to assess for significant differences between the median cytokine levels across the study groups found none of the analyte levels differed.

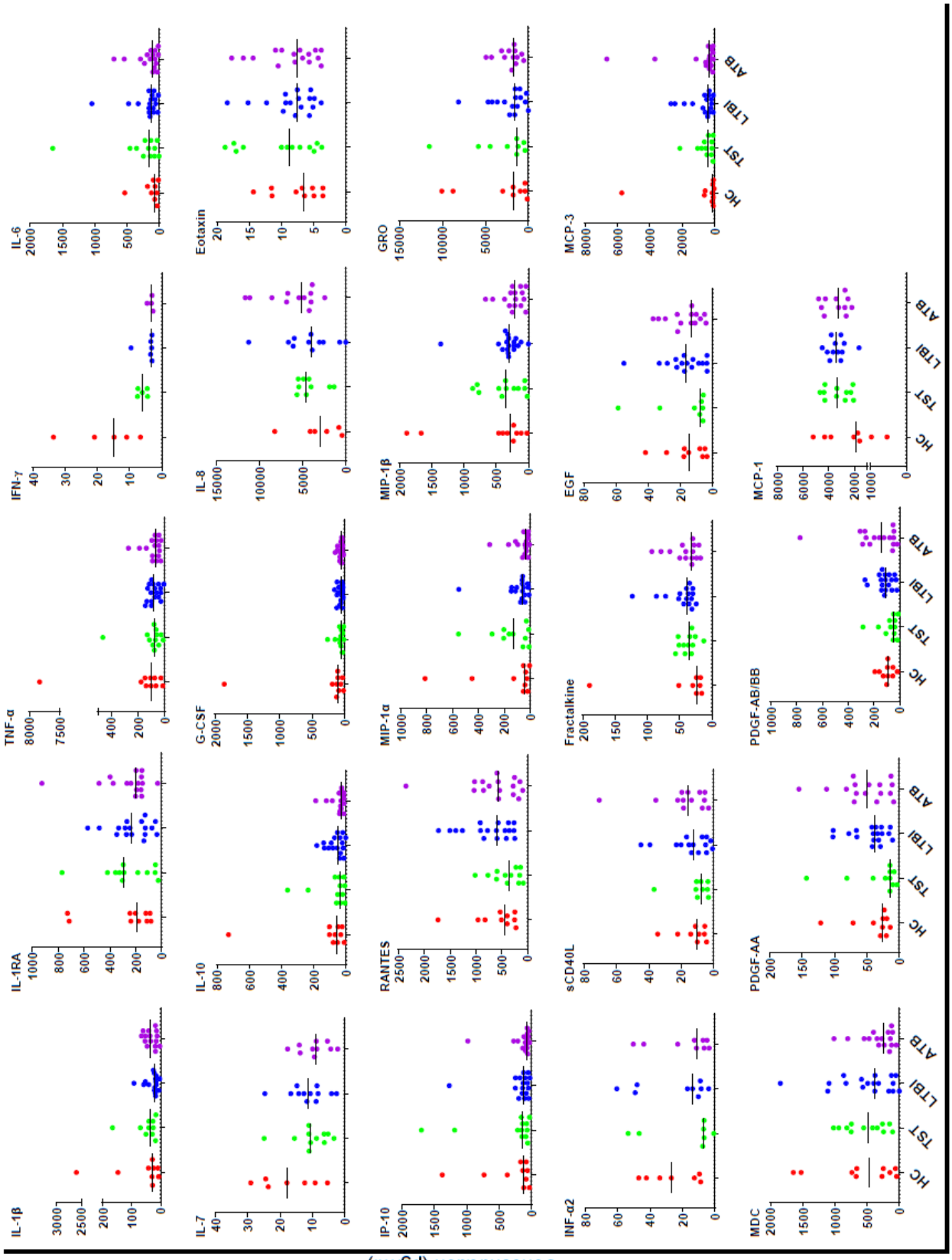
IL-1β
IL-1RA
TNF-α
IFN-γ
IL-6
IL-7
IL-10
G-CSF
IL-8
Eotaxin
IP-10
RANTES
MIP-1α
MIP-1β
GRO
INF-α2
sCD40L
Fractalkine
EGF
MCP-3
MDC
PDGF-AA
PDGF-AB/BB
MCP-1
HC
TST
LTBI
ATB
Concentration (pg/ml)
Clinical phenotype

Figure 30. Cytokine levels in baseline samples from HC, TST, LTBI, and ATB.

Cytokine levels were measured in baseline PBMCs from HC, TST, LTBI, and ATB using a multiplex bead assay. Data are presented as median values. Each dot represents one participant. Kruskal-Wallis test was performed to assess differences between clinical phenotypes. (blue=HC, red=TST, green=LTBI, purple=ATB).

3.4.1.1 Summary

The experiments in this section aimed to assess the production of cytokines at baseline, without stimulation, in the *M. tuberculosis* infection states (TST reactive, LTBI, and ATB) and in healthy controls. We hypothesized that the levels of pro-inflammatory cytokines are higher in ATB than in other clinical phenotypes.

None of the cytokines were statistically significant between clinical phenotypes in the baseline samples. Nevertheless, the levels of the chemokines, IL-8 and GRO, and the growth factors PDGF-AA and PDGF-AB/BB were higher in ATB compared to LTBI. The proinflammatory cytokines - IL-6 and IL-1β; the chemokines-eotaxin, fractalkine, MCP-1, MCP-3, IL-8, and RANTES - some of which have pro-inflammatory activity, including IL-8 and MCP-1; the growth factors-PDGF-AA and PDGF-AB/BB; and the anti-inflammatory receptor antagonist-IL-1RA were all higher in ATB compared to HC.

3.4.2 Comparison of cytokine levels between clinical groups following IFN-α or IFN-β stimulation

Next, each PBMC stimulation sample was tested for differences in cytokine profiles in response to IFN-α or IFN-β stimulation. Samples from the study groups HCs, TST, LTBI, and ATB were stimulated with either 1000IU/ml IFN-α or 10ng/ml IFN-β for 16 to 18 hours. Supernatants were processed using the Milliplex® MAP Human Cytokine / Chemokine kits as described in 2.5.5.

The expression of most of the cytokines were not affected by IFN-α and IFN-β stimulation (Figure 31). Compared to baseline in which IFN-α2 level was highest in HC, then LTBI, ATB, and TST (26.76pg/ml in HC, 6.78pg/m in TST, 13.65pg/ml in LTBI, 11.20pg/ml in ATB), with a similar trend after IFN-β stimulation (35.31pg/ml in HC, 5.86pg/ml in TST, 18.98pg/ml in LTBI, 9.96pg/ml in ATB), IFN-α2 was markedly induced after IFN-α stimulation as expected–with the

highest level in LTBI followed by ATB, TST, and lowest in HC (2316.63pg/ml in HC, 2408.81pg/ml in TST, 2671.14pg/ml in LTBI, 2477.62pg/ml in ATB). IL-1RA and IP-10 levels were elevated with both IFN-α (IL-1RA: 402.06pg/ml in HC, 427.06pg/ml in TST, 592.47pg/ml in LTBI, 702.54pg/ml in ATB; IP-10: 2348.46pg/ml in HC, 3080.27pg/ml in TST, 2455.20pg/ml in LTBI, 2550.82pg/ml in ATB) and IFN-β (IL-1RA: 544.69pg/ml in HC, 610.33pg/ml in TST, 764.58pg/ml in LTBI, 920.51pg/ml in ATB; IP-10: 4542.90pg/ml in HC, 3933.30pg/ml in TST, 4737.47pg/ml in LTBI, 6753.43pg/ml in ATB) compared to baseline levels (IL-1RA: 189.64pg/ml in HC, 293.56pg/ml in TST, 231.32pg/ml in LTBI, 195.41pg/ml in ATB; IP-10: 124.52pg/ml in HC, 139.96pg/ml in TST, 120.14pg/ml in LTBI, 69.22pg/ml in ATB) with higher IL-1RA and IP-10 levels induced by IFN-β in all study groups.

GRO and IL-8 were reduced after both IFN-α (GRO:272.72pg/ml in HC, 348.28pg/ml in TST, 333.38pg/ml in LTBI, 283.84pg/ml in ATB; IL-8: 1342.96pg/ml in HC, 2342.00pg/ml in TST, 2288.06pg/ml in LTBI, 2566.52pg/ml in ATB) and IFN-β stimulation (GRO: 183.39pg/ml in HC, 265.34pg/ml in TST, 233.83pg/ml in LTBI, 237.59pg/ml in ATB; IL-8: 980.74pg/ml in HC, 1059.28pg/min TST, 912.90pg/ml in LTBI, 1256.40pg/ml in ATB) compared to baseline levels (GRO: 1771.44pg/ml in HC, 1369.67pg/ml in TST, 1567.68pg/ml in LTBI, 1769.38pg/ml in ATB; IL-8: 2915..97pg/ml in HC, 4591.42pg/min TST, 4057.15pg/ml in LTBI, 5157.91pg/ml in ATB) with more reduction with IFN-β stimulation as can be seen on Figure 31 and Table S3.

To better understand the responses of individual cytokines, the median levels for each cytokine in the IFN-stimulated samples were compared using a Kruskal-Wallis test to assess for significant differences across the median of the expression values from IFN-stimulation between clinical groups. Following IFN-α stimulation, significant differences in levels across clinical groups were identified for several cytokines – IL-10, MCP-3, MIP-1β, and PDGF-AB/BB (Figure 31 and Table S3). The highest levels of these four cytokines were in LTBI compared to the other clinical groups. the level of IL-10 was highest in LTBI, and lowest in ATB (57.03pg/ml in HC, 40.97pg/ml in TST, 81.89pg/ml in LTBI, 29.06pg/ml in ATB; p=0.036); MCP-3 level was highest in LTBI, followed by ATB, TST, and lowest in HC (349.84pg/ml in HC, 509.59pg/ml in TST, 927.37pg/ml in LTBI, 674.46pg/ml in ATB; p=0.046), MIP-1β level was highest in LTBI, then in TST and HC, and lowest in ATB(388.94pg/ml in HC, 363.92pg/ml in TST, 485.71pg/ml in LTBI, 294.13pg/ml in ATB; p=0.048), and PDGF-AB/BB level was highest in LTBI followed by ATB, HC, and lowest in TST (50.89pg/ml in HC, 32.17pg/ml in TST, 94.20pg/ml in LTBI, 104.35pg/ml

in ATB; p=0.019). Following IFN-β stimulation, only the level of IL-10 showed significant difference between study groups, being highest in HC followed by LTBI, TST, and lowest in ATB (98.54pg/ml in HC, 38.81pg/ml in TST, 83.70pg/ml in LTBI, 27.18pg/ml in ATB; p=0.034).

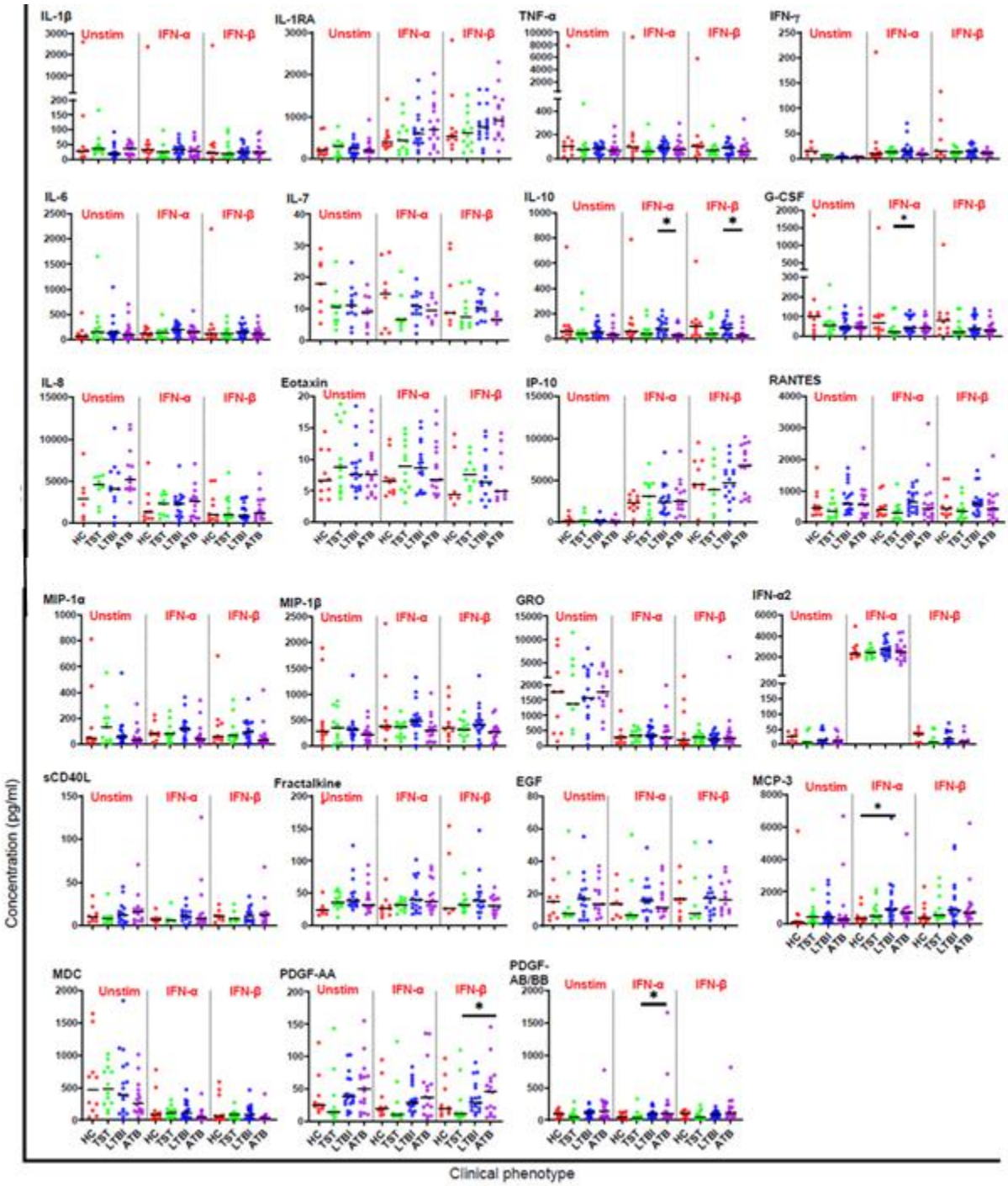
IL-1β
IL-1RA
TNF-α
IFN-γ
IL-6
IL-7
IL-10
G-CSF
IL-8
Eotaxin
IP-10
RANTES
MIP-1α
MIP-1β
GRO
IFN-α2
sCD40L
Fractalkine
EGF
MCP-3
MDC
PDGF-AA
PDGF-AB/BB
Unstim
IFN-α
IFN-β
HC
TST
LTBI
ATB
Concentration (pg/ml)
Clinical phenotype

Figure 31. Cytokine levels in baseline, IFN-α-, or IFN-β- stimulated samples.

Cytokine levels were measured from unstimulated, IFN-α- (α), IFN-β-(β) stimulated PBMCs using a multiplex bead assay. Comparisons between clinical groups were made using Kruskal-Wallis test followed by post hoc analysis with Bonferroni correction. Data are presented as median values. Each dot represents results from one individual. Multiple corrections p-value: * < 0.05; ** ≤ 0.01; *** ≤ 0.001. Symbol color: red=HC, green=TST, blue=LTBI, purple=ATB. x-axis=clinical phenotype; y-axis=cytokine concentrations.

3.4.2.1 Comparison of cytokine levels between clinical groups following IFN-α or IFN-β stimulation

For the levels of IL-10, MCP-3, MIP-1β and PDGF-AB/BB that were differentially expressed across the four study groups following IFN-α or IFN-β stimulation, pairwise comparisons using Dunn's procedure were subsequently performed to identify the specific pairs of medians that differed significantly, followed by post hoc analysis using Bonferroni correction for multiple comparisons with statistical significance set at $p < 0.05$.

3.4.2.1.1 IFN-α stimulation

Pairwise comparisons identified significant differences between clinical groups with IFN-α stimulation for the chemokines MCP-3 (CCL7) between LTBI and HC (median: 927.37pg/ml vs 349.84pg/ml; p=0.046), MIP-1β (CCL4) between LTBI and ATB(median: 485.71pg/ml vs 294.13pg/ml; p=0.048); the immunoregulatory cytokine IL-10 between LTBI and ATB, and between HC and ATB (median: 81.89pg/ml vs 29.06pg/ml, and 57.03pg/ml vs 29.06pg/ml; p=0.036); and the growth factor PDGF-AB/BB between both ATB and LTBI with TST (median: 104.35pg/ml vs 32.17pg/ml, and 94.20pg/ml vs 32.17pg/ml; p=0.019) listed in Table 12. Following correction for multiple comparisons, IL-10 was differentially expressed between LTBI and ATB (median: 81.89pg/ml vs 29.06pg/ml; p=0.032), MCP-3 between LTBI and HC (median: 927.37pg/ml vs 349.84pg/ml; p=0.032), and PDGF-AB/BB between ATB and TST (median: 104.35pg/ml vs 32.17pg/ml; p=0.025) as shown in Table 12.

3.4.2.1.2 IFN-β stimulation

Pairwise comparisons identified significant differences in IL-10 between LTBI and ATB, and between HC and ATB with IFN-β stimulation (median: 83.70pg/ml vs 27.18pg/ml, and 98.54pg/ml vs 27.18pg/ml; p=0.034). Following correction for multiple comparison, IL-10

expression remained statistically significant between LTBI and ATB (median: 83.70pg/ml vs 27.18pg/ml; p=0.048) (Table 12).

Table 12. Cytokine level differences with IFN-α or IFN-β stimulation.

						Post hoc analysis	
Stimulation	**Cytokine**	**N**	**χ2**	**p-value[a]**	**Comparison[b]**	**p-value[c]**	**adjusted p-value[d]**
IFN-α	IL-10	55	8.541	0.036	HC-ATB	0.049	0.292
					LTBI-ATB	0.005	**0.032**
	MCP-3	54	8.017	0.046	LTBI-HC	0.005	**0.032**
	MIP-1β	56	7.906	0.048	LTBI-ATB	0.012	0.075
	PDGF-AB/BB	54	9.945	0.019	ATB-TST	0.004	**0.025**
					LTBI-TST	0.024	0.143
IFN-β	IL-10	55	8.700	0.034	LTBI-ATB	0.008	**0.048**
					HC-ATB	0.019	0.116

ATB-active tuberculosis; TST-Tuberculin skin test positive; LTBI-latent tuberculosis infection; HC-healthy controls. N: total number of individuals in whom each gene is detected. Comparisons of cytokine levels between clinical groups using Kruskal-Wallis test with post hoc pairwise comparisons and Bonferroni correction for multiple comparisons. **Bolded** and yellow highlighted p-values are significant after Bonferroni correction. Chi square (χ^2) is the square of the difference between the observed and the expected values. p-values: [a] – across groups p-value; [c] – pairwise comparison (between groups) p-value; [d] – adjusted p-value using Bonferroni correction for multiple comparisons. [b] – the order in the comparison shows the direction of the difference with the higher expression listed first.

3.4.2.1.3 Summary

The experiments in this section aimed to compare the induction of cytokines in response to IFN-α and IFN-β stimulation in *M. tuberculosis* infection states (LTBI and ATB). We hypothesized that the IFNs would suppress the expression of pro-inflammatory cytokines in ATB while increasing anti-inflammatory cytokines.

The immunoregulatory/ anti-inflammatory cytokine IL-10 was differentially expressed between LTBI and ATB, with higher expression in LTBI following IFN-α and IFN-β stimulation which did not support the sub-hypothesis. The chemokine MCP-3 was differentially expressed between LTBI and HC with higher expression in LTBI and PDGF-AB/BB between ATB and TST

with higher expression in ATB with IFN-α stimulation. Aside from the increased expression of IP-10 with both IFN-α and IFN-β stimulation and of IFN-α2 observed with IFN-α stimulation, most of the cytokines did not show a clear difference in the IFN-stimulated expression compared to the baseline expression. Although not statistically significant, the expression of pro-inflammatory cytokines – IL-1β, IL-6, and TNF-α – was lower in ATB compared to LTBI following IFN-α or IFN-β stimulation.

3.4.2.2 Comparison of cytokine fold changes between clinical groups following IFN-α or IFN-β stimulation

Next, the cytokine fold changes were calculated to assess the quantity of change in cytokine responses with stimulation compared to baseline. This was calculated as the ratio of cytokine level in stimulated sample/cytokine level in unstimulated sample for each IFN stimulation condition. This fold change demonstrated whether a cytokine was up-regulated or down-regulated following stimulation.

3.4.2.2.1 Comparison of cytokine expression (fold changes) across clinical groups following IFN-α or IFN-β stimulation

To determine differences at the single cytokine level, the median fold changes in Table S4 in the IFN-stimulated samples from the four clinical groups were compared. For this comparison a cut-off absolute(log_2FC) of |1| was used, with log $log_2FC \geq$ for upregulated and $log_2FC \leq -1$ for downregulated. Overall, the majority of the cytokines showed little change following IFN-α and IFN-β, as seen in Figure 32 and Table S4. IFN-α stimulation up-regulated the expression of IFN-α2 in all groups with the largest change in TST, followed by LTBI, ATB and HC (log_2FC for HC, TST, LTBI, ATB: 6.39, 8.32, 7.84, 7.19); MCP-3 in HC and ATB with the largest change in HC (log_2FC for HC, TST, LTBI, ATB: 1.49, 0.82, 0.83, 1.01), IL-1RAin all groups with the largest change in ATB, LTBI, HC then TST (log_2FC for HC, TST, LTBI, ATB: 1.41, 1.10, 1.49, 1.61),and IP-10 in all groups with the largest change in ATB followed by LTBI, TST and HC (log_2FC for HC, TST, LTBI, ATB: 3.87, 4.06, 4.66, 4.83). IFN-α stimulation down-regulated the expression of GRO in all groups with the largest change in ATB followed by both LTBI and TST, then HC

(log_2FC for HC, TST, LTBI, ATB:-2.12, -2.25, -2.25, -2.64), MDC in all groups with the largest change in ATB followed by TST then both LTBI and HC (log_2FC for HC, TST, LTBI, ATB: -1.89, -1.94, -1.89, -2.25), and IL-8 only in ATB and TST with the largest change in ATB (log_2FC for HC, TST, LTBI, ATB: -0.97, -1.18, -0.84, -1.36). The remaining cytokines showed no regulation after IFN-α stimulation.

Almost similar responses were observed following IFN-β stimulation in which MCP-3 was upregulated in all groups with the largest change in HC followed by LTBI, ATB and TST (log_2FC for HC, TST, LTBI, ATB: 1.68, 1.08, 1.20, 1.17); IL-1RA with the largest change in ATB then HC, LTBI and TST (log_2FC for HC, TST, LTBI, ATB: 1.87, 1.49, 1.85, 2.22); and IP-10 with the largest change in ATB then LTBI, HC and TST (log_2FC for HC, TST, LTBI, ATB: 5.29, 5.11, 5.61, 6.03); the exception was the expression of IFN-α2 that showed no regulation (log_2FC for HC, TST, LTBI, ATB: 0.10, -0.17, -0.06, -0.10). IFN-β stimulation downregulated the expression of GRO in all groups with the largest change in ATB then LTBI, TST and HC (log_2FC for HC, TST, LTBI, ATB: -2.64, -2.74, -2.94, -3.18); MDC in all groups with the largest change in ATB followed by TST, HC, and LTBI (log_2FC for HC, TST, LTBI, ATB: -2.47, -2.64, -2.25, -2.94); and IL-8 in all groups with the largest change in ATB followed by TST, HC and LTBI (log_2FC for HC, TST, LTBI, ATB: -1.32, -1.40, -1.15, -2.00). The remaining cytokines showed no regulation (Table S4).

The cytokines IL-10, IL-1α, IL-1β, and IP-10 were also assessed at gene level. The expression of the cytokine IL-10 showed no change with both IFN-α (log_2FC for HC, TST, LTBI, ATB: 0.36, -0.03, 0.57, -0.03) and IFN-β stimulation (log_2FC for HC, TST, LTBI, ATB: 0.40, 0.01, 0.45, 0.00) (Table S4). Likewise, the IL-10 gene expression showed no change for almost all groups with IFN-α (log_2FC for HC, TST, LTBI, ATB: 0.77, 0.23, 0.58, 0.37) and IFN-β stimulation (log_2FC for HC, TST, LTBI, ATB: 1.01, -0.07, 0.28, -0.04) except for HC with IFN-β stimulation (Table S2). The expression of the cytokine IL-1β showed no change with IFN-α (log_2FC for HC, TST, LTBI, ATB: -0.10, -0.79, 0.38, 0.14) and IFN-β stimulation (log_2FC for HC, TST, LTBI, ATB: -0.29, -0.81, 0.11, 0.16) although that of the IL-1B gene was downregulated with both stimulations - IFN-α (log_2FC for HC, TST, LTBI, ATB: -1.51, -1.69, -1.69, -1.32) and IFN-β stimulation (log_2FC for HC, TST, LTBI, ATB: -2.25, -2.00, -1.84, -2.12) (Tables S4 and S2). CXCL10 (IP-10) was upregulated at both cytokine level - IFN-α (log_2FC for HC, TST, LTBI, ATB: 3.87, 4.06, 4.66, 4.83) and IFN-β (log_2FC for HC, TST, LTBI, ATB: 5.29, 5.11, 5.61, 6.03)

(Table S4), and at gene level - IFN-α (log_2FC for HC, TST, LTBI, ATB: 7.60, 5.59, 6.49, 6.71) and IFN-β (log_2FC for HC, TST, LTBI, ATB: 7.69, 5.58, 6.73, 7.28) (Table S2).

A Kruskal-Wallis test was then carried out to assess differences in cytokine expression between the clinical groups. None of the cytokines up-regulated or down-regulated following IFN-α stimulation were differentially regulated. Significant differences across the four study groups were identified in the fold changes for G-CSF that was highest in LTBI, followed by ATB, HC, and lowest with TST (log_2FC for HC, TST, LTBI, ATB: -0.22, -0.64, -0.06, -0.18; p=0.031); IL-10 expression was highest in LTBI, followed by HC, and lowest in ATB and TST (log_2FC for HC, TST, LTBI, ATB: 0.36, -0.03, 0.57, -0.03; p=0.022), PDGF-AB/BB expression was highest in ATB then in LTBI, TST, and HC (log_2FC for HC, TST, LTBI, ATB: -0.81, -0.43, -0.12, -0.15; p=0.017) and IL-1β expression was highest in LTBI, followed by ATB, HC, and TST (log_2FC for HC, TST, LTBI, ATB: -0.10, -0.79, 0.38, 0.14; p=0.033) with IFN-α stimulation; and in the expression of IP-10 following IFN-β stimulation with the highest expression in ATB, followed by LTBI, HC, and TST (log_2FC for HC, TST, LTBI, ATB: 5.29, 5.11, 5.61, 6.03; p=0.029) (Figure 32). Although the differences in the expression of G-CSF, IL-10, and IL-1β after IFN-α stimulation were statistically significant, the expression levels did not meet the absolute (log_2FC) of |1| cut-off.

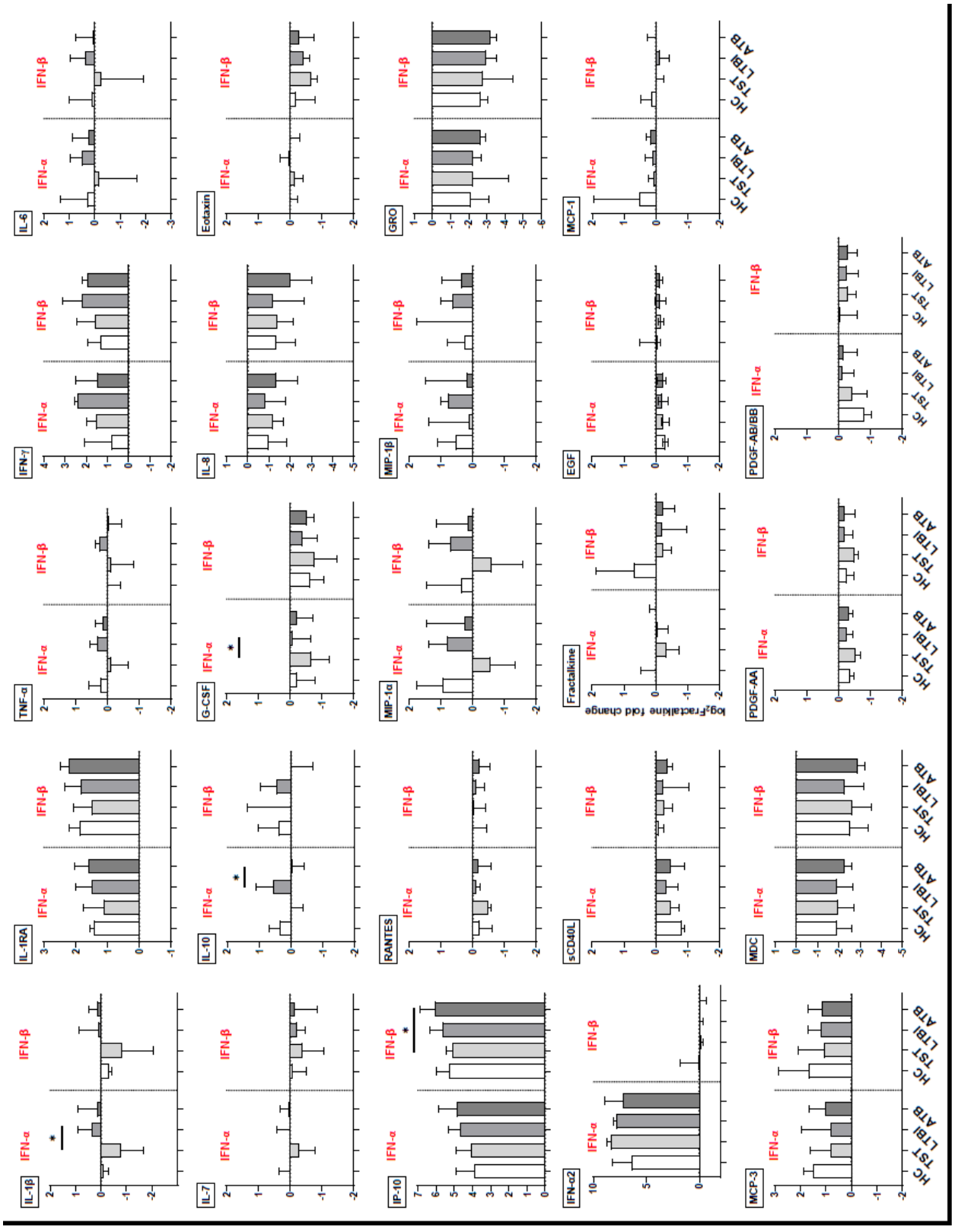
log2fold change
IL-1β
IFN-α
IFN-β
*
IL-1RA
TNF-α
IFN-γ
IL-6
IL-7
IL-10
G-CSF
IL-8
Eotaxin
IP-10
RANTES
MIP-1α
MIP-1β
GRO
IFN-α2
sCD40L
Fractalkine
EGF
MCP-1
MCP-3
MDC
PDGF-AA
PDGF-AB/BB
log2Fractalkine fold change
HC
TST LTBI
TST ATB
Clinical phenotype

Figure 32. Cytokine expression (fold change) responses to IFN-α- or IFN-β- stimulation

Cytokine levels were measured from unstimulated, IFN-α- (α), or IFN-β-(β) stimulated PBMCs using a multiplex bead assay. Fold changes were calculated by dividing each participant's cytokine level from stimulated PBMCs by the level from unstimulated PBMCs. Comparisons of fold changes between clinical groups were made using Kruskal-Wallis test followed by post hoc analysis with Bonferroni correction. Data are presented as median values. Multiple corrections p-value: * < 0.05; ** ≤ 0.01; *** ≤ 0.001. Bars in each section are in the order HC (white), TST, LTBI, and ATB (dark gray).x-axis= clinical phenotype; y-axis=log_2fold change.

3.4.2.2.2 Comparison of cytokine expression (fold changes) between clinical groups following IFN-α or IFN-β stimulation

For the fold changes of G-CSF, IL-10, IL-1β and PDGF-AB/BB that were differentially expressed across the four study groups following IFN-α or IFN-β stimulation, pairwise comparisons using Dunn's procedure were subsequently performed to identify the specific pairs of medians that differed significantly, followed by post hoc analysis using Bonferroni correction for multiple comparisons with statistical significance set at $p< 0.05$.

3.4.2.2.2.1 IFN-α stimulation

Following IFN-α stimulation, significant differences were identified for G-CSF between TST and HC (log_2FC: -0.64 vs -0.22; p=0.037) and between TST and LTBI (log_2FC: -0.64 vs -0.06; p=0.004) with a larger change in TST; IL-10 between LTBI and ATB (log_2FC: 0.57 vs -0.03; p=0.002); PDGF-AB/BB between HC and ATB (log_2FC: -0.81 vs -0.15; p=0.021), HC and LTBI (-0.81 vs -0.12; p=0.009) with larger fold change in HC, and between TST and LTBI (log_2FC: -0.43 vs -0.12; p=0.035) with larger changes in TST; and IL-1β between ATB and TST (log_2FC: 0.14 vs -0.79; p=0.040) being higher in ATB, between TST and HC (log_2FC: -0.79 vs -0.10; p=0.026) with larger change in TST, and between LTBI and TST (log_2FC: 0.38 vs -0.79; p=0.005) with larger change in LTBI. Bonferroni correction for multiple comparisons was then conducted setting the adjusted p-value for significance at $p<0.05$. Following correction for multiple comparisons, G-CSF was differentially expressed between TST and LTBI (log_2FC: -0.64 vs -0.06; p=0.022), IL-10 between LTBI and ATB (log_2FC: 0.57 vs -0.03; p=0.012), and IL-1β between LTBI and TST (log_2FC: 0.38 vs -0.79; p=0.029), as shown in Table 13.

3.4.2.2.2.2 IFN-β stimulation

With IFN-β stimulation, significant differences were identified for IP-10 between ATB and TST (log_2FC: 6.03 vs 5.11; p=0.008) and ATB and HC (log_2FC: 6.03 vs 5.29; p=0.032). Bonferroni correction for multiple comparisons was then carried out setting the adjusted p-value for significance at p<0.05. As shown in Table 13, IP-10 was differentially expressed between ATB and TST (log_2FC: 6.03 vs 5.11; p=0.046).

Table 13. Differentially expressed cytokines between clinical groups with IFN-α or IFN-β stimulation (fold change).

						Post hoc analysis	
Stimulation	**Cytokine**	**N**	**χ2**	**p-value[a]**	**Comparison[b]**	**p-value[c]**	**adjusted p-value[d]**
IFN-α	G-CSF	54	8.886	0.031	TST-HC	0.037	0.221
					TST-LTBI	0.004	**0.022**
	IL-10	55	9.612	0.022	LTBI-ATB	0.002	**0.012**
	IL-1β	48	8.734	0.033	ATB-TST	0.04	0.239
					TST-HC	0.026	0.153
					LTBI-TST	0.005	**0.029**
	PDGF-AB/BB	54	10.153	0.017	HC-ATB	0.021	0.124
					HC-LTBI	0.009	0.052
					TST-LTBI	0.035	0.211
IFN-β	IP-10	48	8.987	0.029	ATB-TST	0.008	**0.046**
					ATB-HC	0.032	0.195

ATB-active tuberculosis; TST- Tuberculin skin test positive; LTBI-latent tuberculosis infection; HC-healthy controls. N: total number of individuals in whom each gene wass detected. Comparisons of fold changes between clinical groups using Kruskal-Wallis test with post hoc pairwise comparisons and Bonferroni correction for multiple comparisons. **Bolded** and yellow highlighted p-values are significant after Bonferroni correction. Chi square (χ^2) is the square of the difference between the observed and the expected values. p-values: [a] – across groups p-value; [c] – pairwise comparison (between groups) p-value; [d] – adjusted p-value using Bonferroni correction for multiple comparisons.[b] – the order in the comparison shows the direction of the difference with the higher expression listed first.

3.4.2.3 Summary

The experiments in this section aimed to compare the induction of cytokines in response to IFN-α and IFN-β stimulation in *M. tuberculosis* infection states (TST reactive, LTBI, and ATB). We hypothesized that stimulation with type I IFNs would suppress the expression of pro-inflammatory cytokines in ATB while increasing that of anti-inflammatory cytokines.

Stimulation with IFN-α or IFN-β either suppressed or down-regulated the expression of the pro-inflammatory cytokine, IL-1β, TNF-α, and IL-6, compared to the unstimulated samples and up-regulated the expression of IL-1RA and IP-10 in all clinical groups which supported the sub-hypothesis. The expression of IL-10 was highest in LTBI but was suppressed in TST and ATB, which did not support the sub-hypothesis. The differences between median values for IL-10 between ATB and LTBI and PDGF-AB/BB between LTBI and TST were observed with both the cytokine levels and the fold changes.

3.4.3 Comparison of cytokine levels across clinical groups following Mtb WCL-stimulation

Differences in cytokine responses following Mtb WCL stimulation of PBMCs from our study participants were also analysed. PBMC stimulation samples from the participant groups HCs, TST, LTBI, and ATB were stimulated with Mtb WCL for 16 to 18 hours with an unstimulated control for each sample. Supernatants were processed using the Milliplex® MAP Human Cytokine / Chemokine kits as described in 2.5.5.

Compared to unstimulated samples, most of the cytokines showed increased levels with Mtb WCL stimulation – eotaxin, G-CSF, fractalkine, IFN-α2, IFN-γ, IL-10, IL-6, IL-7, IP-10, IL-1RA, IL-1β, MIP-1α, MIP-1β, RANTES, and TNF-α – as can be seen in Figure 33. MCP-3 levels were reduced in stimulation with Mtb WCL. A Kruskal-Wallis analysis was conducted to determine whether there were differences in cytokine levels between study groups with Mtb WCL stimulation. Statistically significant differences were identified across clinical groups for the growth factors PDGF-AA, PDGF-AB/BB, and the pro-inflammatory cytokine IL-1β (Figure 32).The levels of PDGF-AA were highest in ATB compared to LTBI and TST(median levels in HC, TST, LTBI, ATB: 26.99pg/ml, 13.80pg/ml, 38.90pg/ml, 72.13pg/ml; p=0.029); PDGF-AB/BB was elevated in ATB compared to HC and LTBI (median levels in HC, TST, LTBI, ATB:

126.14pg/ml, 118.88pg/ml, 178.43pg/ml, 244.34pg/ml; p=0.010); additionally, levels of IL-1β were highest in ATB compared to LTBI (median levels in HC, TST, LTBI, ATB: 1442.62pg/ml, 1188.98pg/ml, 1609.01pg/ml, 2748.40pg/ml; p=0.045).

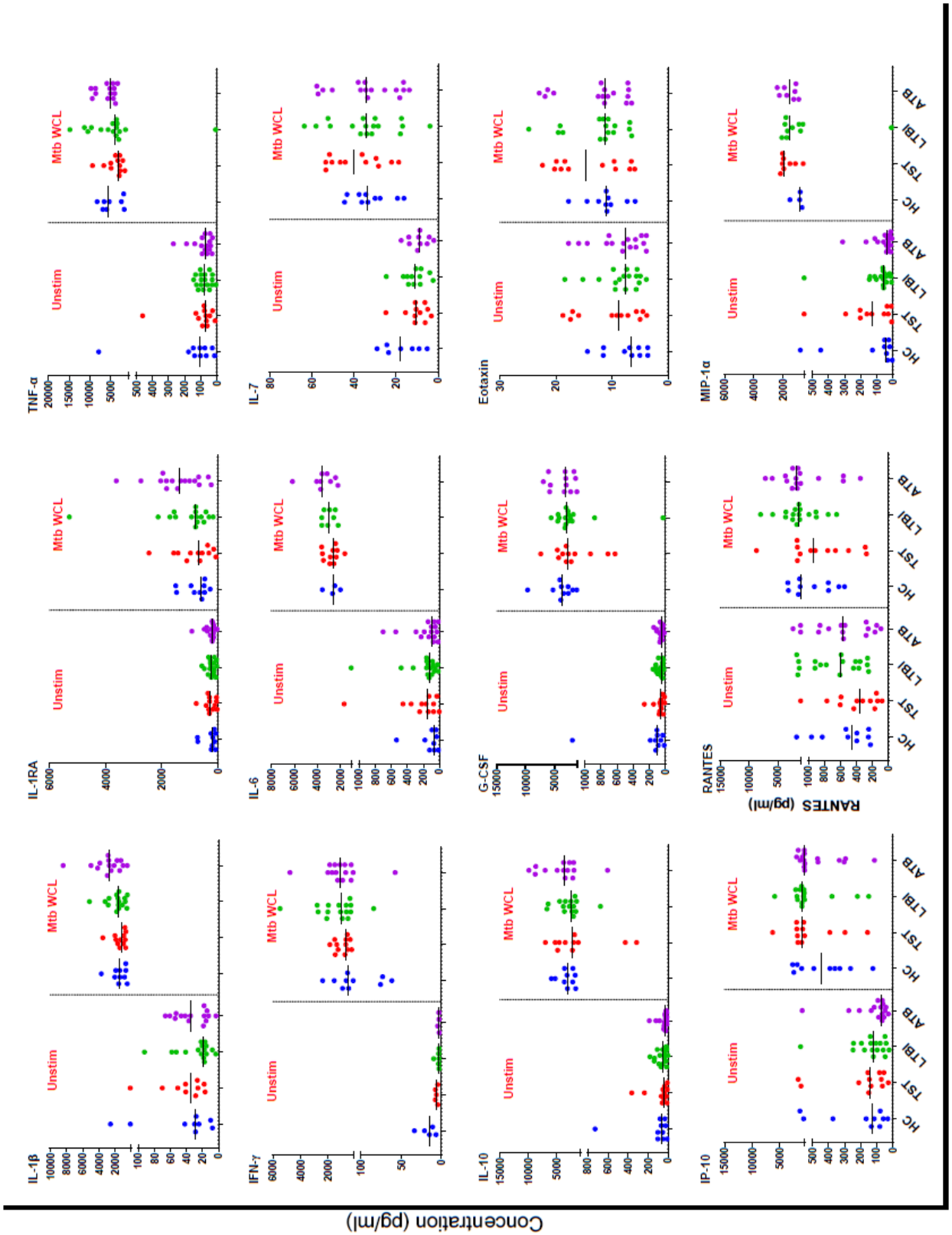
Concentration (pg/ml)
Clinical phenotype
IL-1β
IL-1RA
IL-6
IL-7
IL-10
IFN-γ
G-CSF
Eotaxin
RANTES (pg/ml)
MIP-1α
IP-10
TNF-α
Unstim
Mtb WCL
HC
TST
LTBI
ATB

Figure 33. Cytokine levels in baseline and Mtb WCL stimulated samples.

Cytokine levels were measured from unstimulated or Mtb WCL (Mtb) stimulated PBMCs using a multiplex bead assay. Comparisons between clinical groups were made using Kruskal-Wallis test followed by post hoc analysis with Bonferroni correction. Data are presented as median values. The p-value indicated is the overall for the stimulation calculated using the Kruskal-Wallis test. Multiple corrections p-value: * < 0.05; ** ≤ 0.01; *** ≤ 0.001. (blue=HC, red=TST, green=LTBI, purple=ATB). x-axis= clinical phenotype; y-axis=cytokine levels (pg/ml)

Figure 33: continued

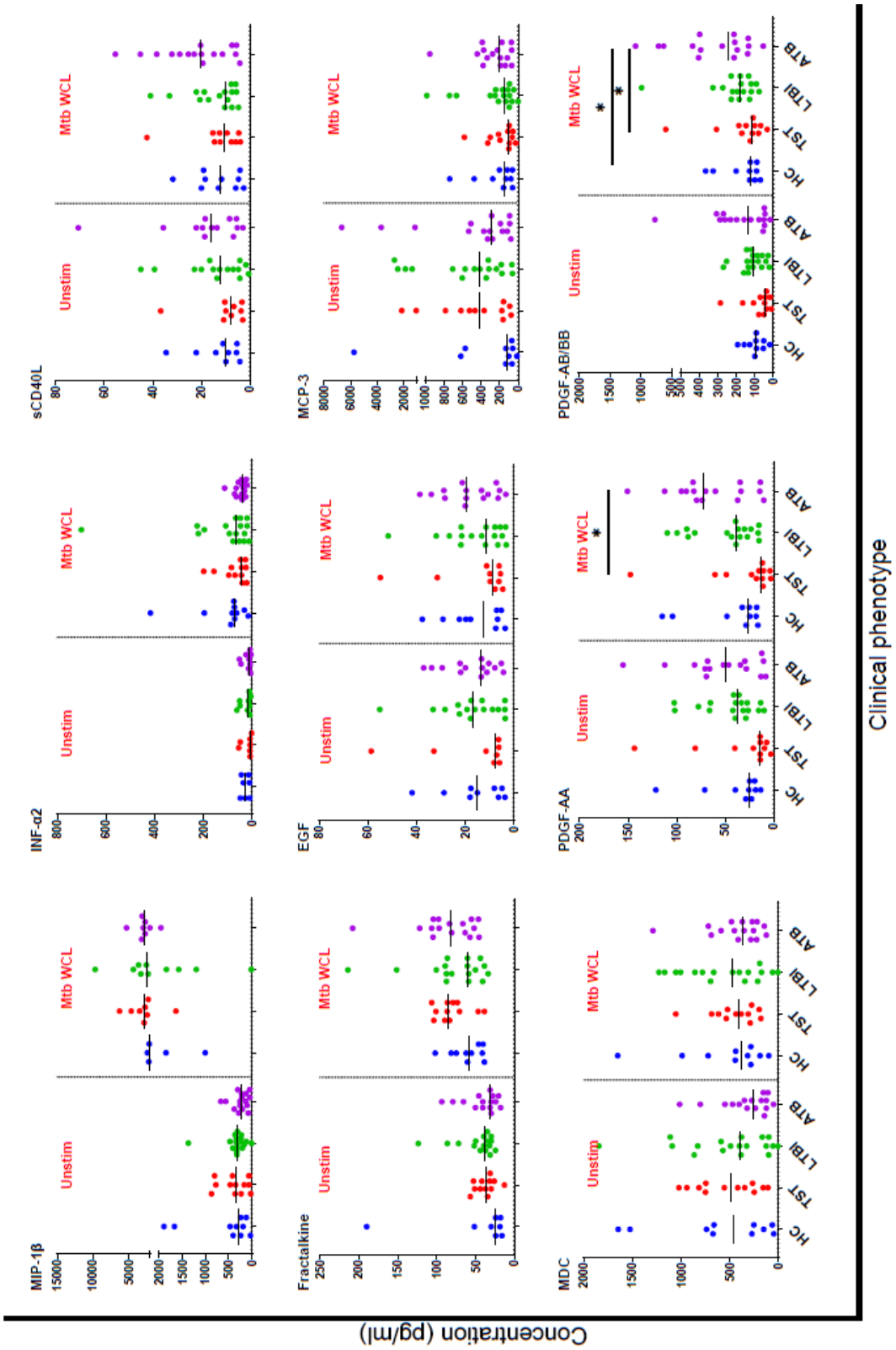

3.4.3.1 Comparison of cytokine levels between clinical groups following Mtb WCL-stimulation

For the level of IL-1β, PDGF-AA, and PDGF-AB/BB that were differentially expressed across the four study groups following Mtb WCL stimulation, pairwise comparisons using Dunn's procedure were subsequently performed to identify the specific pairs of medians that differed significantly, followed by post hoc analysis using Bonferroni correction for multiple comparisons with statistical significance set at $p< 0.05$.

Pairwise comparisons revealed differences in the levels of the growth factors PDGF-AB/BB between ATB and HC (244.34pg/ml vs 126.14pg/ml; p=0.007) and ATB and TST (244.34pg/ml vs 118.88pg/ml; p=0.003); PDGF-AA between ATB and TST(72.13pg/ml vs 13.80pg/ml p=0.004) and between LTBI and TST (38.90pg/ml vs 13.80pg/ml; p=0.021); and of the pro-inflammatory cytokine IL-1β between ATB and HC (2748.40pg/ml vs 1442.62pg/ml; pp=0.022) and between ATB and TST (2748.40pg/ml vs 1188.98pg/ml; p p=0.013). Post hoc analysis with Bonferroni correction did not reach statistical significance ($p<0.0083$) for the cytokines analysed as shown on Table 14.

Table 14. Cytokine level differences with Mtb WCL stimulation.

						Post hoc analysis	
Stimulation	**Cytokine**	**N**	**χ2**	**p-value[a]**	**Comparison[b]**	**p-value[c]**	**adjusted p-value[d]**
Mtb WCL	IL-1β	53	8.061	0.045	ATB-HC	0.022	0.139
					ATB-TST	0.013	0.079
	PDGF-AA	55	9.021	0.029	ATB-TST	0.004	**0.023**
					LTBI-TST	0.021	0.126
	PDGF-AB/BB	55	11.284	0.01	ATB-HC	0.007	**0.045**
					ATB-TST	0.003	**0.02**

ATB-active tuberculosis; TST-Tuberculin skin test positive; LTBI-latent tuberculosis infection; HC-healthy controls. N: total number of individuals in whom gene was detected. Comparisons of cytokine levels between clinical groups using Kruskal-Wallis test with post hoc pairwise comparisons and Bonferroni correction for multiple comparisons. **Bolded** and yellow highlighted p-values are significant after Bonferroni correction. Chi square (χ^2) is the square of the difference between the observed values and the expected values. p-values: [a] – across groups p-value; [c] – pairwise comparison (between groups) p-value; [d] – adjusted p-value using Bonferroni correction for multiple comparisons.[b] – the order in the comparison shows the direction of the difference with the higher expression listed first.

3.4.3.2 Comparison of cytokine expression (fold changes) across clinical groups following Mtb WCL stimulation

Next, cytokines' fold changes were evaluated to assess the cytokine responses with stimulation above the unstimulated sample. This was calculated by dividing the cytokine levels in supernatants from Mtb WCL-stimulated cell cultures by cytokine levels from baseline cell cultures from the same individual.

Following stimulation with Mtb WCL, most cytokines were either up-regulated – HC (43.5%), TST (65.2%), LTBI (60.9%), and ATB (60.9%), or showed no regulation - HC (56.5%), TST (30.4%), LTBI (34.8%), and ATB (34.8%) (Figure 34). Cytokines that were upregulated in all clinical groups with this stimulation included G-CSF, IL-10, IL-1RA, IL-1β, IP-10, MIP-1α, MIP-1β, RANTES and TNF-α with the highest fold change in ATB followed by LTBI, while IFN-α2 expression was highest in LTBI, and IL-6 expression was highest in HC.

The fold change of IFN-α2 was higher with Mtb WCL stimulation (log_2FC in HC, TST, LTBI, ATB: 1.41, 2.57, 3.00, 2.04) compared to that with IFN-β (log_2FC in HC, TST, LTBI, ATB: 0.10, -0.17, -0.06, -0.10) but lower than that after IFN-α stimulation (log_2FC in HC, TST, LTBI, ATB: 6.39, 8.32, 7.84, 7.19). The expression of the cytokine IL-10 was upregulated with Mtb WCL stimulation at both protein (log_2FC for HC, TST, LTBI, ATB: 5.90, 5.70, 6.16, 6.77) (Table S4) and gene level (log_2FC for HC, TST, LTBI, ATB: 2.85, 2.54, 1.98, 2.79) (Table S2), both with higher expression in ATB than in LTBI.

Some of the cytokines assessed were also analysed at the gene level. IL-10 protein and *IL-10* gene fold changes were higher after Mtb WCL stimulation than after IFN-α/β stimulation. The expression of the cytokine IL-1β showed upregulation with Mtb WCL at protein level (log_2FC for HC, TST, LTBI, ATB: 5.53, 5.31, 6.26, 6.66) (Table S4) and for the *IL-1B* gene (log_2FC for HC, TST, LTBI, ATB: 3.65, 2.95, 3.3, 2.98) (Table S2). Similar to IL-10 expression, both IL-1β protein and *IL-1B* gene fold changes were higher after Mtb WCL stimulation than after IFN-α/β stimulation. However, the similarities between protein and gene expression were not observed with CXCL10 (IP-10) which was upregulated at protein level (log_2FC for HC, TST, LTBI, ATB: 2.31, 2.56, 2.53, 2.92) (Table S4), but not at gene level except in ATB (log_2FC for HC, TST, LTBI,

ATB: 0.75, 0.07, 0.49, 1.18) (Table S2). The fold changes of both CXCL10/IP-10 protein and gene were lower after Mtb WCL stimulation than after IFN-α/β stimulation.

A Kruskal-Wallis test was then carried out to identify differences in soluble analyte expression between the clinical groups and identified significant differences between the median log_2FC of IL-1β (HC, TST, LTBI, ATB: 5.53, 5.31, 6.26, 6.66; p=0.019) with Mtb WCL stimulation (Figure 34).

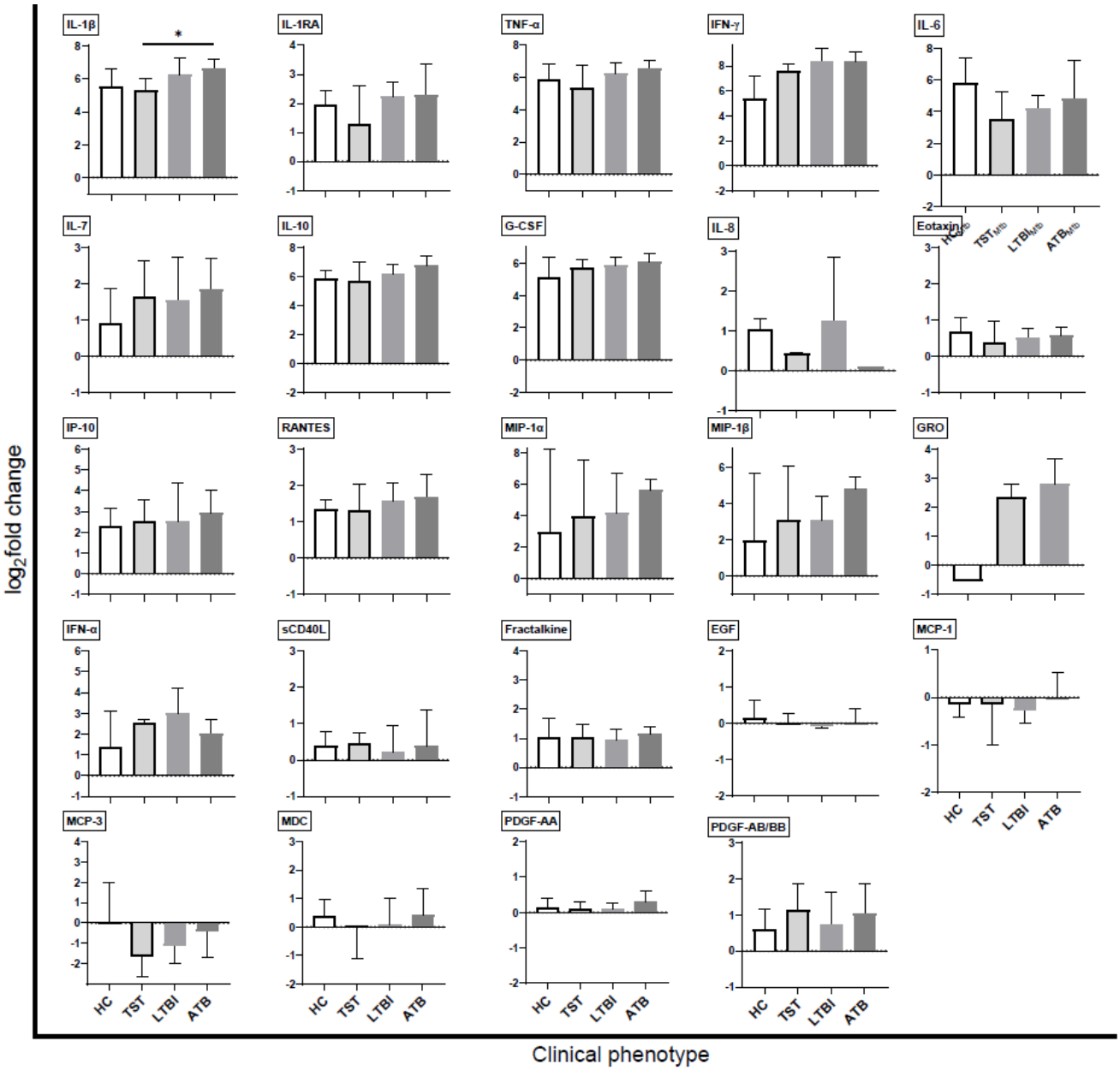

Figure 34. Cytokine expression (fold change) responses to Mtb WCL stimulation.

Cytokine levels were measured from unstimulated, and Mtb WCL (Mtb) stimulated PBMCs using a multiplex bead assay. Fold changes were calculated by dividing the stimulated levels by the unstimulated levels. Comparisons of fold changes between clinical groups were made using Kruskal-Wallis test followed by post hoc analysis with Bonferroni correction. Data are presented as median values. The p-value indicated is the overall for the stimulation calculated using the Kruskal-Wallis test. Multiple corrections p-value: * < 0.05; ** ≤ 0.01; *** ≤ 0.001. Bars in each section are labelled in the order HC (white), TST, LTBI, ATB (dark gray).x-axis=clinical phenotype; y-axis=log_2 fold change

3.4.3.3 Comparison of cytokine expression (fold change) between clinical groups following Mtb WCL stimulation

For the fold changes of IL-1β that were differentially expressed across the four study groups following Mtb WCL stimulation, pairwise comparisons using Dunn's procedure were subsequently performed to identify the specific pairs of medians that differed significantly, followed by post hoc analysis using Bonferroni correction for multiple comparisons with statistical significance set at $p< 0.05$. Significant differences were identified for IL-1β between LTBI and TST (log_2FC: 6.26 vs 5.31; p=0.030), ATB and TST (log_2FC: 6.66 vs 5.31; p=0.006), and between ATB and HC (log_2FC: 6.66 vs 5.53; p=0.035). Bonferroni correction for multiple comparisons was then carried out setting the adjusted p-value for significance at $p<0.05$. As shown in Table 15, IL-1β was differentially expressed between ATB and TST (log_2FC: 6.66 vs 5.31; p=0.034).

Table 15. Differentially expressed cytokines between clinical groups with Mtb WCL stimulation (fold change).

						Post hoc analysis	
Stimulation	**Cytokine**	**N**	**$\chi 2$**	**p-value[a]**	**Comparison[b]**	**p-value[c]**	**adjusted p-value[d]**
Mtb WCL	IL-1β	48	9.948	0.019	ATB-HC	0.035	0.213
					ATB-TST	0.006	**0.034**
					LTBI-TST	0.03	0.183

ATB-active tuberculosis; TST-Tuberculin skin test positive; LTBI-latent tuberculosis infection; HC-healthy controls. N: total number of individuals in whom gene is detected. Comparisons of cytokine fold changes between clinical groups using Kruskal-Wallis test with post hoc pairwise comparisons and Bonferroni correction for multiple comparisons. **Bolded** and yellow highlighted p-values are significant after Bonferroni correction. Chi square (χ^2) is the square of the difference between the observed and the expected values. p-values: [a] – across groups p-value; [c] – pairwise comparison (between groups) p-value; [d] – adjusted p-value using Bonferroni correction for multiple comparisons. [b] – the order in the comparison shows the direction of the difference with the higher expression listed first.

3.4.3.4 Summary

The experiments in this section aimed to compare cytokine responses to Mtb WCL stimulation in different *M. tuberculosis* infection states (TST reactive, LTBI, and ATB). We

hypothesized that the Mtb WCL would increase the expression of pro-inflammatory cytokines in TB while suppressing anti-inflammatory cytokines. We observed increased expression of pro-inflammatory cytokines (IL-1β, IL-6 and TNF-α) in ATB which supported the sub-hypothesis. Increases expression was also observed for chemokines (fractalkine, MIP-1-α, MIP-1β and RANTES) and of the immunoregulatory IL-10 with a more prominent increase in ATB for most of these cytokines. IL-1RA was increased in ATB. The increased expression of the anti-inflammatory cytokines did not support the sub-hypothesis. IP-10 levels were suppressed after Mtb WCL stimulation compared to those induced by type I IFNs, but higher than in the unstimulated samples. IL-10 and IL-1β were both upregulated at both gene and protein level after Mtb WCL stimulation, while CXCL10/IP-10 showed no regulation at gene level but was upregulated at protein level.

3.4.4 Comparison of cytokine expression (fold change) with IFN-α versus IFN-β stimulation across clinical groups

To assess for differences in cytokine fold changes induced by IFN-α and IFN-β, each PBMC sample from the participant groups HCs, TST, LTBI, and ATB was stimulated in parallel with either IFN-α or IFN-β. Calculated fold changes were used to compare the cytokine responses induced by IFN-α with those induced by IFN-β within each clinical phenotype using a Wilcoxon signed-rank test.

The median values are presented as log_2FC in IFN-α vs IFN-β. Higher expression after IFN-β stimulation compared to after IFN-α stimulation was observed in the expression of EGF in HC (-0.32 vs -0.07; 8 pairs; p= 0.0078); IL-1RA gene in HC (1.41 vs 1.87; 10 pairs; p= 0.0137), TST (1.10 vs 1.49; 12 pairs; p= 0.0005), LTBI (1.49 VS 1.85; 17 pairs; p=0.0004) and in ATB (1.61 VS 2.22; 16 pairs; p=0.0063); IP-10 in HC (3.87 vs 5.29; 9 pairs; p =0.0078), TST (4.06 vs 5.11; 8 pairs; 0.0078), LTBI (4.66 vs 5.61; 15 pairs; p=0.0001), and ATB (4.83 vs 6.03; 14 pairs; p=0.0004) (Figure 35). Some demonstrated higher downregulation after IFN-β stimulation compared to after IFN-α stimulation as observed in the expression of MDC in TST (-1.94 vs -2.64; 12 pairs; p=0.0010), LTBI (-1.89 vs -2.25; 17 pairs; p=0.0021), and ATB (-2.25 vs -2.94; 16 pairs; p=0.0001); GRO in LTBI (-2.25 vs -2.94; 16 pairs; 0.0052) and ATB (-2.64 vs -3.18; 13

pairs; p=0.0024); IL-8 in TST (-1.18 vs -1.40; 9 pairs; p=0.0078) and ATB (-1.36 vs 2.00; 12 pairs; p=0.0122).

Higher expression after IFN-αstimulation compared to after IFN-β stimulation was observed in the expression of IFN-α2 in HC (6.39 vs 0.10; 7 pairs; p=0.0156), TST (8.32 vs -0.17; 6 pairs; p=0.0313), LTBI (7.84 vs -0.06; 8 pairs; p=0.0078) and ATB (7.19 vs -0.10; 6 pairs; p=0.0313); MIP-1β in HC (0.56 vs 0.28; 10 pairs; p=0.0020); and TNF-α in HC (0.23 vs 0.00; 10 pairs; p=0.0371) and ATB (0.14 vs -0.06; 16 pairs; 0.0386) (Figure 35). Similar differences were also observed for eotaxin in LTBI (0.04 vs -0.42; 13 pairs; p=0.0081) and ATB (-0.01 vs -0.27; 10 pairs; 0.0039); and fractalkine in ATB (0.00 vs -0.22; 13 pairs; p=0.0049)

3.4.4.1 Summary

The experiments in this section aimed to compare cytokine expression induced by IFN-α and IFN-β. PBMC samples from each study participant were tested in parallel, with one tube of PBMCs stimulated with IFN-α and the other with IFN-β, with an unstimulated control. Supernatants were processed for cytokine levels. Fold changes were calculated by dividing the cytokine level in the stimulated sample by that in the unstimulated sample. Although the different type I IFNs signal through the same receptor, IFNAR, differences in their binding sites and affinities to the receptor suggest functional differences. We, therefore, hypothesized that stimulation with IFN-α and IFN-β would drive similar cytokine profiles in the *M. tuberculosis* infection states.

As expected, IFN-α2 was differentially expressed with exogenous IFN-α in all clinical groups; IL-1RA and IP-10 were also differentially expressed in all clinical groups. Other cytokines differentially expressed in HC were EGF, and the chemokine MIP-1β, and TNF-α; in TST – the chemokines MDC and IL-8; in LTBI – the chemokines MDC, eotaxin, and GRO; and in ATB - TNF-α, and the chemokines MDC, IL-8, eotaxin, GRO and fractalkine. Although most of the cytokines tested supported the sub-hypothesis that stimulation with IFN-α and IFN-β would drive similar cytokine profiles in the *M. tuberculosis* infection states, several genes showed differences in the expression levels between the stimulations in the infection states.

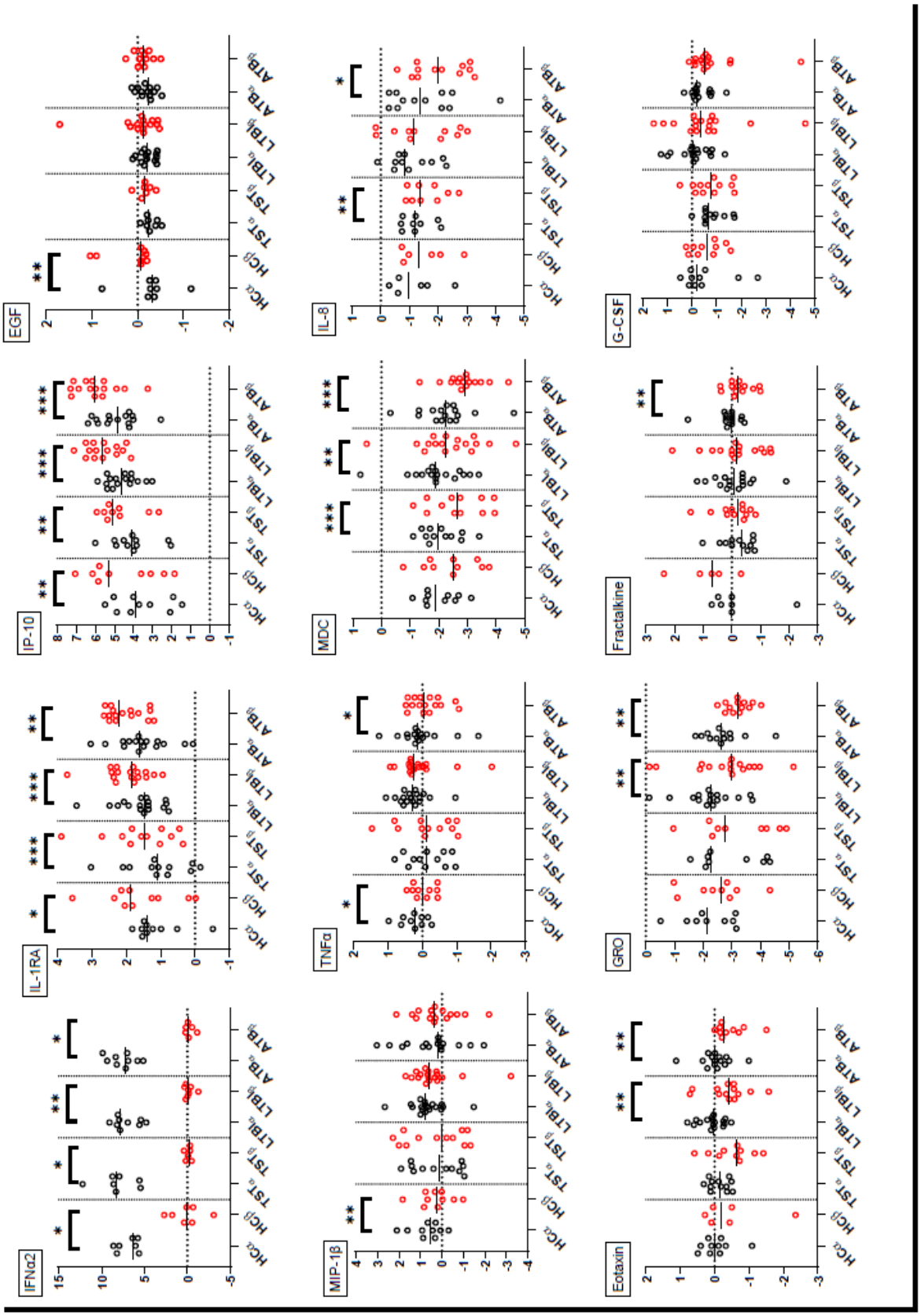
Clinical phenotype
log2fold change
IFNα2
IL-1RA
IP-10
EGF
MIP-1β
TNFα
MDC
IL-8
Eotaxin
GRO
Fractalkine
G-CSF
HCα
HCβ
TSTα
TSTβ
LTBIα
LTBIβ
ATBα
ATBβ

Figure 35. Cytokine expression (fold changes) with IFN-α versus IFN-β stimulation of PBMCs within clinical phenotypes

PBMCs from healthy control (HC), tuberculin skin test (TST), latent TB infection (LTBI), and active TB (ATB) were stimulated for 16-18 hours with IFN-α or IFN-β with an unstimulated control. Cytokine levels were measured from unstimulated, IFN-α- (α) or IFN-β-(β) stimulated PBMCs using a multiplex bead assay. Fold changes were calculated by dividing the stimulated level by the unstimulated level. Data are presented as the median values. The p-value indicated is overall for the stimulation calculated using the Wilcoxon signed-rank test. Adjusted p-value: * < 0.05; ** ≤ 0.01; *** ≤ 0.001. (black open circles=IFN-α responses, red open circles= IFN-β responses).

Figure 35: continued

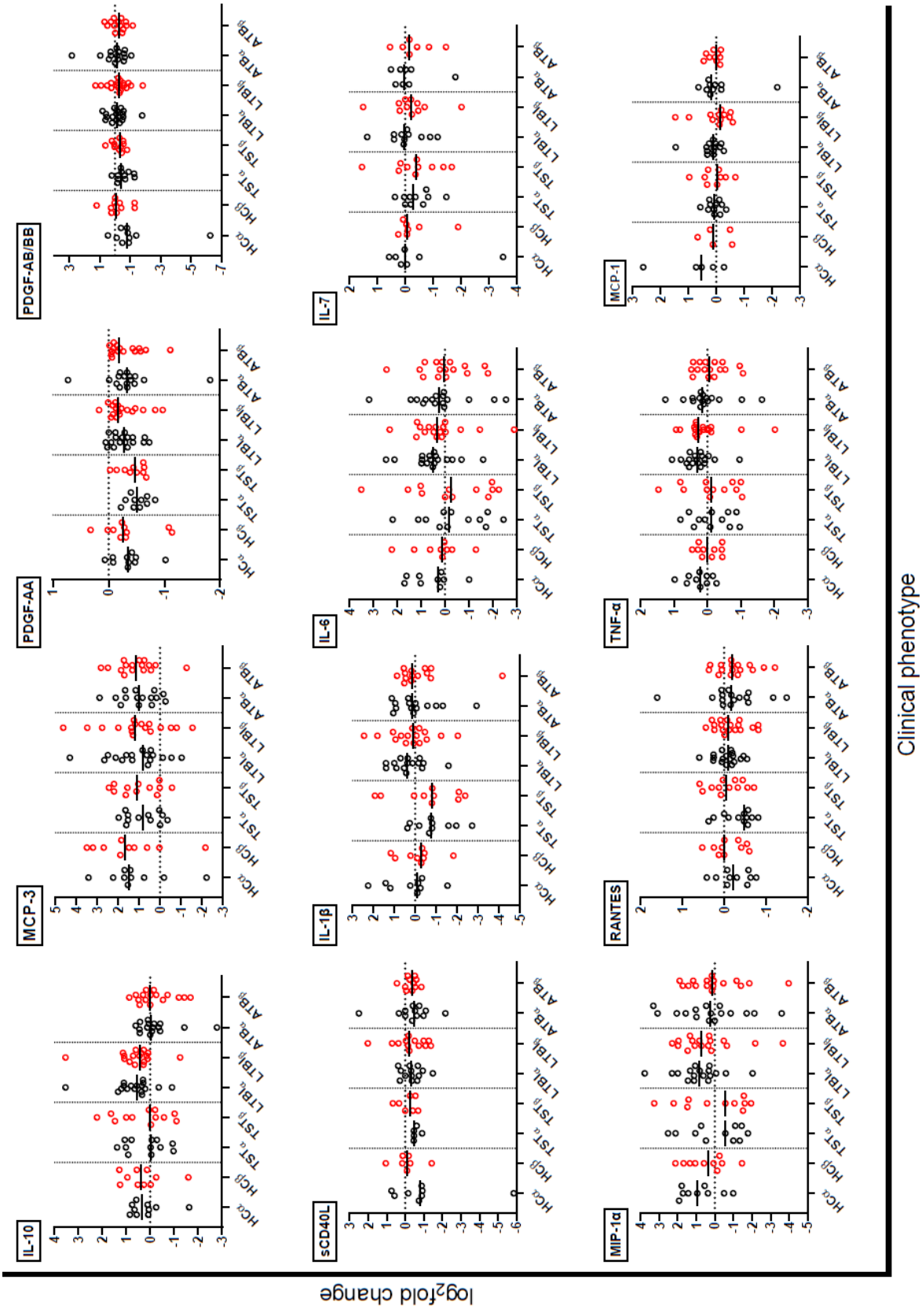

3.5 Assessing associations between differentially expressed genes and participant epidemiological characteristics and cytokines

3.5.1 Assessing the association between differentially expressed genes and participant epidemiologic characteristics

Following the identification of seven genes identified as differentially expressed by the fold change method between clinical groups with IFN-α or IFN-β or Mtb WCL stimulation – *IRF9*, *MSR1*, *SOCS*3, *IFITM3, OAS3*, *SECTM1*, and *STAT1* listed in Table 9 and Table 11, I evaluated the relationship between the expression of these genes and the participant characteristics. The goal was to determine whether the observed differences in gene expression induced by these stimulations in the different clinical groups were confounded by epidemiological or clinical factors. This sought to determine whether there was a significant association between the variables listed in Table 6 (demographic and clinical characteristics of study participants) and the magnitude of the change in gene expression, the fold change, in the clinical phenotypes of *M. tuberculosis* infection–LTBI and ATB for each stimulation using Spearman's correlation analysis.

First, the relationship between sex and the expression of the seven genes by IFN-α, IFN-β, and Mtb WCL was assessed (Table 16). In the ATB group, sex showed a moderate positive correlation with the expression of *IFITM3* and *MSR1* genes following IFN-α stimulation with females showing stronger responses for both genes – for *IFITM3* 12.46-fold, compared to 6.84-fold in males (r= 0.520, p=0.023) and for *MSR1* 12.00-fold, compared to 6.88-fold in males (r= 0.539, p=0.017). None of the genes showed association with sex following IFN-β and Mtb WCL stimulation. Age showed a moderate positive correlation with *IFITM3* gene expression in ATB (r= 0.573, p=0.010), and a moderate negative correlation with LTBI (r= -0.056, p=0.032) following Mtb WCL stimulation. There was no relationship observed between genes induced by IFN-α or IFN-β stimulation and age.

Correlation analysis revealed relationships between ethnicity and several genes following IFN-α and IFN-β stimulations in LTBI and after Mtb WCL stimulation in ATB. Following IFN-α stimulation, a strong positive association was observed with *IFITM3* gene expression with the strongest responses in Canadian-born non-Indigenous, 29.27-fold, Canadian-born Indigenous, 28.36-fold, and then Foreign-born, 12.92-fold (r= 0.714, p=0.001); a moderate positive association

in *IRF9* gene expression with the strongest responses in Canadian-born Indigenous, 6.00-fold, Canadian-born non-Indigenous, 5.14-fold, and Foreign-born, 2.37-fold, (r= 0.532, p=0.023) and *STAT1* gene expression with the strongest responses in Canadian-born Indigenous, 11.02-fold, Canadian-born non-Indigenous, 10.48-fold, and Foreign-born, 5.94-fold (r= 0.599, p=0.009). Conversely, there was a low positive association between ethnicity and the expression of *OAS3* with the strongest responses in Canadian-born Indigenous, 130.21-fold, Canadian-born non-Indigenous, 103.34-fold, and Foreign-born, 16.09-fold (r= 0.478, p=0.045). A similar pattern was observed following IFN-β stimulation - a strong positive association with *IFITM3* gene expression with the strongest responses in Canadian-born non-Indigenous, 28.80-fold, Canadian-born Indigenous, 22.97-fold, and then Foreign-born, 7.18-fold (r= 0.721, p=0.001); a moderate positive association in *IRF9* gene expression with the strongest responses in Canadian-born non-Indigenous, 6.20-fold, Canadian-born Indigenous, 2.91-fold, and Foreign-born, 2.38-fold, (r= 0.523, p=0.031), in *STAT1* gene expression with the strongest responses in Canadian-born non-Indigenous, 9.04-fold, Canadian-born Indigenous, 9.03-fold, and Foreign-born, 5.51-fold, (r= 0.589, p=0.013), and in *OAS3* gene expression with the strongest responses in Canadian-born Indigenous, 121.15-fold, Canadian-born non-Indigenous, 103.11-fold, and Foreign-born, 16.27-fold (r= 0.523, p=0.031). Following Mtb WCL stimulation, a low negative association was observed in ATB between ethnicity and *IFITM3* gene expression, with the strongest responses in Canadian-born non-Indigenous, 0.96-fold, then in Foreign-born, 0.84-fold, and Canadian-born Indigenous, 0.53-fold, (r= -0.473, p=0.041), and a moderate negative correlation with *IRF9* expression with the strongest expression in Foreign-born, 2.61-fold, followed by Canadian-born non-Indigenous, 1.35-fold, and Canadian-born Indigenous, 1.12-fold (r= -0.581, p=0.009).

The BCG status of the study participants negatively correlated with the expression of genes only with IFN-α and IFN-β stimulation in LTBI. Following IFN-α stimulation, a moderate negative correlation was observed with BCG-negative individuals showing stronger responses for *OAS3* gene expression, 131.40-fold, compared to 16.09-fold in BCG-positive (r= -0.511, p=0.030), and for *SOCS3* gene expression, 3.59-fold, compared to 1.49-fold in BCG-positive (r= -0.545, p=0.019). There was a low negative association with *STAT1* with BCG-negative individuals showing stronger responses, 13.44-fold, compared to 6.34-fold in BCG-positive (r= -0.477, p=0.045). Following IFN-β stimulation a low negative correlation was observed with BCG-negative individuals showing stronger responses for *IFITM3* gene expression, 26.49-fold,

compared to 13.35-fold in BCG-positive (r= -0.484, p=0.049), a moderate correlation with BCG-negative individuals showing stronger responses for *IRF9* gene expression, 6.51-fold, compared to 2.39-fold in BCG-positive (r= -0.559, p=0.020), for *OAS3* gene expression, 133.21-fold, compared to 16.27-fold in BCG-positive (r= -0.522, p=0.032), and for *SOCS3* gene expression, 2.63-fold, compared to 1.59-fold in BCG-positive (r= -0.559, p=0.020).

Assessment of the relationship between the expression of the seven genes and chest X-ray results only showed association in the IFN-β-induced *OAS3* expression in the LTBI group (Table 16). The strongest responses were observed in study participants with no CXR done, followed by those with abnormal CXR and normal CXRs, 65.16-fold compared to 17.04-fold and 12.64-fold in the normal CXRs.

None of the genes showed a correlation with TST results (positive or negative) or QFT results (positive or negative) by IFN-α, IFN-β, or Mtb WCL. QFT detects IFN-γ released from lymphocytes in whole blood when stimulated with *M. tuberculosis*-specific antigens (Antigen response), mitogen (Mitogen response), and an unstimulated control (Nil). The IFN-γ amount is calculated by subtracting the IFN-γ from the Nil tube from the IFN-γ in the Antigen response tube or the Mitogen response tube. Using manufacturer's software that uses a predetermined cut-off, a test is positive when the TB antigen response is ≥0.35 IU/ml (Qiagen: www.QuantiFERON.com). Following Mtb WCL stimulation, a low negative correlation was observed between the TB antigen response and *SECTM1* gene expression in ATB, with the strongest response in the QFT-negative (<0.35 IU/ml), 1.33-fold, compared to the QFT-positive (≥0.35 IU/ml), 00.75-fold. None of the genes showed significant association with the TB antigen response with IFN-α or IFN-β stimulations.

3.5.1.1 Summary

This section assessed the association between the fold changes in gene expression and the participant demographic and clinical characteristics. Sex showed a positive correlation with gene expression only in ATB following IFN-α stimulation with stronger responses in females. Ethnicity showed positive correlation with gene expression in LTBI following IFN-α or IFN-β stimulation but a negative correlation following Mtb WCL stimulation. BCG status showed a negative correlation with gene expression in LTBI following IFN-α or IFN-β stimulation but no correlation after Mtb WCL stimulation.

Table 16. Association between differentially expressed genes and participant epidemiologic characteristics by type of stimulation.

Stimulation	Characteristic	Study group	Gene	Correlation coefficient	p-value
IFN-α	Sex	ATB	*IFITM3*	0.520	0.023
			MSR1	0.539	0.017
	Ethnicity	LTBI	*IFITM3*	0.714	0.001
			IRF9	0.532	0.023
			OAS3	0.478	0.045
			STAT1	0.599	0.009
	BCG	LTBI	*OAS3*	-0.511	0.030
			SOCS3	-0.545	0.019
			STAT1	-0.477	0.045
IFN-β	Ethnicity	LTBI	*IFITM3*	0.721	0.001
			IRF9	0.523	0.031
			OAS3	0.523	0.031
			STAT1	0.589	0.013
	BCG	LTBI	*IFITM3*	-0.484	0.049
			IRF9	-0.559	0.020
			OAS3	-0.522	0.032
			SOCS3	-0.559	0.020
	Chest Xray	LTBI	*OAS3*	0.482	0.050
Mtb WCL	Age	ATB	*IFITM3*	0.573	0.010
		LTBI		-0.506	0.032
		TST		-0.677	0.016
	Ethnicity	ATB	*IFITM3*	-0.473	0.041
			IRF9	-0.581	0.009
	TB antigen response	ATB	*SECTM1*	-0.490	0.039

Assessment of association using Spearman's correlation analysis. Values highlighted in yellow indicate positive correlations.

3.5.2 Association between expression levels of ISGs and cytokines

There is a paucity of data on the relationship between expression at the gene level and its downstream effects on cytokines in TB. Therefore, gene expression experiments were carried out in parallel with cytokine assays to assess the relationship between gene expression and cytokine profiles in specific clinical phenotypes of *M. tuberculosis* infection. For each of the 4-hour PBMC cultures set up for gene expression, a parallel 16-18-hour PBMC culture was set up for cytokine analysis.

To explore the potential effect of gene expression levels on the expression levels of cytokines, we ran a correlation analysis of the data focusing on the seven differentially expressed ISGs - *IRF9*, *MSR1*, *SOCS3*, *IFITM3*, *OAS3*, *SECTM1*, and *STAT1*, with gene expression as the independent/ predictor variable and cytokine expression as the dependent/ outcome variable. Here only the significant correlation results between cytokine expression and gene expression in ATB and LTBI are shown.

3.5.2.1 IFN-α stimulation

In ATB, the expression of fractalkine showed a moderate negative correlation with *IFITM3*, *OAS3*, and *STAT1* gene expression; MDC with *SOCS3* expression, and G-CSF with *MSR1* expression; and a moderate positive correlation between the expression of RANTES and *IRF9* gene, and between IP-10/CXCL10 and *SECTM1* gene expression (Table 17). In LTBI, a strong negative correlation was observed between IFN-α2 expression and *MSR1* gene and between PDGF-AA and *SOCS3* gene expression.

3.5.2.2 IFN-β stimulation

In contrast to the observations with IFN-α stimulation in ATB, fractalkine expression showed a positive correlation with *OAS3*, *STAT1*, and *IRF9* (Table 17). PDGF-AA expression showed a moderate negative correlation with *IFITM3*, *MSR1*, and *STAT1* genes, and sCD40L expression with *SOCS3* gene expression. In LTBI, a strong negative correlation was observed between the expression of PDGF-AA and *IFITM3* and a moderate negative correlation with *OAS3*, *STAT1*, and *SECTM1* genes; PDGF-AB/BB and *IFITM3* and *STAT1* genes; EGF and *SECTM1* gene; and a moderate positive correlation between G-CSF and *MSR1* gene.

3.5.2.3 Mtb WCL

In ATB, a moderate negative correlation was observed in the expression of G-CSF and *IFITM3* and *IRF9* gene expression. In LTBI, the expression of fractalkine, RANTES, PDGF-AA, and PDGF-AB/BB showed a positive correlation with *MSR1* gene, IL-8 and sCD40L with *SECTM1*, whereas IFN-α2 showed a strong negative correlation with *IFITM3* gene.

3.5.2.4 Summary

This section examined the association between the fold changes of gene expression and cytokine expression. The hypothesis tested was that there is an association between gene

expression and cytokine profiles in *M. tuberculosis* infection states. Gene expression showed association more commonly with chemokines in ATB following IFN-α and IFN-β stimulation and in LTBI following Mtb WCL stimulation. Differences were observed in correlation results with chemokines with IFN-α stimulation resulting in both positive and negative correlations, while IFN-β stimulation resulted in positive correlations. The correlation of differentially expressed genes with differentially expressed cytokines was only observed following IFN-α stimulation between the *MSR1* gene and G-CSF protein. These findings support the hypothesis of an association between the levels of gene expression and cytokine levels.

Table 17. Significant associations between differentially expressed genes and cytokine expression by clinical phenotype grouping.

Stimulation	Study group	Cytokine	Gene	Correlation coefficient	p-value
IFN-α	ATB	Fractalkine	*IFITM3*	-0.695	0.006
			OAS3	-0.600	0.023
			STAT1	-0.668	0.009
		RANTES	*IRF9*	0.529	0.035
		IP-10	*SECTM1*	0.653	0.011
		MDC	*SOCS3*	-0.556	0.025
		G-CSF	*MSR1*	-0.611	0.016
	LTBI	IFN-α2	*MSR1*	-0.867	0.002
		PDGF-AA	*SOCS3*	-0.588	0.013
	TST	IP-10	*IFITM3*	0.900	<0.001
		Eotaxin	*MSR1*	0.580	0.048
			SOCS3	0.825	0.001
		IL-8	*OAS3*	-0.883	0.002

Stimulation	Study group	Cytokine	Gene	Correlation coefficient	p-value
IFN-β	ATB	Fractalkine	*IRF9*	0.646	0.017
			OAS3	0.677	0.011
			STAT1	0.633	0.020
		PDGF-AA	*IFITM3*	-0.547	0.028
			MSR1	-0.629	0.009
			STAT1	-0.529	0.035
		sCD40L	*SOCS3*	-0.609	0.047
	LTBI	PDGF-AA	*IFITM3*	-0.711	0.001
			OAS3	-0.632	0.006
			STAT1	-0.566	0.018
			SECTM1	-0.632	0.006
		PDGF-AB/BB	*IFITM3*	-0.527	0.030
			STAT1	-0.596	0.012
		G-CSF	*MSR1*	0.550	0.027
		EGF	*SECTM1*	-0.640	0.014
	TST	IL-1β	*STAT1*	-0.770	0.009
		IL-8	*STAT1*	-0.883	0.005
			OAS3	-0.817	0.007
		MIP-1β	*IRF9*	0.608	0.036
		G-CSF	*SECTM1*	0.629	0.028
		EGF	*IRF9*	0.857	0.014

Stimulation	Study group	Cytokine	Gene	Correlation coefficient	p-value
Mtb WCL	ATB	G-CSF	*IFITM3*	-0.629	0.028
			IRF9	-0.692	0.013
	LTBI	Fractalkine	*MSR1*	0.566	0.044
		RANTES		0.596	0.019
		PDGF-AA		0.571	0.026
		PDGF-AB/BB		0.600	0.018
		IFN-α2	*IFITM3*	-0.893	0.007
		IL-8	*SECTM1*	0.900	0.037
		sCD40L	*SECTM1*	0.593	0.033
	TST	IL-1β	*IFITM3*	0.709	0.022
		IL-1RA	*MSR1*	-0.629	0.028
		IFN-α2	*OAS3*	0.929	0.003
		PDGF-AA	*SECTM1*	0.673	0.023

Significant associations between continuous data done using Spearman's correlation analysis. Values highlighted in yellow indicate positive correlations.

CHAPTER 4: DISCUSSION

More than a hundred years after the discovery of *M. tuberculosis* as the causative agent of TB, its relationship with the host immune system is still not fully understood. Ex-vivo whole blood and PBMCs from ATB demonstrate a transcriptional profile enriched for type I IFN-inducible genes (189,352,377,398). However, the specific drivers of this observed transcriptional profile remain unidentified. The role of distinct type I IFN subtypes and *M. tuberculosis*-specific antigens on the expression of IFN-stimulated genes (ISG) in TB has not been studied. Therefore, the primary objective of this study was to characterize responses to type I IFN stimulation in clinical phenotypes of *M. tuberculosis* infection (ATB and LTBI), TST reactive individuals and healthy controls. Response to *M. tuberculosis*-specific stimulation was also assessed to identify linkages to the observed signature. The central hypothesis tested was that **IFN-α- and/or IFN-β-driven transcriptomic signatures and cytokine responses can distinguish clinical TB states.** The research presented aimed to identify similarities or differences in individual gene responses to IFN-α, IFN-β and *M. tuberculosis*-specific stimulation in order to define the drivers of the selected ISGs tested in this thesis. Identification of the drivers of the immunopathogenesis in TB will help discriminate immunologic processes that distinguish LTBI and ATB, which can lead to 1) better identification of individuals with LTBI at high risk of reactivation through the development of discriminant diagnostics and 2) the development of new therapeutics to treat LTBI and prevent the process of reactivation.

Various transcriptional studies have previously identified type IFN signatures that discriminate between ATB and LTBI and between ATB and HC. These include a 393-gene signature for ATB and an 86-gene signature that distinguishes ATB from other inflammatory and infectious disorders (189), a 380-gene signature that distinguishes ATB from HC (386,397), a 27-gene signature that distinguishes ATB from LTBI, and a 44-gene signature that distinguishes TB from other diseases (401), and a 2-gene set for that distinguishes ATB from other pulmonary diseases (421). A 4-gene set (422) and a 16-gene set (357) signature predictive of progression to active disease have also been identified, highlighting the importance of the transcriptional signature in TB pathogenesis. However, discordances have been observed in the individual genes identified in these studies; in an assessment of three gene sets that distinguish ATB from healthy controls that included LTBI - a 393-gene signature, a 27-gene signature, and a 42-gene signature

– only one gene was common to the three gene sets. Similarly, an assessment of four gene sets that distinguish ATB from other pulmonary diseases – a 144- gene signature, a 44-gene signature, an 86-gene signature, and a 51-gene signature found that none of the genes was common to all gene sets (189,356,401,423,424). These studies highlight the limited reproducibility of these signatures, possibly due to the impact of comorbidities, concomitant drug therapy, and genetics on the transcriptional profiles. This identifies a need for more studies, and the use of stimulations may mask some of the underlying variability of transcriptional profiles in ex vivo whole blood and PBMCs. No other study has utilized responses to type I IFN directly to assess the gene components of the type I IFN signature. For this thesis research, a set of 51 significant ISGs previously identified from our unpublished data and other transcriptional studies was utilized (189,425,426) to assess the transcription profiling, after stimulation, of the various clinical phenotypes in parallel with cytokine analysis to understand the patterns of immune responsiveness in clinical groups. This study sought to identify the drivers of the observed type I IFN response and determine whether differences in these responses are driven by distinct type I IFNs.

4.1 ISG responses to stimulation amongst *M. tuberculosis* infection states

In order to determine the effect of stimulation with IFN-α, IFN-β or *M. tuberculosis* whole cell lysate on the expression of ISGs in *M. tuberculosis* infection states, PBMCs from each study participant were divided into four parts and cultured with either IFN-α, IFN-β or *M. tuberculosis* WCL with an unstimulated control. For this section, **the hypotheses tested was that in comparison to LTBI, ISG expression in ATB would be higher following IFN-α/β stimulation and lower following Mtb WCL stimulation and that the ISG expression would not differ between IFN-α and IFN-β.**

4.1.1 Differentially expressed ISGs at baseline show higher expression in ATB

Previous studies have shown an overrepresentation of genes downstream of type I and II IFN signaling pathways in whole blood and PBMCs (189,233,352,375–377,398). Type I IFN-inducible genes identified from these studies demonstrate an increased expression in ATB compared to either controls or LTBI and clustered the groups by their expression patterns. While

baseline gene expression was not the primary focus of this study, analysis of gene expression at baseline was done to assess the expression of these genes and identify genes in our panel that could distinguish between clinical groups. A comparison of the expression of ISGs between the four study groups confirmed the hypothesis that the expression of ISGs at baseline would be higher in ATB than in LTBI and HC, as observed from the trends for most of the ISGs tested.

The trends of higher expression in ATB observed for most ISGs agreed with findings from other transcriptional studies (189,425). The relative expression of three of the 51 genes *FCGR1A*, *MSR1*, and *SECTM1* differed significantly between the four study groups (Table 18). Interestingly, previous studies have identified *FCGR1A* as differentially expressed in TB with increased expression in ATB compared to LTBI and healthy controls, and also discriminates between ATB and other pulmonary diseases (233,387,425,427–432). In agreement with our findings at baseline, *MSR1* and *SECTM1* have previously been shown to distinguish TB from LTBI or HC but not as components of type I IFN signature (387,432,433).

Table 18: Summary of differentially expressed genes

Gene	Unstim relative	IFN-α stim relative	IFN-α stim FC	IFN-β stim relative	IFN-β stim FC	Mtb WCL stim relative	Mtb WCL stim FC
FCGRIA	Up **ATB** v all	Up ATB v HC, LTBI		Up **ATB** v all		Up **ATB** v HC, TST	
SECTM1	Up **ATB** v HC, LTBI					Up **HC v** TST, LTBI	Up **HC** v all
MSR1	Up **ATB** v HC, TST		Up **HC** v ATB			Up **ATB** v TST	
ANKRD22		Up **ATB** v TST		Up **ATB** v TST			
FCGR1B				Up **ATB** v all			
IRF-9			Up **HC** v TST				
SOCS3					Up **LTBI** vs ATB		
IF144						Up **LTBI** vs ATB	
IF144L						Up **LTBI** vs ATB	
IFIT1						Up **LTBI** vs ATB	
IFITM3							Down **ATB** v LTBI
OAS3							Up **HC** v ATB
STAT1							Up **HC** v ATB

ATB-active tuberculosis; TST- Tuberculin skin test; LTBI-latent tuberculosis infection; HC-healthy controls. Table summarizes differentially expressed genes in the stimulation condition in which the adjusted p-value <0.05. Column color codes: gray – unstimulated relative expression, green – IFN-α relative expression and fold change (FC), purple – IFN-β relative expression and fold change (FC), blue – Mtb WCL relative expression and fold change (FC). The **bolded** group showed the higher expression.

The similarities in trends we observed with our targeted PCR results for some of the genes confirmed our choice of methodology. Most studies that described the IFN signature in TB used

microarray platforms that have the advantage of screening many genes at a time compared to PCR. For the studies that used microarrays, the individual genes identified in each gene list of the IFN signature varied between studies (423,434). Several factors may also have contributed to the differences in our findings. These include the type of samples, which have been shown to affect the transcriptional profile with differences in gene expression observed between whole blood and PBMCs (435). These differences may be due to the absence of neutrophils from PBMCs, cells that have been found to play a significant role in driving the IFN-inducible signature in TB (189). Gene expression levels also show variation depending on the stage of the disease, with low levels in LTBI that increase through the different stages in progression to ATB (434). Other factors that may have contributed to the differences in our findings include population differences such as gender and ethnicity that play a role in the immune response to infection (106). These factors are discussed further in section 4.7.

In this analysis of the baseline samples, we hypothesized that the expression of ISGs at baseline would be higher in ATB compared to LTBI and healthy individuals. Although no clear type I IFN-inducible transcriptional pattern was observed, we identified three ISGs *FCGR1A*, *MSR1* and *SECTM1*, which distinguished ATB from the other study groups.

4.1.2 IFN-α or IFN-β upregulate the expression of most ISGs in active TB.

IFN-α and IFN-β play a critical role in driving the innate and adaptive immune responses. The type I IFN signaling pathway leads to the production of ISGs, the effector molecules associated with the downstream effects of IFN-α and IFN-β signaling. Although genes in this pathway are overrepresented in the gene signature previously identified in ATB patients (189,352,375–377), the drivers of this effect are not known. The effects of IFN-α and IFN-β stimulation on individual genes and whether these effects differ between *M. tuberculosis* infection states remains unclear. We, therefore, set out to explore the specificity of IFN-α and IFN-β on ISG expression in *M. tuberculosis* infection states and hypothesized that stimulation of PBMCs with IFN-α or IFN-β would result in the upregulation of distinct ISGs in ATB compared to LTBI. No studies have explored differential outcomes of transcriptional profiles following stimulation with IFN-α or IFN-β as they relate to TB pathogenesis. A literature search revealed a paucity of studies investigating the effect of exogenous IFN-α/β stimulation on ISG expression in TB. Hence most

of the inferences we make on the effects of differentially expressed genes in this thesis research were based on previous findings from either unstimulated samples or other diseases.

In comparing the effect of IFN-α or IFN-β on ISG expression in *M. tuberculosis* infection states, there was an expected increase in the expression of most of our ISGs compared to that from unstimulated samples. The relative expression of three genes, *ANKRD22*, *FCGR1A* and *FCGR1B* differed between study groups after IFN-α/β stimulation (Table 18). The literature shows that these three genes have been described in previous ex vivo transcriptional profiling studies in TB, but this is the first time describing these genes' regulation by IFN-α and IFN-β. Previous ex-vivo transcriptional studies have shown *ANKRD22* to discriminate between ATB and LTBI (189,401,436) and between ATB and HC (386,426). Higher expression of *ANKRD22* has been observed in disease progressors in humans and mouse- and macaque-models of TB (357,437). Our data shows that *FCGR1A* gene expression is higher in ATB at baseline and after IFN-α/β stimulation. Similarly, the *FCGR1A* gene is a component of several gene signatures identified in TB. These include the 393-gene signature that discriminates LTBI from ATB described in a cohort from London (189); a 10-gene signature described in an Indian cohort (425); a 27-gene set from an African cohort (401); and even in a 16-gene signature that predicts risk of progression to ATB in a South African population (357). The observed expression of *FCGR1B* also agreed with findings from baseline expression in previous studies (233,234,426,428,436,438). Both *FCGR1A* and *FCGR1B* have been identified as the most stable genes with increased expression in ATB (233,375,386,400,425,427–429,432).

The *ANKRD22* gene encodes the protein ANKRD22, which induces macrophage apoptosis in TB, a process that has recently been shown with virulent strains of *M. tuberculosis*, leading to cell-to-cell spread through the ESX-1 system and resulting in dissemination (439–441). From this, it can be inferred that a higher expression of *ANKRD22* may induce apoptosis of *M. tuberculosis*-infected macrophages would cause bacillary dissemination leading to disease progression, which is supported by the upregulation of *ANKRD22* observed in TB progression (422).

The *FCGR1A* and *FCGR1B* genes are induced by IFN-γ and encode the high-affinity and low-affinity FCγR1, respectively. The high-affinity FCγR1 is an activating receptor expressed on immune cells such as DCs and macrophages, but not in AECs, that recognizes IgG-coated bacteria and induces phagocytosis (442–445). However, the low-affinity FCγR1 is not well characterized.

FCγR1 has been shown to reduce inflammation through its downregulation by microRNA 127 (miR-127) in lung injury. Our observation of increased *FCGR1A* and *FCGR1B* in ATB compared to LTBI suggests that higher expression of FCγR1 may induce inflammation which may be beneficial in early infection but cause tissue injury if persistent with potential for disease progression (446). Increased FCγR1 expression would also increase PRR signaling and subsequent phagocytosis, promoting bacterial clearance in early infection. However, where bacillary replication persists, this would cause macrophage necrosis that enhances further bacterial replication increasing the bacillary burden and leading to disease progression (447,448). Lower expression in LTBI compared to ATB would result in reduced phagocytosis and bacillary clearance, increasing the possibility of disease progression (Figure 36).

We have used both relative expression and fold change methods to describe differences in expression between study groups throughout our analysis. While the relative expression method gives the normalized gene expression and uses the difference in Crt values between a target gene and a reference gene(s), enabling gene expression analysis for all stimulation conditions, including the unstimulated samples, fold change assess the differences (gain or loss) in gene expression between the stimulated and the unstimulated samples.

Interestingly, the calculation of gene expression following IFN-α or IFN-β stimulation using the fold change method revealed a different set of genes – *IRF9* and *MSR1* following IFN-α stimulation, *SOCS3* following IFN-β stimulation only. The higher expression of IRF9 in LTBI progressors compared to LTBI has previously been described only in unstimulated samples and not in IFN-α/β stimulated samples (357). However, stimulation with IFN-α/β would upregulate *IRF9* expression by inducing the IFN signaling pathway. The body of literature shows that *MSR1* gene expression discriminates ATB from LTBI, in contrast to our findings (432). The pattern of *MSR1* expression observed in our study is similar to what was observed in unstimulated samples in which the highest basal expression was in ATB, suggesting that stimulation with both IFN-α/β upregulates *MSR1* expression in all the clinical phenotypes, but the fold change is lower in ATB compared to the other clinical phenotypes because of its increased expression at baseline. In agreement with our findings, the ability of the *SOCS3* gene to discriminate between LTBI and ATB has also previously been described in unstimulated samples but not previously linked to specific IFN stimulation (449).

IRF9 is a transcription factor that is an integral part of the IFN signaling pathway and a component of the IFN stimulated gene factor 3 (ISGF3) complex found upstream in the IFN signaling pathway. IRF9, induced by type I and II IFNs, binds to the STAT1-STAT2 dimer to form the ISGF3 that binds to the IFN-stimulated response elements in the nucleus, driving transcription of ISGs. IRF9 plays a role in the production of type I IFNs, regulates the expression of downstream ISGs, and IRF7, and has been shown to determine the type I IFN-directed cellular responses by driving the transcriptional profile (450–452). The specific role of IRF9 in TB has not been defined. In viral infections, IRF9 inhibits viral replication and spread in early infection but is also needed for CD8+ T cell responses leading to viral clearance and preventing the establishment of chronic infection, a protective role (451). From this, it can be inferred that IRF9 plays a role in pathogenesis, regulated specifically by IFN-α based on our findings of differential expression driven by IFN-α stimulation and not by IFN-β. Its downstream effects may be related to its expression since IRF9 is also an ISG or to the ISG profile induced.

The *MSR1* gene is induced by type I IFNs and IFN-γ and encodes a pattern recognition receptor (PRR), MSR1, also known as CD204 or macrophage scavenger receptor class A1 (SR-A1), a receptor located in the plasma membrane and Golgi apparatus of macrophages; the receptor is also not expressed on AECs (453,454). MSR1 belongs to a family of scavenger receptors that have a wide array of ligands. Although the ligands in *M. tuberculosis* are unknown, a glycolipid trehalose 6,6'-dimycolate is recognized by a closely related receptor MARCO and CpG DNA by other members of the family (455). MSR1 suppresses the nuclear translocation of IRF5, shifting macrophage polarization from the pro-inflammatory M1 to the anti-inflammatory M2 macrophage phenotype switching from a Th1 immune response to a Th2 response which leads to a loss of the protection conferred by the Th1 response in *M. tuberculosis* infection (390,456,457). Conversely, the deficiency of this receptor drives an M1 macrophage polarization and appears to protect against *M. tuberculosis* infection (458,459). The stepwise increase in the expression of *MSR1* from HC to TST, LTBI with the highest expression in ATB suggests that its expression increases with disease progression. Higher upregulation of the *MSR1* gene induced by IFN-α stimulation in LTBI would drive macrophage polarization to the M2 phenotype, which drives a Th2 immune response, and suppress Th1 cytokines, particularly TNF-α, that are key in the formation and maintenance of the granuloma (5,211,244). In the absence of this protection, infected phagocytic cells in the centre of the granuloma die releasing the bacilli that get disseminated. Macrophages with increased MSR1

expression would, therefore, likely show increased bacterial uptake and intracellular replication within the macrophage that may result in further cell death releasing more bacilli that spread leading to disease progression.

SOCS3 is expressed on Th2 cells and negatively regulates type I and II IFNs (460). The lower expression of the *SOCS3* gene in ATB would remove its inhibitory effect on type I IFN production driving IFN-α/β production. SOCS3 has also been shown to regulate macrophage polarization driving an M1 macrophage phenotype in contrast to MSR1 (461) and boosting the phagocytic function of M1 macrophages (462) (Figure 36). The expression of SOCS3 also plays a protective role against *M. tuberculosis* infection by curtailing the inhibitory effects of IL-6 on the production of TNF and IL-12 in myeloid and lymphoid cells (463). The magnitude of expression was greater in LTBI than in ATB, which may imply a protective role in LTBI. It also implies that the basal expression of this gene is lowest in LTBI and HC compared to ATB. While this pattern was also observed in our unstimulated comparison, it did not reach statistical significance.

Taken together, we observed a paucity of studies assessing the effect of distinct type I IFNs on ISG expression in TB despite a significant body of evidence identifying a type I IFN-driven signature contributing to TB pathogenesis. We hypothesized that stimulation of PBMCs with IFN-α or IFN-β would result in upregulation of ISGs in ATB compared to LTBI, which was observed for most genes. An almost equal number of genes had higher expression in ATB than LTBI and vice versa with the relative expression method and the fold change method. The findings from ISG expression following IFN-α/β suggest that some the genes may induce protective effects such as *SOCS3* expression or *FCGR1A* expression in early infection. In contrast, the expression of other ISGs such as *ANKRD22*, *MSR1*, and *FCGR1A* may drive disease progression. The specific mechanisms of these ISGs in *M. tuberculosis* infection are not known. Although the *SECTM1* gene was observed in baseline samples, the gene was not differentially expressed following IFN-α or IFN-β stimulation suggesting its expression is possibly regulated by alternative mechanisms; the gene is differentially expressed following Mtb WCL stimulation. For the first time, we show that IFN-α/β stimulation drives a myriad of distinct ISG responses in our TB groups, both protective and detrimental, including macrophage polarization to either M1 or M2 phenotype, macrophage apoptosis, and inflammation. The outcome of IFN-α and IFN-β activity in infection may depend on the balance of the gene components of the ISG profile induced. Although most ISGs showed

similar responses following stimulation with IFN-α and IFN-β, some differed. The within-study group ISG responses to IFN-α and IFN-β were assessed and are discussed in section 4.1.4. The differences in ISG expression may be related to differences in binding affinities to IFNAR observed with IFN-α and IFN-β (304,305).

4.1.3 Mtb WCL downregulates the expression of most ISGs in TB

Previous microarray testing of PBMCs from ATB, LTBI, and HC stimulated with *M. tuberculosis*-specific antigens failed to identify genes enriched for type I IFN signaling pathway (384,385). Therefore, aside from the stimulation with IFN-α and IFN-β, we also stimulated samples with Mtb WCL to determine its effect on the expression of the ISGs. The lysate contains the bacillary cell wall components - proteins, lipids, and carbohydrates – and was used as a surrogate for infection with *M. tuberculosis* and represented the events at the site of bacterial replication and enabled us to compare the immune responses to those observed with IFN-α/β. In addition, based on the findings from previous genome-wide transcriptome analysis from PBMCs stimulated with ESAT-6/CFP-10 or PPD, we expected that Mtb WCL would suppress the expression of ISGs in ATB more than in LTBI.

The relative expression method identified *IFI44*, *IFI44L*, *IFIT1*, *FCGR1A*, *MSR1*, and *SECTM1* genes were identified as differentially expressed following Mtb WCL stimulation (Table 18). The fold change method revealed more unique differences between clinical phenotypes in the expression of *IFITM3*, *OAS3*, *SECTM1*, and *STAT1*, which showed higher expression in LTBI than in ATB. Aside from *FCGR1A*, *MSR1*, and *SECTM1*, the remaining genes were only observed following Mtb WCL stimulation and not at baseline or after IFN-α/β stimulation.

In agreement with our findings, previous transcriptional studies of unstimulated samples show that the expression of *IFI44* and *IFI44L* genes can discriminate between ATB and both LTBI and HC and decline with LTBI treatment (189,375,425,464). However, in contrast with these studies in which higher *IFI44* and *IFI44L* gene expression were observed in ATB, the expression in our study was higher in LTBI following Mtb WCL stimulation, a difference that may be due to the stimulation. In a study on TST-reactive individuals, IFI44L shows higher expression in IGRA-

negative individuals than in IGRA-positive, whereas no differences are observed in *IFI44* gene expression (465).

IFI44 gene encodes for the protein IFI44 while the *IFI44L* gene encodes the protein IFI44L, which shows antiproliferative activity and inhibits viral replication (466–468). In *M. tuberculosis* infection, IFI44L is upregulated and demonstrates antimicrobial activity in macrophages showing potential as a marker for treatment monitoring (469). The IFI44L is accompanied by the production of chemokines, including CXCL10 and CXCL11, and the pro-inflammatory cytokines IL8 and IL18, compared to non-infected macrophages. IFI44 also induces latency in HIV-1 infection (468). Our findings of significant difference between LTBI and ATB with Mtb WCL stimulation, with lower expression in ATB, may suggest a protective role for IFI44 and IFI44L in TB, especially since the genes negatively regulate type I IFN responses (470). The higher expression in LTBI may induce antiproliferative activity similar to what has been observed in viruses such as HIV and RSV (466–468). Higher expression of the *IFI44L* gene in LTBI may also play a protective role by enhancing bacterial clearance, as observed in the *M. tuberculosis*-infected macrophages, thereby preventing disease progression (469).

Upon stimulation with Mtb WCL, the expression of the *IFIT1* gene was higher in LTBI than in ATB and differentially expressed between LTBI and ATB. IFIT1 is upregulated in alveolar macrophages and in primary bronchial epithelial cells infected in vitro with *M. tuberculosis* but downregulated in bone marrow-derived macrophages infected with the virulent *M. tuberculosis* H37RV strain (471–473). The *IFIT1* (*ISG56*) gene encodes the protein P56 and is induced by IFNs (primarily IFN-α/β, but also by IFN-γ), LPS, dsRNA, and viruses, and binds to the stimulator of IFN genes (STING), inhibiting its activation of the TBK1 (474,475). Overexpression of the gene has been found to inhibit activation of IRF3 and NFκB and inhibition of IFN-β production, dampening the innate immune responses in viral infection (460,475). IFIT1 also inhibits translation initiation resulting in cell growth inhibition and impeding viral replication, negatively regulates the production of pro-inflammatory cytokines, including TNF-α, and induces *IFN-B* gene expression and downstream expression of ISGs (460,474–476). The higher expression in LTBI may be associated with inhibition of replication or IFN-β production, hence protective. On the other hand, higher levels of IFT1 in LTBI may also suppress pro-inflammatory cytokines such as TNF-α, which is crucial for maintaining the granuloma structure, possibly leading to reactivation

and disease progression. Nevertheless, the specific mechanism and role in *M. tuberculosis* infection remain unknown.

FCGR1A gene expression was highest in ATB following Mtb WCL stimulation, showing a similar pattern to that observed at baseline. The gene was differentially expressed between ATB and HC and ATB and TST, suggesting a potential detrimental role for FCGR1A in TB. The progression from latency resulting from the higher expression in ATB compared to LTBI increases the bacterial burden. Increased *FCGR1A* expression and the FCγR1 would result in increased phagocytosis and cell necrosis leading to bacterial replication and disease progression. Although the high-affinity *FCGR1A* was induced following Mtb WCL stimulation, the low-affinity FCGR1B, commonly identified in ATB, was not induced in any of the clinical phenotypes with Mtb WCL stimulation. In a similar study in which PBMCs were stimulated with the *M. tuberculosis* antigen PPD, the gene was induced though not differentially expressed between TB clinical phenotypes (385). The mechanism by which the *FCGR1B* gene was not induced following stimulation with Mtb WCL is not known but may suggest differences in the stimulation ability of *M. tuberculosis*-specific antigens with undetectable induction or inhibition by Mtb WCL.

The expression of the *MSR1* gene after Mtb WCL stimulation was also highest n in ATB as seen in baseline expression and with IFN-α/β stimulation. Mtb WCL stimulation repressed the expression of the *MSR1* gene in all clinical groups compared to the unstimulated condition. The gene was differentially expressed between TST and ATB with higher expression in ATB, suggesting a detrimental role for MSR1 in TB, as discussed in section 4.1.2.

The expression of the *IFITM3* gene showed little change for all clinical phenotypes with Mtb WCL stimulation but was differentially expressed between LTBI and ATB, with higher expression in LTBI. Previous studies showed upregulation of this gene in ATB in unstimulated samples (189,375,399,426). The expression of *IFITM3* is induced by *M. tuberculosis* and TLR 2 and 4. The gene encodes the IFITM3 protein that restricts the bacillary intracellular growth by increasing endosomal acidification (477). Although the role of IFITM3 in TB is not established, the higher induction of the *IFITM3* gene with Mtb WCL stimulation in LTBI than in ATB may suggest it plays a protective role by restricting bacillary burden and maintaining latency.

OAS3 gene expression was highest in HC. *OAS3* and other related genes, *OAS1* and *OAS2*, have been described in several transcriptional signatures in TB, with their upregulation

discriminating between ATB and LTBI and between HC and ATB (189,233,352,426)(426). The expression of the *OAS3* gene is induced by type I and II IFNs with downstream inhibition of apoptosis, protein synthesis in viral infections, intracellular replication of mycobacteria, and enhanced production of pro-inflammatory cytokines – TNF-α, IL-1β, and MCP-1 (478,479). The suppression of *OAS3* by Mtb WCL in ATB observed in our study may therefore drive bacillary replication and suppress the synthesis of pro-inflammatory cytokines required for controlling early *M. tuberculosis* infection.

The expression of the *SECTM1* gene was highest in HC with Mtb WCL stimulation, and the gene was differentially expressed with both the relative expression method and the fold change method. This *SECTM1* gene expression trend differed from that observed at baseline, in which the gene was differentially expressed with the highest expression in ATB. However, *SECTM1* was not differentially expressed with IFN-α/β, suggesting that alternative mechanisms regulate its expression. A literature search shows that in unstimulated whole blood samples, SECTM1 is upregulated in ATB compared to HC (426,438). The *SECTM1* gene is induced by type I IFNs and IFN-γ and encodes the SECTM1 protein, a ligand for CD7 expressed on NK cells and T cells that acts as a co-stimulatory ligand for the proliferation of CD4 and CD8 T lymphocytes and production of pro-inflammatory cytokines, and a chemoattractant for monocytes (433,480–482). In TB, the SECTM1 chemoattractant role would be necessary for granuloma formation, which has a core of monocyte-derived macrophages and in the macrophage-related control of infection, a role that has not been established. SECTM1 is also induced in lung epithelial cells during pneumococcal pneumonia, a process that requires type I IFN signaling. In early infection, the SECTM1 binds to neutrophils in the infected lung and induces the expression of CXCL2, a neutrophil chemoattractant that drives the influx of neutrophils to the infection site, and that is involved in IL-1β production leading to bacterial clearance (483,484). The lower expression in LTBI and ATB following Mtb WCL stimulation possibly suggests that this stimulation suppresses CXCL2 expression, neutrophil influx and bacterial clearance resulting in failure of early infection control. However, this remains an unstudied area in TB.

STAT1 gene was differentially expressed between HC and ATB with higher expression in LTBI. This gene has previously been found upregulated in ATB (189,375,387,425,426). The *STAT1* gene encodes the STAT1 protein, a transcriptional regulator that is a component of type I IFN and IFN-γ signaling pathways. Early in *M. tuberculosis* infection, phosphorylation of STAT1

activates apoptotic factors leading to bacillary elimination. Over time, there is an accumulation of non-phosphorylated STAT1 that inhibits cellular apoptosis allowing for bacillary evasion (485). STAT1 has also been shown to promote macrophage polarization to the M1 phenotype, which is involved in eliminating the bacilli (486). These defensive roles of STAT in *M. tuberculosis* infection may explain the higher expression of the gene in LTBI rather than in ATB.

In summary, we hypothesized that stimulation of PBMCs with *M. tuberculosis* WCL would suppress ISGs to a greater extent in ATB than LTBI. In LTBI and ATB, most of the genes showed little effect following Mtb WCL stimulation being outside the absolute(log_2FC) of |1| cutoff. They would therefore not be defined as either up-regulated or down-regulated. This is in agreement with the studies that failed to identify the IFN signature in PBMCs stimulated with ESAT-6/CFP-10 or PPD (384,385), but in contrast to the expression of the same gene panel in response to IFN-α/β stimulation in which most genes were upregulated in all clinical phenotypes. The kinetics of gene expression has been shown to vary between genes and depend on the stimulation used, its signaling pathway, and the cell type (487). This was demonstrated in fibrosarcoma cells in which stimulation with IFN-β resulted in high levels of *IFIT1* (*ISG56*) mRNA and *IFIT2* (*ISG54*) mRNA at 6 hours with sustained *IFIT1* mRNA but reduced *IFIT2* mRNA at 24 hours post-stimulation whereas TLR3 stimulation using dsRNA caused a decline in the two genes between 12 to 24 hours; and infection with Sendai virus causes a rapid decline by 12 hours (487). Following stimulation of THP-1 cells with IFN-α, a strong type I IFN signal was observed, whereas infection of the cell-line with *M. tuberculosis* led to increased negative regulation of IFN-α/β that led to a low type I IFN signal (488). The findings from these studies suggest an inhibitory effect of *M. tuberculosis* on the type I IFN signal and ISGs, although the specific mechanism induced by stimulation has not been defined.

The findings from ISG expression following Mtb WCL stimulation suggest that some of the genes may induce protective effects, such as *IFI44*, *IFI44L*, *IFITM3*, and *STAT1* genes, while the expression of other ISGs such as *FCGR1A*, *MSR1*, *SECTM1*, and *OAS3* genes may drive disease progression (Figure 36). However, the specific mechanisms of these ISGs in *M. tuberculosis* infection are not known.

4.1.4 IFN-α and IFN-β-induced differential ISG expression within clinical groups

The previous sections assessed differential responses to IFN-α or IFN-β stimulation between TB clinical groups following either IFN-α or IFN-β stimulation. It is also important to consider within-group differences to determine whether in ATB or LTBI, responsiveness to either of the IFNs predominates. In this section, ISG expression was compared between IFN-α and IFN-β stimulation within each study group. These better highlights any distinct differences between the two stimulations and answers the question whether, within a study group, the two IFNs stimulated similar or different ISG gene expression patterns.

In section 4.1.2, IFN-α and IFN-β showed a similar but not exact profile for the majority of the 51 differentially expressed genes interrogated but importantly, some of the ISGs did show significant differences and specificity to IFN-α or IFN-β. In agreement with some of our findings in HC, a study that compared the effects of type I IFN subtypes stimulation on ISGs in healthy donors found no differences in IFN-α versus IFN-β in the expression of *OAS1*, *MSR1*, *CCL8*, *CXCL10*, *CXCL11*, *IFITM1*, *IFITM2*, *IFITM3*, *IFIT1*, and *IFI44* genes (390). However, in this thesis research, differences were observed in the expression of ISGs tested between IFN-α and IFN-β in all clinical phenotypes, with most genes showing higher expression with IFN-β than IFN-α. This may be related to the high binding affinity of IFN-β for IFNAR and previous observation in HSV-2 infected mice that IFN-β regulates the production of IFN-α (304,305,309,314). Differences in the induction of ISG expression between IFN-α and IFN-β would suggest that the components of the type I IFN signature may be driven by either IFN-α or IFN-β. This is important if modulation of specific IFN-α or IFN-β induced ISGs are identified as potential therapeutic targets in TB, then treatment monitoring can utilize specific ISG detection.

In summary, we identified a set of ISGs that differentiated LTBI from ATB at baseline *FCGR1A* and *SECTM1* genes; following IFN-α stimulation *FCGR1A* gene; following IFN-β stimulation *FCGR1A*, *FCGR1B*, and *SOCS3* genes; and following Mtb WCL stimulation *IFITM3*, *IFI44*, *IFI44L* and *IFIT1* genes (Figure 36). These roles of these genes have not been identified in TB pathogenesis but have been inferred from roles in other diseases; these genes play a protective role in disease through various mechanisms. The protective roles of *SECTM1* and *FCGR1A* genes appear to be in early infection, but the ISGs also show a potential role in disease progression. This thesis work also identified a set of ISGs involved in macrophage polarization *MSR1*, *STAT1*, and

SOCS3 genes that differentiated HC/TST or LTBI from ATB and drive M1 polarization (*STAT1* and *SOCS3* genes) or M2 polarization (*MSR1* gene). Some genes showed significant differences in expression between IFN-α and IFN-β stimulation. Stimulation with IFN-α/β enhances the expression of most ISGs. In contrast, stimulation with Mtb WCL has little effect on most ISGs but suppresses *MSR1* gene expression, which would be protective in *M. tuberculosis* infection. The data suggest that ISGs show specificity to IFN-α or IFN-β, and the individual genes induced in an ISG profile possibly determine *M. tuberculosis* infection outcomes. Most of the genes induced by IFN-α/β during infection may drive disease progression, while genes induced by *M. tuberculosis* were protective. However, the specific mechanisms have not been elucidated.

4.2 Cytokine responsiveness to stimulation amongst *M. tuberculosis* infection states

In addition to assessing select transcript regulation to our stimulation panel, we also looked at cytokine production in response to stimulation using Milliplex® MAP Human Cytokine / Chemokine kits.

To quantify cytokine responses to IFN-α, IFN-βor *M. tuberculosis* whole cell lysate in various *M. tuberculosis* infection states, PBMCs from each study participant were cultured for 16 to 18 hours with either IFN-α, IFN-β or *M. tuberculosis* WCL and an unstimulated control. The hypotheses tested were that **compared to LTBI, pro-inflammatory cytokine responses in ATB would be suppressed by IFN-α/β and increased by Mtb WCL stimulation and would not differ between IFN-α and IFN-β stimulation.**

4.2.1 Unstimulated PBMCs showed no differences in cytokine levels between *M. tuberculosis* phenotypes

In assessing cytokine levels following culture with no stimulation, none of the cytokines assessed showed significant differences between the clinical phenotypes (Table 19). Similar results were observed in a study that analysed cytokines from unstimulated plasma cultured for 16 to 24 hours from culture-confirmed TB patients in which no differences were observed between the TB

patients and HC (489). This may be related to the length of culture, which was between 16 and 18 hours in our study.

Table 19: Summary of cytokine expression

Cyokine	**Unstim**	**IFN-α stim level**	**IFN-α stim FC**	**IFN-β stim level**	**IFN-β stim FC**	**Mtb WCL stim level**	**Mtb WCL stim FC**
IL-10		Up **LTBI** v ATB	Up **LTBI** v ATB	Up **LTBI** v ATB			
MCP-3		Up **LTBI** v HC					
PDGF-AB/BB		Up **ATB** v TST				Up **ATB** v HC, TST	
PDGF-AA						Up **ATB** v TST	
G-CSF			Down **TST** v LTBI				
IP-10					Up **ATB** v TST		
IL-1β			Up **LTBI** v TST				Up **ATB** v TST

ATB-active tuberculosis; TST- Tuberculin skin test; LTBI-latent tuberculosis infection; HC-healthy controls. Table summarizes differentially expressed genes in the stimulation condition in which the comparison adjusted p-value <0.05. Column color codes: gray – unstimulated relative expression, green – IFN-α relative expression and fold change (FC), purple – IFN-β relative expression and fold change (FC), blue – Mtb WCL relative expression and fold change (FC). The **bolded** group showed the higher expression.

4.2.2 IFN-α and IFN-β suppresses the expression of pro-inflammatory cytokines in TB

Previous studies in mice and human macrophages show that infection with *M. tuberculosis* drives the production of type I IFNs. In TB, type I IFNs suppress or inhibit the production of protective cytokines such as IFN-γ, IL-12, IL-1, TNF-α, and IL-6 (26,366,367,420,490,491). In these studies, in which human or murine cells were infected with *M. tuberculosis* and then treated with type I IFNs, the effects of type I IFNs on IL-10 differed, showing a reduction in production in some studies and enhanced production in others.

In our study, following IFN-α and IFN-β stimulation, IL-10 was interestingly higher among the LTBI group as compared to the other groups (Table 19). In this study, IFN-α stimulation showed little effect on the expression of IL-10, although the cytokine was differentially expressed between LTBI and ATB. These mirrored the findings at the transcriptional level, where we found higher expression of the *IL-10* gene was observed in LTBI compared to ATB. However, the difference in gene expression did not reach statistical significance. Increased levels of IL-10 have previously been reported in ATB from pleural fluid, PBMCs, serum, bronchoalveolar lavage cells and *M. tuberculosis*-stimulated cell culture supernatants, whereas higher levels in LTBI compared to ATB have also been reported from *M. tuberculosis*-specific antigen-stimulated whole blood cell culture supernatants (492–495). IL-10 is an immunoregulatory cytokine produced by many cell types, including macrophages, neutrophils, all CD4+ T cell subsets, and B cells (496). In *M. tuberculosis*-infected macrophages, IFN-α/β induces the production of IL-10, which inhibits the production of the pro-inflammatory cytokines IL-12 and TNF-α, phagocytosis, and the production of reactive intermediates, ROIs and RNIs, processes that are crucial for clearing *M. tuberculosis* (263,496–498). The cytokine impairs the host immune response against *M. tuberculosis* at all stages of infection (364). In a mouse model of infection, IL-10 expression in early infection was not associated with increased susceptibility to infection; in latent infection, however, expression was associated with increased lung bacterial burden and reactivation (499). Therefore, the higher levels of IL-10 induced after stimulation with IFN-α and IFN-β in LTBI could potentially drive disease progression by suppressing the immune response necessary for clearance of the bacilli.

PDGF-AB/BB level was higher in the ATB group compared to the other groups following IFN-α stimulation but not with IFN-β stimulation, and similar to the response following Mtb WCL

stimulation (Table 19). Differences in the levels of PDGF-AB/BB were observed between TST and ATB with IFN-α with higher expression in ATB. Elevated levels of PDGF-BB in serum from ATB patients have been observed previously, and increased levels have been observed in ATB compared to HC. However, no study has linked these increased levels directly to type I IFN responsiveness (500,501). There is scarce information on PDGF-AB/BB responses in different phenotypes of *M. tuberculosis* infection. PDGF-AB/BB is an angiogenic growth factor produced by platelets and macrophages that negatively affects *M. tuberculosis* growth (502). The role of this cytokine in TB is not well defined, but its release from alveolar macrophages induces the proliferation of myofibroblasts and drives fibrogenesis leading to fibrosis in disorders with chronic lung inflammation (503,504), which is possibly related to the higher expression in ATB in our study. IFN-γ and IL-1β induce the expression of PDGF-B and PDGF-AA, respectively (505). However, the link between this cytokine and type I IFNs in TB is not established. In dermal fibrosis, monocyte/ macrophage recruitment, tissue injury, and effect on blood vessels appear to be dependent on IFNAR (506). This is the first study to identify a specificity of PDGF in response to IFN-α; more studies on a possible interaction of type I IFNs and PDGFs and the role of PDGFs in TB are required.

After stimulation with IFN-α, the MCP-3 level was highest in LTBI, followed by ATB, TST, and lowest in HC (Table 19). The cytokine level showed differences between HC and LTBI for MCP-3 with higher expression in LTBI. The levels of MCP-3 were also higher in LTBI than in ATB, as previously described (507), although this difference was not statistically significant. MCP-3/ CCL7 is a chemokine produced by macrophages that recruits monocytes and neutrophils to the site of infection (508). Increased MCP-3 levels have been observed in ATB compared to LTBI and HC in both unstimulated and *M. tuberculosis*-specific antigen-stimulated samples (509–511). Increased levels in ATB increase the cellular immune responses leading to bacillary clearance. In addition, increased expression of MCP-3 has been observed in type I IFN-driven diseases such as systemic lupus erythematosus (SLE), in which the cytokine is associated with systemic inflammation (512). Similar observations are found in PBMCs cultured with either measles virus, dsRNA, IFN-α, or IFN-β, all of which induced MCP-3 (513). This is the first study to link MCP-3 levels to IFN-α in TB.

The expression of IL-1β protein showed little change in all clinical groups following stimulation with both IFN-α and IFN-β. It was differentially expressed between LTBI and TST with IFN-α stimulation with the highest expression in LTBI (Table 19). In contrast to our findings, a recent study demonstrated higher levels of IL-1β in ATB compared to LTBI in unstimulated samples and identified an association between IL-1β and disease severity (514). The trend in protein data also differed from our transcriptional data in which IFN-α stimulation downregulated the *IL-1B* gene in all clinical phenotypes with the largest change in ATB. This suppressive effect of type I IFNs on IL-1β has previously been described in cells exposed to *M. tuberculosis* and IFN-β (419,490). IL-1β is secreted by a wide range of cells, including mononuclear phagocytes and T and B lymphocytes. It is a pro-inflammatory cytokine that is crucial for controlling *M. tuberculosis* infection. The higher expression in LTBI compared to ATB at protein level may be an attempt to control disease progression by preventing reactivation, although a study in a mouse-model of infection observed no increase in reactivation with individual neutralization of IL-1β (and IL-1α) (268).

Stimulation with IFN-α showed little effect on G-CSF production with fold change differences between TST and LTBI (Table 19). Tumor immune surveillance studies in mice downregulated the expression of G-CSF following IFN-α stimulation (515,516). G-CSF drives the survival of neutrophils, their differentiation and proliferation. It is also an immune cell chemotactic factor recruiting cells to injury sites (517). In *M. tuberculosis* infection, neutrophils may be involved in controlling early infection by their participation in granuloma formation and the formation of effector T cells (185). Neutropenia resulting from G-CSF downregulation by type I IFNs in LTBI may affect granuloma formation and the adaptive immune response to infection leading to disease progression.

IP-10/ CXCL10 was differentially expressed between TST and ATB with IFN-β stimulation with higher expression in ATB (Table 19). Although not statistically significant, a similar trend was observed with IFN-α stimulation. IP-10 has been assessed as a potential biomarker for TB in various studies and has shown the potential to discriminate between ATB and both LTBI and HC with higher expression in ATB, and between LTBI and both ATB and HC with higher levels in LTBI in unstimulated samples (518,519). A correlation between IP-10 levels and disease severity was observed, with extensive disease presenting higher levels than localized

disease. In samples stimulated with *M. tuberculosis*-specific antigens, IP-10 discriminates between LTBI and ATB (507,520–522). IP-10 levels are higher in ATB than in household contacts, in HIV-positive TB patients than in HIV-negative patients, and in QFT-positive than in QFT-negative (507,523). Indeed, IP-10 has higher levels than IFN-γ in TB and shows more reproducible results than QFT, which is CD4+ T cell-dependent (524). IP-10/ CXCL10 is a chemokine secreted by many cells, including leukocytes, neutrophils, and monocytes, in response to IFN-α, IFN-β, and IFN-γ (525,526). It induces the migration of macrophages, DCs, NK cells and leukocytes to the infection site, their binding to and activation of the CXCR3 receptor, apoptosis, and cell growth inhibition (527). In *M. tuberculosis*-infected human DCs, type I IFN induced by the infection drives the production of IP-10, as confirmed by its downregulated when the IFNs were neutralized (525). Increased IP10 protein in ATB may therefore have a role to play in the elimination of *M. tuberculosis* that our data would indicate is driven by IFN-β and not by IFN-α or Mtb WCL.

Previous studies demonstrated that high levels of type IFNs induced during infection drive the production of the regulatory cytokine, IL-10, and inhibit protective pro-inflammatory cytokines including IL-1α, IL-1β, TNF-α, and IL-12 (364,366,367,369,373,490). However, few studies have assessed the effect of distinct type I IFNs on cytokine expression in TB. We hypothesized that stimulation of PBMCs with IFN-α or IFN-β would suppress pro-inflammatory cytokines in ATB compared to LTBI and observed the suppression of the pro-inflammatory cytokines –IL-1β, IL-6, and TNF-α – in ATB compared to LTBI although these differences were not statistically significant. Following IFN-α or IFN-β stimulation, IL-10 was the only cytokine that was differentially expressed between LTBI and ATB, which in LTBI would drive reactivation and disease progression (499).

4.2.3 Mtb WCL drives pro-inflammatory cytokines in TB

Most cytokines tested showed little change after stimulation with IFN-α and IFN-β, but stimulation with Mtb WCL upregulated the expression of most cytokines in ATB and LTBI. Stimulation with Mtb WCL resulted in trends of increased expression of the pro-inflammatory cytokines IL-1β, IL-6, and TNF-α in ATB compared to LTBI; increased expression of the anti-inflammatory cytokines IL-1RA and IL-10 in ATB compared to LTBI; and showed different effects on chemokines with upregulation of IP-10, MIP-1α, MIP-1β, and RANTES, and little change on MCP-3, eotaxin, and MDC. Most of these cytokines showed higher expression in ATB

compared to LTBI. However, these differences in fold changes observed between ATB and LTBI did not reach statistical significance for any of the cytokines.

The PDGF-AA and PDGF-AB/BB levels differed between ATB and HC or TST. As described in section 4.2.2, there is scarce evidence on the role of these cytokines in TB, but they have been shown to drive fibrogenesis in chronic lung disease, causing lung fibrosis (503,504). Pulmonary fibrosis is a feature of chronic TB or resolving disease commonly occurring post-TB treatment (18,528,529). However, the possible role of PDGFs in lung fibrosis in TB has not been elucidated.

Only IL-1β protein was differentially expressed in our study in the fold change method analysis (Table 19). IL-1β expression was upregulated and differentially expressed between TST and ATB with Mtb WCL with the largest fold change in ATB. This finding was the opposite effect from what we observed following stimulation with IFN-α/β, whereby the expression of IL-1β protein was suppressed, and that of the *IL-1B* gene downregulated. Our findings agree with those observed with both live *M. tuberculosis* and its product, ESAT-6, inducing the production of IL-1β from macrophages (530). The role of IL-1β in TB is discussed in 4.2.2.

Increased expression of the pro-inflammatory cytokines IL-1β, IL-6 and TNF-α was observed in ATB compared to LTBI, confirming our hypothesis that Mtb WCL drives a pro-inflammatory cytokine milieu in *M. tuberculosis* infection states, although this difference was only significant for IL-1β.

4.2.4 Differences between IFN-α and IFN-β-induced cytokine expression within clinical groups

To further define the effect of the individual IFNs used in this study, the expression of the cytokines in each clinical phenotype was compared between IFN-α and IFN-β stimulation. As we observed in a similar gene expression analysis described in section 4.1.4, most of the cytokines that showed significant differences between IFN-α and IFN-β stimulation had higher expression following IFN-β stimulation. Cytokines that showed higher expression following IFN-β stimulation in ATB included chemokines IP-10, MDC, GRO, IL-8, and anti-inflammatory cytokines IL-1RA; in LTBI, they included chemokines IP-10, MDC and GRO, and the anti-inflammatory cytokine IL-1RA. Similarly, this could be related to the high binding affinity and

slow dissociation rate of IFN-β that is associated with more prolonged induction of ISGs and the regulation of IFN-α production by IFN-β

In summary, IL-10 protein showed the ability to differentiate LTBI from ATB following IFN-α and IFN-β stimulation (Figure 36). IL-10 is an immunoregulatory cytokine that could drive disease progression by suppressing the immune response to infection. Notably, stimulation with IFN-α and IFN-β had little effect on most cytokines tested, whereas stimulation with Mtb WCL upregulated cytokine expression. These findings were in contrast to what we observed in ISG expression, whereby IFN-α and IFN-β upregulated ISG expression while Mtb WCL had little effect on most ISGs. Stimulation with IFN-α and IFN-β suppressed the expression of IL-1β, IL-6 and TNF-α in ATB, which would be detrimental. In contrast, stimulation with Mtb WCL upregulated the expression of these pro-inflammatory cytokines in ATB, which would be protective. The difference between groups was not significant except for IL-1β. Differences in cytokine expression were also observed between IFN-α and IFN-β stimulation. In agreement with our findings in the gene expression study, IFN-α/β may drive disease progression while Mtb WCL stimulation induces protective responses.

4.3 Differentially expressed genes show association with cytokine expression

The effects of type I IFNs in TB are partly related to their downstream effects on the production of other cytokines. These include their inhibition of pro-inflammatory cytokines such as IL-1, IL-12, TNF-α, and IFN-γ; and enhanced production of anti-inflammatory cytokines such as IL-10 that play a role in the aforementioned inhibition of pro-inflammatory cytokines. The association between the expression of ISGs and their downstream cytokine effects has, however, not been investigated in TB. For the first time, we assessed the association between ISG and cytokine responses to IFN-α, or IFN-β, or Mtb WCL stimulation in *M. tuberculosis* infection states.

Spearman's correlation analysis revealed that the expression of multiple ISGs correlated with chemokines that differed by stimulation conditions, with the majority of the ISG-chemokine correlation observed in ATB following IFN-α/β stimulation but in LTBI following Mtb WCL. Differences were also observed in the correlations identified with IFN-α and IFN-β. Following

IFN-α stimulation in ATB, the expression of ISGs correlated mainly with chemokines with fractalkine and MDC showing a negative correlation, whereas RANTES and IP-10 showed a positive correlation; following IFN-β stimulation in ATB, ISG expression showed a positive correlation with fractalkine; and following Mtb WCL stimulation in LTBI, ISG expression showed a positive correlation with fractalkine, RANTES, and IL-8. Chemokines are known for cell migration but also play a role in the differentiation and polarization of macrophages. For instance, in obesity, CCR5, the receptor for RANTES, has been shown to regulate macrophage polarization to an M2 phenotype similar to the *MSR1* gene, with which the cytokine showed a moderate positive correlation in LTBI following Mtb WCL stimulation (456,457,531). RANTES is chemotactic for and induces activation and proliferation of mononuclear cells such as T cells and macrophages, is involved in granuloma formation, and suppresses the intracellular growth of *M. tuberculosis* in macrophages (532). In our study following Mtb WCL stimulation, the *MSRI* gene was downregulated more in LTBI, suggesting polarization to the M1 phenotype in LTBI that is protective. At the same time, RANTES was upregulated in LTBI, suggesting an M2 phenotype. Given that the *MSR1* gene showed a positive correlation with RANTES following stimulation with Mtb WCL but appears to drive different macrophage phenotypes, the mechanism and outcome of this potential interaction in TB require further investigation.

IL-8, a neutrophil chemoattractant, showed a positive correlation with *SECTM1* gene expression, a gene that binds to neutrophils and induces the expression of MIP-2α/ CXCL2, a neutrophil chemoattractant of the IL-8/CXCL8 family (483,484,533). The expression of both IL-8 and *SECTM1* were higher in LTBI, which would increase the influx of neutrophils, cells that are a structural component of the granuloma. In addition, neutrophils are a source of CXCL10, a chemokine that showed a positive correlation with *SECTM1* gene expression in ATB.

Our findings show associations between ISG expression and cytokine expression. These associations between ISG expression and downstream cytokine production require further investigation to determine the role of specific ISGs in the cytokine response and whether the effects are protective or detrimental in TB.

4.4 Major findings

The research in this thesis examined the effects of type I IFN, IFN-α/β, and an *M. tuberculosis*-specific antigen, Mtb WCL, on the expression of ISGs and soluble immune responses in individuals who had ATB disease, LTBI as defined by the QFT test, TST-reactive but QFT negative, and in healthy controls. The major findings uncovered by this research are as follows:

4.4.1 IFN-α and IFN-β-driven ISGs and cytokine responses can distinguish clinical states of TB

Comparisons between ISG expression from the clinical groups identified three ISGs that differentiated LTBI from ATB following stimulation. These were the FCGR1A gene following IFN-α stimulation and the *FCGR1A*, *FCGR1B* and *SOCS3* genes following IFN-β stimulation (Figure 36). The *FCGR1A* and *FCGR1B* genes have been described as the most stable genes in transcriptional studies in TB with high expression in ATB, and our study identifies that both IFN-α and IFN-β can drive regulation of these genes (233,375,400,425,427–429,432,534). The expression of *SOCS3* has shown variation in TB studies, some show higher expression in ATB, while the gene has also been found downregulated in TB progressors, and our study identifies that IFN-β can drive regulation of this gene (535–537). IL-10 expression distinguished LTBI from ATB in cytokine analysis following both IFN-α and IFN-β stimulation. IL-10 as a biomarker to distinguish between LTBI and ATB has previously been demonstrated at baseline; our data identifies both IFN-α and IFN-β as drivers of this important immunomodulatory cytokine (538). Various factors may be responsible for the differences in the response patterns observed between LTBI and ATB. These could include differences between the clinical phenotypes in bacterial burden, IFNAR expression, and innate imprinting. ATB shows a higher bacterial load while bacterial load is not detectable in LTBI (539). The association of bacterial load with virulence suggests different mechanisms by which IFNs may act in *M. tuberculosis* infection. In vivo studies using ifnar$^{-/-}$ mice infected with *M. tuberculosis* show reduced bacterial burden and pathology (323,420,540,541). Hence, type I IFN signaling may be a factor in progression from LTBI to active TB. Elevated ISG expression have been detected up to 18 months prior to TB diagnosis and to differentiate LTBI from ATB (542). Given that the available IGRAs cannot distinguish ATB from LTBI, these and other IFN-α and IFN-β-driven ISGs and cytokines should be further assessed for TB diagnostics.

Differences have also been observed in other aspects of innate memory in LTBI and ATB. For instance, memory-like NK cells expansion is observed in individuals with LTBI but not in ATB (190,543,544). Antibodies from LTBI demonstrate a higher FCγRIII binding ability compared to ATB, leading to effector functions of macrophages and NK cells. This difference in binding affinity is related to unique Fab domain glycosylation patterns that differ between the two clinical phenotypes of infection (227,544).

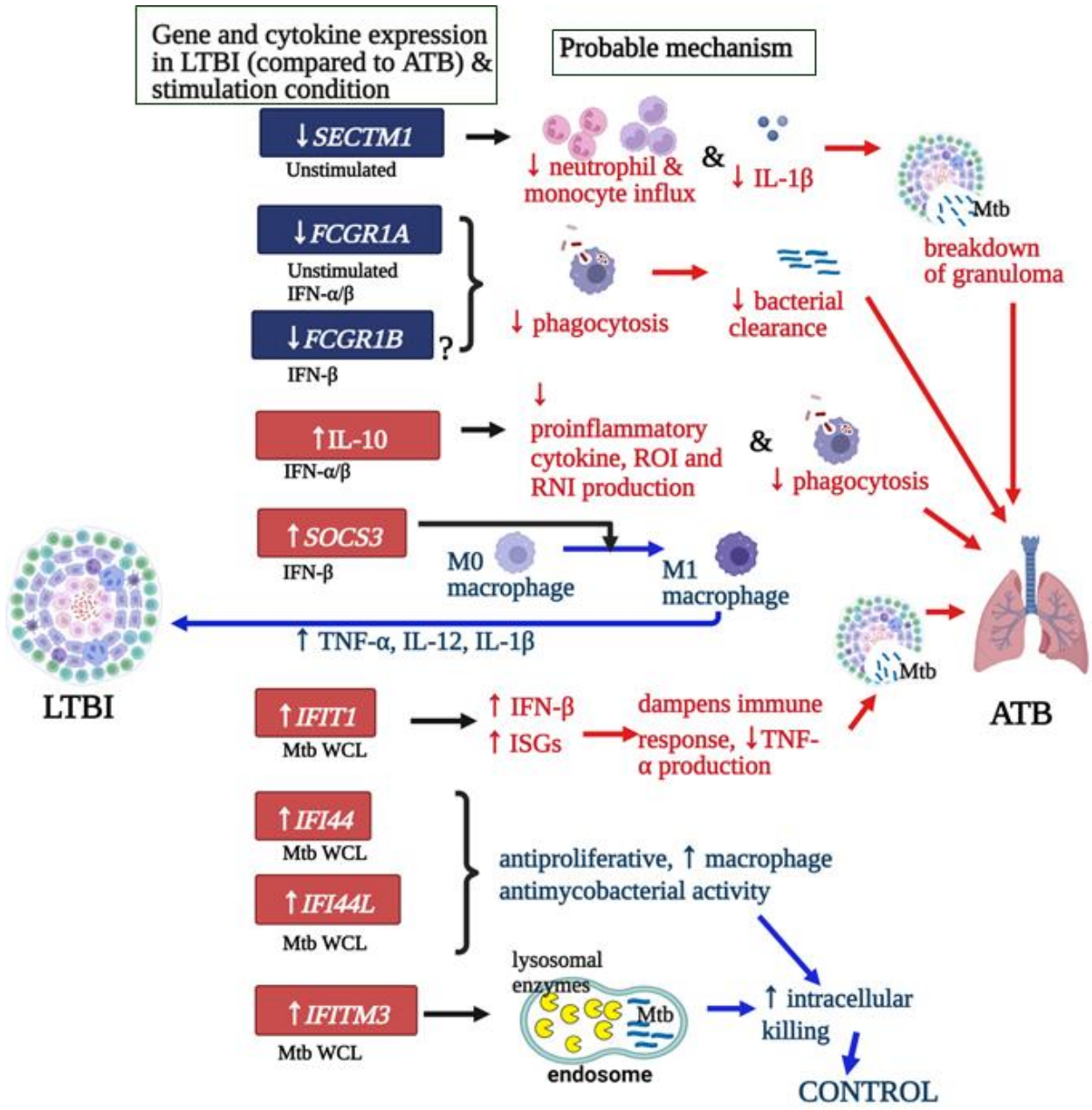

LEGEND

Mycobacterium tuberculosis	Cytokines	M0 macrophage
Tuberculous granuloma	Phagocytosis	M1 macrophage
Lysosomal enzymes	Monocyte	Neutrophil

Figure 36. Model of ISGs and cytokines that distinguish LTBI from ATB.

At baseline, lower *SECTM1* gene expression in LTBI suppresses CXCL2 expression which decreases neutrophil and monocyte influx to the infection site and reduces production of pro-inflammatory cytokines (IL-1β), leading to loss of infection control, breakdown of the granuloma and bacillary replication resulting in disease progression. Lower expression *FCGR1A* and *FCGR1B* genes in LTBI decreases antibody production leading to reduced opsonization of *M. tuberculosis* with subsequent reduction in phagocytosis and bacterial clearance resulting in disease progression. IFN-α or IFN-β stimulation reduces *FCGR1A* gene expression, and IFN-β stimulation reduces *FCGR1B* gene expression. This decreases antibody production leading to reduced opsonization of *M. tuberculosis* with subsequent reduction in phagocytosis and bacterial clearance resulting in disease progression. IFN-β stimulation increases *SOCS3* expression in LTBI that drives M1 macrophage phenotype producing pro-inflammatory cytokines and controlling infection. IFN-α and IFN-β stimulation increases IL-10 protein expression suppressing production of pro-inflammatory cytokines, inhibits phagocytosis, and inhibits ROI and RNI production, leading to disease progression. Mtb WCL stimulation increases *IFITM3* expression that induces acidification of the endosome leading to restricted bacillary growth and intracellular killing controlling or clearing infection. Increased *IFI44* and *IFI44L* induce an antiproliferative state inhibiting growth, and production of chemokines ad pro-inflammatory cytokines that increase intracellular killing leading to clearance or control of infection. Increased *IFIT1* inhibits production of pro-inflammatory cytokines leading to disease progression. *IFIT1* increases ISG production which may lead to either protection or disease progression depending on the ISG profile induced. (Blue boxes represent genes with lower expression in LTBI than in ATB, red boxes represent genes/ cytokines with higher expression in LTBI than in ATB, red arrows represent disease progression, blue arrows represent controlled infection; red font – mechanisms for disease progression, blue font – protective mechanisms). Created with BioRender.com

4.4.2 Expression of genes involved in macrophage polarization in TB

Three genes, *MSR1*, *SOCS3*, and *STAT1*, with a role in macrophage polarization, were also found to have the potential to differentiate between ATB and either LTBI or HC. *MSR1* shifts macrophage polarization from the M1 pro-inflammatory phenotype to the M2 anti-inflammatory phenotype resulting in a Th2 immune response that leads to disease progression that could explain the higher expression of this gene observed in ATB at baseline and after IFN-α stimulation (165). *SOCS3* and *STAT1* drive polarization to the M1 macrophage phenotype, which in early *M. tuberculosis* infection has a protective role by promoting the granuloma formation and enhancing the phagocytic and bactericidal functions of the granuloma resulting in bacterial elimination (Figure 36) (164,460,545,546). The expression of *SOCS3* and *STAT1* genes was higher in LTBI in response to IFN-β and Mtb WCL stimulation, respectively. IFN-α via MSR1 drives a detrimental M2 phenotype, whereas IFN-β via *SOCS3* and Mtb WCL via *STAT1* drive a protective M1

phenotype. This demonstrates divergent responses with direct implications on *M. tuberculosis* pathogenesis that have not previously been described particularly for the roles of IFN-α and IFN-β in TB pathogenesis.

4.4.3 IFN-α/β and Mtb WCL stimulate divergent immune responses

For the first time, the effects of IFN-α/β and Mtb WCL stimulation on ISGs and cytokines were compared. Differences were observed in immune responses induced in response to IFN-α/β and Mtb WCL with IFN-α/β upregulated expression of most ISGs, whereas Mtb WCL showed little effect for most ISGs. Differences were also observed in cytokine responses to IFN-α/β and Mtb WCL stimulation, with most of the cytokines showing little effect in response to IFN-α/β stimulation while Mtb WCL stimulation upregulated most cytokines. These findings suggest a polyfunctional immune response in which the kinetics and outcomes of the response are dependent on the stimulation. IFN-β via *SOCS3* (Figure 36) and Mtb WCL via *IFI44* and *IFI44L* drive a protective role, whereas IFN-α and IFN-β via *ANKRD22*, IFN-α via *IRF9* and *MSR1*, and Mtb WCL via *MSR1* drive disease progression. These findings demonstrate the effects of type I IFNs on ISGs not previously described in the pathogenesis of *M. tuberculosis*. These genes can be investigated further for therapeutic application, for instance, using clustered regularly interspaced short palindromic repeats (CRISPR) gene editing targeting specific genes for therapy.

4.4.4 IFN-α and IFN-β -induced responses show similarities and differences

Comparing IFN-α and IFN-β-induced responses in the LTBI and ATB groups revealed similar effects in the expression of most ISGs except for *BATF2*, *FCGR1A*, and *IFIT2* genes in LTBI, and *CCL8*, *FAM26F*, *IFIT1*, *IFIT2*, *IL-1A*, and *IL-1B* genes in ATB that showed differences in expression with higher expression following IFN-β stimulation compared to IFN-α. Similarly, we also observed differences in cytokine expression between IFN-α and IFN-β, most of which had higher expression following IFN-β stimulation, including IL-1RA, IP-10, MDC, and GRO in LTBI, and IL-1RA, IP-10, MDC, IL-8, and GRO in ATB. These findings may be related to the higher binding affinity and lower dissociation rate of IFN-β, leading to the larger effects on ISG expression, although the impact of higher ISG response following IFN-β stimulation versus with IFN-α stimulation is not clear. IFN-α/β have been used as therapeutic agents for viral infections such as viral hepatitis B and C and in cancers such as melanoma, in preventive therapy of viral infections such as herpes therapy, and are also under investigation for use as vaccine adjuvants

(547). However, their use was accompanied by adverse effects that included the reactivation of LTBI (548–551). Additional studies are needed to understand the effect of these unique ISG differences, the effect of the distinct type I IFNs on ISGs and their effect on the immune response to *M. tuberculosis* infection and whether the response is protective or detrimental in cases where IFN-α/β therapy is necessary, and to define which ISGs define successful therapy. This knowledge can be applied in the development of diagnostic tests and of host-directed therapy.

4.5 Conclusion

Type I IFNs play a role in TB that is not fully understood. Transcriptional profiling studies have shown a potential for using ISGs in TB diagnosis, identification of individuals at risk of disease progression, and treatment monitoring. Each stimulant used in this study appears to play a significant part in TB pathogenesis with distinct downstream effects that have not been previously elucidated. This thesis research found that PBMC stimulation with IFN-α or IFN-β drives ISG and cytokine responses that can distinguish LTBI and ATB (Figure 36). The results also showed that IFN-α drives a detrimental M2 phenotype through the *MSR1* gene while IFN-β or Mtb WCL drive a protective M1 phenotype through *SOCS3* and *STAT1* genes, respectively (Figure 36). The immune responses induced by IFN-α/β or Mtb WCL stimulation were divergent, with IFN-α/β largely showing upregulated ISGs and little effect on cytokines. In contrast, Mtb WCL showed little effect on ISGs but upregulated cytokines. IFN-α and IFN-β induced similar responses for most but not all ISGs, a difference that may affect their potential use as therapeutic agents. Therefore, the specific components of an ISGs profile may determine the outcome of *M. tuberculosis* infection.

The IFN signature has been under investigation by many researchers but is not well understood. Studying the individual ISGs may determine differences in their responses that can be used to better define the roles the ISGs play in different *M. tuberculosis* infection states. Knowledge of the specific roles can be used to identify possible therapeutic targets, improve the use of ISGs to discriminate between different infection states and identify individuals with LTBI at high risk of reactivation.

4.6 Study limitations

The assessment of the gene and cytokine responses in this thesis research was done in vitro, which is not an exact replication of what occurs in the human body. Furthermore, unlike in these experiments where each stimulation was acting independently, in the human body, autocrine production of IFNs may include the production of many subtypes of IFNs, leading to a response different from what we found in these experiments.

For the TST reactive group (remote TST-positive test but IGRA negative at recruitment), the TST results were accessed from records and not tested at the time of recruitment; this meant that the study participants in this group had previous exposure to TB or cross reactivity to the BCG vaccine. We could not confirm the participants' current TST status at the time of sample collection, which may have re-classified some of the participants. The TST group was considered to be closest to the HC, but the expression of some genes *IRF9* and *SECTM1* differed between the two groups suggesting there were differences between the two populations.

Differences may result from the nature of the samples used. Transcriptional profiling studies in TB have utilized PBMCs (352,377,385,400,552) or whole blood (189,233,355,356,375,398,399,401,537). A comparison of transcript expression between whole blood and PBMCs described larger expression differences for some of the genes in whole blood compared to PBMCs (435), differences that may be attributed to the contribution of cells, such as neutrophils, found in whole blood but that are removed in the isolation of PBMCs. Indeed, the transcriptional signature in TB has been shown to be driven primarily by neutrophils (189). We also did not control for differences in the monocyte/ lymphocyte ratio (MLR) in the PBMCs a ratio that have been shown to contribute to the transcriptional changes observed in disease, with genes associated with the MLR enriched for IFN signaling (553).

Other sources of differences in our findings could be population differences. Geographic location plays an important role because of the variation in microorganisms to which individuals are exposed. These include the microbiome that appears to relate to the susceptibility to and severity of the infection and correlates with host immune response and exposure to non-tuberculous mycobacteria in the environment (106,554–556). Demographic factors such as gender and ethnicity may also have played a role in our findings (106). More than half of our study

population (70.5%) was female, in contrast to what is observed globally. For example, in 2019, adult females made up only 32% of cases, while adult males made up 56% (71). The impact of sex hormones on the transcriptional profile in TB has not been studied, considering that sex hormones affect immune cells and modulate immune responses in tuberculosis. Given that progesterone increases the production of PGE2 while testosterone inhibits it and that this hormone has a role in the inhibition of type I IFN production (72), its potential effect on the expression of ISGs warrants more research. Ethnicity also influences the host immune responses (557). Interestingly, transcriptional signatures from areas with high TB endemicity show low sensitivity and specificity in regions of low endemicity (423,558). For this study, we could not control for these potential confounders.

Although we do not understand the potential impact of these limitations on our study results, we did identify differences in the expression of genes between clinical phenotypes. In the analysis of baseline gene expression, some of our findings were similar to those from previous studies regarding the identification of differentially expressed genes, while others showed similar trends but were not statistically significant. The differences in gene profiles identified in different studies

4.7 Future Directions

Based on the findings in this thesis, several experiments will be carried out in the future. We observed differentially expressed genes between the clinical phenotypes, including between HC and TST, that we expected to show similar responses. To validate our findings, transcriptional profiling will be carried out on whole blood and PBMCs from healthy controls (TST- and IGRA-negative), LTBI-1 (TST-positive and IGRA-negative at enrolment), LTBI-2 (TST-negative and IGRA-positive at enrolment), LTBI-3 (TST-positive IGRA-positive at enrolment), and ATB (culture-positive). The samples will be cultured with IFN-α/β and Mtb WCL with an unstimulated control for each sample. RNA Seq will be used for analysis of the samples to identify a wider range of transcripts. This will further delineate the transcriptional profiles and identify potential gene sets that can define the different groups in the spectrum of *M. tuberculosis* infection.

Three genes – *MSR1*, *SOCS3*, and *STAT1* – that were differentially expressed with the stimulation conditions have some interactions with macrophage polarization. The *MSR1* gene was differentially expressed at baseline and with both IFN-α and Mtb WCL, whereas the *SOCS3* gene was differentially expressed with IFN- β and *STAT1* with Mtb WCL. The *MSR1* gene drives an M2 macrophage phenotype, while *SOCS3* and *STAT1* drive an M1 phenotype. We hypothesize that in ATB, IFN-α suppresses MSR1 inhibiting M2 polarization, IFN-β suppresses *SOCS3* inhibiting M1 polarization, and Mtb WCL suppresses *STAT1* inhibiting M1 polarization and set out to investigate the effect of type I IFNs on macrophage polarization in TB. Briefly, PBMCs will be isolated from healthy donors' blood and monocytes will be extracted using the adherence method. Monocyte cultures will be set up with or without Mtb WCL and incubated for 6 hours, then washed and cultured with M-CSF ± IFN-α, -β, -γ or -all IFNs for 4 hours and 24 hours. After the 4-hour cell cultures, the cells will be washed, and the cell pellet will be used for gene expression assays and the supernatant for cytokine assays. The 24-hour cell cultures will also be used for gene expression and cytokine assays. In addition, the 24-hour cell cultures will be used for flow cytometry analysis for the detection of markers for monocyte lineage - CD68, M1 phenotype – CD80, M1-like cells – CD197, M2 phenotype – CD163, M2-like cells – CD206, and MSR1 – CD204. Optimization tests were completed for all steps. These functional studies were to be a major component of this thesis research; however, due to the lockdown imposed due to the COVID-19 pandemic and restricted access to the laboratory, the objective was put on hold. These experiments could also be carried out on PBMCs from individuals with ATB and LTBI with HCs as controls.

It is important to further characterize the effect of the stimulations with IFN-α, -β, -γ, and *M. tuberculosis*-specific antigens using platforms such as microarrays which allow for the study of a broader range of gene transcripts. Since neutrophils have been shown to drive the IFN transcriptional signature observed in TB (189), the effects of these stimulations should be assessed from whole blood and in individual cell populations to appreciate the main contributors to the type I IFN response at different stages of *M. tuberculosis* infection. For these experiments, stimulation with individual IFNs and IFN combinations can be used to investigate their effect on the immune responses since the individual IFNs do not act in isolation in the human body.

This research identified several potentially important ISGs not previously assessed for their role in TB pathogenesis. The functions of ISGs in TB have not been defined. These can be studied in knockout experiments using murine models of infection and may identify potential therapeutic targets against TB. The *SECTM1* gene distinguished between HC and ATB or LTBI at baseline and following Mtb WCL stimulation, respectively. In pneumococcal pneumonia, the expression of the *SECTM1* gene is associated with neutrophil influx, a relation that has not been studied in TB (483,484,559,560). The effect of the *SECTM1* gene in TB can be studied using SECTM1 knockout (KO) mice infected with *M. tuberculosis* with healthy mice as controls. The lungs can be assessed for infection using microscopy, and neutrophil accumulation in the lungs determined using flow cytometry and compared between infected SECTM1 KO mice, uninfected SECTM1 KO mice, and infected and uninfected wild-type mice. Similar studies can also be applied to the functional analysis studies for other ISGs to define their roles in *M. tuberculosis* infection states, in LTBI and in ATB.

Although this study provides pilot data, future studies can utilize replication studies. In replication studies, the research study is repeated using a different set of study participants to assess whether study findings are applicable in a different population, in larger sample sizes, or in a meta-analysis. In addition, research can be extended to cover different geographical regions, especially TB-endemic countries and cohorts from different ethnicities. Finally, there is also a need to study the effect of different *M. tuberculosis* strains on the transcriptional profile and how these effects relate to the immune response. These studies will build on the current knowledge of the immune response to TB.

The interplay between cells in the respiratory tract also requires further research. For instance, whether type I IFNs act on AECs to affect other immune responses in the lung microenvironment in *M. tuberculosis* infection and the role in determining infection outcome (176). This can be studied using M. tuberculosis-infected AECs co-cultured with macrophages or DCs in the presence or absence of type I IFNs with mechanistic assessment of the infection pathway and transcriptional profiling of responses from the co-cultures. These experiments would better define the role of AECs in TB pathogenesis.

Future studies should aim to assess molecular profiles for stratification of subgroups of infection which would identify the role of specific pathways in different phases of the infection

spectrum. The understanding of these mechanisms at different stages of infection feeds into our knowledge of the immune response to *M. tuberculosis* infection but also to the pharmacological interventions leading to development of specific targeted therapies.

CHAPTER 5: REFERENCES

1. World Health Organization. Global Tuberculosis Report 2021. 2021.
2. Lafreniere M, Hussain H, He N, Mcguire M. Tuberculosis in Canada: 2017. Canada Commun Dis Rep. 2019;45(3):68–74.
3. World Health Organization. The End TB Strategy [Internet]. World Health Organization. 2015. Available from: https://www.who.int/tb/End_TB_brochure.pdf
4. Salgame P, Geadas C, Collins L, Jones-Lopez E, Ellner JJ. Latent tuberculosis infection - Revisiting and revising concepts. Tuberculosis. 2015;95:373–84.
5. O'Garra A, Redford PS, McNab FW, Bloom CI, Wilkinson RJ, Berry MPR. The Immune Response in Tuberculosis. Annu Rev Immunol. 2013;31(1):475–527.
6. Barry CE, Boshoff HI, Dartois V, Dick T, Ehrt S, Flynn JA, et al. The spectrum of latent tuberculosis: Rethinking the biology and intervention strategies. Nat Rev Microbiol. 2009;7(12):845–55.
7. Cadena AM, Fortune SM, Flynn JL. Heterogeneity in tuberculosis. Nat Rev Immunol. 2017;17(11):691–702.
8. Churchyard GJ, Swindells S. Controlling latent TB tuberculosis infection in high-burden countries: A neglected strategy to end TB. PLoS Med. 2019;16(4):e1002787.
9. Uplekar M, Weil D, Lonnroth K, Jaramillo E, Lienhardt C, Dias HM, et al. WHO's new end TB strategy. Lancet. 2015;385(9979):1799–801.
10. World Health Organization. The END TB Strategy: global strategy and targets for tuberculosis prevention, care and control after 2015 [Internet]. World Health Organization. 2014 [cited 2020 Sep 7]. Available from: https://www.who.int/tb/strategy/End_TB_Strategy.pdf
11. Houben RMGJ, Dodd PJ. The Global Burden of Latent Tuberculosis Infection: A Re-estimation Using Mathematical Modelling. PLoS Med. 2016;13(10):1–13.
12. Cohen A, Mathiasen VD, Schön T, Wejse C. The global prevalence of latent tuberculosis: A systematic review and meta-analysis. Eur Respir J. 2019;54(3):1900655.
13. Millet JP, Moreno A, Fina L, Baño L Del, Orcau A, De Olalla PG, et al. Factors that influence current tuberculosis epidemiology. Eur Spine J. 2013;22(Suppl.4):S539–48.
14. Narasimhan P, Wood J, MacIntyre CR, Mathai D. Risk factors for tuberculosis. Pulm Med. 2013;2013:Article ID 828939.
15. Hick S. The Enduring Plague: How Tuberculosis in Canadian Indigenous Communities is Emblematic of a Greater Failure in Healthcare Equality. J Epidemiol Glob Health. 2019;9(2):89–92.
16. Courtwright A, Turner AN. Tuberculosis and Stigmatization: Pathways and Interventions. Public Health Rep. 2010;125(Suppl 4):34–42.

17. Craig GM, Daftary A, Engel N, O'driscoll S, Ioannaki A. Tuberculosis stigma as a social determinant of health: a systematic mapping review of research in low incidence countries. Int J Infect Dis. 2017;56:90–100.

18. Fitzgerald DW, Sterling TR, Haas DW. 249 - Mycobacterium tuberculosis. In: Mandell, Douglas, and Bennett's Principles and Practice of Infectious Diseases. Ninth Edit. Elsevier Inc.; 2020. p. 2985-3021.e7.

19. Malone KM, Gordon S V. Mycobacterium tuberculosis complex members adapted to wild and domestic animals. In: Advances in Experimental Medicine and Biology. Springer New York LLC; 2017. p. 135–54.

20. Brodin P, Eiglmeier K, Marmiesse M, Billault A, Garnier T, Niemann S, et al. Bacterial artificial chromosome-based comparative genomic analysis identifies Mycobacterium microti as a natural ESAT-6 deletion mutant. Infect Immun. 2002;70(10):5568–78.

21. Cousins D V., Bastida R, Cataldi A, Quse V, Redrobe S, Dow S, et al. Tuberculosis in seals caused by a novel member of the Mycobacterium tuberculosis complex: Mycobacterium pinnipedii sp. nov. Int J Syst Evol Microbiol. 2003;53(5):1305–14.

22. Tientcheu LD, Koch A, Ndengane M, Andoseh G, Kampmann B, Wilkinson RJ. Immunological consequences of strain variation within the Mycobacterium tuberculosis complex. Eur J Immunol. 2017;47(3):432–45.

23. Forrellad MA, Klepp LI, Gioffré A, García JS, Morbidoni HR, de la Paz Santangelo M, et al. Virulence factors of the Mycobacterium tuberculosis complex. Virulence. 2013;4(1):3–66.

24. de Jong BC, Antonio M, Gagneux S. Mycobacterium africanum-review of an important cause of human tuberculosis in West Africa. PLoS Negl Trop Dis. 2010;4(9):e744.

25. Brites D, Gagneux S. The Nature and Evolution of Genomic Diversity in the Mycobacterium tuberculosis Complex. In: Advances in Experimental Medicine and Biology. 2017. p. 1–25.

26. Manca C, Tsenova L, Bergtold A, Freeman S, Tovey M, Musser JM, et al. Virulence of a Mycobacterium tuberculosis clinical isolate in mice is determined by failure to induce Th1 type immunity and is associated with induction of IFN-α/β. PNAS. 2001;98(10):5752–5257.

27. Tsenova L, Ellison E, Harbacheuski R, Moreira AL, Kurepina N, Reed MB, et al. Virulence of selected Mycobacterium tuberculosis clinical isolates in the rabbit model of meningitis is dependent on phenolic glycolipid produced by the bacilli. J Infect Dis. 2005;192(1):98–106.

28. Moopanar K, Mvubu NE. Lineage-specific differences in lipid metabolism and its impact on clinical strains of Mycobacterium tuberculosis. Microb Pathog. 2020;146:104250.

29. Sarkar R, Lenders L, Wilkinson KA, Wilkinson RJ, Nicol MP. Modern Lineages of Mycobacterium tuberculosis Exhibit Lineage-Specific Patterns of Growth and Cytokine Induction in Human Monocyte-Derived Macrophages. Neyrolles O, editor. PLoS One. 2012;7(8):e43170.

30. Coscolla M, Gagneux S. Consequences of genomic diversity in mycobacterium tuberculosis. Semin Immunol. 2014;26(6):431–44.

31. Ribeiro SCM, Gomes LL, Amaral EP, Andrade MRM, Almeida FM, Rezende AL, et al. Mycobacterium tuberculosis strains of the modern sublineage of the beijing family are more likely to display increased virulence than strains of the ancient sublineage. J Clin Microbiol. 2014;52(7):2615–24.

32. Portevin D, Gagneux S, Comas I, Young D. Human macrophage responses to clinical isolates from the Mycobacterium tuberculosis complex discriminate between ancient and modern lineages. PLoS Pathog. 2011;7(3):e1001307.

33. Manca C, Tsenova L, Freeman S, Barczak AK, Tovey M, Murray PJ, et al. Hypervirulent M. tuberculosis W/Beijing Strains Upregulate Type I IFNs and Increase Expression of Negative Regulators of the Jak-Stat Pathway. J Interf Cytokine Res. 2005;25(11):694–701.

34. Gagneux S. Ecology and evolution of Mycobacterium tuberculosis. Nat Rev Microbiol. 2018;16:202–13.

35. Ngabonziza JCS, Loiseau C, Marceau M, Jouet A, Menardo F, Tzfadia O, et al. A sister lineage of the Mycobacterium tuberculosis complex discovered in the African Great Lakes region. Nat Commun. 2020;11(1):2917.

36. Brites D, Gagneux S. Co-evolution of Mycobacterium tuberculosis and Homo sapiens. Immunol Rev. 2015;264(1):6–24.

37. Cole ST, Brosch R, Parkhill J, Garnier T, Churcher C, Harris D, et al. Deciphering the biology of mycobacterium tuberculosis from the complete genome sequence. Nature. 1998;393(6685):537–44.

38. Behr MA, Wilson MA, Gill WP, Salamon H, Schoolnik GK, Rane S, et al. Comparative genomics of BCG vaccines by whole-genome DNA microarray. Science (80-). 1999;284(5419):1520–3.

39. Samten B, Wang X, Barnes PF. Immune regulatory activities of early secreted antigenic target of 6-kD protein of Mycobacterium tuberculosis and implications for tuberculosis vaccine design. Tuberculosis. 2011;91:S114–8.

40. Wong K-W. The Role of ESX-1 in Mycobacterium tuberculosis Pathogenesis. In: Microbiology Spectrum. 2017. p. 627–34.

41. Simeone R, Brosch R, Bobard A, Lippmann J, Bitter W, Enninga J, et al. Phagosomal Rupture by Mycobacterium tuberculosis Results in Toxicity and Host Cell Death. PLoS Pathog. 2012;8(2):e1002507.

42. Houben D, Demangel C, van Ingen J, Perez J, Baldeón L, Abdallah AM, et al. ESX-1-mediated translocation to the cytosol controls virulence of mycobacteria. Cell Microbiol. 2012;14(8):1287–98.

43. van der Wel N, Hava D, Houben D, Fluitsma D, van Zon M, Pierson J, et al. M. tuberculosis and M. leprae Translocate from the Phagolysosome to the Cytosol in Myeloid

Cells. Cell. 2007;129(7):1287–98.

44. Welin A, Björnsdottir H, Winther M, Christenson K, Oprea T, Karlsson A, et al. CFP-10 from Mycobacterium tuberculosis selectively activates human neutrophils through a pertussis toxin-sensitive chemotactic receptor. Infect Immun. 2015;83(1):205–13.

45. Coppola M, Ottenhoff TH. Genome wide approaches discover novel Mycobacterium tuberculosis antigens as correlates of infection, disease, immunity and targets for vaccination. Semin Immunol. 2018;39:88–101.

46. Babaki MKZ, Soleimanpour S, Rezaee SA. Antigen 85 complex as a powerful Mycobacterium tuberculosis immunogene: Biology, immune-pathogenicity, applications in diagnosis, and vaccine design. Microb Pathog. 2017;112:20–9.

47. Rosser A, Stover C, Pareek M, Mukamolova G V. Resuscitation-promoting factors are important determinants of the pathophysiology in Mycobacterium tuberculosis infection. Crit Rev Immunol. 2017;43(5):621–30.

48. Churchyard G, Kim P, Shah N, Rustomjee R, Gandhi N, Mathema B, et al. What We Know About Tuberculosis Transmission: An Overview. J Infect Dis. 2017;216(Suppl 6):S629–35.

49. Patterson B, Wood R. Is cough really necessary for TB transmission? Tuberculosis. 2019;117:31–5.

50. Stetzenbach LD, Buttner MP, Cruz P. Detection and enumeration of airborne biocontaminants. Curr Opin Biotechnol. 2004;15:170–4.

51. Diel R, Nienhaus A, Witte P, Ziegler R. Protection of healthcare workers against transmission of Mycobacterium tuberculosis in hospitals: a review of the evidence. ERJ Open Res. 2020;6(1):00317–2019.

52. Fox GJ, Barry SE, Britton WJ, Marks GB. Contact investigation for tuberculosis: A systematic review and meta-analysis. Eur Respir J. 2013;41(1):140–56.

53. Acuña-Villaorduña C, Jones-López EC, Fregona G, Marques-Rodrigues P, Gaeddert M, Geadas C, et al. Intensity of exposure to pulmonary tuberculosis determines risk of tuberculosis infection and disease. Eur Respir J. 2018;51(1):1701578.

54. Winthrop KL. Risk and prevention of tuberculosis and other serious opportunistic infections associated with the inhibition of tumor necrosis factor. Nat Clin Pract Rheumatol. 2006;2(11):602–10.

55. Torres-Castiblanco JL, Carrillo JA, Hincapié-Urrego D, Rojas-Villarraga A. Tuberculosis in the era of anti-TNF-alpha therapy: Why does the risk still exist? Biomedica. 2018;38(1):17–26.

56. Corbett EL, Watt CJ, Walker N, Maher D, Williams BG, Raviglione MC, et al. The Growing Burden of Tuberculosis. Arch Intern Med. 2003;163(9):1009–21.

57. Al-Rifai RH, Pearson F, Critchley JA, Abu-Raddad LJ. Association between diabetes mellitus and active tuberculosis: A systematic review and meta-analysis. PLoS One.

2017;12(11):e0187967.

58. Hensel R, Kempker R, Tapia J, Oladele A, Blumberg H, Magee M. Increased risk of latent tuberculosis infection among persons with pre-diabetes and diabetes mellitus. Int J Tuberc Lung Dis. 2016;20(1):71–8.

59. Lee M-R, Huang Y-P, Kuo Y-T, Luo C-H, Shih Y-J, Shu C-C, et al. Diabetes Mellitus and Latent Tuberculosis Infection: A Systemic Review and Metaanalysis. Clin Infect Dis. 2017;64(6):719–27.

60. Martinez L, Zhu L, Castellanos ME, Liu Q, Chen C, Hallowell BD, et al. Glycemic Control and the Prevalence of Tuberculosis Infection: A Population-based Observational Study. Clin Infect Dis. 2017;65(12):2060–8.

61. Cegielski JP, McMurray DN. The relationship between malnutrition and tuberculosis: Evidence from studies in humans and experimental animals. Int J Tuberc Lung Dis. 2004;8(3):286–98.

62. Chandrasekaran P, Saravanan N, Bethunaickan R, Tripathy S. Malnutrition: Modulator of immune responses in tuberculosis. Front Immunol. 2017;8:1316.

63. Kant S, Gupta H, Ahluwalia S. Significance of Nutrition in Pulmonary Tuberculosis. Crit Rev Food Sci Nutr. 2015;55(7):955–63.

64. Zhang Z, Fan W, Yang G, Xu Z, Wang J, Cheng Q, et al. Risk of tuberculosis in patients treated with TNF-α antagonists: A systematic review and meta-analysis of randomised controlled trials. BMJ Open. 2017;7(3):12567.

65. Yorke E, Atiase Y, Akpalu J, Sarfo-Kantanka O, Boima V, Dey ID. The Bidirectional Relationship between Tuberculosis and Diabetes. Tuberc Res Treat. 2017;2017:1–6.

66. Lin HH, Wu CY, Wang CH, Fu H, Lönnroth K, Chang YC, et al. Association of obesity, diabetes, and risk of tuberculosis: Two population-based cohorts. Clin Infect Dis. 2018;66(5):699–705.

67. Yen YF, Yen MY, Lin YS, Lin YP, Shih HC, Li LH, et al. Smoking increases risk of recurrence after successful anti-tuberculosis treatment: A population-based study. Int J Tuberc Lung Dis. 2014;18(4):492–8.

68. Mahishale V, Patil B, Lolly M, Eti A, Khan S. Prevalence of Smoking and Its Impact on Treatment Outcomes in Newly Diagnosed Pulmonary Tuberculosis Patients: A Hospital-Based Prospective Study. Chonnam Med J. 2015;51(2):86–90.

69. Lönnroth K, Williams BG, Stadlin S, Jaramillo E, Dye C. Alcohol use as a risk factor for tuberculosis - a systematic review. BMC Public Health. 2008;8:289.

70. Crews FT, Bechara R, Brown LA, Guidot DM, Mandrekar P, Oak S, et al. Cytokines and alcohol. In: Alcoholism: Clinical and Experimental Research. John Wiley & Sons, Ltd; 2006. p. 720–30.

71. World Health Organization. Global tuberculosis report 2020. World Health Organization. 2020.

72. Nhamoyebonde S, Leslie A. Biological differences between the sexes and susceptibility to tuberculosis. J Infect Dis. 2014;209(Suppl. 3):S100–6.

73. Meyer CG, Thye T. Host genetic studies in adult pulmonary tuberculosis. Semin Immunol. 2014;26(6):445–53.

74. Greenwood CMT, Fujiwara TM, Boothroyd LJ, Miller MA, Frappier D, Fanning EA, et al. Linkage of Tuberculosis to Chromosome 2q35 Loci, Including NRAMP1, in a Large Aboriginal Canadian Family. Am J Hum Genet. 2000;67:405–16.

75. Yanlin L, Tao Y, Weiping L, Ming C, Xiaoxing C, Shaoli D. Association of tuberculosis and polymorphisms in the promoter region of macrophage migration inhibitory factor (MIF) in a Southwestern China Han population. Cytokine. 2012;60:64–7.

76. Thye T, Niemann S, Walter K, Homolka S, Intemann CD, Chinbuah MA, et al. Variant G57E of Mannose Binding Lectin associated with protection against tuberculosis caused by mycobacterium africanum but not by M. tuberculosis. PLoS One. 2011;6(6):e20908.

77. Cormier M, Schwartzman K, N'Diaye DS, Boone CE, dos Santos AM, Gaspar J, et al. Proximate determinants of tuberculosis in Indigenous peoples worldwide: a systematic review. Lancet Glob Heal. 2019;7(1):e68–80.

78. Devi Kanabalan R, Jie Lee L, Yan Lee T, Pei Chong P, Hassan L, Ismail R, et al. Human tuberculosis and Mycobacterium tuberculosis complex: A review on genetic diversity, pathogenesis and omics approaches in host biomarkers discovery. Sci Technol. 2021;246:126674.

79. Kumar A, Farhana A, Guidry L, Saini V, Hondalus M, Steyn AJC. Redox homeostasis in mycobacteria: the key to tuberculosis control? Expert Rev Mol Med. 2011;13:e39.

80. Parvaresh L, Crighton T, Martinez E, Bustamante A, Chen S, Sintchenko V. Recurrence of tuberculosis in a low-incidence setting: A retrospective cross-sectional study augmented by whole genome sequencing. BMC Infect Dis. 2018;18(1):1–6.

81. Dobler CC, Crawford ABH, Jelfs PJ, Gilbert GL, Marks GB. Recurrence of tuberculosis in a low-incidence setting. Eur Respir J. 2009;33(1):160–7.

82. Karakousis PC, Dutta NK, Manabe YC. Clinical features and diagnosis of tuberculosis: Primary infection and progressive pulmonary tuberculosis. In: Handbook of Tuberculosis. Springer International Publishing; 2017. p. 17–34.

83. Selwyn PA, Hartel D, Lewis VA, Schoenbaum EE, Vermund SH, Klein RS, et al. A Prospective Study of the Risk of Tuberculosis among Intravenous Drug Users with Human Immunodeficiency Virus Infection. N Engl J Med. 1989;320(9):545–50.

84. Ai JW, Ruan QL, Liu QH, Zhang WH. Updates on the risk factors for latent tuberculosis reactivation and their managements. Emerg Microbes Infect. 2016;5(2):e10.

85. World Health Organization. International Standards for Tuberculosis Care. Vol. 3rd editio. 2014.

86. Pai M, Denkinger CM, Kik S V., Rangaka MX, Zwerling A, Oxlade O, et al. Gamma

Interferon Release Assays for Detection of Mycobacterium tuberculosis Infection. Clin Microbiol Rev. 2014;27(1):3–20.

87. Centers for Disease Control and Prevention. Updated Guidelines for Using Interferon Gamma Release Assays to Detect Mycobacterium tuberculosis Infection-United States, 2010. Morb Mortal Wkly Rep. 2010;59(RR-5).

88. Nayak S, Acharjya B. Mantoux test and its interpretation. Indian Dermatol Online J. 2012;3(1):2.

89. Pai M, Kunimoto D, Jamieson F, Menzies D. Diagnosis of latent tuberculosis infection. In: Canadian Tuberculosis Standard, 7th edition. 2014.

90. Lawn SD. Advances in diagnostic assays for tuberculosis. Cold Spring Harb Perspect Med. 2015;5(12):a017806.

91. Yamasue M, Komiya K, Usagawa Y, Umeki K, Nureki S ichi, Ando M, et al. Factors associated with false negative interferon-γ release assay results in patients with tuberculosis: A systematic review with meta-analysis. Sci Rep. 2020;10:1607.

92. Nguyen DT, Teeter LD, Graves J, Graviss EA. Characteristics associated with negative interferon-γ release assay results in culture-confirmed tuberculosis patients, Texas, USA, 2013–2015. Emerg Infect Dis. 2018;24(3):534–40.

93. Liao C, Lai C, Tan C, Chou C, Hsu H, Tasi T, et al. False-negative results by enzyme-linked immunospot assay for interferon-gamma; among patients with culture-confirmed tuberculosis. J Infect. 2009;59:421–5.

94. Kobashi Y, Mouri K, Obase Y, Fukuda M, Miyashita N, Oka M. Clinical evaluation of QuantiFERON TB-2G test for immunocompromised patients. Eur Respir J. 2007;30(5):945–50.

95. Mancuso J, Bernardo J, Mazurek GH. The Elusive “Gold” Standard for Detecting Mycobacterium tuberculosis Infection. Am J Respir Crit Care Med. 2013;187(2):122–4.

96. Palomino JC. Nonconventional and new methods in the diagnosis of tuberculosis: Feasibility and applicability in the field. Eur Respir J. 2005;26(2):339–50.

97. Steingart KR, Henry M, Ng V, Hopewell PC, Ramsay A, Cunningham J, et al. Fluorescence versus conventional sputum smear microscopy for tuberculosis: a systematic review. Lancet Infect Dis. 2006;6(9):570–81.

98. World Health Organization. Fluorescent light-emitting diode (LED) microscopy for diagnosis of tuberculosis: Policy statement [Internet]. 2011 [cited 2020 Aug 3]. Available from: http://www.who.int/about/licensing/copyright_form/en/index.html

99. Lewinsohn DM, Leonard MK, Lobue PA, Cohn DL, Daley CL, Desmond E, et al. Official American Thoracic Society/Infectious Diseases Society of America/Centers for Disease Control and Prevention Clinical Practice Guidelines: Diagnosis of Tuberculosis in Adults and Children. Clin Infect Dis. 2017;64(2):e1–33.

100. Kirwan DE, Ugarte-Gil C, Gilman RH, Caviedes L, Rizvi H, Ticona E, et al. Microscopic

Observation Drug Susceptibility Assay for Rapid Diagnosis of Lymph Node Tuberculosis and Detection of Drug Resistance. J Clin Microbiol. 2015;54(1):185–9.

101. World Health Organization. Molecular line probe assays for rapid screening of patients at risk of multidrug-resistant tuberculosis (MDR-TB). 2008.

102. World Health Organization. Policy statement: Automated Real-time Nucleic Acid Amplification Technology for Rapid and Simultaneous Detection of Tuberculosis and Rifampicin Resistance: Xpert MTB/RIF System [Internet]. 2011 [cited 2020 Sep 7]. Available from: www.who.int

103. World Health Organization. WHO Meeting Report of a Technical Expert Consultation: Non-inferiority analysis of Xpert MTB/RIF Ultra compared to Xpert MTB/RIF [Internet]. 2017 [cited 2021 Feb 23]. Available from: http://apps.who.int/bookorders.

104. Lewinsohn DM, Leonard MK, LoBue PA, Cohn DL, Daley CL, Desmond E, et al. Official American Thoracic Society / Infectious Diseases Society of America / Centers for Disease Control and Prevention Clinical Practice Guidelines : Diagnosis of Tuberculosis in Adults and Children. Clin Infect Dis. 2016;00(0):1–33.

105. MacLean E, Kohli M, Weber SF, Suresh A, Schumacher SG, Denkinger CM, et al. Advances in molecular diagnosis of tuberculosis. J Clin Microbiol. 2020;58(10):e01582-19.

106. Burel JG, Babor M, Pomaznoy M, Lindestam Arlehamn CS, Khan N, Sette A, et al. Host transcriptomics as a tool to identify diagnostic and mechanistic immune signatures of tuberculosis. Front Immunol. 2019;10:Article 221.

107. Hopewell PC, Pai M, Maher D, Uplekar M, Raviglione MC. International Standards for Tuberculosis Care. Lancet Infect Dis. 2006;6(11):710–25.

108. Harries A, Kumar A. Challenges and Progress with Diagnosing Pulmonary Tuberculosis in Low- and Middle-Income Countries. Diagnostics. 2018;8(4):78.

109. Tiemersma EW, van der Werf MJ, Borgdorff MW, Williams BG, Nagelkerke NJD. Natural history of tuberculosis: Duration and fatality of untreated pulmonary tuberculosis in HIV negative patients: A systematic review. PLoS One. 2011;6(4):e17601.

110. World Health Organization. WHO consolidated guidelines on tuberculosis. Module 1, Prevention : tuberculosis preventive treatment. 2020.

111. Public Health Agency of Canada. Tuberculosis prevention and control in Canada: A federal framework for action. 2014.

112. World Health Organization. Early detection of Tuberculosis: An overview of approaches, guidelines and tools. World Health Organization; 2011.

113. World Health Organization. WHO consolidated guidelines on tuberculosis: module 4: treatment: drug-resistant tuberculosis treatment. 2020.

114. World Health Organization. Companion handbook to the WHO guidelines for the programmatic management of drug-resistant tuberculosis. 2014.

115. Laurence Y V., Griffiths UK, Vassall A. Costs to Health Services and the Patient of Treating Tuberculosis: A Systematic Literature Review. Pharmacoeconomics. 2015;33(9):939–55.

116. Viney K, Linh NN, Gegia M, Zignol M, Glaziou P, Ismail N, et al. New definitions of pre-extensively and extensively drug-resistant tuberculosis: update from the World Health Organization. Eur Respir J. 2021;57:2100361.

117. Mirzayev F, Viney K, Linh NN, Gonzalez-Angulo L, Gegia M, Jaramillo E, et al. World Health Organization recommendations on the treatment of drug-resistant tuberculosis, 2020 update. Eur Respir J. 2021;57(6):2003300.

118. Hatherill M. Prospects for elimination of childhood tuberculosis: The role of new vaccines. Arch Dis Child. 2011;96(9):851–6.

119. Narayanan PR. Fifteen year follow up of trial of BCG vaccines in south India for tuberculosis prevention. Indian J Med Res. 1999;110:56–69.

120. de Gijsel D, von Reyn CF. A Breath of Fresh Air: BCG Prevents Adult Pulmonary Tuberculosis. Int J Infect Dis. 2019;80:S6–8.

121. Sable SB, Posey JE, Scriba TJ. Tuberculosis Vaccine Development: Progress in Clinical Evaluation. Clin Microbiol Rev. 2019;33(1):e00100-19.

122. Li J, Zhao A, Tang J, Wang G, Shi Y, Zhan L, et al. Tuberculosis vaccine development: from classic to clinical candidates. Eur J Clin Microbiol Infect Dis. 2020;39(8):1405–25.

123. Whitlow E, Mustafa AS, Hanif SNM. An Overview of the Development of New Vaccines for Tuberculosis. Vaccines. 2020;8:586.

124. Martin C, Aguilo N, Marinova D, Gonzalo-Asensio J. Update on TB vaccine pipeline. Appl Sci. 2020;10(7):2632.

125. Scriba TJ, Kaufmann SHE, Lambert PH, Sanicas M, Martin C, Neyrolles O. Vaccination against tuberculosis with whole-cell mycobacterial vaccines. J Infect Dis. 2016;214(5):659–64.

126. Bhatt K, Verma S, Ellner JJ, Salgame P. Quest for correlates of protection against tuberculosis. Clin Vaccine Immunol. 2015;22(3):258–66.

127. Hmama Z, Peña-Díaz S, Joseph S, Av-Gay Y. Immunoevasion and immunosuppression of the macrophage by Mycobacterium tuberculosis. Immunol Rev. 2015;264(1):220–32.

128. Hossain MM, Norazmi MN. Pattern recognition receptors and cytokines in Mycobacterium tuberculosis infection - The double-edged sword? Biomed Res Int. 2013;2013:179174.

129. Schlesinger LS. Macrophage phagocytosis of virulent but not attenuated strains of Mycobacterium tuberculosis is mediated by mannose receptors in addition to complement receptors. J Immunol. 1993;150(7):2920–30.

130. Rajaram MVS, Arnett E, Azad AK, Guirado E, Ni B, Gerberick AD, et al. M. tuberculosis-Initiated Human Mannose Receptor Signaling Regulates Macrophage

Recognition and Vesicle Trafficking by FcRγ-Chain, Grb2, and SHP-1. Cell Rep. 2017;21(1):126–40.

131. Kang PB, Azad AK, Torrelles JB, Kaufman TM, Beharka A, Tibesar E, et al. The human macrophage mannose receptor directs Mycobacterium tuberculosis lipoarabinomannan-mediated phagosome biogenesis. J Exp Med. 2005;202(7):987–99.

132. Zimmerli S, Edwards S, Ernst JD. Selective Receptor Blockade during Phagocytosis Does Not Alter the Survival and Growth of Mycobacterium tuberculosis in Human Macrophages. Am J Respir Cell Mol Biol. 1996;15(6):760–70.

133. Kleinnijenhuis J, Oosting M, Joosten LAB, Netea MG, Van Crevel R. Innate immune recognition of mycobacterium tuberculosis. Clin Dev Immunol. 2011;2011:405310.

134. Faridgohar M, Nikoueinejad H. New findings of Toll-like receptors involved in Mycobacterium tuberculosis infection. Pathog Glob Health. 2017;111(5):256–64.

135. Mortaz E, Adcock IM, Tabarsi P, Masjedi MR, Mansouri D, Velayati AA, et al. Interaction of Pattern Recognition Receptors with Mycobacterium Tuberculosis. J Clin Immunol. 2015;35(1):1–10.

136. Mortaz E. Role of pattern recognition receptors in Mycobacterium tuberculosis infection. Int J Mycobacteriology. 2015;4:66.

137. Jo EK, Yang CS, Choi CH, Harding C V. Intracellular signalling cascades regulating innate immune responses to Mycobacteria: Branching out from Toll-like receptors. Cell Microbiol. 2007;9(5):1087–98.

138. Mishra A, Akhtar S, Jagannath C, Khan A. Pattern recognition receptors and coordinated cellular pathways involved in tuberculosis immunopathogenesis: Emerging concepts and perspectives. Mol Immunol. 2017;87:240–8.

139. Stamm CE, Collins AC, Shiloh MU. Sensing of Mycobacterium tuberculosis and consequences to both host and bacillus. Immunol Rev. 2015;264(1):204–19.

140. Ishikawa E, Ishikawa T, Morita YS, Toyonaga K, Yamada H, Takeuchi O, et al. Direct recognition of the mycobacterial glycolipid, trehalose dimycolate, by C-type lectin Mincle. J Exp Med. 2009;206(13):2879–88.

141. Wagener M, Hoving JC, Ndlovu H, Marakalala MJ. Dectin-1-Syk-CARD9 signaling pathway in TB immunity. Front Immunol. 2018;9:225.

142. Manzanillo PS, Shiloh MU, Portnoy DA, Cox JS. Mycobacterium tuberculosis activates the DNA-dependent cytosolic surveillance pathway within macrophages. Cell Host Microbe. 2012;11(5):469–80.

143. Wassermann R, Gulen MF, Sala C, Perin SG, Lou Y, Rybniker J, et al. Mycobacterium tuberculosis Differentially Activates cGAS- and Inflammasome-Dependent Intracellular Immune Responses through ESX-1. Cell Host Microbe. 2015;17(6):799–810.

144. Collins AC, Cai H, Li T, Franco LH, Li XD, Nair VR, et al. Cyclic GMP-AMP Synthase Is an Innate Immune DNA Sensor for Mycobacterium tuberculosis. Cell Host Microbe.

2015;17(6):820–8.

145. Hossain MM, Norazmi M-N. Pattern recognition receptors and cytokines in Mycobacterium tuberculosis infection--the double-edged sword? Biomed Res Int. 2013;179174.

146. Silva Miranda M, Breiman A, Allain S, Deknuydt F, Altare F. The tuberculous granuloma: An unsuccessful host defence mechanism providing a safety shelter for the bacteria? Clin Dev Immunol. 2012;2012:Article ID 139127.

147. Pagán AJ, Ramakrishnan L. The Formation and Function of Granulomas. Annu Rev Immunol. 2018;36:639–65.

148. Schluger NW, Rom WN. The Host Immune Response to Tuberculosis. Am J Respir Crit Care Med. 1998;157:679–91.

149. Russell DG, Cardona PJ, Kim MJ, Allain S, Altare F. Foamy macrophages and the progression of the human tuberculosis granuloma. Nat Immunol 2009 109. 2009;10(9):943–8.

150. Shah KK, Pritt BS, Alexander MP. Histopathologic review of granulomatous inflammation. J Clin Tuberc Other Mycobact Dis. 2017;7:1–12.

151. Ehlers S, Schaible UE. The granuloma in tuberculosis: Dynamics of a host-pathogen collusion. Front Immunol. 2012;3:1–9.

152. Flynn JL, Chan J. Immunology of Tuberculosis. Annu Rev Immunol. 2001;19:93–129.

153. Ramakrishnan L. Revisiting the role of the granuloma in tuberculosis. Nat Rev Immunol. 2012;12(5):352–66.

154. Gengenbacher M, Kaufmann SHE. Mycobacterium tuberculosis : success through dormancy. FEMS Microbiol Rev. 2012;36:514–32.

155. Martinot AJ. Microbial Offense vs Host Defense: Who Controls the TB Granuloma? Vet Pathol. 2018;55(1):14–26.

156. Zumla A, Atun R, Maeurer M, Mwaba P, Ma Z, Grady JO, et al. Scientific dogmas , paradoxes and mysteries of latent Mycobacterium tuberculosis infection. Trop Med Int Heal. 2011;16(1):79–83.

157. Saunders BM, Britton WJ. Life and death in the granuloma: immunopathology of tuberculosis. Immunol Cell Biol. 2007;85(2):103–11.

158. Vogel DYS, Glim JE, Stavenuiter AWD, Breur M, Heijnen P, Amor S, et al. Human macrophage polarization in vitro: Maturation and activation methods compared. Immunobiology. 2014;219:695–703.

159. Marino S, Cilfone NA, Mattila JT, Linderman JJ, Flynn JL, Kirschner DE. Macrophage polarization drives granuloma outcome during Mycobacterium tuberculosis infection. Infect Immun. 2015;83(1):324–38.

160. Chai Q, Lu Z, Cui ·, Liu H. Host defense mechanisms against Mycobacterium

tuberculosis. Cell Mol Life Sci. 2020;77:1859–78.

161. Chávez-Galán L, Olleros ML, Vesin D, Garcia I. Much more than M1 and M2 macrophages, there are also CD169+ and TCR+ macrophages. Front Immunol. 2015;6:263.

162. Kahnert A, Seiler P, Stein M, Bandermann S, Hahnke K, Mollenkopf H, et al. Alternative activation deprives macrophages of a coordinated defense program to Mycobacterium tuberculosis. Eur J Immunol. 2006;36(3):631–47.

163. El Kasmi KC, Qualls JE, Pesce JT, Smith AM, Thompson RW, Henao-Tamayo M, et al. Toll-like receptor-induced arginase 1 in macrophages thwarts effective immunity against intracellular pathogens. Nat Immunol. 2008;9(12):1399–406.

164. Huang Z, Luo Q, Guo Y, Chen J, Xiong G, Peng Y, et al. Mycobacterium tuberculosis-induced polarization of human macrophage orchestrates the formation and development of tuberculous granulomas in vitro. PLoS One. 2015;10(6):e0129744.

165. Xu Z, Xu L, Li W, Jin X, Song X, Chen X, et al. Innate scavenger receptor-A regulates adaptive T helper cell responses to pathogen infection. Nat Commun. 2017;8(1):16035.

166. Moreira-Teixeira L, Sousa J, McNab FW, Torrado E, Cardoso F, Machado H, et al. Type I IFN Inhibits Alternative Macrophage Activation during *Mycobacterium tuberculosis* Infection and Leads to Enhanced Protection in the Absence of IFN-γ Signaling. J Immunol. 2016;197(12):4714–26.

167. Desvignes L, Wolf AJ, Ernst JD. Dynamic Roles of Type I and Type II IFNs in Early Infection with Mycobacterium tuberculosis. J Immunol. 2012;188(12):6205–15.

168. Queval CJ, Brosch R, Simeone R. The macrophage: A disputed fortress in the battle against Mycobacterium tuberculosis. Front Microbiol. 2017;8:2284.

169. Behar SM, Divangahi M, Remold HG. Evasion of innate immunity by mycobacterium tuberculosis: Is death an exit strategy? Nat Rev Microbiol. 2010;8(9):668–74.

170. Goldberg MF, Saini NK, Porcelli SA. Evasion of Innate and Adaptive Immunity by Mycobacterium tuberculosis. Microbiol Spectr. 2014;2(5):MGM2-0005–2013.

171. De Waal AM, Hiemstra PS, Ottenhoff TH, Joosten SA, Van Der Does AM. Lung epithelial cells interact with immune cells and bacteria to shape the microenvironment in tuberculosis. Thorax. 2022;77:408–16.

172. Reuschl A-K, Edwards MR, Parker R, Connell DW, Hoang L, Halliday A, et al. Innate activation of human primary epithelial cells broadens the host response to Mycobacterium tuberculosis in the airways. PLOS Pathog. 2017;13(9):e1006577.

173. Scordo JM, Knoell DL, Torrelles JB. E-Mail Alveolar Epithelial Cells in Mycobacterium tuberculosis Infection: Active Players or Innocent Bystanders? J Innate Immun. 2016;8:3–14.

174. Rodrigues TS, Conti BJ, Fraga-Silva TF de C, Almeida F, Bonato VLD. Interplay between alveolar epithelial and dendritic cells and Mycobacterium tuberculosis. J Leukoc

Biol. 2020;108(4):1139–56.

175. Ryndak MB, Singh KK, Peng Z, Laal S. Transcriptional Profile of Mycobacterium tuberculosis Replicating in Type II Alveolar Epithelial Cells. PLoS One. 2015;10(4):e0123745.

176. Ioannidis I, Ye F, McNally B, Willette M, Flaño E. Toll-Like Receptor Expression and Induction of Type I and Type III Interferons in Primary Airway Epithelial Cells. J Virol. 2013;87(6):3261–70.

177. Maier BB, Hladik A, Lakovits K, Korosec A, Martins R, Kral JB, et al. Type I interferon promotes alveolar epithelial type II cell survival during pulmonary Streptococcus pneumoniae infection and sterile lung injury in mice HHS Public Access. Eur J Immunol. 2016;46(9):2175–86.

178. Major J, Crotta S, Llorian M, Mccabe TM, Gad HH, Priestnall SL, et al. Type I and III interferons disrupt lung epithelial repair during recovery from viral infection. Science (80-). 2020;369:712–7.

179. Henderson RA, Watkins SC, Flynn JL. Activation of human dendritic cells following infection with Mycobacterium tuberculosis. J Immunol. 1997;159(2):635–43.

180. Giacomini E, Iona E, Ferroni L, Miettinen M, Fattorini L, Orefici G, et al. Infection of Human Macrophages and Dendritic Cells with Mycobacterium tuberculosis Induces a Differential Cytokine Gene Expression That Modulates T Cell Response. J Immunol. 2001;166:7033–41.

181. Marino S, Pawar S, Fuller CL, Reinhart TA, Flynn JL, Kirschner DE. Dendritic Cell Trafficking and Antigen Presentation in the Human Immune Response to Mycobacterium tuberculosis. J Immunol. 2004;173(1):494–506.

182. Mihret A. The role of dendritic cells in Mycobacterium tuberculosis infection. Virulence. 2012;3(7):654–9.

183. Hanekom WA, Mendillo M, Manca C, Haslett PAJ, Siddiqui MR, Barry III C, et al. Mycobacterium tuberculosis Inhibits Maturation of Human Monocyte-Derived Dendritic Cells In Vitro. J Infect Dis. 2003;188(2):257–66.

184. Eum SY, Kong JH, Hong MS, Lee YJ, Kim JH, Hwang SH, et al. Neutrophils are the predominant infected phagocytic cells in the airways of patients with active pulmonary TB. Chest. 2010;137(1):122–8.

185. Lyadova I V. Neutrophils in Tuberculosis: Heterogeneity Shapes the Way? Mediators Inflamm. 2017;2017:Article ID 8619307.

186. Kisich KO, Higgins M, Diamond G, Heifets L. Tumor necrosis factor alpha stimulates killing of Mycobacterium tuberculosis by human neutrophils. Infect Immun. 2002;70(8):4591–9.

187. Corleis B, Korbel D, Wilson R, Bylund J, Chee R, Schaible UE. Escape of Mycobacterium tuberculosis from oxidative killing by neutrophils. Cell Microbiol. 2012;14(7):1109–21.

188. Moreira-Teixeira L, Stimpson PJ, Stavropoulos E, Hadebe S, Chakravarty P, Ioannou M, et al. Type I IFN exacerbates disease in tuberculosis-susceptible mice by inducing neutrophil-mediated lung inflammation and NETosis. Nat Commun. 2020;11(1):5566.

189. Berry MPR, Graham CM, McNab FW, Xu Z, Bloch SAA, Oni T, et al. An interferon-inducible neutrophil-driven blood transcriptional signature in human tuberculosis. Nature. 2010;466(7309):973–7.

190. Choreño Parra JA, Martínez Zúñiga N, Jiménez Zamudio LA, Jiménez Álvarez LA, Salinas Lara C, Zúñiga J. Memory of natural killer cells: A new chance against Mycobacterium tuberculosis? Front Immunol. 2017;8:Article 967.

191. Vankayalapati R, Wizel B, Weis SE, Safi H, Lakey DL, Mandelboim O, et al. The NKp46 Receptor Contributes to NK Cell Lysis of Mononuclear Phagocytes Infected with an Intracellular Bacterium. J Immunol. 2002;168(7):3451–7.

192. Vankayalapati R, Barnes PF. Innate and adaptive immune responses to human Mycobacterium tuberculosis infection. Tuberculosis. 2009 Dec;89(SUPPL.1):S77–80.

193. Chancellor A, White A, Tocheva AS, Fenn JR, Dennis M, Tezera L, et al. Quantitative and qualitative iNKT repertoire associations with disease susceptibility and outcome in macaque tuberculosis infection Europe PMC Funders Group. Tuberculosis. 2017;105:86–95.

194. Sada-Ovalle I, Chiba A, Gonzales A, Brenner MB, Behar SM. Innate invariant NKT cells recognize Mycobacterium tuberculosis-infected macrophages, produce interferon-γ, and kill intracellular bacteria. PLoS Pathog. 2008;4(12):e1000239.

195. Ruibal P, Voogd L, Joosten SA, Ottenhoff THM. The role of donor-unrestricted T-cells, innate lymphoid cells, and NK cells in anti-mycobacterial immunity. Immunol Rev. 2021;301(1):30.

196. Gold MC, Napier RJ, Lewinsohn DM. MR1-restricted mucosal associated invariant T (MAIT) cells in the immune response to Mycobacterium tuberculosis. Immunol Rev. 2015;264(1):154–66.

197. Kjer-Nielsen L, Patel O, Corbett AJ, Nours J Le, Meehan B, Liu L, et al. MR1 presents microbial vitamin B metabolites to MAIT cells. Nature. 2012;491(7426):717–23.

198. Kwon Y-S, Cho Y-N, Kim M-J, Jin H-M, Jung H-J, Kang J-H, et al. Mucosal-associated invariant T cells are numerically and functionally deficient in patients with mycobacterial infection and reflect disease activity. Tuberculosis. 2015;95:267–74.

199. Jiang J, Yang B, An H, Wang X, Liu Y, Cao Z, et al. Mucosal-associated invariant T cells from patients with tuberculosis exhibit impaired immune response. J Infect. 2015;72:338–52.

200. Malka-Ruimy C, Youssef G Ben, Lambert M, Tourret M, Ghazarian L, Faye A, et al. Mucosal-Associated Invariant T Cell Levels Are Reduced in the Peripheral Blood and Lungs of Children With Active Pulmonary Tuberculosis. Front Immunol. 2019;10:206.

201. Suliman S, Gela A, Mendelsohn SC, Iwany SK, Tamara KL, Mabwe S, et al. Peripheral

blood mucosal-associated invariant T cells in tuberculosis patients and healthy mycobacterium tuberculosis-exposed controls. J Infect Dis. 2020;222(6):995–1007.

202. Gold MC, Napier RJ, Lewinsohn DM. MR1-restricted mucosal associated invariant T (MAIT) cells in the immune response to Mycobacterium tuberculosis. Immunol Rev. 2015;264(1):154–66.

203. Sia JK, Rengarajan J. Immunology of Mycobacterium tuberculosis infections. Microbiol Spectr. 2019;7(4).

204. Pinheiro MB, Antonelli LR, Sathler-Avelar R, Vitelli-Avelar DM, Spindola-de-Miranda S, Guimarães TMPD, et al. CD4-CD8-αβ and γδ T Cells Display Inflammatory and Regulatory Potentials during Human Tuberculosis. PLoS One. 2012;7(12):e50923.

205. Wolf AJ, Desvignes L, Linas B, Banaiee N, Tamura T, Takatsu K, et al. Initiation of the adaptive immune response to Mycobacterium tuberculosis depends on antigen production in the local lymph node, not the lungs. J Exp Med. 2008;205(1):105–15.

206. Cooper AM. Cell-Mediated Immune Responses in Tuberculosis. Annu Rev Immunol. 2009;27(1):393–422.

207. de Martino M, Lodi L, Galli L, Chiappini E. Immune Response to Mycobacterium tuberculosis: A Narrative Review. Front Pediatr. 2019;7:350.

208. Meraviglia S, Daker S El, Dieli F, Martini F, Martino A. γδ T Cells Cross-Link Innate and Adaptive Immunity in Mycobacterium tuberculosis Infection. Clin Dev Immunol. 2011;2011:Article ID 587315.

209. Caruso AM, Serbina N, Klein E, Triebold K, Bloom BR, Flynn JL. Mice Deficient in CD4 T Cells Have Only Transiently Diminished Levels of IFN- γ, Yet Succumb to Tuberculosis. J Immunol. 1999;162:5407–16.

210. Luo J, Zhang M, Yan B, Zhang K, Chen M, Deng S. Imbalance of Th17 and Treg in peripheral blood mononuclear cells of active tuberculosis patients. Brazilian J Infect Dis. 2017;21(2):155–61.

211. Domingo-Gonzalez R, Prince O, Cooper A, Khader SA. Cytokines and Chemokines in Mycobacterium tuberculosis Infection. Microbiol Spectr. 2016;4(5):TBTB2-0018–2016.

212. Lyadova I V., Panteleev A V. Th1 and Th17 Cells in Tuberculosis: Protection, Pathology, and Biomarkers. Mediators Inflamm. 2015;2015:Article ID 854507.

213. Cardona P, Cardona PJ. Regulatory T Cells in Mycobacterium tuberculosis Infection. Front Immunol. 2019;10:2139.

214. Pang H, Yu Q, Guo B, Jiang Y, Li W, Li J, et al. Frequency of Regulatory T-Cells in the Peripheral Blood of Patients with Pulmonary Tuberculosis from Shanxi Province, China. PLoS One. 2013;8(6):e65496.

215. Kumar NP, Sridhar R, Hanna LE, Banurekha V V., Nutman TB, Babu S. Decreased Frequencies of Circulating CD4+ T Follicular Helper Cells Associated with Diminished Plasma IL-21 in Active Pulmonary Tuberculosis. PLoS One. 2014;9(10):e111098.

216. Booty MG, Barreira-Silva P, Carpenter SM, Nunes-Alves C, Jacques MK, Stowell BL, et al. IL-21 signaling is essential for optimal host resistance against Mycobacterium tuberculosis infection. Sci Rep. 2016;6:36720.

217. Lin PL, Flynn JAL. CD8 T cells and Mycobacterium tuberculosis infection. Semin Immunopathol. 2015;37(3):239–49.

218. Canaday DH, Wilkinson RJ, Li Q, Harding C V., Silver RF, Boom WH. CD4 + and CD8 + T Cells Kill Intracellular Mycobacterium tuberculosis by a Perforin and Fas/Fas Ligand-Independent Mechanism. J Immunol. 2001;167(5):2734–42.

219. Rao M, Valentini D, Poiret T, Dodoo E, Parida S, Zumla A, et al. B in TB: B Cells as Mediators of Clinically Relevant Immune Responses in Tuberculosis. Clin Infect Dis. 2015;61(Suppl 3):S225–34.

220. Loxton AG. Bcells and their regulatory functions during Tuberculosis: Latency and active disease. Mol Immunol. 2019;111:145–51.

221. Abebe F, Bjune G. The protective role of antibody responses during Mycobacterium tuberculosis infection. Clin Exp Immunol. 2009;157(2):235–43.

222. Achkar JM, Casadevall A. Antibody-mediated immunity against tuberculosis: Implications for vaccine development. Cell Host Microbe. 2013;13(3):250–62.

223. Rijnink WF, Ottenhoff THM, Joosten SA. B-Cells and Antibodies as Contributors to Effector Immune Responses in Tuberculosis. Front Immunol. 2021;12:640168.

224. Hamasur B, Haile M, Pawlowski A, Schröder U, Källenius G, Svenson SB. A mycobacterial lipoarabinomannan specific monoclonal antibody and its F(ab′)2 fragment prolong survival of mice infected with Mycobacterium tuberculosis. Clin Exp Immunol. 2004;138(1):30–8.

225. Teitelbaum R, Glatman-Freedman A, Chen B, Robbins JB, Unanue E, Casadevall A, et al. A mAb recognizing a surface antigen of Mycobacterium tuberculosis enhances host survival. Proc Natl Acad Sci U S A. 1998;95(26):15688–93.

226. Kawahara JY, Irvine EB, Alter G. A case for antibodies as mechanistic correlates of immunity in tuberculosis. Front Immunol. 2019;10:996.

227. Lu LL, Chung AW, Rosebrock TR, Ghebremichael M, Yu WH, Grace PS, et al. A Functional Role for Antibodies in Tuberculosis. Cell. 2016;167(2):433-443.e14.

228. Robbins JB, Schneerson R, Szu SC. Perspective: Hypothesis: Serum IgG Antibody Is Sufficient to Confer Protection against Infectious Diseases by Inactivating the Inoculum. J Infect Dis. 1995;171(6):1387–98.

229. Tameris MD, Hatherill M, Landry BS, Scriba TJ, Snowden MA, Lockhart S, et al. Safety and efficacy of MVA85A, a new tuberculosis vaccine, in infants previously vaccinated with BCG: A randomised, placebo-controlled phase 2b trial. Lancet. 2013;381(9871):1021–8.

230. Ndiaye BP, Thienemann F, Ota M, Landry BS, Camara M, Dièye S, et al. Safety,

immunogenicity, and efficacy of the candidate tuberculosis vaccine MVA85A in healthy adults infected with HIV-1: A randomised, placebo-controlled, phase 2 trial. Lancet Respir Med. 2015;3(3):190–200.

231. Fletcher HA, Snowden MA, Landry B, Rida W, Satti I, Harris SA, et al. T-cell activation is an immune correlate of risk in BCG vaccinated infants. Nat Commun. 2016;7:11290.

232. Corrêa RDS, Rodrigues LS, Pereira LHL, Nogueira OC, Leung J, Sousa MDS, et al. Neutrophil CD64 expression levels in IGRA-positive individuals distinguish latent tuberculosis from active disease. Mem Inst Oswaldo Cruz. 2019;114(2):1–8.

233. Maertzdorf J, Repsilber D, Parida SK, Stanley K, Roberts T, Black G, et al. Human gene expression profiles of susceptibility and resistance in tuberculosis. Genes Immun. 2011;12(1):15–22.

234. Wu K, Li M, Chen Z, Lowrie DB, Fan X-Y. Probe signal values in mRNA Arrays Imply an Excessive Involvement of Neutrophil FCGR1 in Tuberculosis. Front Medi. 2020;7:19.

235. Paola Etna M, Giacomini E, Severa M, Marina Coccia E. Pro-and anti-inflammatory cytokines in tuberculosis: A two-edged sword in TB pathogenesis. Semin Immunol. 2014;26:543–51.

236. Wajant H, Pfizenmaier K, Scheurich P. Tumor necrosis factor signaling. Cell Death Differ. 2003;10(1):45–65.

237. Flynn JAL, Goldstein MM, Chan J, Triebold KJ, Pfeffer K, Lowenstein CJ, et al. Tumor necrosis factor-α is required in the protective immune response against mycobacterium tuberculosis in mice. Immunity. 1995;2(6):561–72.

238. Scott Algood HM, Lin PL, Flynn JL. Tumor Necrosis Factor and Chemokine Interactions in the Formation and Maintenance of Granulomas in Tuberculosis. Clin Infect Dis. 2005;41(Suppl 3):S189–93.

239. Roach DR, Bean AGD, Demangel C, France MP, Briscoe H, Britton WJ. TNF Regulates Chemokine Induction Essential for Cell Recruitment, Granuloma Formation, and Clearance of Mycobacterial Infection. J Immunol. 2002;168(9):4620–7.

240. Arriaga AK, Orozco EH, Aguilar LD, Rook GAW, Hernández Pando R. Immunological and pathological comparative analysis between experimental latent tuberculous infection and progressive pulmonary tuberculosis. Clin Exp Immunol. 2002;128(2):229–37.

241. Domingo-Gonzalez R, Prince O, Cooper A, Khader SA. Cytokines and Chemokines in Mycobacterium tuberculosis Infection. Microbiol Spectr. 2016;4(5):TBTB2-0018–2016.

242. Farber JM. MIG and IP-10: CXC chemokines that target lymphocytes. J Leukoc Biol. 1997;61(3):246–57.

243. Cole KE, Strick CA, Paradis TJ, Ogborne KT, Loetscher M, Gladue RP, et al. Interferon-inducible T Cell Alpha Chemoattractant (I-TAC): A Novel Non-ELR CXC Chemokine with Potent Activity on Activated T Cells through Selective High Affinity Binding to CXCR3. J Exp Med. 1998;187:2009–21.

244. Mohan VP, Scanga CA, Yu K, Scott HM, Tanaka KE, Tsang E, et al. Effects of Tumor Necrosis Factor Alpha on Host Immune Response in Chronic Persistent Tuberculosis: Possible Role for Limiting Pathology. Infect Immun. 2001;69(3):1847–55.

245. Solovic I, Sester M, Gomez-Reino JJ, Rieder HL, Ehlers S, Milburn HJ, et al. The risk of tuberculosis related to tumour necrosis factor antagonist therapies: A TBNET consensus statement. Eur Respir J. 2010;36(5):1185–206.

246. Liao H, Zhong Z, Liu Z, Zou X. Comparison of the risk of infections in different anti-TNF agents: a meta-analysis. Int J Rheum Dis. 2017;20(2):161–8.

247. Wallis RS. Reactivation of latent tuberculosis by TNF blockade: The role of interferon γ. J Investig Dermatology Symp Proc. 2007;12(1):16–21.

248. Keane J, Katarzyna Balcewicz-Sablinska M, Remold HG, Chupp GL, Meek BB, Fenton MJ, et al. Infection by Mycobacterium tuberculosis Promotes Human Alveolar Macrophage Apoptosis. Infect Immun. 1997;65(1):298–304.

249. Mootoo A, Stylianou E, Arias MA, Reljic R. TNF-α in tuberculosis: A cytokine with a split personality. Inflamm Allergy - Drug Targets. 2009;8(1):53–62.

250. María Rocha-Ramírez L, Estrada-García I, María López-Marín L, Segura-Salinas E, Méndez-Aragón P, Van Soolingen D, et al. Mycobacterium tuberculosis lipids regulate cytokines, TLR-2/4 and MHC class II expression in human macrophages. Tuberculosis. 2008;88:212–20.

251. Méndez-Samperio P. Role of interleukin-12 family cytokines in the cellular response to mycobacterial disease. Int J Infect Dis. 2010;14(5):e366–71.

252. Romero-Adrian TB, Leal-Montiel J, Fernández G, Valecillo A. Role of cytokines and other factors involved in the Mycobacterium tuberculosis infection. World J Immunol. 2015;5(1):16–50.

253. Cooper BAM, Magram J, Ferrante J, Orme IM. Interleukin 12 (IL-12) Is Crucial to the Development of Protective Immunity in Mice Intravenously Infected with Mycobacterium tuberculosis. Tuberculosis. 1997;186(1):39–45.

254. Cooper AM, Roberts AD, Rhoades ER, Callahan JE, Getzy DM, Orme IM. The role of interleukin-12 in acquired immunity to Mycobacterium tuberculosis infection. Immunology. 1995;84(3):423–32.

255. Flynn JL, Goldstein MM, Triebold KJ, Sypek J, Wolf S, Bloom BR. IL-12 increases resistance of BALB/c mice to Mycobacterium tuberculosis infection. J Immunol. 1995;155(5):2515–24.

256. Khader SA, Partida-Sanchez S, Bell G, Jelley-Gibbs DM, Swain S, Pearl JE, et al. Interleukin 12p40 is required for dendritic cell migration and T cell priming after Mycobacterium tuberculosis infection. J Exp Med. 2006;203(7):1805–15.

257. Feng CG, Jankovic D, Kullberg M, Cheever A, Scanga CA, Hieny S, et al. Maintenance of Pulmonary Th1 Effector Function in Chronic Tuberculosis Requires Persistent IL-12 Production. J Immunol. 2005;174(7):4185–92.

258. Fremond CM, Togbe D, Doz E, Rose S, Vasseur V, Maillet I, et al. IL-1 Receptor-Mediated Signal Is an Essential Component of MyD88-Dependent Innate Response to Mycobacterium tuberculosis Infection. J Immunol. 2007;179(2):1178–89.

259. Schneider BE, Korbel D, Hagens K, Koch M, Raupach B, Enders J, et al. A role for IL-18 in protective immunity against Mycobacterium tuberculosis. Eur J Immunol. 2010;40(2):396–405.

260. Saraiva M, O'Garra A. The regulation of IL-10 production by immune cells. Nat Rev Immunol. 2010;10(3):170–81.

261. Richardson ET, Shukla S, Sweet DR, Wearsch PA, Tsichlis PN, Henry Boom W, et al. Toll-like receptor 2-dependent extracellular signal-regulated kinase signaling in Mycobacterium tuberculosis-infected macrophages drives anti-inflammatory responses and inhibits Th1 polarization of responding T cells. Infect Immun. 2015;83(6):2242–54.

262. Bai W, Liu H, Ji Q, Zhou Y, Liang L, Zheng R, et al. TLR3 regulates mycobacterial RNA-induced IL-10 production through the PI3K/AKT signaling pathway. Cell Signal. 2014;26:942–50.

263. McNab FW, Ewbank J, Howes A, Moreira-Teixeira L, Martirosyan A, Ghilardi N, et al. Type I IFN Induces IL-10 Production in an IL-27–Independent Manner and Blocks Responsiveness to IFN-γ for Production of IL-12 and Bacterial Killing in Mycobacterium tuberculosis –Infected Macrophages. J Immunol. 2014;193(7):3600–12.

264. Couper KN, Blount DG, Riley EM. IL-10: The Master Regulator of Immunity toInfection. J Immunol Ref. 2008;180:5771–7.

265. Dinarello CA. Overview of the IL-1 family in innate inflammation and acquired immunity. Immunol Rev. 2018;281(1):8–27.

266. Feghali-Bostwick CA, Wright TM. Cytokines in acute and chronic inflammation. Front Biosci. 1997;2:12–26.

267. Werman A, Werman-Venkert R, White R, Lee JK, Werman B, Krelin Y, et al. The precursor form of IL-1α is an intracrine proinflammatory activator of transcription. Proc Natl Acad Sci U S A. 2004;101(8):2434–9.

268. Guler R, Parihar SP, Spohn G, Johansen P, Brombacher F, Bachmann MF. Blocking IL-1α but not IL-1β increases susceptibility to chronic Mycobacterium tuberculosis infection in mice. Vaccine. 2011;29:1339–46.

269. Mayer-Barber KD, Barber DL, Shenderov K, White SD, Wilson MS, Cheever A, et al. Caspase-1 Independent IL-1β Production Is Critical for Host Resistance to Mycobacterium tuberculosis and Does Not Require TLR Signaling In Vivo. J Immunol. 2010;184(7):3326–30.

270. Cooper AM, Mayer-Barber KD, Sher A. Role of innate cytokines in mycobacterial infection. Mucosal Immunol. 2011;4(3):252–60.

271. Saunders BM, Cooper AM. Restraining mycobacteria: Role of granulomas in mycobacterial infections. Immunol Cell Biol. 2000;78(4):334–41.

272. Peters VA, Joesting JJ, Freund GG. IL-1 receptor 2 (IL-1R2) and its role in immune regulation. Brain Behav Immun. 2013;32:1–8.

273. Dorhoi A, Kaufmann SHE, De K-BM. Pathology and immune reactivity: understanding multidimensionality in pulmonary tuberculosis. Semin Immunopathol. 2016;38:153–66.

274. Monin L, Khader SA. Chemokines in tuberculosis: The good, the bad and the ugly. Semin Immunol. 2014;26(6):552–8.

275. Kang DD, Lin Y, Moreno JR, Randall TD, Khader SA. Profiling early lung immune responses in the mouse model of tuberculosis. PLoS One. 2011;6(1):e16161.

276. Kumar NP, Moideen K, Nancy A, Viswanathan V, Shruthi BS, Sivakumar S, et al. Plasma chemokines are biomarkers of disease severity, higher bacterial burden and delayed sputum culture conversion in pulmonary tuberculosis. Sci Rep. 2019;9(1):18217.

277. Zhao Y, Yang X, Zhang X, Yu Q, Zhao P, Wang J, et al. IP-10 and RANTES as biomarkers for pulmonary tuberculosis diagnosis and monitoring. Tuberculosis. 2018;111:45–53.

278. Wergeland I, Pullar N, Assmus J, Ueland T, Aukrust P, Mollnes TE, et al. IP-10 differentiates between active and latent tuberculosis irrespective of HIV status and declines during therapy. J Infect. 2015;70:381–91.

279. Estévez O, Anibarro L, Garet E, Angeles P, Pena A, Villaverde C, et al. Identification of candidate host serum and saliva biomarkers for a better diagnosis of active and latent tuberculosis infection. PLoS One. 2020;15(7):e0235859.

280. Bastos HN, Osório NS, Gagneux S, Comas I, Saraiva M. The Troika Host-Pathogen-Extrinsic Factors in Tuberculosis: Modulating Inflammation and Clinical Outcomes. Front Immunol. 2017;8:1948.

281. Isaacs A, Lindenmann J. Virus Interference . I . The Interferon. Proc R Soc London Ser B, Biol Sci. 1957;147(927):258–67.

282. Schreiber G. The molecular basis for differential type I interferon signaling. J Biol Chem. 2017;292(18):7285–94.

283. Pestka S, Krause CD, Walter MR. Interferons, interferon-like cytokines, and their receptors. Immunol Rev. 2004;202:8–32.

284. Schroder K, Hertzog PJ, Ravasi T, Hume DA. Interferon-γ: an overview of signals, mechanisms and functions. J Leukoc Biol. 2004;75(2):163–89.

285. Kotenko S V., Gallagher G, Baurin V V., Lewis-Antes A, Shen M, Shah NK, et al. IFN-λs mediate antiviral protection through a distinct class II cytokine receptor complex. Nat Immunol. 2003;4(1):69–77.

286. Sheppard P, Kindsvogel W, Xu W, Henderson K, Schlutsmeyer S, Whitmore TE, et al. IL-28, IL-29 and their class II cytokine receptor IL-28R. Nat Immunol. 2003;4(1):63–8.

287. Dorman SE, Picard C, Lammas D, Heyne K, Van Dissel JT, Baretto R, et al. Clinical features of dominant and recessive interferon γ receptor 1 deficiencies. Lancet.

2004;364(9451):2113–21.

288. Bustamante J, Boisson-Dupuis S, Abel L, Casanova JL. Mendelian susceptibility to mycobacterial disease: Genetic, immunological, and clinical features of inborn errors of IFN-γ immunity. Semin Immunol. 2014;26(6):454–70.

289. Mogues T, Goodrich ME, Ryan L, LaCourse R, North RJ. The relative importance of T cell subsets in immunity and immunopathology of airborne Mycobacterium tuberculosis infection in mice. J Exp Med. 2001;193(3):271–80.

290. Hemann EA, Gale M, Savan R. Interferon lambda genetics and biology in regulation of viral control. Front Immunol. 2017;8:1707.

291. Travar M, Vucic M, Petkovic M. Interferon lambda-2 levels in sputum of patients with pulmonary mycobacterium tuberculosis infection. Scand J Immunol. 2014;80(1):43–9.

292. Mattila JT, Talukdar P, Junecko BA. Type 3 interferons expressed in tuberculous granulomas may influence signaling in epithelioid macrophages. J Immunol. 2018;200(1 Supplement):117.25.

293. Talukdar P, Mattila JT, Fallert Junecko BA. Type III interferons are expressed in tuberculosis granulomas and promote an inflammatory phenotype in macrophages that differs from type I interferon. J Immunol. 2020;204(1 Supplement):62.2.

294. Bierne H, Travier L, Mahlakõiv T, Tailleux L, Subtil A, Lebreton A, et al. Activation of Type III Interferon Genes by Pathogenic Bacteria in Infected Epithelial Cells and Mouse Placenta. Gorvel J-P, editor. PLoS One. 2012;7(6):e39080.

295. Carrero JA. Confounding roles for type I interferons during bacterial and viral pathogenesis. Int Immunol. 2013;25(12):663–9.

296. Monroe KM, McWhirter SM, Vance RE. Induction of type I interferons by bacteria. Cell Microbiol. 2010;12(7):881–90.

297. Snyder DT, Hedges JF, Jutila MA. Getting “Inside” Type I IFNs: Type I IFNs in Intracellular Bacterial Infections. J Immunol Res. 2017;2017:Article 9361802.

298. McNab F, Mayer-barber K, Sher A, Wack A, Garra AO. Type I interferons in infectious disease. Nat Rev Immunol. 2015;15(2):87–103.

299. Dussurget O, Bierne H, Cossart P. The bacterial pathogen Listeria monocytogenes and the interferon family : type I , type II and type III interferons. Front Cell Infect Microbiol. 2014;4:Article 50.

300. Eshleman EM, Lenz LL. Type I interferons in bacterial infections: Taming of myeloid cells and possible implications for autoimmunity. Front Immunol. 2014;5:Article 431.

301. Li SF, Gong MJ, Zhao FR, Shao JJ, Xie YL, Zhang YG, et al. Type i interferons: Distinct biological activities and current applications for viral infection. Cell Physiol Biochem. 2018;51(5):2377–96.

302. Siegal FP, Kadowaki N, Shodell M, Fitzgerald-Bocarsly PA, Shah K, Ho S, et al. The nature of the principal Type 1 interferon-producing cells in human blood. Science (80-).

1999;284:1835–7.

303. Ng CT, Mendoza JL, Garcia KC, Oldstone MBA. Alpha and Beta Type 1 Interferon Signaling: Passage for Diverse Biologic Outcomes. Cell. 2016;164(3):349–52.

304. Wittling MC, Cahalan SR, Levenson EA, Rabin RL. Shared and Unique Features of Human Interferon-Beta and Interferon-Alpha Subtypes. Front Immunol. 2021;11:3325.

305. Piehler J, Thomas C, Christopher Garcia K, Schreiber G. Structural and dynamic determinants of type I interferon receptor assembly and their functional interpretation. Immunol Rev. 2012;250(1):317–34.

306. Schreiber G, Piehler J. The molecular basis for functional plasticity in type I interferon signaling. Trends Immunol. 2015;36(3):139–49.

307. Welsh RM, Bahl K, Marshall HD, Urban SL. Type 1 Interferons and Antiviral CD8 T-Cell Responses. PLOS Pathog. 2012;8(1):e1002352.

308. Wagner TC, Velichko S, Chesney SK, Biroc S, Harde D, Vogel D, et al. Interferon receptor expression regulates the antiproliferative effects of interferons on cancer cells and solid tumors. Int J Cancer. 2004;111(1):32–42.

309. Erlandsson L, Blumenthal R, Eloranta ML, Engel H, Alm G, Weisst S, et al. Interferon-β is required for interferon-α production in mouse fibroblasts. Curr Biol. 1998;8(4):223–6.

310. Lienenklaus S, Cornitescu M, Ziętara N, Łyszkiewicz M, Gekara N, Jabłońska J, et al. Novel Reporter Mouse Reveals Constitutive and Inflammatory Expression of IFN-β In Vivo. J Immunol. 2009;183(5):3229–36.

311. Taniguchi T, Takaoka A. A weak signal for strong responses: Interferon-α/β revisited. Nat Rev Mol Cell Biol. 2001;2(5):378–86.

312. Koerner I, Kochs G, Kalinke U, Weiss S, Staeheli P. Protective Role of Beta Interferon in Host Defense against Influenza A Virus. J Virol. 2007;81(4):2025–30.

313. Lee AJ, Ashkar AA. The dual nature of type I and type II interferons. Front Immunol. 2018;9:Article 2061.

314. Gill N, Deacon PM, Lichty B, Mossman KL, Ashkar AA. Induction of innate immunity against herpes simplex virus type 2 infection via local delivery of Toll-like receptor ligands correlates with beta interferon production. J Virol. 2006;80(20):9943–50.

315. Génin P, Lin R, Hiscott J, Civas A. Differential Regulation of Human Interferon A Gene Expression by Interferon Regulatory Factors 3 and 7. Mol Cell Biol. 2009;29(12):3435–50.

316. Bierne H, Milohanic E, Kortebi M. To Be Cytosolic or Vacuolar: The Double Life of Listeria monocytogenes. Front Cell Infect Microbiol. 2018;8:136.

317. O'Riordan M, Yi CH, Gonzales R, Lee K-D, Portnoy DA. Innate recognition of bacteria by a macrophage cytosolic surveillance pathway. Proc Natl Acad Sci. 2002;99(21):13861–6.

318. Vergne I, Chua J, Singh SB, Deretic V. Cell biology of Mycobacterium tuberculosis phagosome. Annu Rev Cell Dev Biol. 2004;20:367–94.

319. Rahman A, Sobia P, Gupta N, Kaer L Van, Das G. Mycobacterium tuberculosis Subverts the TLR-2 - MyD88 Pathway to Facilitate Its Translocation into the Cytosol. PLoS One. 2014;9(1):e86886.

320. Gao L-Y, Guo S, McLaughlin B, Morisaki H, Engel JN, Brown EJ. A mycobacterial virulence gene cluster extending RD1 is required for cytolysis, bacterial spreading and ESAT-6 secretion. Mol Microbiol. 2004;53(6):1677–93.

321. Peng X, Sun J, Paso E. Mechanism of ESAT-6 membrane interaction and its roles in pathogenesis of Mycobacterium tuberculosis Pore-forming toxins. Toxicon. 2016;116:29–34.

322. Conrad WH, Osman MM, Shanahan JK, Chu F, Takaki KK, Cameron J, et al. Mycobacterial ESX-1 secretion system mediates host cell lysis through bacterium contact-dependent gross membrane disruptions. Proc Natl Acad Sci U S A. 2017;114(6):1371–6.

323. Stanley SA, Johndrow JE, Manzanillo P, Cox JS. The Type I IFN Response to Infection with Mycobacterium tuberculosis Requires ESX-1-Mediated Secretion and Contributes to Pathogenesis. J Immunol. 2007;178(5):3143–52.

324. Dey B, Dey RJ, Cheung LS, Pokkali S, Guo H, Lee JH, et al. A bacterial cyclic dinucleotide activates the cytosolic surveillance pathway and mediates innate resistance to tuberculosis. Nat Med. 2015;21(4):401–8.

325. Saiga H, Kitada S, Shimada Y, Kamiyama N, Okuyama M, Makino M, et al. Critical role of AIM2 in Mycobacterium tuberculosis infection. Int Immunol. 2012;24(10):637–44.

326. Remoli ME, Giacomini E, Lutfalla G, Dondi E, Orefici G, Battistini A, et al. Selective Expression of Type I IFN Genes in Human Dendritic Cells Infected with Mycobacterium tuberculosis. J Immunol. 2002;169:366–74.

327. Watson RO, Bell SL, Macduff DA, Stallings CL, Virgin HW, Cox JS, et al. Short Article The Cytosolic Sensor cGAS Detects Mycobacterium tuberculosis DNA to Induce Type I Interferons and Activate Autophagy Short Article The Cytosolic Sensor cGAS Detects Mycobacterium tuberculosis DNA to Induce Type I Interferons and Activate Aut. Cell Host Microbe. 2015;17(6):811–9.

328. Mourik BC, Lubberts E, de Steenwinkel JEM, Ottenhoff THM, Leenen PJM. Interactions between type 1 interferons and the Th17 response in tuberculosis: Lessons learned from autoimmune diseases. Front Immunol. 2017;8:Article 294.

329. Ivashkiv LB, Donlin LT. Regulation of type I interferon responses. Nat Rev Immunol. 2014 Jan 1;14(1):36–49.

330. Banks DA, Ahlbrand SE, Hughitt VK, Shah S, Mayer-Barber KD, Vogel SN, et al. Mycobacterium tuberculosis Inhibits Autocrine Type I IFN Signaling to Increase Intracellular Survival. J Immunol. 2019;202(8):2348–59.

331. Chen K, Liu J, Cao X. Regulation of type I interferon signaling in immunity and

inflammation: A comprehensive review. J Autoimmun. 2017;83:1–11.

332. Schoggins JW. Interferon-Stimulated Genes: What Do They All Do? Annu Rev Virol. 2019;6(1):567–84.

333. Green R, Ireton RC, Gale M. Interferon-stimulated genes: new platforms and computational approaches. Mamm Genome. 2018;29(7):593–602.

334. Schneider WM, Chevillotte MD, Rice CM. Interferon-Stimulated Genes: A Complex Web of Host Defenses. Annu Rev Immunol. 2014;32:513–45.

335. Yan N, Chen ZJ. Intrinsic Antiviral Immunity. Nat Immunol. 2013;13(3):214–22.

336. Versteeg GA, García-Sastre A. Viral tricks to grid-lock the type I interferon system. Curr Opin Microbiol. 2010;13(4):508–16.

337. Davidson S, Crotta S, McCabe TM, Wack A. Pathogenic potential of interferon αβ in acute influenza infection. Nat Commun. 2014;5:3864.

338. Garcia-Sastre A, Biron CA. Type 1 Interferons and the Virus-Host Relationship: A Lesson in Détente. Science (80-). 2006;312(5775):879–82.

339. Wilson EB, Yamada DH, Elsaesser H, Herskovitz J, Deng J, Cheng G, et al. Blockade of chronic type I interferon signaling to control persistent LCMV infection. Science (80-). 2013;340(6129):202–7.

340. Teijaro JR, Ng C, Lee AM, Sullivan BM, Sheehan KCF, Welch M, et al. Persistent LCMV Infection Is Controlled by Blockade of Type I Interferon Signaling. Science (80-). 2013;340:207–11.

341. Parker D, Martin FJ, Soong G, Harfenist BS, Aguilar JL, Ratner AJ, et al. Streptococcus pneumoniae DNA initiates type I interferon signaling in the respiratory tract. MBio. 2011;2(3):e00016-11.

342. Damjanovic D, Khera A, Medina MF, Ennis J, Turner JD, Gauldie J, et al. Type 1 interferon gene transfer enhances host defense against pulmonary Streptococcus pneumoniae infection via activating innate leukocytes. Mol Ther - Methods Clin Dev. 2014;1:14005.

343. Mancuso G, Midiri A, Biondo C, Beninati C, Zummo S, Galbo R, et al. Type I IFN Signaling Is Crucial for Host Resistance against Different Species of Pathogenic Bacteria. J Immunol. 2007;178(5):3126–33.

344. Rothfuchs AG, Trumstedt C, Mattei F, Schiavoni G, Hidmark Å, Wigzell H, et al. STAT1 Regulates IFN-αβ- and IFN-γ-Dependent Control of Infection with Chlamydia pneumoniae by Nonhemopoietic Cells . J Immunol. 2006;176(11):6982–90.

345. De La Maza LM, Peterson EM, Goebel JM, Fennie CW, Czarniecki CW. Interferon-induced inhibition of Chlamydia trachomatis: Dissociation from antiviral and antiproliferative effects. Infect Immun. 1985;47(3):719–22.

346. Schiavoni G, Mauri C, Carlei D, Belardelli F, Castellani Pastoris M, Proietti E. Type I IFN Protects Permissive Macrophages from Legionella pneumophila Infection through an

IFN-γ-Independent Pathway . J Immunol. 2004;173(2):1266–75.

347. Plumlee CR, Lee C, Beg AA, Decker T, Shuman HA, Schindler C. Interferons direct an effective innate response to Legionella pneumophila infection. J Biol Chem. 2009;284(44):30058–66.

348. Carrero JA, Calderon B, Unanue ER. Type I interferon sensitizes lymphocytes to apoptosis and reduces resistance to Listeria infection. J Exp Med. 2004;200(4):535–40.

349. Taniguchi T, Takaoka A. A weak signal for strong responses: Interferon-α/β revisited. Nat Rev Mol Cell Biol. 2001;2(5):378–86.

350. Wang S, Zhang X, Ju Y, Zhao B, Yan X, Hu J, et al. MicroRNA-146a Feedback Suppresses T Cell Immune Function by Targeting Stat1 in Patients with Chronic Hepatitis B. J Immunol. 2013;191:293–301.

351. Hou J, Wang P, Lin L, Liu X, Ma F, An H, et al. MicroRNA-146a Feedback Inhibits RIG-I-Dependent Type I IFN Production in Macrophages by Targeting TRAF6, IRAK1, and IRAK2. J Immunol. 2009;183(3):2150–8.

352. Ottenhoff THM, Dass RH, Yang N, Zhang MM, Wong HEE, Sahiratmadja E, et al. Genome-Wide Expression Profiling Identifies Type 1 Interferon Response Pathways in Active Tuberculosis. PLoS One. 2012;7(9):e45839.

353. Antonelli LR V, Rothfuchs AG, Gonçalves R, Roffê E, Cheever AW, Bafica A, et al. Intranasal Poly-IC treatment exacerbates tuberculosis in mice through the pulmonary recruitment of a pathogen-permissive monocyte/macrophage population. J Clin Invest. 2010;120(5):1674–82.

354. Ordway D, Henao-Tamayo M, Harton M, Palanisamy G, Troudt J, Shanley C, et al. The Hypervirulent Mycobacterium tuberculosis Strain HN878 Induces a Potent TH1 Response followed by Rapid Down-Regulation. J Immunol. 2007;179:522–31.

355. Cliff JM, Lee J-S, Constantinou N, Cho J-E, Clark TG, Ronacher K, et al. Distinct Phases of Blood Gene Expression Pattern Through Tuberculosis Treatment Reflect Modulation of the Humoral Immune Response. J Infect Dis. 2013;207:18–29.

356. Bloom CI, Graham CM, Berry MPR, Wilkinson KA, Oni T, Rozakeas F, et al. Detectable Changes in The Blood Transcriptome Are Present after Two Weeks of Antituberculosis Therapy. PLoS One. 2012;7(10):e46191.

357. Zak DE, Penn-Nicholson A, Scriba TJ, Thompson E, Suliman S, Amon LM, et al. A blood RNA signature for tuberculosis disease risk: a prospective cohort study. Lancet. 2016;387:2312–22.

358. McNab FW, Ewbank J, Rajsbaum R, Stavropoulos E, Martirosyan A, Paul S, et al. TPL-2 − ERK1/2 Signaling Promotes Host Resistance against Intracellular Bacterial Infection by Negative Regulation of Type I IFN Production. J Immunol. 2013;191:1732–43.

359. Flynn JL, Chan J. What's good for the host is good for the bug. Trends Microbiol. 2005;13(3):98–102.

360. Parker D, Planet PJ, Soong G, Narechania A, Prince A. Induction of Type I Interferon Signaling Determines the Relative Pathogenicity of Staphylococcus aureus Strains. PLoS Pathog. 2014;10(2):e1003951.

361. Wiens KE, Ernst JD. The Mechanism for Type I Interferon Induction by Mycobacterium tuberculosis is Bacterial Strain-Dependent. PLoS Pathog. 2016;12(8):e1005809.

362. Ward CM, Jyonouchi H, Kotenko S V., Smirnov S V., Patel R, Aguila H, et al. Adjunctive treatment of disseminated Mycobacterium avium complex infection with interferon alpha-2b in a patient with complete interferon-gamma receptor R1 deficiency. Eur J Pediatr. 2007;166(9):981–5.

363. Carmona J, Cruz A, Moreira-Teixeira L, Sousa C, Sousa J, Osorio NS, et al. Mycobacterium tuberculosis Strains Are Differentially Recognized by TLRs with an Impact on the Immune Response. PLoS One. 2013;8(6):e67277.

364. Donovan ML, Schultz TE, Duke TJ, Blumenthal A. Type I Interferons in the Pathogenesis of Tuberculosis: Molecular Drivers and Immunological Consequences. Front Immunol. 2017;8:Article 1633.

365. McNab FW, Ewbank J, Howes A, Moreira-Teixeira L, Martirosyan A, Ghilardi N, et al. Type I IFN Induces IL-10 Production in an IL-27–Independent Manner and Blocks Responsiveness to IFN- g for Production of IL-12 and Bacterial Killing in Mycobacterium tuberculosis –Infected Macrophages. J Immunol. 2014;193(7):3600–12.

366. Byrnes AA, Xiaojing M, Cuomo P, Park K, Wahl L, Wolf SF, et al. Type I interferons and IL-12: Convergence and cross-regulation among mediators of cellular immunity. Eur J Immunol. 2001;31(7):2026–34.

367. Gautier G, Humbert M, Deauvieau F, Scuiller M, Hiscott J, Bates EEM, et al. A type I interferon autocrine–paracrine loop is involved in Toll-like receptor-induced interleukin-12p70 secretion by dendritic cells. J Exp Med. 2005;201(9):1435–46.

368. Reinhardt RL, Hong S, Kang S-J, Wang Z, Locksley RM. Visualization of IL-12/23p40 In Vivo Reveals Immunostimulatory Dendritic Cell Migrants that Promote Th1 Differentiation. J Immunol. 2006;177(3):1618–27.

369. Paus RA De, Wengen A Van, Schmidt I, Visser M, Verdegaal EME, Dissel JT Van, et al. Inhibition of the type I immune responses of human monocytes by IFN-α and IFN-β. Cytokine. 2013;61(2):645–55.

370. Mayer-Barber KD, Andrade BB, Oland SD, Amaral EP, Barber DL, Gonzales J, et al. Host-directed therapy of tuberculosis based on interleukin-1 and type I interferon crosstalk. Nature. 2014;511:99–103.

371. Bourigault ML, Segueni N, Rose S, Court N, Vacher R, Vasseur V, et al. Relative contribution of IL-1α, IL-1β and TNF to the host response to mycobacterium tuberculosis and attenuated M. bovis BCG. Immun Inflamm Dis. 2013;1(1):47–62.

372. Novikov A, Cardone M, Thompson R, Shenderov K, Kirschman KD, Mayer-Barber KD, et al. Mycobacterium tuberculosis Triggers Host Type I IFN Signaling To Regulate IL-1 Production in Human Macrophages. J Immunol. 2011;187(5):2540–7.

373. Moreira-Teixeira L, Mayer-Barber K, Sher A, Garra AO. Type I interferons in tuberculosis : Foe and occasionally friend. J Exp Med. 2018;215(5):1273–85.

374. Wang S, He L, Wu J, Zhou Z, Gao Y, Chen J, et al. Transcriptional Profiling of Human Peripheral Blood Mononuclear Cells Identifies Diagnostic Biomarkers That Distinguish Active and Latent Tuberculosis. Front Immunol. 2019;10:Article 2948.

375. Bloom CI, Graham CM, Berry MPR, Rozakeas F, Redford PS, Wang Y, et al. Transcriptional Blood Signatures Distinguish Pulmonary Tuberculosis, Pulmonary Sarcoidosis, Pneumonias and Lung Cancers. PLoS One. 2013;8(8):e70630.

376. Kwan PKW, Periaswamy B, De Sessions PF, Lin W, Molton JS, Naftalin CM, et al. A blood RNA transcript signature for TB exposure in household contacts. BMC Infect Dis. 2020;20(1):403.

377. Lesho E, Forestiero FJ, Hirata MH, Hirata RD, Cecon L, Melo FF, et al. Transcriptional responses of host peripheral blood cells to tuberculosis infection. Tuberculosis. 2011;91:390–9.

378. Lee SW, Wu LSH, Huang GM, Huang KY, Lee TY, Weng JTY. Gene expression profiling identifies candidate biomarkers for active and latent tuberculosis. BMC Bioinformatics. 2016;17(Suppl 1):3.

379. Roe J, Venturini C, Gupta RK, Gurry C, Chain BM, Sun Y, et al. Blood Transcriptomic Stratification of Short-term Risk in Contacts of Tuberculosis. Clin Infect Dis. 2019;70(5):731–7.

380. Prada-Medina CA, Fukutani KF, Kumar NP, Gil-Santana L, Babu S, Lichtenstein F, et al. Systems Immunology of Diabetes-Tuberculosis Comorbidity Reveals Signatures of Disease Complications. Sci Rep. 2017;7(1):1999.

381. Taneja V, Kalra P, Goel M, Khilnani CG, Saini V, Prasad GBKS, et al. Impact and prognosis of the expression of IFN-α among tuberculosis patients. PLoS One. 2020;15(7):e0235488.

382. Llibre A, Bilek N, Bondet V, Darboe F, Mbandi SK, Penn-Nicholson A, et al. Plasma Type I IFN Protein Concentrations in Human Tuberculosis. Front Cell Infect Microbiol. 2019;9:296.

383. Dunning J, Blankley S, Hoang LT, Cox M, Graham CM, James PL, et al. Progression of whole-blood transcriptional signatures from interferon-induced to neutrophil-associated patterns in severe influenza. Nat Immunol. 2018;19(6):625–35.

384. Pan L, Wei N, Jia H, Gao M, Chen X, Wei R, et al. Genome-wide transcriptional profiling identifies potential signatures in discriminating active tuberculosis from latent infection. Oncotarget. 2017;8(68):112907–16.

385. Lu C, Wu J, Wang H, Wang S, Diao N, Wang F, et al. Novel biomarkers distinguishing active tuberculosis from latent infection identified by gene expression profile of peripheral blood mononuclear cells. PLoS One. 2011;6(8):e24290.

386. Blankley S, Graham CM, Turner J, Berry MP, Bloom CI, Xu Z, et al. The Transcriptional

Signature of Active Tuberculosis Reflects Symptom Status in Extra-Pulmonary and Pulmonary Tuberculosis. PLoS One. 2016;11(10):e0162220.

387. Koh GC, Schreiber MF, Bautista R, Maude RR, Dunachie S, Limmathurotsakul D, et al. Host responses to melioidosis and tuberculosis are both dominated by interferon-mediated signaling. PLoS One. 2013;8(1):e54961.

388. Moreira-Teixeira L, Tabone O, Graham CM, Singhania A, Stavropoulos E, Redford PS, et al. Mouse transcriptome reveals potential signatures of protection and pathogenesis in human tuberculosis. Nat Immunol. 2020;21(4):464–76.

389. Singhania A, Verma R, Graham CM, Lee J, Trang T, Lecine P, et al. A modular transcriptional signature identifies heterogeneity of human tuberculosis infection phenotypic. Nat Commun. 2018;9:2308.

390. Waddell SJ, Popper SJ, Rubins KH, Griffiths MJ, Brown PO, Levin M, et al. Dissecting Interferon-Induced Transcriptional Programs in Human Peripheral Blood Cells. PLoS One. 2010;5(3):e9753.

391. Borden EC. Interferons α and β in cancer: therapeutic opportunities from new insights. Nat Rev Drug Discov. 2019;18(3):219–34.

392. Asmana Ningrum R. Human Interferon Alpha-2b: A Therapeutic Protein for Cancer Treatment. Scientifica (Cairo). 2014;2014:1–8.

393. Limmroth V, Putzki N, Kachuck NJ. The interferon beta therapies for treatment of relapsing-remitting multiple sclerosis: Are they equally efficacious? A comparative review of open-label studies evaluating the efficacy, safety, or dosing of different interferon beta formulations alone or i. Ther Adv Neurol Disord. 2011;4(5):281–96.

394. Woo ASJ, Kwok R, Ahmed T. Alpha-interferon treatment in hepatitis B. Ann Transl Med. 2017;5(7):159.

395. de Oliveira Uehara SN, Emori CT, Perez RM, Mendes-Correa MCJ, de Souza Paiva Ferreira A, de Castro Amaral Feldner AC, et al. High incidence of tuberculosis in patients treated for hepatitis C chronic infection. Brazilian J Infect Dis. 2016;20(2):205–9.

396. Mr. Frosty™ Freezing Container [Internet]. [cited 2021 Nov 26]. Available from: https://www.thermofisher.com/order/catalog/product/5100-0001

397. Blankley S, Graham CM, Levin J, Turner J, Berry MPR, Bloom CI, et al. A 380-gene meta-signature of active tuberculosis compared with healthy controls. Eur Respir J. 2016;47(6):1873–6.

398. Maertzdorf J, Weiner J, Mollenkopf HJ, Network TbT, Bauer T, Prasse A, et al. Common patterns and disease-related signatures in tuberculosis and sarcoidosis. Proc Natl Acad Sci U S A. 2012;109(20):7853–8.

399. Maertzdorf J, McEwen G, Weiner J, Tian S, Lader E, Schriek U, et al. Concise gene signature for point-of-care classification of tuberculosis. EMBO Mol Med. 2016;8(2):86–95.

400. Jacobsen M, Repsilber D, Gutschmidt A, Neher A, Feldmann K, Mollenkopf HJ, et al. Candidate biomarkers for discrimination between infection and disease caused by Mycobacterium tuberculosis. J Mol Med. 2007;85(6):613–21.

401. Kaforou M, Wright VJ, Oni T, French N, Anderson ST, Bangani N, et al. Detection of Tuberculosis in HIV-Infected and -Uninfected African Adults Using Whole Blood RNA Expression Signatures: A Case-Control Study. PLoS Med. 2013;10(10):e1001538.

402. Thermo Fisher Scientific. Crt, a relative threshold method for qPCR data analysis on the QuantStudio 12K Flex system with OpenArray technology [Internet]. 2016 [cited 2022 Mar 15]. Available from: http://tools.thermofisher.com/content/sfs/brochures/CO28730-Crt-Tech-note_FLR.pdf

403. Taylor SC, Nadeau K, Abbasi M, Lachance C, Nguyen M, Fenrich J. The Ultimate qPCR Experiment: Producing Publication Quality, Reproducible Data the First Time. Trends Biotechnol. 2019;37(7):761–74.

404. Zhao B, Erwin A, Xue B. How many differentially expressed genes: A perspective from the comparison of genotypic and phenotypic distances. Genomics. 2018;110(1):67–73.

405. Mccarthy DJ, Smyth GK. Testing significance relative to a fold-change threshold is a TREAT. Bioinformatics. 2009;25(6):765–71.

406. Mehta CR. The exact analysis of contingency tables in medical research. Stat Methods Med Res. 1994;3:135–56.

407. Dinno A. Nonparametric pairwise multiple comparisons in independent groups using Dunn's test. Stata J. 2015;15(1):292–300.

408. Mukaka MM. Statistics corner: A guide to appropriate use of correlation coefficient in medical research. Malawi Med J. 2012;24(3):69–71.

409. Karaulov A V, Shulzhenko AE, Karsonova A V. Expression of IFN-Inducible Genes with Antiviral Function OAS1 and MX1 in Health and under Conditions of Recurrent Herpes Simplex Infection. Bull Exp Biol Med. 2017;163(3):355–8.

410. Ignatius IJ, Contreras D, Spurka L, Subramanian A, Allen J, French SW, et al. Characterization of type I interferon pathway during hepatic differentiation of human pluripotent stem cells and hepatitis C virus infection. Stem Cell Res. 2015;15(2):354–64.

411. Critchley-Thorne RJ, Simons DL, Yan N, Miyahira AK, Dirbas FM, Johnson DL, et al. Impaired interferon signaling is a common immune defect in human cancer. Proc Natl Acad Sci U S A. 2009;106(22):9010–5.

412. Sheikh F, Dickensheets H, Gamero AM, Vogel SN. An essential role for IFN-β in the induction of IFN-stimulated gene expression by LPS in macrophages. J Leukoc Biol. 2017;96(4):591–600.

413. Song J, Guan M, Zhao Z, Zhang J. Type i interferons function as autocrine and paracrine factors to induce autotaxin in response to TLR activation. PLoS One. 2015;10(8):e0136629.

414. Livak KJ, Schmittgen TD. Analysis of Relative Gene Expression Data Using Real-Time Quantitative PCR and the 2-ΔΔCt Method. Methods. 2001;25:402–8.

415. Thuong NTT, Dunstan SJ, Chau TTH, Thorsson V, Simmons CP, Quyen NTH, et al. Identification of Tuberculosis Susceptibility Genes with Human Macrophage Gene Expression Profiles. Cox JS, editor. PLoS Pathog. 2008;4(12):e1000229.

416. Sharma B, Upadhyay R, Dua B, Khan NA, Katoch VM, Bajaj B, et al. Mycobacterium tuberculosis secretory proteins downregulate T cell activation by interfering with proximal and downstream T cell signalling events. BMC Immunol. 2015;16(1):67.

417. Schmittgen TD, Livak KJ. Analyzing real-time PCR data by the comparative CT method. Nat Protoc. 2008;3(6):1101–8.

418. McNab FW, Ewbank J, Howes A, Moreira-Teixeira G, Martirosyan A, Ghilardi N, et al. Type I IFN Induces IL-10 Production in an IL-27−Independent Manner and Blocks Responsiveness to IFN- γ for Production of IL-12 and Bacterial Killing in Mycobacterium tuberculosis−Infected Macrophages. J Immunol. 2014;193:3600–12.

419. Mayer-Barber KD, Andrade BB, Barber DL, Hieny S, Feng CG, Caspar P, et al. Innate and Adaptive Interferons Suppress IL-1α and IL-1β Production by Distinct Pulmonary Myeloid Subsets during Mycobacterium tuberculosis Infection. Immunity. 2011;35(6):1023–34.

420. Ordway D, Henao-Tamayo M, Harton M, Palanisamy G, Troudt J, Shanley C, et al. The Hypervirulent Mycobacterium tuberculosis Strain HN878 Induces a Potent TH1 Response followed by Rapid Down-Regulation. J Immunol. 2007;179(1):522–31.

421. Francisco NM, Fang Y-M, Ding L, Feng S, Yang Y, Wu M, et al. Diagnostic accuracy of a selected signature gene set that discriminates active pulmonary tuberculosis and other pulmonary diseases. J Infect. 2017;75:499–510.

422. Suliman S, Thompson EG, Sutherland J, Weiner J, Ota MOC, Shankar S, et al. Four-gene pan-African blood signature predicts progression to tuberculosis. Am J Respir Crit Care Med. 2018;197(9):1198–208.

423. Haas CT, Roe JK, Pollara G, Mehta M, Noursadeghi M. Diagnostic "omics" for active tuberculosis. BMC Med. 2016;14(1):37.

424. Anderson ST, Kaforou M, Brent AJ, Wright VJ, Banwell CM, Chagaluka G, et al. Diagnosis of Childhood Tuberculosis and Host RNA Expression in Africa. N Engl J Med. 2014;370:1712–23.

425. Sambarey A, Devaprasad A, Mohan A, Ahmed A, Nayak S, Swaminathan S, et al. Unbiased Identification of Blood-based Biomarkers for Pulmonary Tuberculosis by Modeling and Mining Molecular Interaction Networks. EBioMedicine. 2017;15:112–26.

426. Alam A, Imam N, Ahmed MM, Tazyeen S, Tamkeen N, Farooqui A, et al. Identification and Classification of Differentially Expressed Genes and Network Meta-Analysis Reveals Potential Molecular Signatures Associated With Tuberculosis. Front Genet. 2019;10:Article 932.

427. Kassa D, Ran L, Jager W De, Broek T Van Den, Jacobi R, Haks C, et al. Discriminative expression of whole blood genes in HIV patients with latent and active TB in Ethiopia. Tuberculosis. 2016;100:25–31.

428. Satproedprai N, Wichukchinda N, Suphankong S, Inunchot W, Kuntima T, Kumpeerasart S, et al. Diagnostic value of blood gene expression signatures in active tuberculosis in Thais: a pilot study. Genes Immun. 2015;16:253–60.

429. Sutherland JS, Loxton AG, Haks MC, Kassa D, Ambrose L, Lee JS, et al. Differential gene expression of activating Fcγ receptor classifies active tuberculosis regardless of human immunodeficiency virus status or ethnicity. Clin Microbiol Infect. 2014;20(4):O230–8.

430. Mihret A, Loxton AG, Bekele Y, Kaufmann SHE, Kidd M, Haks MC, et al. Combination of gene expression patterns in whole blood discriminate between tuberculosis infection states. BMC Infect Dis. 2014;14(1):257.

431. Maertzdorf J, Ota M, Repsilber D, Mollenkopf HJ, Weiner J, Hill PC, et al. Functional Correlations of Pathogenesis-Driven Gene Expression Signatures in Tuberculosis. Doherty TM, editor. PLoS One. 2011;6(10):e26938.

432. Petrilli JD, Araújo LE, da Silva LS, Laus AC, Müller I, Reis RM, et al. Whole blood mRNA expression-based targets to discriminate active tuberculosis from latent infection and other pulmonary diseases. Sci Rep. 2020;10(1):22072.

433. Young BL, Mlamla Z, Gqamana PP, Smit S, Roberts T, Peter J, et al. The identification of tuberculosis biomarkers in human urine samples. Eur Respir J. 2014;43(6):1719–29.

434. Tabone O, Verma R, Singhania A, Chakravarty P, Branchett WJ, Graham CM, et al. Blood transcriptomics reveal the evolution and resolution of the immune response in tuberculosis. J Exp Med. 2021;218(10):e20210915.

435. Darboe F, Kimbung Mbandi S, Thompson EG, Fisher M, Rodo M, van Rooyen M, et al. Diagnostic performance of an optimized transcriptomic signature of risk of tuberculosis in cryopreserved peripheral blood mononuclear cells. Tuberculosis. 2018;108:124–6.

436. Leong S, Zhao Y, Joseph NM, Hochberg NS, Sarkar S, Pleskunas J, et al. Existing blood transcriptional classi fi ers accurately discriminate active tuberculosis from latent infection in individuals from south India. Tuberculosis. 2018;109:41–51.

437. Ahmed M, Thirunavukkarasu S, Rosa BA, Thomas KA, Das S, Rangel-Moreno J, et al. Immune correlates of tuberculosis disease and risk translate across species. Sci Transl Med. 2020;12(528):eaay0233.

438. Singhania A, Verma R, Graham CM, Lee J, Tran T, Richardson M, et al. A modular transcriptional signature identifies phenotypic heterogeneity of human tuberculosis infection. Nat Commun. 2018;9:2308.

439. Lavalett L, Ortega H, Barrera LF. Infection of Monocytes From Tuberculosis Patients With Two Virulent Clinical Isolates of Mycobacterium tuberculosis Induces Alterations in Myeloid Effector Functions. Front Cell Infect Microbiol. 2020;10:Article 163.

440. Aguilo JI, Alonso H, Uranga S, Marinova D, Arbués A, Martino A de, et al. ESX-1-induced apoptosis is involved in cell-to-cell spread of Mycobacterium tuberculosis. Cell Microbiol. 2013;15(12):1994–2005.

441. Augenstreich J, Arbues A, Simeone R, Haanappel E, Wegener A, Sayes F, et al. ESX-1 and phthiocerol dimycocerosates of Mycobacterium tuberculosis act in concert to cause phagosomal rupture and host cell apoptosis. Cell Microbiol. 2017;19(7):e12726.

442. van der Poel CE, Spaapen RM, van de Winkel JGJ, Leusen JHW. Functional Characteristics of the High Affinity IgG Receptor, FcγRI. J Immunol. 2011;186(5):2699–704.

443. Hargreaves CE, Rose-Zerilli MJJ, Machado LR, Iriyama C, Hollox EJ, Cragg MS, et al. Fcγ receptors: genetic variation, function, and disease. Immunol Rev. 2015;268(1):6–24.

444. Sibéril S, Dutertre C-A, Boix C, Bonnin E, Ménez R, Stura E, et al. Molecular aspects of human FcR interactions with IgG: Functional and therapeutic consequences. Immunol Lett. 2006;106:111–8.

445. Zimmermann N, Thormann V, Hu B, Köhler A, Imai-Matsushima A, Locht C, et al. Human isotype-dependent inhibitory antibody responses against Mycobacterium tuberculosis. EMBO Mol Med. 2016;8(11):1325–39.

446. McLean MR, Lu LL, Kent SJ, Chung AW. An Inflammatory Story: Antibodies in Tuberculosis Comorbidities. Front Immunol. 2019;10:2846.

447. Dallenga T, Repnik U, Corleis B, Eich J, Reimer R, Griffiths GW, et al. M. tuberculosis-Induced Necrosis of Infected Neutrophils Promotes Bacterial Growth Following Phagocytosis by Macrophages. Cell Host Microbe. 2017;22(4):519–30.

448. Lerner TR, Borel S, Greenwood DJ, Repnik U, Russell MRG, Herbst S, et al. Mycobacterium tuberculosis replicates within necrotic human macrophages. J Cell Biol. 2017;216(3):583–94.

449. Masood KI, Rottenberg ME, Salahuddin N, Irfan M, Rao N, Carow B, et al. Expression of M. tuberculosis-induced suppressor of cytokine signaling (SOCS) 1, SOCS3, FoxP3 and secretion of IL-6 associates with differing clinical severity of tuberculosis. BMC Infect Dis. 2013;13:13.

450. Paul A, Tang TH, Ng SK. Interferon regulatory factor 9 structure and regulation. Front Immunol. 2018;9:Article 1831.

451. Huber M, Suprunenko T, Ashhurst T, Marbach F, Raifer H, Wolff S, et al. IRF9 Prevents CD8 + T Cell Exhaustion in an Extrinsic Manner during Acute Lymphocytic Choriomeningitis Virus Infection. J Virol. 2017;91(22):1219–36.

452. Suprunenko T, Hofer MJ. The emerging role of interferon regulatory factor 9 in the antiviral host response and beyond. Cytokine Growth Factor Rev. 2016;29:35–43.

453. PrabhuDas MR, Baldwin CL, Bollyky PL, Bowdish DME, Drickamer K, Febbraio M, et al. A Consensus Definitive Classification of Scavenger Receptors and Their Roles in Health and Disease. J Immunol. 2017;198(10):3775–89.

454. Dieudonné A, Torres D, Blanchard S, Taront S, Jeannin P, Delneste Y, et al. Scavenger receptors in human airway epithelial cells: Role in response to double-stranded RNA. PLoS One. 2012 Aug 7;7(8).

455. Canton J, Neculai D, Grinstein S. Scavenger receptors in homeostasis and immunity. Nat Rev Immunol. 2013;13(9):621–34.

456. Bowdish DME, Sakamoto K, Kim MJ, Kroos M, Mukhopadhyay S, Leifer CA, et al. MARCO, TLR2, and CD14 are required for macrophage cytokine responses to mycobacterial trehalose dimycolate and Mycobacterium tuberculosis. PLoS Pathog. 2009;5(6):e1000474.

457. Xu Z, Xu L, Li W, Jin X, Song X, Chen X, et al. Innate scavenger receptor-A regulates adaptive T helper cell responses to pathogen infection. Nat Commun. 2017;8:16035.

458. Sever-Chroneos Z, Tvinnereim A, Hunter RL, Chroneos ZC. Prolonged survival of scavenger receptor class A-deficient mice from pulmonary Mycobacterium tuberculosis infection. Tuberculosis. 2011;91(Suppl.1):S69–74.

459. Qin H, Holdbrooks AT, Liu Y, Reynolds SL, Yanagisawa LL, Benveniste EN. SOCS3 Deficiency Promotes M1 Macrophage Polarization and Inflammation. J Immunol. 2012;189(7):3439–48.

460. Porritt RA, Hertzog PJ. Dynamic control of type I IFN signalling by an integrated network of negative regulators. Trends Immunol. 2015;36(3):150–60.

461. Arnold CE, Whyte CS, Gordon P, Barker RN, Rees AJ, Wilson HM. A critical role for suppressor of cytokine signalling 3 in promoting M1 macrophage activation and function in vitro and in vivo. Immunology. 2014;141(1):96–110.

462. Gordon P, Okai B, Hoare JI, Erwig LP, Wilson HM. SOCS3 is a modulator of human macrophage phagocytosis. J Leukoc Biol. 2016;100(4):771–80.

463. Carow B, Reuschl AK, Gavier-Widén D, Jenkins BJ, Ernst M, Yoshimura A, et al. Critical and Independent Role for SOCS3 in Either Myeloid or T Cells in Resistance to Mycobacterium tuberculosis. PLoS Pathog. 2013;9(7):e1003442.

464. Wu K, Dong D, Fang H, Levillain F, Jin W, Mei J, et al. An interferon-related signature in the transcriptional core response of human macrophages to Mycobacterium tuberculosis infection. PLoS One. 2012/06/04. 2012;7(6):e38367.

465. Oyarzabal E de, García-García L, Rangel-Escareño C, Ferreyra-Reyes L, Orozco L, Herrera MT, et al. Expression of USP18 and IL2RA Is Increased in Individuals Receiving Latent Tuberculosis Treatment with Isoniazid. J Immunol Res. 2019;2019:13.

466. Busse DC, Habgood-Coote D, Clare S, Brandt C, Bassano I, Kaforou M, et al. Interferon-induced Protein-44 and Interferon-induced Protein 44-like restrict replication of Respiratory Syncytial Virus. J Virol. 2020;94(18):e00297-20.

467. Carlton-Smith C, Elliott RM. Viperin, MTAP44, and Protein Kinase R Contribute to the Interferon-Induced Inhibition of Bunyamwera Orthobunyavirus Replication. J Virol. 2012;86(21):11548–57.

468. Power D, Santoso N, Dieringer M, Yu J, Huang H, Simpson S, et al. IFI44 suppresses HIV-1 LTR promoter activity and facilitates its latency. Virology. 2015;481:142–50.

469. Jiang H, Tsang L, Wang H, Liu C. IFI44L as a Forward Regulator Enhancing Host Antituberculosis Responses. J Immunol Res. 2021;2021:Article 5599408.

470. DeDiego ML, Martinez-Sobrido L, Topham DJ. Novel Functions of IFI44L as a Feedback Regulator of Host Antiviral Responses. J Virol. 2019;93(21):e01159-19.

471. Banks DA, Ahlbrand SE, Hughitt VK, Shah S, Mayer-Barber KD, Gel SN, et al. Mycobacterium tuberculosis Inhibits Autocrine Type I IFN Signaling to Increase Intracellular Survival. J Immunol. 2019;202:2348–59.

472. Lavalett L, Ortega H, Barrera LF. Human Alveolar and Splenic Macrophage Populations Display a Distinct Transcriptomic Response to Infection With Mycobacterium tuberculosis. Front Immunol. 2020;11:Article 630.

473. Reuschl A, Edwards MR, Parker R, Connell DW, Hoang L, Halliday A, et al. Innate activation of human primary epithelial cells broadens the host response to Mycobacterium tuberculosis in the airways. PLoS Pathog. 2017;13(9):e1006577.

474. Fensterl V, Sen GC. The ISG56/IFIT1 Gene Family. J Interf Cytokine Res. 2011;31(1):71–8.

475. Li Y, Li C, Xue P, Zhong B, Mao A-P, Ran Y, et al. ISG56 is a negative-feedback regulator of virus-triggered signaling and cellular antiviral response. Proc Natl Acad Sci. 2009;106(19):7945–50.

476. John SP, Sun J, Carlson RJ, Song J, Smelkinson M, Fraser IDC. IFIT1 Exerts Opposing Regulatory Effects on the Inflammatory and Interferon Gene Programs in LPS-Activated Human Macrophages. Cell Rep. 2018;25:95–106.

477. Ranjbar S, Haridas V, Jasenosky LD, Falvo J V., Goldfeld AE. A Role for IFITM Proteins in Restriction of Mycobacterium tuberculosis Infection. Cell Rep. 2015;13(5):874–83.

478. Castelli JC, Hassel BA, Maran A, Paranjape J, Hewitt JA, Li X, et al. The role of 2′-5′ oligoadenylate-activated ribonuclease L in apoptosis. Cell Death Differ. 1998;5(4):313–20.

479. Leisching G, Cole V, Ali AT, Baker B. OAS1, OAS2 and OAS3 restrict intracellular M. tb replication and enhance cytokine secretion. Int J Infect Dis. 2019;80:S77–84.

480. Lyman SD, Escobar S, Rousseau A-M, Armstrong A, Fanslow WC. Identification of CD7 as a Cognate of the Human K12 (SECTM1) Protein *. J Biol Chem. 2000;275(5):3431–7.

481. Wang T, Huang C, Lopez-Coral A, Slentz-Kesler KA, Xiao M, Wherry EJ, et al. K12/SECTM1, an interferon-γ regulated molecule, synergizes with CD28 to costimulate human T cell proliferation. J Leukoc Biol. 2012;91(3):449.

482. Wang T, Ge Y, Xiao M, Lopez-Coral A, Li L, Roesch A, et al. SECTM1 produced by tumor cells attracts human monocytes via CD7-mediated activation of the PI3K pathway. J Invest Dermatol. 2014;134(4):1108–18.

483. Kamata H, Yamamoto K, Wasserman GA, Zabinski MC, Yuen CK, Lung WY, et al. Epithelial Cell–Derived Secreted and Transmembrane 1a Signals to Activated Neutrophils during Pneumococcal Pneumonia. Am J Respir Cell Mol Biol. 2016;55(3):407–18.

484. Kumar V. Pulmonary Innate Immune Response Determines the Outcome of Inflammation During Pneumonia and Sepsis-Associated Acute Lung Injury. Front Immunol. 2020;11:Article 1722.

485. Yao K, Chen Q, Wu Y, Liu F, Chen X, Zhang Y. Unphosphorylated STAT1 represses apoptosis in macrophages during Mycobacterium tuberculosis infection. 2017;1740–51.

486. Lim Y-J, Yi M-H, Choi J-A, Lee J, Han J-Y, Jo S-H, et al. Roles of endoplasmic reticulum stress-mediated apoptosis in M1-polarized macrophages during mycobacterial infections. Sci Rep. 2016;6:37211.

487. Terenzi F, Hui DJ, Merrick WC, Sen GC. Distinct Induction Patterns and Functions of Two Closely Related Interferon-inducible Human Genes, ISG54 and ISG56 *. J Biol Chem. 2006;281:34064–71.

488. Prabhakar S, Qiao Y, Hoshino Y, Weiden M, Canova A, Giacomini E, et al. Inhibition of Response to Alpha Interferon by Mycobacterium tuberculosis. Infect Immun. 2003;71(5):2487–97.

489. Kellar KL, Gehrke J, Weis SE, Mahmutovic-Mayhew A, Davila B, Zajdowicz MJ, et al. Multiple Cytokines Are Released When Blood from Patients with Tuberculosis Is Stimulated with Mycobacterium tuberculosis Antigens. PLoS One. 2011;6(11):e26545.

490. Novikov A, Cardone M, Thompson R, Shenderov K, Kirschman KD, Mayer–Barber KD, et al. Mycobacterium tuberculosis triggers host type I interferon signaling to regulate IL-1β production in human macrophages. J Immunol. 2011;187(5):2540–7.

491. McNab FW, Ewbank J, Howes A, Moreira-Teixeira L, Martirosyan A, Ghilardi N, et al. Type I IFN induces IL-10 production in an IL-27-independent manner and blocks responsiveness to IFN-γ for production of IL-12 and bacterial killing in Mycobacterium tuberculosis-infected macrophages. J Immunol. 2014;193(7):3600–12.

492. Barnes PF, Lu S, Abrams JS, Wang E, Yamamura M, Modlin3 RL. Cytokine Production at the Site of Disease in Human Tuberculosis. Infect Immun. 1993;61(8):3482–9.

493. Bonecini-Almeida MG, Ho JL, Boéchat N, Huard RC, Chitale S, Doo H, et al. Down-Modulation of Lung Immune Responses by Interleukin-10 and Transforming Growth Factor β (TGF-β) and Analysis of TGF-β Receptors I and II in Active Tuberculosis. Infect Immun. 2004;72(5):2628–34.

494. Verbon A, Juffermans N, Deventer SJH Van, Speelman P, Deutekom H Van, Poll T Van Der. Serum concentrations of cytokines in patients with active tuberculosis (TB) and after treatment. Clin Exp Immunol. 1999;115(1):110.

495. Kumar NP, Gopinath V, Sridhar R, Hanna LE, Banurekha V V., Jawahar MS, et al. IL-10 Dependent Suppression of Type 1, Type 2 and Type 17 Cytokines in Active Pulmonary Tuberculosis. PLoS One. 2013;8(3):e59572.

496. Redford PS, Murray PJ, O'Garra A. The role of IL-10 in immune regulation during M. tuberculosis infection. Mucosal Immunol. 2011;4(3):261–70.

497. Ma J, Yang B, Yu S, Zhang Y, Zhang X, Lao S, et al. Tuberculosis antigen-induced expression of IFN-α in tuberculosis patients inhibits production of IL-1β. FASEB J. 2014;28(7):3238–48.

498. Abdalla AE, Lambert N, Duan X, Xie J. Interleukin-10 family and tuberculosis: An old story renewed. Int J Biol Sci. 2016;12(6):710–7.

499. Turner J, Gonzalez-Juarrero M, Ellis DL, Basaraba RJ, Kipnis A, Orme IM, et al. In Vivo IL-10 Production Reactivates Chronic Pulmonary Tuberculosis in C57BL/6 Mice. J Immunol. 2002;169(11):6343–51.

500. Ameglio F, Casarini M, Capoluongo E, Mattia P, Puglisi G, Giosuè S. Post-treatment changes of six cytokines in active pulmonary tuberculosis: differences between patients with stable or increased fibrosis. Int J Tuberc Lung Dis. 2005;9(1):98–104.

501. Fox KA, Kirwan DE, Whittington AM, Krishnan N, Robertson BD, Gilman RH, et al. Platelets Regulate Pulmonary Inflammation and Tissue Destruction in Tuberculosis. Am J Respir Crit Care Med. 2018;198(2):245–55.

502. O'Shea MK, Tanner R, Müller J, Harris SA, Wright D, Stockdale L, et al. Immunological correlates of mycobacterial growth inhibition describe a spectrum of tuberculosis infection. Sci Rep. 2018;8(1):14480.

503. Andrae J, Gallini R, Betsholtz C. Role of platelet-derived growth factors in physiology and medicine. Genes Dev. 2008;22(10):1276.

504. Wangoo A, Taylor IK, Haynes AR, Shaw RJ. Up-regulation of alveolar macrophage platelet-derived growth factor-B (PDGF-B) mRNA by interferon-gamma from Mycobacterium tuberculosis antigen (PPD)-stimulated lymphocytes. Clin Exp Immunol. 1993;94(1):43.

505. Bonner JC. Regulation of PDGF and its receptors in fibrotic diseases. Cytokine Growth Factor Rev. 2004;15:255–73.

506. Cho JS, Fang TC, Reynolds TL, Sofia DJ, Hamann S, Burkly LC. PDGF-BB Promotes Type I IFN-Dependent Vascular Alterations and Monocyte Recruitment in a Model of Dermal Fibrosis. PLoS One. 2016;11(9):e0162758.

507. Mihret A, Bekele Y, Bobosha K, Kidd M, Aseffa A, Howe R, et al. Plasma cytokines and chemokines differentiate between active disease and non-active tuberculosis infection. J Infect. 2013;66:357–65.

508. Proost P, Wuyts A, Damme J van. Human monocyte chemotactic proteins-2 and -3: structural and functional comparison with MCP-1. J Leukoc Biol. 1996;59(1):67–74.

509. Yao X, Liu Y, Liu Y, Liu W, Ye Z, Zheng C, et al. Multiplex analysis of plasma cytokines/chemokines showing different immune responses in active TB patients, latent TB infection and healthy participants. Tuberculosis. 2017;107:88–94.

510. Ruhwald M, Bjerregaard-Andersen M, Rabna P, Eugen-Olsen J, Ravn P. IP-10, MCP-1, MCP-2, MCP-3, and IL-1RA hold promise as biomarkers for infection with M. tuberculosis in a whole blood based T-cell assay. BMC Res Notes. 2009;2:19.

511. Rambaran S, Naidoo K, Lewis L, Hassan-Moosa R, Govender D, Samsunder N, et al. Effect of Inflammatory Cytokines/Chemokines on Pulmonary Tuberculosis Culture Conversion and Disease Severity in HIV-Infected and -Uninfected Individuals From South Africa. Front Immunol. 2021;12:Article 641065.

512. Bauer JW, Baechler EC, Petri M, Batliwalla FM, Crawford D, Ortmann WA, et al. Elevated Serum Levels of Interferon-Regulated Chemokines Are Biomarkers for Active Human Systemic Lupus Erythematosus. PLoS Med. 2006;3(12):e491.

513. Menten P, Proost P, Struyf S, Van Coillie E, Put W, Lenaerts JP, et al. Differential induction of monocyte chemotactic protein-3 in mononuclear leukocytes and fibroblasts by interferon-α/β and interferon-γ reveals MCP-3 heterogeneity. Eur J Immunol. 1999;29(2):678–85.

514. Kumar NP, Moideen K, Banurekha V V, Nair D, Babu S. Plasma Proinflammatory Cytokines Are Markers of Disease Severity and Bacterial Burden in Pulmonary Tuberculosis. Open Forum Infect Dis. 2019;6(7):ofz257.

515. Wu CF, Andzinski L, Kasnitz N, Kröger A, Klawonn F, Lienenklaus S, et al. The lack of type i interferon induces neutrophil-mediated pre-metastatic niche formation in the mouse lung. Int J Cancer. 2015;137(4):837–47.

516. Andzinski L, Wu CF, Lienenklaus S, Kröger A, Weiss S, Jablonska J. Delayed apoptosis of tumor associated neutrophils in the absence of endogenous IFN-β. Int J Cancer. 2015;136(3):572–83.

517. Chung HK, Kim SW, Byun SJ, Ko EM, Chung HJ, Woo JS, et al. Enhanced biological effects of Phe140Asn, a novel human granulocyte colony-stimulating factor mutant, on HL60 cells. BMB Rep. 2011;44(10):686–91.

518. Latorre I, Díaz J, Mialdea I, Serra-Vidal M, Altet N, Prat C, et al. IP-10 is an accurate biomarker for the diagnosis of tuberculosis in children. J Infect. 2014;69:590–9.

519. Whittaker E, Gordon A, Kampmann B. Is IP-10 a Better Biomarker for Active and Latent Tuberculosis in Children than IFNγ? PLoS One. 2008;3(12):e3901.

520. Qiu X, Tang Y, Zou R, Zeng Y, Yue Y, Li W, et al. Diagnostic accuracy of interferon-gamma-induced protein 10 for differentiating active tuberculosis from latent tuberculosis: A meta-analysis. Sci Rep. 2019;9:11408.

521. Qiu X, Xiong T, Su X, Qu Y, Ge L, Yue Y, et al. Accumulate evidence for IP-10 in diagnosing pulmonary tuberculosis. BMC Infect Dis. 2019;19:924.

522. Suárez I, Rohr S, Stecher M, Lehmann C, Winter S, Jung N, et al. Plasma interferon-γ-inducible protein 10 (IP-10) levels correlate with disease severity and paradoxical reactions in extrapulmonary tuberculosis. Infection. 2020;49(3):437–45.

523. Bhattacharyya C, Majumder PP, Pandit B. CXCL10 is overexpressed in active

tuberculosis patients compared to M. tuberculosis-exposed household contacts. Tuberculosis. 2018;109:8–16.

524. Aabye MG, Ruhwald M, PrayGod G, Jeremiah K, Faurholt-Jepsen M, Faurholt-Jepsen D, et al. Potential of interferon-γ-inducible protein 10 in improving tuberculosis diagnosis in HIV-infected patients. Eur Respir J. 2010;36(6):1488–90.

525. Lande R, Giacomini E, Grassi T, Remoli E, Iona E, Miettinen M, et al. IFN- αβ Released by Mycobacterium tuberculosis -Infected Human Dendritic Cells Induces the Expression of CXCL10: Selective Recruitment of NK and Activated T Cells. J Immunol. 2003;170:1174–82.

526. Metzemaekers M, Vanheule V, Janssens R, Struyf S, Proost P. Overview of the Mechanisms that May Contribute to the Non-Redundant Activities of Interferon-Inducible CXC Chemokine Receptor 3 Ligands. Front Immunol. 2018;8:1970.

527. Liu M, Guo S, Hibbert JM, Jain V, Singh N, Wilson NO, et al. CXCL10/IP-10 in infectious diseases pathogenesis and potential therapeutic implications. Cytokine Growth Factor Rev. 2011;22(3):121–30.

528. Hunter RL. Pathology of post primary tuberculosis of the lung: an illustrated critical review. Tuberculosis (Edinb). 2011;91(6):497–509.

529. Evans S, Butler JR, Mattila JT, Kirschner DE. Systems biology predicts that fibrosis in tuberculous granulomas may arise through macrophage-to-myofibroblast transformation. PLOS Comput Biol. 2020 Dec 28;16(12):e1008520.

530. Mishra BB, Moura-Alves P, Sonawane A, Hacohen N, Griffiths G, Moita LF, et al. Mycobacterium tuberculosis protein ESAT-6 is a potent activator of the NLRP3/ASC inflammasome. Cell Microbiol. 2010;12(8):1046–63.

531. Kitade H, Sawamoto K, Nagashimada M, Inoue H, Yamamoto Y, Sai Y, et al. CCR5 plays a critical role in obesity-induced adipose tissue inflammation and insulin resistance by regulating both macrophage recruitment and M1/M2 status. Diabetes. 2012;61(7):1680–90.

532. Saukkonen JJ, Bazydlo B, Thomas M, Strieter RM, Keane J, Kornfeld H. β-Chemokines Are Induced by Mycobacterium tuberculosis and Inhibit Its Growth. Infect Immun. 2002;70(4):1684.

533. Russo RC, Garcia CC, Teixeira MM, Amaral FA. The CXCL8/IL-8 chemokine family and its receptors in inflammatory diseases. Expert Rev Clin Immunol. 2014;10(5):593–619.

534. Laux L, Delcroix M, Dalla ER, Prestes I V, Milano M, Francis SS, et al. A real-time PCR signature to discriminate between tuberculosis and other pulmonary diseases. Tuberculosis. 2015;95(4):421–5.

535. Ashenafi S, Aderaye G, Bekele A, Zewdie M, Aseffa G, Hoang AT, et al. Progression of clinical tuberculosis is associated with a Th2 immune response signature in combination with elevated levels of SOCS3. Clin Immunol. 2014;151(2):84–99.

536. Ruan Q ling, Yang Q luan, Gao Y xin, Wu J, Lin S ran, Zhou JY, et al. Transcriptional signatures of human peripheral blood mononuclear cells can identify the risk of tuberculosis progression from latent infection among individuals with silicosis. Emerg Microbes Infect. 2021;10(1):1536–44.

537. Mistry R, Cliff JM, Clayton CL, Beyers N, Mohamed YS, Wilson PA, et al. Gene-Expression Patterns in Whole Blood Identify Subjects at Risk for Recurrent Tuberculosis. J Infect Dis. 2007;195:357–65.

538. Wu J, Wang S, Lu C, Shao L, Gao Y, Zhou Z, et al. Multiple cytokine responses in discriminating between active tuberculosis and latent tuberculosis infection. Tuberculosis. 2017;102:68–75.

539. Tram TTB, Nhung HN, Vijay S, Hai HT, Thu DDA, Ha VTN, et al. Virulence of Mycobacterium tuberculosis Clinical Isolates Is Associated With Sputum Pre-treatment Bacterial Load, Lineage, Survival in Macrophages, and Cytokine Response. Front Cell Infect Microbiol. 2018;8:417.

540. Wiens KE, Ernst JD. The Mechanism for Type I Interferon Induction by Mycobacterium tuberculosis is Bacterial Strain-Dependent. PLoS Pathog. 2016;12(8):e1005809.

541. Dorhoi A, Yeremeev V, Nouailles G, Weiner J, Jörg S, Heinemann E, et al. Type I IFN signaling triggers immunopathology in tuberculosis-susceptible mice by modulating lung phagocyte dynamics. Eur J Immunol. 2014;44(8):2380.

542. Scriba TJ, Penn-Nicholson A, Shankar S, Hraha T, Thompson EG, Sterling D, et al. Sequential inflammatory processes define human progression from M. tuberculosis infection to tuberculosis disease. PLoS Pathog. 2017;13(11):e1006687.

543. Venkatasubramanian S, Cheekatla S, Paidipally P, Tripathi D, Welch E, Tvinnereim AR, et al. IL-21-dependent expansion of memory-like NK cells enhances protective immune responses against Mycobacterium tuberculosis. Mucosal Immunol. 2017;10(4):1031.

544. Choreño-Parra JA, Weinstein LI, Yunis EJ, Zúñiga J, Hernández-Pando R. Thinking Outside the Box: Innate- and B Cell-Memory Responses as Novel Protective Mechanisms Against Tuberculosis. Front Immunol. 2020;11:226.

545. Sica A, Mantovani A. Macrophage plasticity and polarization: In vivo veritas. J Clin Invest. 2012;122(3):787–95.

546. Lawrence T, Natoli G. Transcriptional regulation of macrophage polarization: enabling diversity with identity. Nat Rev Immunol 2011 1111. 2011;11:750–61.

547. Bergman SJ, Ferguson MC, Santanello C. Interferons as Therapeutic Agents for Infectious Diseases. Infect Dis Clin North Am. 2011;25(4):819–34.

548. Farah R, Awad J. The association of interferon with the development of pulmonary tuberculosis. Int J Clin Pharmacol Ther. 2007;45(11):598–600.

549. Lin S-Y, Chen T-C, Lu P-L, Lin C-Y, Lin W-R, Yang Y-H, et al. Incidence rates of tuberculosis in chronic hepatitis C infected patients with or without interferon based therapy: a population-based cohort study in Taiwan. BMC Infect Dis. 2014;14:705.

550. Sirbu CA, Dantes E, Plesa CF, Axelerad AD, Ghinescu MC. Active pulmonary tuberculosis triggered by interferon beta-1b therapy of multiple sclerosis: Four case reports and a literature review. Med. 2020;56:202.

551. Telesca C, Angelico M, Piccolo P, Nosotti L, Morrone A, Longhi C, et al. Interferon-alpha treatment of hepatitis D induces tuberculosis exacerbation in an immigrant. J Infect. 2007;54(4):e223–6.

552. Dawany N, Showe LC, Kossenkov A V., Chang C, Ive P, Conradie F, et al. Identification of a 251 gene expression signature that can accurately detect M. tuberculosis in patients with and without HIV co-infection. PLoS One. 2014;9(2):e89925.

553. Naranbhai V, Fletcher HA, Tanner R, O'Shea MK, McShane H, Fairfax BP, et al. Distinct Transcriptional and Anti-Mycobacterial Profiles of Peripheral Blood Monocytes Dependent on the Ratio of Monocytes: Lymphocytes. EBioMedicine. 2015;2(11):1619–26.

554. Gupta VK, Paul S, Dutta C. Geography, Ethnicity or Subsistence-Specific Variations in Human Microbiome Composition and Diversity. Front Microbiol. 2017;8:Article 1162.

555. Namasivayam S, Kauffman KD, McCulloch JA, Yuan W, Thovarai V, Mittereder LR, et al. Correlation between Disease Severity and the Intestinal Microbiome in Mycobacterium tuberculosis-Infected Rhesus Macaques. MBio. 2019;10(3):e01018-19.

556. Khaliq A, Ravindran R, Afzal S, Jena PK, Akhtar MW, Ambreen A, et al. Gut microbiome dysbiosis and correlation with blood biomarkers in active-tuberculosis in endemic setting. PLoS One. 2021;16(1):e0245534.

557. Coussens AK, Wilkinson RJ, Nikolayevskyy V, Elkington PT, Hanifa Y, Islam K, et al. Ethnic Variation in Inflammatory Profile in Tuberculosis. PLOS Pathog. 2013;9(7):e1003468.

558. Walter ND, Miller MA, Vasquez J, Weiner M, Chapman A, Engle M, et al. Blood transcriptional biomarkers for active tuberculosis among patients in the United States: A case-control study with systematic cross-classifier evaluation. J Clin Microbiol. 2016;54(2):274–82.

559. Hilda JN, Das S, Tripathy SP, Hanna LE. Role of neutrophils in tuberculosis: A bird's eye view. Innate Immun. 2020;26(4):240–7.

560. Huyton T, Göttmann W, Bade-Döding C, Paine A, Blasczyk R. The T/NK cell co-stimulatory molecule SECTM1 is an IFN "early response gene" that is negatively regulated by LPS in Human monocytic cells. Biochim Biophys Acta - Gen Subj. 2011;1810(12):1294–301.

Appendix 1: Abbreviations

ACTB	Beta-actin
ADCC	Antibody-dependent cellular cytotoxicity
AEC	Airway epithelial cell
AIM2	Absent in melanoma 2
ANKRD22	Ankyrin Repeat Domain 22
APC	Antigen presenting cells
APOL1	Apolipoprotein L1
Arg1	Arginase 1
ASL	Airway surface liquid
ATB	Active tuberculosis
BAL	Broncho-alveolar lavage
BATF2	Basic Leucine Zipper ATF-Like Transcription Factor 2
β -ME	β-mercaptoethanol
BMI	Body mass index
BCG	Bacillus Calmette–Guérin
CAMP	Cathelicidin Antimicrobial Peptide
CARD9	Caspase recruitment domain-containing protein 9
CCL	Chemokine (C-C motif) ligand
CXCL	C-X-C Motif Chemokine Ligand
CD	Cluster of Differentiation
cDNA	Complementary Deoxyribonucleic acid
CFP-10	Culture filtrate protein 10
cGAS	cyclic GMP-AMP synthase
CLR	C-type lectin receptors
CR	Complement receptors
CRISPR	Clustered regularly interspaced short palindromic repeats
CXCL	Chemokine (C-X-C motif) ligand
DC	Dendritic cell
DEG	Differentially expressed genes
DEPC	Diethyl pyrocarbonate
DMSO	Dimethyl sulfoxide
DNA	Deoxyribonucleic acid
DsDNA	Double-stranded Deoxyribonucleic acid
DUSP2	Dual Specificity Phosphatase 2
EGF	Epidermal growth factor
EPTB	Extra-pulmonary tuberculosis
ESAT-6	Early secretory antigen target
ESRD	End-stage renal disease
ESX-1	(ESAT)-6 secretion system-1
ETV7	ETS Variant Transcription Factor 7
FAM26F	Family with Sequence Similarity 26 Member F
FBS	Fetal bovine serum
FCγR	Fc gamma receptors
FGF-2	Fibroblast growth factor 2
FM	Fluorescence microscopy
GBS	Group B streptococci
GBP	Guanylate Binding Protein
G-CSF	Granulocyte colony-stimulating factor
γδ T cells	Gamma-delta T cells

gDNA	Genomic Deoxyribonucleic acid
GM-CSF	Granulocyte-macrophage colony-stimulating factor
GRO	Growth-regulated protein
HIV	Human immunodeficiency virus
HPRT1	Hypoxanthine phosphoribosyltransferase 1
IFI	Interferon Induced Protein
IFI44L	Interferon Induced Protein 44 Like
IFIT	Interferon Induced Protein with Tetratricopeptide Repeats
IFITM	Interferon Induced Transmembrane Protein
IFN	Interferon
IFN-α	Interferon alpha
IFN-β	Interferon beta
IFN-γ	Interferon gamma
IFNAR	Interferon alpha receptor
IFNGR	Interferon gamma receptor
IFNLR	Interferon lambda receptor
IgG	Immunoglobulin G
IGRA	Interferon gamma release assay
IL	Interleukin
IL-1RA	Interleukin 1 receptor antagonist
IL-15RA	Interleukin 15 Receptor Subunit Alpha
iNKT	Invariant natural killer T cell
iNOS	Inducible nitric oxide synthase
IP-10	Interferon gamma-induced protein 10
IRAK	Interleukin-1 receptor-associated kinase
IRF	Interferon regulatory factor
ISG	Interferon stimulated gene
ISGF3	Interferon Stimulated Gene Factor 3
ISRE	Interferon-stimulated Response Element
JAK	Janus kinase
LAG3	Lymphocyte Activating 3
LTBI	Latent tuberculosis infection
MAIT	Mucosal-associated invariant T cells
MAPK	Mitogen-activated protein kinase
MARCO	Macrophage receptor with collagenous structure
MCP	Macrophage-derived chemokine
MGIT	Mycobacterial growth in tube
MHC	Major Histocompatibility Complex
MIP-1	Macrophage inflammatory protein 1
MLR	Monocyte/ lymphocyte ratio
MODS	Microscopic observation drug susceptibility
MR	Mannose receptor
MSMD	Mendelian susceptibility to mycobacterial diseases
MSR1	Macrophage Scavenger Receptor
MTBC	*Mycobacterium tuberculosis* complex

Mtb WCL	*Mycobacterium tuberculosis* Whole cell lysate
MX	MX Dynamin-Like GTPase
MyD88	Myeloid differentiation factor 88
NAAT	Nucleic acid amplification test
NET	Neutrophil extracellular traps
NFκB	Nuclear Factor kappa-light-chain-enhancer of activated B cells
NK cells	Natural killer cells
NLR	Nucleotide-binding and oligomerization domain (NOD)-like receptors
NO	Nitric oxide
Nos2	Nitric Oxide Synthase 2
NTM	Non-tuberculous mycobacteria
OAS	2'-5'-Oligoadenylate Synthetase
OSM	Oncostatin M
P13K	Phosphoinositide 3-kinases
PAMP	Pathogen-associated molecular patterns
PBMC	Peripheral blood mononuclear cells
PBS	Phosphate-buffered saline
PCA	Principal component analysis
PCR	Polymerase chain reaction
pDC	Plasmacytoid dendritic cell
PDGF	Platelet Derived Growth Factor
PFMC	Pleural fluid mononuclear cells
PPD	Purified protein derivative
PRR	Pattern recognition receptor
PSMB8	Proteasome Subunit Beta 8
PTB	Pulmonary tuberculosis
QC	Quality control
QFT	QuantiFERON test
RANTES	Regulated on Activation, Normal T Expressed and Secreted
RD	Region of Difference
RNA	Ribonucleic acid
RNI	Reactive nitrogen intermediates
ROI	Reactive oxygen intermediates
Rpm	Rotations per minute
RPMI	Roswell Park Memorial Institute
RT-qPCR	Reverse transcription-quantitative Polymerase Chain Reaction
SAGE	Serial Analysis of Gene Expression
SCARF1	Scavenger Receptor Class F Member 1
sCD40L	Soluble CD40 ligand
SECTM1	Secreted and Transmembrane 1
SEPT1	Septin 4
SERPING1	Serpin Family G Member 1
SLE	Systemic lupus erythematosus
SOCS	Suppressor Of Cytokine Signaling
SR	Scavenger receptor
ssRNA	single-stranded Ribonucleic acid

STAT	Signal transducers and activators of transcription
STING	STimulator of Interferon Genes
TAK1	Transforming growth factor-β-activated kinase 1
TAP1	Transporter 1, ATP Binding Cassette Subfamily B Member
TB	Tuberculosis
TbD1	Tuberculosis–specific deletion region 1
TCR	T-cell receptor
TDM	Trehalose 6′6-dimycolate
Th	T helper
TNF	Tumor necrosis factor
TNFSF10	TNF Superfamily Member 10
TRAFD1	TRAF-Type Zinc Finger Domain Containing 1
TRAM	TRIF-related adaptor molecule
TRIF	TIR-domain-containing adapter-inducing interferon-β
TST	Tuberculin skin test
TYK	Tyrosine kinase
UBE2L6	Ubiquitin Conjugating Enzyme E2 L6
USP18	Ubiquitin Specific Peptidase 18
VEGF	Vascular endothelial growth factor
WHO	World Health Organization
ZN	Ziehl-Neelsen staining

Appendix 2: Supplementary Tables

Table S1. Median relative gene expression results in unstimulated, IFN-α -, IFN-β- and Mtb-WCL-stimulated PBMCs

	unstimulated					IFN-α				
Genes	HC	TST	LTBI	ATB	**p-value**	HC	TST	LTBI	ATB	**p-value**
ANKRD22	0.00011	0.000131	0.00015	0.000234	**0.136**	0.002588	0.002376	0.002482	0.003765	**0.019**
APOL1	0.000564	0.000584	0.000539	0.00048	**0.833**	0.00548	0.005767	0.005673	0.005006	**0.783**
BATF2	0.000564	0.00005	0.000057	0.000051	**0.719**	0.000647	0.000699	0.000768	0.001109	**0.075**
CAMP	0.000013		0.000086							
CCL8	0.000116	0.000175	0.000084	0.000222	**0.091**	0.015753	0.014111	0.013818	0.022401	**0.046**
CXCL10	0.000249	0.000928	0.000492	0.000527	**0.323**	0.039424	0.055564	0.057678	0.054174	**0.816**
CXCL11	0.000054	0.000117	0.000126	0.000077	**0.638**	0.055503	0.046279	0.041297	0.045151	**0.912**
CXCL9		0.000086	0.000047			0.001645	0.002309	0.002553	0.002781	**0.164**
ETV7	0.000043	0.000054	0.000069	0.000064	**0.963**	0.001193	0.000968	0.001213	0.000941	**0.749**
FAM26F	0.00012	0.000131	0.000132	0.000184	**0.367**	0.001443	0.001268	0.001124	0.001771	**0.069**
FCGR1A	0.000108	0.000116	0.000078	0.000239	**0.001**	0.000742	0.0007	0.000604	0.001381	**0.008**
FCGR1B	0.00005	0.000044	0.000032	0.000067		0.00009	0.000114	0.000122	0.000305	**0.013**
GBP1	0.003171	0.003786	0.004385	0.00466	**0.158**	0.043329	0.050718	0.060482	0.054715	**0.433**
GBP2	0.005688	0.005727	0.004646	0.005754	**0.601**	0.020685	0.019823	0.018834	0.017138	**0.774**
GBP4	0.001214	0.001264	0.001406	0.001366	**0.793**	0.013551	0.011843	0.015673	0.012629	**0.404**
GBP5	0.002819	0.003615	0.002967	0.003958	**0.253**	0.026405	0.031067	0.031576	0.032506	**0.665**
IFI35	0.000514	0.000655	0.000621	0.00064	**0.551**	0.007842	0.007452	0.009024	0.008171	**0.581**
IFI44	0.000629	0.000698	0.000913	0.000507	**0.685**	0.007139	0.007267	0.009396	0.008277	**0.15**
IFI44L	0.000279	0.000403	0.000637	0.000122	**0.196**	0.005681	0.005439	0.007206	0.005836	**0.188**
IFIT1	0.00055	0.000763	0.001051	0.000556	**0.654**	0.045927	0.032507	0.037956	0.038357	**0.479**
IFIT2	0.000306	0.00054	0.000696	0.000363	**0.285**	0.016122	0.01575	0.016811	0.017696	**0.592**
IFIT3	0.000799	0.00124	0.001134	0.00082	**0.558**	0.035667	0.034889	0.037251	0.035466	**0.476**
IFITM1	0.0096	0.011109	0.00774	0.007629	**0.556**	0.07033	0.06038	0.066242	0.062917	**0.411**
IFITM2	0.003429	0.003965	0.00382	0.003449	**0.764**	0.00725	0.007135	0.007772	0.007555	**0.928**
IFITM3	0.000746	0.001308	0.001192	0.001762	**0.076**	0.017227	0.02052	0.020051	0.022765	**0.519**
IL10	0.000087	0.000136	0.00012	0.000186	**0.144**	0.000156	0.000143	0.00023	0.000211	**0.203**
IL12B										
IL1A	0.000614	0.0009	0.001099	0.001177	**0.482**	0.000112	0.000186	0.00025	0.000318	**0.165**
IL1B	0.019846	0.027808	0.034321	0.04258	**0.149**	0.005867	0.009211	0.011542	0.017254	**0.107**
IRF1	0.003582	0.00314	0.00291	0.003361	**0.743**	0.006818	0.007148	0.007708	0.006891	**0.359**
IRF7	0.001497	0.001461	0.001776	0.001396	**0.867**	0.011922	0.010364	0.012225	0.011458	**0.386**
IRF9	0.000756	0.001109	0.001	0.000926	**0.183**	0.002319	0.002255	0.00283	0.00266	**0.168**
ISG15	0.000806	0.001039	0.001111	0.000695	**0.776**	0.026189	0.024768	0.027473	0.022801	**0.955**
LAG3	0.000079	0.000133	0.000063	0.000077	**0.546**	0.000674	0.0014	0.001284	0.00102	**0.381**
MSR1	0.000406	0.000575	0.000809	0.001292	**0.002**	0.008749	0.007011	0.008058	0.01169	**0.039**
MX1	0.002899	0.004824	0.003813	0.002563	**0.902**	0.05739	0.050541	0.054943	0.05197	**0.627**
MX2	0.002776	0.003126	0.002994	0.00203	**0.854**	0.036448	0.032262	0.039269	0.039301	**0.445**
OAS1	0.001177	0.001325	0.001168	0.000846	**0.827**	0.018486	0.01342	0.017537	0.01523	**0.387**
OAS3	0.000799	0.001577	0.001218	0.000882	**0.551**	0.02252	0.025872	0.027976	0.023716	**0.615**
OASL	0.005609	0.00462	0.006289	0.00658	**0.474**	0.03108	0.027698	0.031903	0.031941	**0.344**
PSMB8	0.001799	0.001954	0.001622	0.001763	**0.931**	0.005802	0.005855	0.006266	0.005427	**0.738**
SCARF1	0.000069	0.000062	0.000066	0.000078	**0.467**	0.000081	0.000143	0.000131	0.000126	**0.746**
SECTM1	0.000293	0.000413	0.000356	0.000587	**0.002**	0.003362	0.003956	0.003012	0.004438	**0.289**
SEPTIN4	0.000037	0.000038	0.00004	0.000042		0.000056	0.000038	0.000059	0.00006	
SERPING1	0.000056	0.000053	0.000054	0.000086	**0.448**	0.001128	0.001535	0.00144	0.001703	**0.192**
SOCS1	0.000557	0.000699	0.000721	0.000814	**0.426**	0.001257	0.001912	0.002079	0.001955	**0.091**
SOCS3	0.00511	0.004519	0.00379	0.005842	**0.282**	0.006572	0.006053	0.007316	0.006826	**0.823**
STAT1	0.007869	0.009211	0.007031	0.008607	**0.523**	0.051015	0.046615	0.048865	0.050301	**0.562**
TAP1	0.003352	0.003661	0.003723	0.004353	**0.684**	0.013332	0.013112	0.016349	0.016653	**0.251**
TNFSF10	0.000535	0.000615	0.000549	0.000756	**0.415**	0.016218	0.013778	0.014643	0.01848	**0.186**
TRAFD1	0.000874	0.00099	0.000913	0.001078	**0.904**	0.005231	0.004791	0.006006	0.005073	**0.582**
UBE2L6	0.004183	0.004692	0.004269	0.003404	**0.618**	0.028125	0.024986	0.029083	0.024952	**0.258**
USP18	0.000169	0.000119	0.000089	0.000117	**0.701**	0.004143	0.003456	0.004587	0.004365	**0.634**

	IFN-β					Mtb WCL				
Genes	HC	TST	LTBI	ATB	**p-value**	HC	TST	LTBI	ATB	**p-value**
ANKRD22	0.00263	0.00213	0.00281	0.00469	**0.024**	0.00012	0.00015	0.00014	0.00023	**0.055**
APOL1	0.00486	0.00534	0.00628	0.00498	**0.444**	0.0011	0.00111	0.00126	0.00082	**0.207**
BATF2	0.00077	0.00071	0.0011	0.00134	**0.1**	7.4E-05	5.8E-05	0.00014	7.7E-05	**0.209**
CAMP										
CCL8	0.02069	0.01684	0.01678	0.02862	**0.045**	.000073	5.1E-05	0.00005	6.5E-05	
CXCL10	0.04644	0.05638	0.0629	0.07674	**0.263**	0.00047	0.00114	0.00105	0.0011	**0.502**
CXCL11	0.04623	0.03142	0.04792	0.04973	**0.941**	0.00013	0.00015	0.00025	0.00013	**0.73**
CXCL9	0.00155	0.00207	0.00287	0.00272	**0.247**	0.00016	0.0002	0.00025	0.0003	**0.583**
ETV7	0.00114	0.00106	0.0013	0.00101	**0.884**	0.00016	0.00012	9.1E-05	6.6E-05	**0.211**
FAM26F	0.00123	0.00131	0.00152	0.00234	**0.036**	0.00008	0.00011	8.3E-05	0.0001	**0.581**
FCGR1A	0.00063	0.00055	0.00085	0.00157	**0.001**	4.5E-05	4.9E-05	0.00013	0.00016	
FCGR1B	7.8E-05	9.3E-05	0.00016	0.00032	**0.001**					
GBP1	0.0505	0.04939	0.06743	0.06568	**0.286**	0.00497	0.00616	0.00791	0.00754	**0.354**
GBP2	0.0183	0.01872	0.02011	0.0194	**0.798**	0.00943	0.00949	0.01061	0.0101	**0.889**
GBP4	0.01274	0.01249	0.0151	0.0128	**0.507**	0.00368	0.00308	0.00342	0.0031	**0.524**
GBP5	0.02506	0.03066	0.03297	0.03184	**0.371**	0.0043	0.00699	0.00796	0.00657	**0.222**
IFI35	0.00823	0.00769	0.0089	0.00922	**0.408**	0.00109	0.00117	0.0013	0.00106	**0.672**
IFI44	0.00728	0.00765	0.00866	0.00811	**0.378**	0.00147	0.0017	0.00234	0.00107	**0.03**
IFI44L	0.00599	0.00671	0.00817	0.00535	**0.377**	0.00072	0.00092	0.00161	0.00049	**0.015**
IFIT1	0.05302	0.03516	0.04419	0.04112	**0.185**	0.00305	0.00308	0.00476	0.00153	**0.036**
IFIT2	0.01839	0.01767	0.02082	0.02198	**0.357**	0.00116	0.00115	0.00188	0.0008	**0.077**
IFIT3	0.03922	0.03444	0.04099	0.03793	**0.467**	0.0032	0.00367	0.00381	0.00181	**0.096**
IFITM1	0.06377	0.05934	0.06817	0.05099	**0.389**	0.01837	0.0182	0.02053	0.01494	**0.058**
IFITM2	0.00697	0.00802	0.00847	0.00704	**0.928**	0.00421	0.004	0.00428	0.00318	**0.164**
IFITM3	0.01559	0.01809	0.02095	0.02496	**0.195**	0.00082	0.00115	0.00196	0.00136	**0.184**
IL10	0.0002	0.00012	0.00022	0.00012	**0.135**	0.00102	0.00077	0.00071	0.00099	**0.354**
IL12B						0.00016	0.0001	0.00012	0.00009	**0.578**
IL1A	0.00016	0.00012	0.00022	0.0002	**0.506**	0.01051	0.01094	0.01353	0.01579	**0.24**
IL1B	0.00418	0.00729	0.01014	0.01366	**0.2**	0.31071	0.26943	0.29854	0.39398	**0.061**
IRF1	0.00594	0.00772	0.00797	0.00711	**0.575**	0.00566	0.0059	0.00589	0.00625	**0.823**
IRF7	0.00993	0.01028	0.01363	0.01064	**0.35**	0.00233	0.00244	0.00365	0.00216	**0.305**
IRF9	0.00249	0.00299	0.00326	0.00279	**0.948**	0.00103	0.00137	0.00144	0.00109	**0.533**
ISG15	0.02686	0.02353	0.02534	0.02472	**0.964**	0.00249	0.00232	0.00296	0.00131	**0.125**
LAG3	0.00091	0.00149	0.00144	0.00121	**0.53**	9.5E-05	0.00013	0.00017	0.00018	**0.241**
MSR1	0.00866	0.00727	0.00993	0.01322	**0.041**	0.00014	8.1E-05	0.00014	0.00018	**0.012**
MX1	0.04251	0.04648	0.05644	0.04247	**0.537**	0.0073	0.00692	0.01358	0.00621	**0.426**
MX2	0.03137	0.03391	0.0377	0.03663	**0.518**	0.00582	0.00596	0.00764	0.00368	**0.178**
OAS1	0.01655	0.01405	0.0179	0.01488	**0.273**	0.0026	0.00248	0.003	0.00161	**0.153**
OAS3	0.02236	0.02286	0.02931	0.02604	**0.205**	0.00281	0.00317	0.00366	0.00196	**0.314**
OASL	0.02745	0.02636	0.03165	0.03201	**0.325**	0.00805	0.00801	0.00949	0.00714	**0.327**
PSMB8	0.00558	0.00623	0.00733	0.00529	**0.685**	0.00215	0.00219	0.00265	0.00198	**0.229**
SCARF1	0.00012	8.2E-05	0.00011	0.00012	**0.662**	8.5E-05	0.00013	0.00013	0.00013	**0.726**
SECTM1	0.00367	0.00412	0.0039	0.00454	**0.175**	0.00089	0.00057	0.00054	0.00073	**0.006**
SEPTIN4	6.3E-05	5.3E-05	0.00004	6.6E-05	**0.58**	.000029	2.1E-05	3.7E-05	0.00004	
SERPING1	0.00109	0.00129	0.0018	0.00185	**0.178**	.000044	0.00004	7.8E-05	7.6E-05	
SOCS1	0.00146	0.00199	0.00203	0.00229	**0.263**	0.00114	0.00134	0.00153	0.00124	**0.575**
SOCS3	0.00619	0.00521	0.00717	0.00627	**0.477**	0.01048	0.00744	0.00955	0.01341	**0.09**
STAT1	0.05191	0.04843	0.05545	0.04856	**0.934**	0.01202	0.01417	0.01316	0.01142	**0.423**
TAP1	0.01267	0.01276	0.01589	0.01744	**0.392**	0.00598	0.00542	0.00569	0.00616	**0.948**
TNFSF10	0.01512	0.01503	0.01586	0.01602	**0.457**	0.00104	0.00088	0.00102	0.00091	**0.914**
TRAFD1	0.00499	0.00548	0.00645	0.00528	**0.494**	0.00136	0.00134	0.00177	0.00111	**0.203**
UBE2L6	0.02494	0.02517	0.02786	0.02317	**0.644**	0.00685	0.0068	0.0079	0.00588	**0.208**
USP18	0.0039	0.00396	0.00483	0.00407	**0.539**	0.00035	0.0004	0.00037	0.00023	**0.132**

HC: healthy controls; TST: TST+QFT-; LTBI: latent TB infection, ATB: active TB, Mtb WCL: *M. tuberculosis* whole cell lysate. Yellow highlighted and **bolded** p-values are statistically significant. Genes without a p-value had < 60% detectability in one or more clinical phenotypes.

Table S2. Median gene expression (fold changes) in IFN-α -, IFN-β- and Mtb-WCL-stimulated PBMCs

	IFN-α					IFN-β				
Genes	**HC**	**TST**	**LTBI**	**ATB**	**p-value**	**HC**	**TST**	**LTBI**	**ATB**	**p-value**
ANKRD22	4.75	4.38	4.17	4.23	**0.91**	4.66	4.39	4.18	4.44	**0.862**
APOL1	3.49	2.97	3.14	3.09	**0.972**	3.20	3.10	3.26	3.18	**0.924**
BATF2		3.59	3.62	4.76			3.75	3.86	5.14	
CAMP										
CCL8	7.12	6.67	7.13	6.70	**0.718**	7.23	6.73	7.37	7.19	**0.821**
CXCL10	7.60	5.59	6.49	6.71	**0.461**	7.69	5.58	6.73	7.28	**0.318**
CXCL11	8.26	8.09	8.66	8.69	**0.743**	8.51	8.25	8.42	8.78	**0.613**
CXCL9			5.71				4.77	5.79	5.66	**0.422**
ETV7	4.29	4.01	4.21	3.85	**0.856**	4.23	3.98	4.25	4.01	**0.898**
FAM26F	3.85	3.31	3.40	3.58	**0.76**	3.48	3.69	3.76	3.89	**0.809**
FCGR1A	2.77	2.72	2.96	2.59	**0.541**	2.39	2.19	3.08	2.62	**0.454**
FCGR1B				2.20					2.78	
GBP1	4.38	3.99	3.84	3.62	**0.194**	4.27	3.94	3.63	3.88	**0.453**
GBP2	1.91	1.82	1.97	1.72	**0.242**	1.77	1.79	2.01	1.82	**0.503**
GBP4	3.52	3.29	3.33	3.35	**0.888**	3.16	3.14	3.28	3.18	**0.961**
GBP5	3.44	3.22	3.42	3.39	**0.26**	3.43	3.04	3.41	3.14	**0.346**
IFI35	4.01	3.12	3.60	3.71	**0.251**	4.07	3.33	3.54	3.73	**0.144**
IFI44	4.36	3.31	3.55	3.79	**0.425**	4.30	3.26	3.14	3.76	**0.646**
IFI44L	4.66	3.84	4.05	5.54	**0.338**	4.63	3.93	3.26	4.96	**0.206**
IFIT1	6.36	5.38	5.50	6.21	**0.572**	6.50	5.23	5.41	6.10	**0.424**
IFIT2	5.92	5.00	4.84	5.86	**0.239**	6.21	5.07	4.99	5.97	**0.223**
IFIT3	5.39	4.66	5.00	5.34	**0.383**	5.91	4.65	4.99	5.41	**0.401**
IFITM1	3.19	2.48	2.75	2.90	**0.653**	3.10	2.49	2.76	2.72	**0.842**
IFITM2	1.59	0.96	1.13	1.23	**0.599**	1.29	1.06	1.12	1.10	**0.674**
IFITM3	4.29	3.74	3.96	3.56	**0.198**	4.25	3.68	3.76	3.56	**0.506**
IL10	0.77	0.23	0.58	0.37	**0.12**	1.01	-0.07	0.28	-0.04	**0.087**
IL12B										
IL1A	-2.25	-2.12	-2.40	-1.69	**0.789**	-2.40	-2.47	-2.64	-2.06	**0.964**
IL1B	-1.51	-1.69	-1.69	-1.32	**0.994**	-2.25	-2.00	-1.84	-2.12	**0.481**
IRF1	1.22	1.16	1.36	1.12	**0.508**	1.06	1.34	1.39	1.21	**0.483**
IRF7	2.88	2.88	3.04	3.22	**0.93**	3.03	2.99	2.98	2.87	**0.875**
IRF9	2.22	1.09	1.27	1.58	**0.002**	1.95	1.44	1.33	1.47	**0.181**
ISG15	5.08	4.39	4.66	4.96	**0.632**	5.25	4.50	4.31	4.97	**0.332**
LAG3	3.03	3.54	4.34	3.89	**0.128**	3.38	3.80	4.29	3.83	**0.314**
MSR1	4.09	3.59	3.38	3.36	**0.013**	4.08	3.84	3.62	3.39	**0.09**
MX1	4.22	3.42	3.73	3.61	**0.566**	4.19	3.08	3.60	3.66	**0.634**
MX2	3.97	3.39	3.65	3.87	**0.682**	3.97	3.37	3.51	3.84	**0.503**
OAS1	4.26	3.59	3.82	4.00	**0.721**	4.07	3.41	3.40	4.22	**0.598**
OAS3	4.99	3.99	4.20	4.82	**0.607**	4.78	3.72	4.09	4.21	**0.573**
OASL	3.10	2.57	2.45	2.62	**0.401**	2.82	2.56	2.32	2.62	**0.412**
PSMB8	1.83	1.60	1.80	1.63	**0.416**	1.84	1.65	1.76	1.73	**0.619**
SCARF1	0.21	0.94	0.90	0.29	**0.497**	1.11	0.79	0.69	1.28	**0.716**
SECTM1	3.26	3.02	3.22	2.78	**0.055**	3.58	3.26	3.39	3.09	**0.106**
SEPTIN4				0.28					0.25	
SERPING1	4.01	4.41	4.87	4.18	**0.307**	4.02	4.42	4.81	4.38	**0.616**
SOCS1	1.74	1.45	1.73	1.55	**0.643**	1.90	1.69	1.71	1.58	**0.862**
SOCS3	0.63	0.44	0.68	0.40	**0.069**	0.66	0.26	0.90	0.19	**0.043**
STAT1	3.24	2.43	2.83	2.66	**0.269**	3.07	2.44	2.54	2.56	**0.315**
TAP1	1.98	1.86	2.08	2.01	**0.536**	1.95	1.82	2.01	2.15	**0.416**
TNFSF10	4.58	4.24	4.43	4.59	**0.733**	4.93	4.38	4.41	4.55	**0.576**
TRAFD1	2.70	2.26	2.59	2.31	**0.458**	2.63	2.41	2.57	2.61	**0.555**
UBE2L6	3.11	2.42	2.79	2.81	**0.265**	2.88	2.43	2.72	2.72	**0.306**
USP18		5.26	5.29	4.96		5.16	4.85	5.12	5.11	**0.914**

Genes	Mtb WCL				
	HC	TST	LTBI	ATB	p-value
ANKRD22	0.10	1.40	-0.18	0.16	**0.796**
APOL1	0.96	1.03	0.72	0.69	**0.426**
BATF2			0.73	0.86	
CAMP					
CCL8		-1.74		-1.09	
CXCL10	0.75	0.07	0.49	1.18	**0.835**
CXCL11	0.29	-0.47	0.18	0.75	**0.616**
CXCL9		0.92	1.88	2.24	**0.56**
ETV7	2.21	0.31	0.82	0.55	**0.609**
FAM26F	-0.23	-0.71	-0.47	-0.81	**0.79**
FCGR1A	-1.06	-1.36	0.23	-0.51	**0.121**
FCGR1B					
GBP1	1.03	0.64	0.41	0.76	**0.593**
GBP2	1.06	0.83	0.81	0.83	**0.165**
GBP4	1.59	1.13	1.21	1.18	**0.724**
GBP5	1.16	1.00	0.92	1.01	**0.836**
IFI35	1.09	0.65	0.77	0.86	**0.1**
IFI44	1.16	1.44	1.24	0.82	**0.055**
IFI44L	1.22	1.36	1.15	1.89	**0.818**
IFIT1	2.45	2.16	1.88	1.66	**0.125**
IFIT2	2.07	1.51	0.91	1.18	**0.18**
IFIT3	2.34	1.43	1.14	1.35	**0.278**
IFITM1	0.93	0.96	0.86	0.64	**0.15**
IFITM2	0.18	0.18	0.23	0.06	**0.25**
IFITM3	-0.22	-0.18	-0.29	-0.86	**0.019**
IL10	2.85	2.54	1.98	2.79	**0.34**
IL12B					
IL1A	4.02	3.50	3.61	3.86	**0.403**
IL1B	3.65	2.95	3.13	2.98	**0.589**
IRF1	1.00	0.99	0.86	1.04	**0.812**
IRF7	1.01	0.65	0.83	0.55	**0.057**
IRF9	0.87	0.34	0.28	0.23	**0.345**
ISG15	1.46	0.92	0.96	0.83	**0.471**
LAG3	0.59	0.68	1.37	1.10	**0.32**
MSR1	-1.51	-2.32	-2.47	-2.40	**0.55**
MX1	1.73	1.02	0.94	0.69	**0.068**
MX2	1.10	1.01	0.93	0.62	**0.144**
OAS1	1.38	0.99	1.27	0.67	**0.252**
OAS3	1.91	0.87	1.31	0.91	**0.045**
OASL	0.78	0.71	0.44	0.36	**0.126**
PSMB8	0.23	0.34	0.25	0.12	**0.301**
SCARF1	0.32	1.62	0.69	0.74	**0.252**
SECTM1	1.99	0.49	0.53	0.06	**<0.001**
SEPTIN4					
SERPING1					
SOCS1	1.21	1.21	0.93	0.90	**0.436**
SOCS3	1.10	0.86	0.85	1.07	**0.84**
STAT1	1.44	0.69	0.62	0.49	**0.024**
TAP1	0.84	0.62	0.57	0.45	**0.271**
TNFSF10	0.96	0.70	0.30	-0.07	**0.044**
TRAFD1	0.80	0.61	0.49	0.28	**0.058**
UBE2L6	1.00	0.78	0.56	0.58	**0.103**
USP18	1.60	1.40	1.38	0.99	**0.357**

	$\log_2FC \geq 1.0$
	$-1.0 < \log_2FC > 1.0$
	$\log_2FC \leq -1.0$

HC: healthy controls; TST: TST+QFT-; LTBI: latent TB infection, ATB: active TB, Mtb WCL: *M. tuberculosis* whole cell lysate. Yellow highlighted and **bolded** p-values are statistically significant. Genes without a p-value had < 60% detectability in one or more clinical phenotypes. Red-filled boxes – upregulated genes, blue-filled boxes – downregulated genes, white-filled boxes -no change.

Table S3. Median cytokine levels in supernatants from unstimulated, IFN-α -, IFN-β- and Mtb-WCL-stimulated PBMCs

	Unstimulated					IFN-α				
Cytokine	**HC**	**TST**	**LTBI**	**ATB**	**p-value**	**HC**	**TST**	**LTBI**	**ATB**	**p-value**
EGF	14.91	7.49	16.71	13.27	**0.819**	13.53	6.37	15.46	11.14	**0.452**
Eotaxin	6.65	8.76	7.57	7.56	**0.704**	6.55	8.85	8.68	6.77	**0.629**
G-CSF	102.1	55.36	48.31	48.14	**0.292**	69.93	23.2	42.83	42.67	**0.195**
Fractalkine	23.98	35.55	38.03	31.14	**0.205**	25.78	31.79	39.25	36.46	**0.127**
IFNα2	26.76	6.78	13.65	11.2	**0.368**	2316.63	2408.81	2671.14	2477.62	**0.541**
IFN-γ						10.28	13.7	14.06	8.66	**0.184**
GRO	1771.44	1369.67	1567.68	1769.38	**0.928**	272.72	348.28	333.38	283.84	**0.946**
IL-10	61.5	40.06	54.31	31.53	**0.387**	57.03	40.97	81.89	29.06	**0.036**
MCP-3	119.53	418.64	415.09	298.36	**0.212**	349.84	509.59	927.37	674.46	**0.046**
MDC	465.7	485.57	390.3	253.29	**0.429**	88.35	116.83	111.9	48.1	**0.155**
PDGF-AA	25.33	14.13	37.69	49.37	**0.174**	19.98	10.39	28.85	36.83	**0.177**
PDGF-AB/BB	93.18	48.79	112.1	140.18	**0.127**	50.89	32.17	94.2	104.35	**0.019**
sCD40L	9.9	7.7	12.5	15.78	**0.48**	6.73	6.48	11.05	8.41	**0.518**
IL-1RA	189.64	293.56	231.32	195.41	**0.922**	402.06	427.06	592.47	702.54	**0.304**
IL-1β	28.8	34.8	19.63	34.99	**0.35**	31.78	23.36	34.43	26.52	**0.344**
IL-6	70.2	154.02	128.2	100.69	**0.493**	124.89	140.1	196.12	152.2	**0.22**
IL-7	17.84	10.52	11.12	9	**0.216**	14.62	6.45	10.73	9.53	**0.396**
IL-8	2915.97	4591.42	4057.15	5157.91	**0.195**	1342.96	2342	2288.06	2566.52	**0.768**
IP-10	124.52	139.96	120.14	69.22	**0.474**	2348.46	3080.27	2455.2	2550.82	**0.913**
MCP-1	1743.05	3366.47	3290.3	3233.34	**0.203**	3325.97	3391.6	3736.77	3379.83	**0.939**
MIP-1α	45.11	131.3	59.61	36.11	**0.365**	82.57	78.12	122.76	40.14	**0.052**
MIP-1β	282.26	353.09	309.94	213.72	**0.398**	388.94	363.92	485.71	294.13	**0.048**
RANTES	453.3	360.66	600.22	568.39	**0.173**	414.2	301.54	634.05	430	**0.055**
TNFα	103.12	72.38	79.32	67.12	**0.538**	98.44	62.58	89.76	75.98	**0.304**

	IFN-β					Mtb WCL				
Cytokine	**HC**	**TST**	**LTBI**	**ATB**	**p-value**	**HC**	**TST**	**LTBI**	**ATB**	**p-value**
EGF	16.33	7.58	17.05	15.79	**0.648**	12.54	8.61	11.59	19.49	**0.67**
Eotaxin	4.35	7.56	6.41	4.96	**0.86**	10.96	14.73	11.14	11.34	**0.907**
G-CSF	79.87	22.77	36.89	30.22	**0.327**	3597.62	2740.02	2799.77	3072.48	**0.552**
Fractalkine	25.78	31.48	38.23	29.9	**0.72**	57.66	84.66	60.24	81.92	**0.147**
IFNα2	35.31	5.86	18.98	9.96	**0.583**	72.13	43.92	64.17	39.22	**0.169**
IFN-γ	14.74	12.33	14.2	10.55	**0.5**	491.68	695.16	387.61	1094.29	**0.268**
GRO	183.39	265.34	233.83	237.59	**0.95**	6040.79	6495.61	1544.69		**0.223**
IL-10	98.54	38.81	83.7	27.18	**0.034**	3105.28	2179.16	2454.26	3602.12	**0.471**
MCP-3	389.14	544.95	885.76	687.35	**0.323**	146.64	107.07	157.93	209.7	**0.477**
MDC	65.27	80.82	88.46	27.37	**0.148**	375.95	407.9	468.71	359.92	**0.855**
PDGF-AA	20.27	11.54	29.2	45.55	**0.244**	26.99	13.8	38.9	72.13	**0.029**
PDGF-AB/BB	93.53	51.87	91.29	113.94	**0.205**	126.14	118.88	178.43	244.34	**0.01**
sCD40L	10.92	7.7	10.66	12.52	**0.948**	12.34	10.87	10.37	20.18	**0.177**
IL-1RA	544.69	610.33	764.58	920.51	**0.239**	604.75	668.59	788.66	1380.03	**0.094**
IL-1β	22.67	19.19	24.52	23.36	**0.807**	1442.62	1188.98	1609.01	2748.4	**0.045**
IL-6	111.57	123.11	146.66	116.35	**0.787**	2566.5	2623.6	3000.23	3589.28	**0.217**
IL-7	8.69	7.22	10.3	6.49	**0.338**	33.94	40.2	34	34	**0.674**
IL-8	980.74	1059.28	912.9	1256.4	**0.891**	5714.12	6279.05	6281.61	5186.76	**0.589**
IP-10	4542.9	3933.3	4737.47	6753.43	**0.256**	441.34	974.09	1009.22	549.93	**0.351**
MCP-1	2731.41	3503.62	2870.76	3456.57	**0.239**	2164.86	2449.76	2571.36	3951.17	**0.08**
MIP-1α	59.23	69.95	94.98	36.1	**0.165**	837.48	1961.03	1535.86	1512.54	**0.129**
MIP-1β	348.82	322.25	409.01	272.57	**0.133**	2118.36	2758.79	2385.63	2830.02	**0.188**
RANTES	436	347.79	588.47	441.56	**0.239**	1022.46	942.91	1327.9	1677.04	**0.132**
TNFα	101.55	67.67	91.12	61.8	**0.556**	5591.92	3014.02	3934.04	5055.63	**0.176**

HC: healthy controls; TST: TST+QFT-; LTBI: latent TB infection, ATB: active TB, Mtb WCL: *M. tuberculosis* whole cell lysate. Yellow highlighted and **bolded** p-values are statistically significant.

Table S4. Median cytokine expression (fold changes) supernatants from IFN-α -, IFN-β- and Mtb-WCL-stimulated PBMCs

	IFN-α					IFN-β				
Cytokines	**HC**	**TST**	**LTBI**	**ATB**	**p-value**	**HC**	**TST**	**LTBI**	**ATB**	**p-value**
EGF	-0.32	-0.23	-0.18	-0.22	0.425	-0.07	-0.17	-0.12	-0.12	0.517
Eotaxin	0.00	-0.15	0.04	-0.01	0.494	-0.17	-0.64	-0.42	-0.27	0.796
G-CSF	-0.22	-0.64	-0.06	-0.18	**0.031**	-0.62	-0.76	-0.36	-0.51	0.738
Fractalkine	0.00	-0.32	-0.07	0.00	0.402	0.70	-0.22	-0.18	-0.22	0.130
IFNα2	6.39	8.32	7.84	7.19	0.645	0.10	-0.17	-0.06	-0.10	0.975
GRO	-2.12	-2.25	-2.25	-2.64	0.433	-2.64	-2.74	-2.94	-3.18	0.304
IL-10	0.36	-0.03	0.57	-0.03	**0.022**	0.40	0.01	0.45	0.00	0.087
MCP-3	1.49	0.82	0.83	1.01	0.723	1.68	1.08	1.20	1.17	0.712
MDC	-1.89	-1.94	-1.89	-2.25	0.802	-2.47	-2.64	-2.25	-2.94	0.419
PDGF-AA	-0.36	-0.51	-0.27	-0.32	0.056	-0.25	-0.47	-0.17	-0.18	0.310
PDGF-AB/BB	-0.81	-0.43	-0.12	-0.15	**0.017**	-0.06	-0.30	-0.27	-0.29	0.970
sCD40L	-0.81	-0.47	-0.34	-0.47	0.788	-0.10	-0.25	-0.22	-0.38	0.730
IL-1RA	1.41	1.10	1.49	1.61	0.167	1.87	1.49	1.85	2.22	0.237
IL-1β	-0.10	-0.79	0.38	0.14	**0.033**	-0.29	-0.81	0.11	0.16	0.268
IL-6	0.30	-0.18	0.52	0.24	0.187	0.11	-0.23	0.34	0.06	0.482
IL-7	0.01	-0.29	0.03	0.04	0.392	-0.06	-0.40	-0.20	-0.15	0.960
IL-8	-0.97	-1.18	-0.84	-1.36	0.860	-1.32	-1.40	-1.15	-2.00	0.403
IP-10	3.87	4.06	4.66	4.83	0.062	5.29	5.11	5.61	6.03	**0.029**
MCP-1	0.53	0.07	0.10	0.16	0.448	0.12	-0.03	-0.14	0.01	0.729
MIP-1α	0.95	-0.56	0.82	0.26	0.346	0.36	-0.58	0.72	0.16	0.719
MIP-1β	0.56	0.14	0.79	0.19	0.636	0.28	0.03	0.64	0.34	0.807
RANTES	-0.22	-0.47	-0.09	-0.17	0.233	0.00	-0.04	-0.09	-0.20	0.747
TNFα	0.23	-0.10	0.30	0.14	0.166	0	-0.12	0.26	-0.06	0.313

Cytokines	Mtb WCL				
	HC	**TST**	**LTBI**	**ATB**	**p-value**
EGF	0.16	0.01	-0.09	0.01	0.307
Eotaxin	0.70	0.38	0.53	0.57	0.655
G-CSF	5.14	5.73	5.87	6.08	0.368
Fractalkine	1.02	1.04	0.95	1.16	0.491
IFNα2	1.41	2.57	3.00	2.04	0.947
GRO	-0.54	2.37	2.81		0.368
IL-10	5.90	5.70	6.16	6.77	0.110
MCP-3	0.07	-1.69	-1.15	-0.42	0.199
MDC	0.39	-0.01	0.08	0.42	0.613
PDGF-AA	0.15	0.11	0.11	0.30	0.207
PDGF-AB/BB	0.62	1.14	0.76	1.05	0.296
sCD40L	0.39	0.48	0.23	0.39	0.921
IL-1RA	1.96	1.29	2.25	2.30	0.085
IL-1β	5.53	5.31	6.26	6.66	**0.019**
IL-6	5.86	3.52	4.23	4.84	0.345
IL-7	0.91	1.66	1.56	1.85	0.153
IL-8	1.04	0.44	1.26	0.10	0.154
IP-10	2.31	2.56	2.53	2.92	0.526
MCP-1	-0.14	-0.15	-0.27	0.00	0.270
MIP-1α	2.94	3.96	4.18	5.62	0.629
MIP-1β	1.99	3.07	3.08	4.80	0.296
RANTES	1.34	1.33	1.57	1.70	0.209
TNFα	5.94	5.37	6.25	6.61	0.387

	$\log_2FC \geq 1.0$
	$-1.0 < \log_2FC > 1.0$
	$\log_2FC \leq -1.0$

HC: healthy controls; TST: TST+QFT-; LTBI: latent TB infection, ATB: active TB, Mtb WCL: *M. tuberculosis* whole cell lysate. Yellow highlighted and **bolded** p-values are statistically significant. Red-filled boxes – upregulated genes, blue-filled boxes – downregulated genes, white-filled boxes -no change.